Université du Québec à Chicoutimi

THÈSE PRÉSENTÉE COMME EXIGENCE PARTIELLE

DU

DOCTORAT EN INGÉNIERIE

Par

Sudeshna Saha

ÉTUDE SUR LE CHANGEMENT DE COULEUR DU BOIS TRAITÉ THERMIQUEMENT PROVOQUÉ PAR UV: DÉVELOPPEMENT DE REVÊTEMENT

Novembre, 2011

University of Quebec at Chicoutimi

A THESIS SUBMITTED IN PARTIAL FULFILMENT OF

THE REQUIREMENTS FOR THE DEGREE

OF

DOCTOR OF PHILOSOPHY

By

Sudeshna Saha

STUDY ON THE COLOR CHANGE OF HEAT-TREATED WOOD CAUSED BY UV LIGHT: COATING DEVELOPMENT

November, 2011

ABSTRACT

High temperature heat treatment of wood is an alternative to chemical treatment which is harmful to the environment as well as human health. The heat-treated woods have higher durability against biological attacks, higher dimensional stability, and higher thermal insulating capacity, and attractive dark brown color compared to conventionally oven-dried wood. Unfortunately, this dark brown color is not stable in outer environment and turns to grey or white if not protected. Especially sunlight (UV and visible light) and water (moisture or rain) are the two main components responsible for the discoloration of heat-treated wood. Although numerous research studies are published which are devoted to understanding the degradation behavior of natural wood and their protection mechanism, few are reported on the discoloration of heat-treated wood and none is available on their protection mechanism. Commercially available coatings are usually highly pigmented and contain toxic compounds. This thesis focuses on the development of a transparent or semitransparent non toxic coating to prevent or delay discoloration and degradation of heat-treated wood. In this study, one soft wood species (jack pine) and two hard wood species (quaking aspen, white birch) are considered.

This study has two parts. The first part is to study potential components of the transparent non toxic protective coatings. The second part involves the evaluation of these coatings.

Several approaches are used for the first part. The first approach is based on the development of different organic and inorganic UV stabilizers and natural antioxidants

(bark extracts, needle extracts, and even organosolv nano lignins). The second approach is the investigation of different inorganic micro and nano UV absorbers (micro and nano titania particles, ZnO nano particles, and CeO_2 nano particles) alone or together with natural antioxidants. The third approach concerns with the investigation of different base polymers (sol-gel coating, soy based polymer coating, and acrylic polyurethane coatings) to be used with the above mentioned additives. In the second part, effectiveness of the coatings with different additives is examined and compared with that of an industrial coating commonly used.

The results showed that the acrylic polyurethane with bark extracts and lignin stabilizer or with CeO_2 nano particles alone or together with lignin stabilizer performed better than the industrial coatings considered during this study for the protection of heat-treated wood during accelerated aging. Up to date, there are no coatings available in the market developed especially for heat-treated woods. Therefore, this study gives an insight into the protection mechanism of heat-treated wood. The results indicate that highly toxic and pigmented industrial coatings could be replaced by the coatings developed during this study as they are more effective. Bark extracts, due to their high antioxidant properties, can be a potential additive for the wood coatings. A lot of research focuses on the inorganic UV absorbers; however, there exist one or two studies on CeO_2 nano particles. This thesis will provide a pathway for the use of CeO_2 nano particles in wood coatings. Therefore, the findings of this thesis constitute a major contribution to the wood coatings industry.

RÉSUMÉ

Le traitement du bois à haute température est un alternatif au traitement chimique qui est néfaste pour l'environnement aussi bien que à la santé humaine. Le bois traité thermiquement a plus de durabilité face à l'attaque biologique, une plus haute stabilité dimensionnelle, une meilleure capacité d'isolation thermique et une couleur brun foncé plus attrayante que le bois séché dans le séchoir conventionnel. Malheureusement, cette couleur brun foncé n'est pas stable dans l'environnement externe et devient gris ou blanc si non protégée. Particulièrement les rayons du soleil (UV et lumière visible) et l'eau (humidité ou pluie) sont les deux facteurs principaux responsables de la décoloration du bois traité thermiquement. Bien que plusieurs études sur le bois naturel se soient penchées sur la compréhension de la dégradation et sur les mécanismes de protection, un nombre très limité d'études porte sur la décoloration du bois traité thermiquement et sur les approches potentielles de protection. Les revêtements disponibles commercialement sont hautement pigmentés et contiennent des composés toxiques. Cette thèse met l'emphase sur le développement des revêtements transparents ou semi-transparents non toxiques, pour empêcher ou retarder la décoloration ou la dégradation du bois traité thermiquement. Une espèce de bois mou (pin gris) et deux espèces de bois durs (peuplier faux tremble, bouleau blanc) ont été considérées dans cette étude.

Cette étude est faite en deux parties. La première partie porte sur les composantes potentielles de revêtements protecteurs transparents non toxiques. La deuxième partie traite de l'évaluation de ces revêtements.

Plusieurs démarches sont utilisées pour la première partie. La première est basée sur le développement de différents stabilisateurs UV organiques et inorganiques et antioxydants naturels. La deuxième façon est l'examen de différents micro et nano absorbeurs UV inorganiques (micro et nano particules de titane, nano particules de ZnO et CeO_2), seuls ou avec des antioxydants naturels. La troisième approche concerne l'analyse des différents polymères de base utilisés avec les additifs mentionnés ci-dessus.

L'efficacité des revêtements avec différents additifs a été examinée dans la deuxième partie et comparée à celle d'un revêtement industriel couramment utilisés. Les résultats démontrent que l'acrylique polyuréthane avec l'extrait d'écorce et le stabilisateur de la lignine ou avec les nano particules de CeO_2 seul ou avec le stabilisateur de la lignine performent mieux que le revêtement industriel considéré lors de l'étude de la protection du bois traité thermiquement pendant le vieillissement accéléré. Jusqu'à présent, aucun revêtement développé spécialement pour le bois traité thermiquement n'est disponible sur le marché. Cette étude fournit donc un regard sur le mécanisme de protection du bois traité thermiquement. Les résultats indiquent que les revêtements industriels pigmentés et hautement toxiques peuvent être remplacés par des revêtements développés lors de cette étude parce qu'ils sont plus efficaces. Les extraits d'écorces, à cause de leurs propriétés hautement anti-oxydantes, peuvent être un additif potentiel pour le revêtement du bois. Bien que plusieurs recherches se concentrent sur l'absorbeur UV inorganique, il existe cependant une ou deux études sur les nano particules de CeO_2. Cette thèse pave la voie à l'usage des nano particules de CeO_2 dans le revêtement de bois. Par conséquent, les

résultats de cette thèse constituent une contribution majeure pour l'industrie du revêtement de bois.

ACKNOWLEDGEMENT

I would like to express sincere gratitude and thanks to my supervisor, Dr. Duygu Kocaefe, for her tireless patience, continuous support, supervision, guidance, trusts on me and valuable suggestions throughout my doctorate research. I have been fortunate enough to have her as my supervisor.

I would also like to extend my sincere appreciation and thanks to my co supervisors, Dr. Yaman Boluk and Dr. Andre Pichette for their valuable inputs, discussions, and their support during the course of this work.

I would like to convoy my thanks to Dr. Yasar Kocaefe, Dr. Cornelia Krause, Dr. Vakhtang Mshvildadze for their valuable contributions to this project.

I have been fortunate enough to work with a number of expert technicians, Rénald Delisle, Jacques Allaire, Pattrice Pacquette, and Jean Pacquette who are not only expert in their field but very good human beings.

I would like to thank all colleagues and professionals in GRTB (Groupe de recherché sur la thermotransformation du bois), LASEVE (Laboratoire d'analyse et de séparation des essences végétales) and other laboratories in UQAC, in Alberta Research Council (now Alberta Innovates) and in University of Alberta who helped me during the course of this work. Special mention to Dr. Jean Legault, Dr. Zhan Zhang. Ms. Xian ai Huang, Dr. Thierry Lekounougou, Dr. Noura Oumarou, Dr, Sandor Poncsak, and Dr. Ramdan Younsi.

I would like to extend my deep gratitude and thanks to Dr. Ujjanini Sarkar and Dr. Jayanta Guha for their support.

I would like to thank Fonds québécois de la recherche sur la nature et les technologies (FRQ_NT, now Fonds de recherche du Québec-Nature et technologie), Développement Économique Canada (DEC), Ministère du Développement Économique, de l'Innovation et de l'Exportation (MDEIE), Conférence Régionale des Élus du Saguenay-Lac-St-Jean (CRÉ), University of Quebec at Chicoutimi (UQAC), Fondation of the University of Quebec at Chicoutimi (FUQAC), FPInnovation, Alberta Innovates, and our industrial partners (PCI Industries, Ohlin Thermo Tech, Industries ISA, Kisis Technologies) for the financial contributions and their valuable collaboration.

I would like to thank all my friends in Chicoutimi for their help, support and continuous encouragement without whom life would not be so easy.

I would like to express my sincere gratefulness to my family members and friends back in India. Thank you very much Maa (mother), baba (father), dadabhai (elder brother) and everyone else in the family and my friends for their continuous moral support and faith in me.

Finally I would extend my appreciation to my husband (Shipan Das) for his love, affection, and understanding throughout my study.

Table of Contents

List of Figures

List of Tables

Chapter 1

INTRODUCTION

Mankind from the primitive age is highly dependent on forests and the wood they produce. Wood has been used as a building material for houses, boats, roads, bridges, agricultural implements and tools, furniture and thousand others from prehistoric and historic periods to the very modern day society. Wood was not only used as a building material but was the main source of fuel in the beginning of mankind survival. It also gained importance for the production of charcoal, tar and pitch, and potash as a chemical raw material. In addition, its use as the basic substance for pulp and paper industry should not be overlooked

In 2010, world consumption of fuel and charcoal was a little more than half of the world's wood consumption whereas 25% of world's wood harvest was accounted for construction and building industry. Out of 3.2 billion cubic meters of wood consumption, 0.15 billion cubic meters was used as source of pulp in 2009 (Figure 1.1). Increased demand of industrial round wood and continuous decrease in supply due to industrialization and deforestation of limited natural resources forced wood industries to consider different options in order to increase the durability of this natural product in construction and building industry.

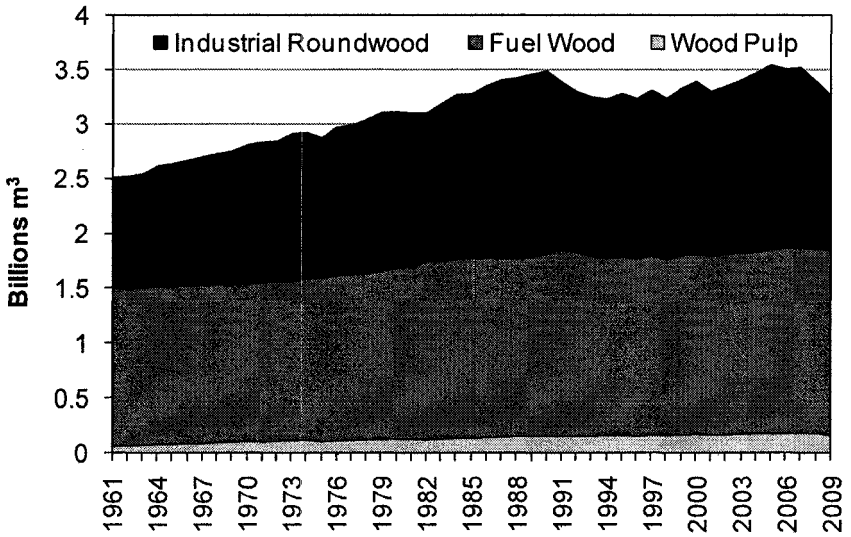

Figure 1.1 Wood consumption since 1991 (FAOStat 2009)

Wood is world's most important building material and the wood industry is one of the major industries in North America, especially in Canada. The Canadian sawmills and wood preservation industry contributed nearly $7.6 billion to the national Gross Domestic Product (GDP) in 2006. This is equivalent of 4.4% of the manufacturing sector's GDP, and 0.7% of the entire Canadian economy. This industry is also a key player in the export market, accounting for more than 4% of total Canadian merchandise exports [1]. It is also of utmost importance to the economy of the Saguenay-Lac-St-Jean region.

Wood is a naturally occurring polymer composite, constituted mainly of polysaccharides and polyphenolics including three biopolymers: lignin, cellulose and hemicelluloses [2-5]. Cellulose, a long, linear cellobiose-based homopolysaccharide composed of β-D-glucopyranose units linked together by (1—›4)-glycosidic bonds, is the main component of wood and constitutes 40-45% of the wood substance. Cellulose molecules are randomly oriented and have a tendency to form intra- and intermolecular

hydrogen bonds. In contrast to cellulose, hemicellulose consists of branched heteropolysaccharides mainly the sugars, D-xylopyranose, D-glucopyranose, D-galactopyranose, L-arabinofuranose, D-mannopyranose, D-glucopyranosyluronic acid, and D-galactopyranosyluronic acid with minor amounts of other sugars, surrounding the cellulose fibers and have a degree of polymerization of only 200. The hemicellulose content of wood is usually between 20-30%. Lignin, on the other hand; is an amorphous polyphenolic aromatic 3D polymer based on polymerization of three poly propanoid units. It mainly acts as a binder between the cells and essentially plays the important role of strength provider [6-10]. Lignin content of normal softwood varies between 26-32% while that of hardwood varies between 20-25% [10]. Unlike cellulose which has a single repeating unit of the hemicelluloses, lignin consists of a complex arrangement of substituted phenolic units.

1.1. Background

Wood preservation is a very important and cost bearing part for wood industries. Since wood is a biological material, it tends to deteriorate with time without proper preservation techniques and material loss due to deterioration is a big problem for wood industries. At this stage, wood deterioration is caused by mainly biological attacks. There are several wood preservation techniques available in the market. Chemical treatment is one of the most useful and practiced method. In the late 1940s and early 1950s, creosote and creosote/petroleum mixtures received high attention for wood preservation and are still practiced by Canadian wood industry mainly for railway roads, utility poles, and marine

structures. It was later replaced by pentacholorophenol in P9 type A oil mainly for utility poles in 1970s, which later substituted by cromated copper arsenate (CCA). Until 2003, CCA treatment was the main wood preservation technique in Canada which was replaced recently by alkaline copper quaternary and copper azole due to its high toxicity. These amine copper-organic co-bioside systems are more corrosive than CCA. All these chemicals are toxic in nature, and they affect environment and human health adversely.

Motivated by growing environmental concerns and growing demand for sustainable use of natural resources, there are many studies on new technologies for enhancing durability and service life of wood due to its unique properties (e.g., wood is recyclable, renewable, and biodegradable) [8, 11, 12]. High temperature heat treatment of wood is a viable and environment-friendly wood preservation method, and it is one of the alternatives to chemical treatment which is harmful to the environment as well as to human health [13]. Heat treatment modifies wood both physically and chemically. The heat-treated woods are highly popular among consumers because of their attractive dark brown color. In addition, it is also dimensionally more stable and less prone to biological attack compared to natural wood due to decrease in hygroscopicity during heat-treatment [13-23]. The heat treatment also improves thermal insulating capacity of wood by modifying its chemical structure. High temperature heat treatment of wood leads to decrease in amorphous polysaccharide content, condensation and demethoxylation of lignin, softening of cellulose and hemicelluloses structure, and removal of certain extractives. Although high-temperature heat treatment has many advantages, it does not restrain the heat-treated wood from aging. On prolonged exposure to outer environment without any protection, these heat-treated

woods undergo several chemical modifications which manifest itself with color change, loss of gloss, and formation of cracks on the surface. Aging of heat-treated wood differs from untreated wood due to the condensed structure of lignin and presence of antioxidant compound, consequent to the thermal modification [24-26]. Modified structure of lignin in heat-treated wood could partially inhibit UV-light-induced free-radical reactions due to reduction in leaching of degraded product and decrease in the formation of low molecular weight degradation products such as quinones [26].

1.2. Statement of the Problem

From the end user's perspective, heat-treated wood is a very beneficial product that has good outdoor fungal resistance, improved swelling and shrinkage properties although less strength and flexibility compared to untreated wood. The main application of these heat-treated woods is for decorative purposes as building material. For the outdoor application of wood, it must satisfy a number of criteria most importantly a prolonged exposure to the outer environment without much degradation. In the natural outdoor environment, heat-treated wood surface undergoes varieties of chain scission reactions due to environmental stresses if not protected with coating. Photo-oxidation of wood refers to a process where this polymer undergoes chemical modifications such as bond cleavage and hydrogen abstraction resulting in radical formation, formation of peroxides with oxygen, and finally decomposition resulting in production of colored and hydrophilic by-products, known as chromophores. These modifications induce surface property changes leading to discoloration, increased water sensitivity followed by hydrolysis, leaching, and cracking.

Apart from a decrease in methoxyl content, and an increase in carboxyl on the wood surface, photo-degradation also results in an increase in cellulose and a decrease in lignin concentration on wood surface [11, 27, 28].

With the move towards value-added products as well as higher quality product specifications, discolorations have become an important economic problem. Therefore, color defects are less tolerable, and they ultimately lead to deterioration of various physical, chemical, and biological properties of heat-treated wood. Wood discolorations can affect the natural appearance of many wood species causing considerable economic problems to the wood industry, especially for heat-treated woods as they are mainly used for decorative purposes. Since heat treatment does not protect wood from UV, development of UV protective coating is of utmost importance to improve the durability and service life for this new product.

In order to prevent photodegradation of the natural wood used in outdoor applications, a great deal of effort has been put forward for the development of protective systems [29]. Numerous researchers work in different directions with similar objectives. A part of the research is directed towards the treatment of natural wood with inorganic substances (ferric chloride, chromium trioxide, zinc oxide, titanium oxide) which imparts some beneficial properties but also imparts some unwanted stain on the wood surface. On the other hand, a wide variety of wood finishes are available such as paints, solid color stains, and semi-transparent coatings. However, these cover the natural beauty and color of wood. In addition, most have toxic components. Although a lot of literature is devoted to the

development of coatings for the protection of natural wood, to our knowledge, there is no study reported on the protection of heat-treated wood.

When choosing a wood finish, there are two elements to consider: aesthetics and protection. These two qualities can sometimes be conflicting. Aesthetically, there is a growing trend among consumers to maintain the clear natural look of wood. However, the best protection from the sun's ultraviolet radiation is obtained from pigmented products which tend to cover the wood's natural grain and texture. Thus, the problem lies in balancing aesthetic and protection. Protective coatings should [30]:

- ✓ have photochemical resistance,
- ✓ dampen the variations of wood moisture content
- ✓ prevent the growth of dark color fungi and
- ✓ be weather resistant

The chemical modification and mechanical breakdown at the wood and clear or semitransparent coating interface due to UV radiation of sunlight often result in the failure of coatings [6, 30] (See Figure 1.2). In order to overcome this problem, UV light should be screened before reaching the wood surface. To enhance the durability of protective coatings, light stabilizers, UV absorbers, and antioxidants are incorporated in coating formulations as additives. UV absorbers are inorganic and organic materials which preferentially absorb the UV radiation and prevent the excitation state, thus, they protect the coating [31, 32]. Light stabilizer must be effective over a long period of time and must not, therefore, degrade, evaporate from the matrix, and be leached out by solvents from the material [33, 34]. Furthermore, the additive must be uniformly distributed, which requires

its compatibility with the base polymer. For UV protective coatings, both inorganic and organic UV absorbers can be used, but no single UV absorber exhibits an ideal absorption in the desired range. Different combinations of organic and inorganic UV absorbers are studied in the search for efficient UV protective coatings [35]. Natural antioxidants also stabilize UV protective coatings by transforming hydrogen peroxide into a more stable product. Therefore, the effects of antioxidants on protection of heat-treated wood surface from UV degradation are also studied.

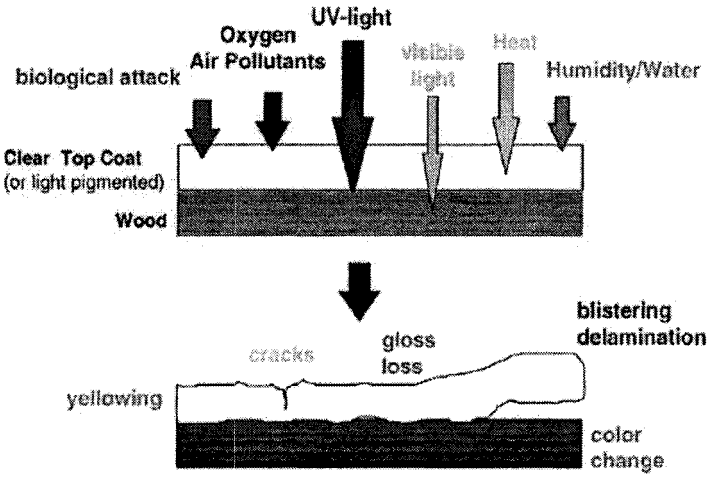

Figure 1.2 Factors influencing wood and coating [6]

1.3. Objectives

The main objective of this doctoral research project is to protect the heat-treated wood in an outdoor environment from mainly two important aging factors, UV light and water. In order to achieve this goal, development of a non-toxic and transparent coating which can prevent the color change for long periods without altering the heat-treated wood's natural color is the most important part. Several specific objectives have been listed below to achieve the main objective of this project:

I. to synthesize and investigate the efficiency of sol-gel coatings alone or together with organic UV absorbers in order to enhance the exterior durability of heat-treated wood,

II. to extract natural antioxidants and investigate their effectiveness alone or together with other organic and inorganic UV stabilizers for photo protection of heat-treated wood,

III. to study different base polymers (soy polymer, acrylic polyurethane) in order to find the best suitable polymer to be mixed with UV protection agents for the protection of heat-treated wood,

IV. to study the affinity of newly developed coatings for different heat-treated wood species, e.g., jack pine, quaking aspen, and white birch,

V. to perform accelerated aging tests with coated and different heat-treated wood species (jack pine, quaking aspen and white birch) to examine the usefulness of the developed coatings during this study and compare their performances with each other as well as with those of the commercially available coatings, and

VI. to study the degradation behavior of the coated heat-treated wood surface and wood-coating interface by carrying out different morphological and compositional studies at different stages of accelerated aging tests.

1.4. Scope

There is no specific information in the literature concerning the protection of heat-treated wood from UV light and water. The majority of the research was carried out with untreated wood. Therefore, the originality of the project lies in the development of protective coatings for heat-treated wood and investigating their protection mechanisms. Since heat-treated wood is a green product, no chemicals are used for the heat treatment. Therefore, the main challenge was the development of a non-toxic natural coating with minimal use of chemicals. Also, this coating should be as transparent as possible because consumers buy the product due to its attractive color. Balance between aesthetics and protection was another challenge for this work as they are usually opposing each other. Highest protection can usually be achieved with opaque and highly pigmented coating whereas transparent coatings keep the natural look of heat-treated wood. For this purpose, the effect of UV stabilizers in different polymer coatings (soy-based and acrylic polyurethane) on the color change of heat-treated wood have been studied on three different North American wood species- jack pine, quaking aspen, and white birch-upon prolonged exposure to accelerated aging.

This thesis consists of five chapters. Detailed literature review is discussed in chapter 2 after a brief background given on wood in this chapter. The experimental materials and

methods are given in chapter 3. Chapter 4, the results and discussions part, consists of six major subdivisions. In the first subdivision, different methods for calculating surface energy of coated heat-treated wood are compared. The development of natural antioxidants and their characterization is the subject of the next subdivision followed by effectiveness of sol-gel derived nano coatings on heat-treated jack pine. In the following two subdivisions, degradation of soy polymer and acrylic polyurethane coated heat-treated surfaces during accelerated aging tests are presented, respectively. This chapter ends with the results of the study on fungal degradation of coated heat-treated surface before and after aging. Finally, in the last chapter, the conclusions and recommendations are given.

Chapter 2

LITERATURE REVIEW

In this chapter, a detailed literature review is presented.

2.1. Wetting, Contact Angle, and Surface Tension

Great attention has been paid to wetting processes in literature on the surface properties of wood and multiphase systems [36]. The wetting behavior is important in order to know the surface properties of wood and also to assess the adhesion of paints or coatings which are used to protect wood from environmental degradation. In literature, the term wetting is defined in many ways. Simply it is what happens when a liquid comes in contact with a solid surface [37]. As reviewed by Stehr and coworkers [38], Berg has defined wetting as "macroscopic manifestations of molecular interactions between liquids and solids in direct contact at the interface between them". For rough and porous materials, such as wood, several wetting phenomena may occur. The term wetting includes (1) the formation of a contact angle, at the solid/liquid/fluid interline, (2) the spreading of liquid over solid surface, and (3) the wicking (penetration) of liquid into the porous solid. The wetting behavior of wood is dependent not only on the chemical composition of wood, but also on the surface roughness of the wood, the density of wood (i.e., early wood or late wood), porosity, heterogeneity, bulk sorption, liquid viscosity, reorientation of the functional

groups at the wood-liquid interface, and influences related to the contamination of the liquid by wood extractives.

The first widely accepted relationship between interfacial tension and contact angle for a liquid drop on a solid surface was expressed by Young's Equation [39] as suggested by Young in 1805 [40]:

$$\Upsilon_{SL} - \Upsilon_{SVo} + \Upsilon_{LV}\cos\theta = 0 \qquad [2.1]$$

where: Υ_{SVo}: Interfacial tension between solid and vapor

Υ_{SL}: Interfacial tension between solid and liquid (also called surface energy)

Υ_{LV}: Interfacial tension between liquid and vapor (also called surface tension)

θ: Contact angle

Later in 1869, Dupré [41] developed an equation for the thermodynamic energy of interaction, which is widely known as work of adhesion, W_A

$$W_A = \Upsilon_{SV} + \Upsilon_{LV} - \Upsilon_{SL} \qquad [2.2]$$

As can be seen from Equation 2.2, the work of adhesion is a simple summation of the energy per unit area involved when a surface is destroyed or created by separating a liquid-solid interface. Combining equations [2.1] and [2.2]:

$$W_A = \Upsilon_{LV}(1 + \cos\theta) \qquad [2.3]$$

This relationship is most commonly known as Young-Dupré equation. The phases are mutually in equilibrium and the designation Υ_{SVo} indicates that the solid surface is in equilibrium with the saturated air. If π^0 is adsorbed film pressure, then

$$\Upsilon_{LV}\cos\theta = \Upsilon_S - \Upsilon_{SL} - \pi^0 \qquad [2.4]$$

where

$$\pi^0 = \gamma_S - \gamma_{SVo} = \frac{RT}{\Sigma}\int_0^{P0} n\, d\ln P \qquad [2.5]$$

where P^0: Vapor pressure of the pure liquid adsorbate

P: Pressure of the adsorbate vapor

$\sum$: Specific surface area

n: Moles adsorbed per gram.

The methods of modifying the wettability of solid surface by the adsorption from a solution of oleo phobic monolayers of oriented polar compounds were reported in the literature. In this case, a drop of liquid placed on the treated sample remained as a discrete droplet and exhibited a finite contact angle. Fox and Zisman in 1950 [42] studied the wetting of such low energy surfaces with a wide variety of liquids which were not good solvents for the monolayers. Later in the 1960 Good and Girifalco [43] proposed a theory for the estimation of surface and interfacial energies as shown below:

$$\gamma_{AB} = \gamma_A + \gamma_B - 2\Phi(\gamma_A\gamma_B)^{1/2} \qquad [2.6]$$

where A, B refer to two phases (solid and liquid), and

Φ: ratio involving the free energies of adhesion and cohesion for two phases.

In the zeroth order approximation, Φ is equal to unity. In the first order approximation for regular interfaces, the value of Φ is given by the equation 2.7 [44]:

$$\Phi = \frac{4(V_A V_B)}{\left(V_A^{\frac{1}{2}} + V_B^{\frac{1}{2}}\right)^2} \qquad [2.7]$$

where V is the molar volume.

When V_A and V_B are not extremely different, the value of Φ is close to unity. A unifying theory was needed which could take the different types of intermolecular forces

between a solid and a liquid into account. Fowkes in 1964 [45] developed a theory to predict the effect of interfacial attraction on the tension of the interface, which could be calculated by the geometric mean of the dispersion force components of the interfacial tensions of the two phases. He assumed that the total free energy at a surface is equal to the sum of contributions from the different intermolecular forces at the surface as shown below:

$$\gamma_{LV} = \gamma_L^d + \gamma_L^p \qquad [2.8]$$

where $\gamma_L{}^d$: Dispersion forces

$\gamma_L{}^p$: Polar forces

Fowkes [45] proposed the following geometric mean relationship for the prediction of intermolecular forces by considering only dispersion forces involved in the interaction of solid-liquid interface:

$$\gamma_{SL} = \gamma_S + \gamma_{LV} - 2\left(\gamma_S^d \gamma_L^d\right)^{1/2} \qquad [2.9]$$

By combining equation [2.1] and [2.9] and assuming $\gamma_S = \gamma_{SVo}$, an expression is derived which is often known as Fowkes's relation:

$$\gamma_{LV}(1 + cos\theta) = 2\left(\gamma_L^d \gamma_S^d\right)^{1/2} \qquad [2.10]$$

In order to determine the non-dispersion forces of attraction, Tamai and co workers have modified Fowkes's equation by including a general term $I_{12}{}^p$ to represent electrostatic, metallic, hydrogen bonding, and dipole-dipole interactions [46]. The modified equation becomes:

$$\gamma_{SL} = \gamma_S + \gamma_{LV} - 2\left(\gamma_S^d \gamma_L^d\right)^{1/2} - I_{SL}^p \qquad [2.11]$$

Owens and Wendent [47] further modified equation [2.11] by introducing the polar force contribution which was presented by the geometric mean of the polar components. Thus the equation [2.11] became

$$\gamma_{LV}(1+\cos\theta) = 2\left(\gamma_S^d\gamma_L^d\right)^{1/2} + 2\left(\gamma_S^p\gamma_L^p\right)^{1/2} \qquad [2.12]$$

where γ_S^p denotes the polar component of surface energy.

The geometric mean relationship was further improvised by using a reciprocal mean or harmonic mean by Wu [48]. He indicated that the harmonic mean model shown below gave better result which was further proved by Nguyen and Jones [46]:

$$\gamma_{SL} = \gamma_S + \gamma_{LV} - \frac{4\gamma_S^d\gamma_L^d}{\gamma_S^d\gamma_L^d} - \frac{4\gamma_S^p\gamma_L^p}{\gamma_S^p\gamma_L^p} \qquad [2.13]$$

This was further innovated considering the Lifshitz-van der Waals and polar interactions by Van Oss and coworkers [49]. The equation [2.14] was developed by taking into account the acid-base components of solids and liquids

$$(1+\cos\theta)\gamma_L = 2\left(\sqrt{\gamma_S^{LW}\gamma_L^{LW}} + \sqrt{\gamma_S^+\gamma_L^-} + \sqrt{\gamma_S^-\gamma_L^+}\right) \qquad [2.14]$$

where γ_L^{LW} : Lifshitz-van der Waals component of solid surface energy

γ_S^+ : Electron donner component of solid surface energy

γ_S^-: Electron acceptor component of solid surface energy

Thus, by contact angle (θ) measurement with three different liquids (of which two must be polar) with known γ_L^{LW}, γ_S^+ and values, γ_S^- using Equation [2.14] three times, the γ_S^{LW}, γ_S^+ and γ_S^- of any solid can be determined.

They had also derived the following equation which can be used in interpretation of contact angle data

$$\gamma = \gamma^{LW} + \gamma^{AB} \qquad [2.15]$$

The polar component of the free energy of cohesion of any compound is given by:

$$\gamma_L^{AB} = 2\sqrt{\gamma_L^+ \gamma_L^-} \qquad [2.16]$$

Based on these theories, a wide range of publications are devoted for the experimental work aimed at understanding the surface chemistry of wood and the adhesion and gluability of different molecular probes, coatings, and resins.

The anatomical wood structures have a complex surface morphology due to the non homogeneity, at the macro-, micro-, as well as sub micro-structural level. The chemical composition of wood is reflected by the free surface energy. The free surface energy of materials is result of unsaturated fields of force belonging to the surfaces of these materials.

The contact angle of a liquid with a solid surface is a convenient measure of wettability; it is an indicator of the affinity of a liquid for a solid [37]. When a liquid does not completely spread on a substrate (usually a solid), a contact angle (θ) is formed, which is geometrically defined as the angle on the liquid side of the tangential line drawn through the three-phase boundary where a liquid, gas and solid intersect, or two immiscible liquids and solid intersect (Figure 2.1). The complete spreading corresponds to a contact angle of 0°.

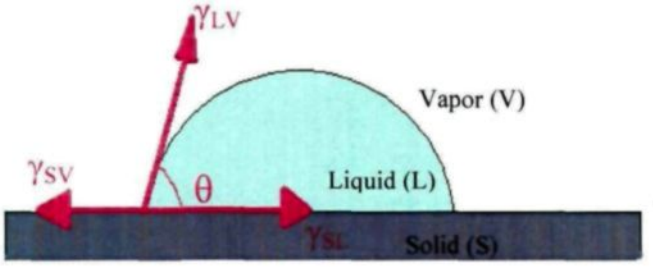

Figure 2.1 Contact angle and interfacial tensions at equilibrium

Contact angle measurements are reported in the literature in several ways.

a) The static sessile drop method - In the static sessile drop method the contact angle of a pure liquid drop on solid substrate is measured by contact angle goniometer, after an equilibrium contact angle is reached.

b) The dynamic sessile drop method – The dynamic sessile drop method is similar to that of static sessile drop method. However, the change of contact angle with time data is measured.

c) Dynamic Wilhelmy method – For dynamic Wilhelmy method, wetting force on the solid substrate is measured by immersing the solid into a liquid or withdrawing it from a liquid of known surface tension. In this case, advancing and receding contact angles are measured.

d) Single-fiber Wilhelmy method – When dynamic Wilhelmy method applied to single fibers to measure advancing and receding contact angles, it is known as Single-fiber Wilhelmy method.

e) Powder contact angle method – This method enables measurement of average contact angle and sorption speed for powders and other porous materials.

When the liquid is put in contact with powder, liquid penetrates through its porous structure. Measuring the weight change with time gives the quantity of liquid penetrated. Then, the contact angle can be calculated from Washburn equation using the measured weight data as given below:

$$T = [\eta / C \,.\, \rho^2 . \gamma \,.\, \cos\theta] \,.\, M^2 \qquad [2.17]$$

The terms are defined as follows:

T = time after contact

η = viscosity of liquid

C = material constant characteristic of solid sample

ρ = density of liquid

γ = surface tension of liquid

θ = contact angle

M = mass of liquid adsorbed on solid

The determination of surface energy of solids is indirect and complicated. One of the first approaches to the characterization of low-energy solid surface was an empirical one developed by Fox and Zisman [42]. They established that a linear relationship often existed between the cosine of the contact angle of several liquids and their surface tension. Zisman introduced the concept of critical surface tension, which represents a value of the surface energy of an actual or hypothetical liquid that just spread on the solid surface (complete wetting), giving a zero contact angle [50]. The meaning of "critical surface tension" is not the surface energy of the solid but only an empirical parameter closely related to this

quantity. However, Zisman [51] reported critical surface tension as even more useful parameter because it is a characteristic of the solid only [52].

A severe contamination of some probe liquids was reported in reference [53] during wetting measurement on non-extracted wood by Wilhelmy method. The contamination was detected as a decrease in the surface tension, which was caused by dissolution or the presence of wood extractives at the wood-liquid interface or at the wood-liquid-air interline. Though Meijer et al. [54] had the same results for probe liquids but they did not found any influence of extractives on the penetration of wood coatings into the surfaces. Direct measurement of a contact angle of liquid on wood is very difficult as wood interacts with many liquids and the contact angle starts changing soon after contact. To overcome this difficulty a direct image analysis method was first used at a forest product laboratory [55] to measure the contact angle and was compared with the result of modified Wilhelmy procedure.

Liptakova and Kudela [36] studied the change of water droplet shape with time on microtomed beech wood and observed a distinct decrease of the apparent contact angle with time. Mantanis and Young [39] measured the thermodynamic work of adhesion, contact angle, wettability, and acid base contribution of the wetting of four North American wood species (Sitka spruce, Douglas fir, sugar maple, quaking aspen) using the Wilhelmy technique. All the wood surfaces had very strong acidic character according to their study whereas Gindl and his co workers [56] found higher basicity component of Norway spruce, larch, beech, and oak. The wetting behavior of sanded wood surfaces was compared with that of the microtomed surfaces of four different wood species (Norway

spruce, larch, beech and oak) by Gindl et al [56]. It was shown that there was a significant influence of the mechanical treatment on the surface energy and all its components whereas differences among wood species were significant only for the total surface energy and its electron donor component. A higher basicity component was also reported for all wood species than the acidity component based on contact angle obtained by the application of the van-Oss et al. [49] approach. Liptakova et al [57] found that type of wood surface treatment as an important factor influencing the wetting process since mechanical treatment of wood surface not only modifies morphology, but also changes chemical composition of surface layer by increasing lignin content of the wood surface. The same observation was also supported by Sinn et al [58]. They investigated the changes in surface properties of wood (Norway spruce and Beech) due to utilization of different grain sizes during sanding, and they found maximum surface energy at the mean grain size. A hypothesis describing tip crack generation during different machining operations on sapwood of pine surfaces and the differences between the pith side and bark side were investigated by Stehr and Ostlund [59]. The wetting dynamics of phenol resorcinol formaldehyde, polyvinyl acetate, and a series of probe liquids on sawed, planed, sanded, and razor blade cut wood surfaces of Southern pine were studied by Stehr et al [38]. The fastest wetting of probe liquids occurred on the sanded surfaces because of the greater surface roughness, resulting increase in capillary forces as compared with the other smoother surfaces. This was in good agreement with the results obtained by Scheikl and Dunky [60]. A similar result was achieved by Hse [61]. He found a lower contact angle on rougher early wood than on the smoother latewood which was also supported by Jinzhen

and Kamdem [62]. But Stehr et al. [38] concluded that a smoother surface improved wetting and penetration properties for high viscosity liquids such as adhesives. It was reported by Scheikl and Dunky [60] that there was no influence of wood moisture content on wetting.

The wettability of four different European heat-treated wood species (pine, spruce, beech, and poplar) was studied by Pétrissans and coworkers [63] and a declination in wettability with the heat treatment was reported which was in good agreement with the results obtained by Hakkou et al [64, 65]. Surface free energies of pine and beech wood were investigated before and after heat treatment using the Lifshitz–van der Waals/acid–base approach by Gerardin et al. [66]. They found that the decrease in electron-donating part of the acid-base component of surface energy was the major parameter affecting the wetting of the modified wood's surface.

A decrease in the total surface energy with surface aging was reported by Sinn and coworkers [58]. Kalnins and Feist [67] suggested that aging of wood increases the wettability by 1) reducing or removing the water repellent effect of extractives; 2) degrading the hydrophobic lignin component of wood; and 3) allowing cellulose to become more abundant on the surface. It is likely that major differences exist between species of wood. The feasibility of UV light exposure for the activation of wood surface to increase the wettability, using radial and tangential surface of two wood species, spruce and teak were assessed by Ginld et al. [68]. At specific UV light, the surface energy, especially that of the base component of wood, increased significantly, i.e., it improved the adhesion properties of wood.

As reviewed by Liptakova and Kudela [69], the surface energy of coating material increased after drying compared to that of the liquid containing state which was due to the increase in their polar shares by keeping the disperse share almost similar. Also during drying, interactions between polar components of surface energy of the adjacent phases increase the work of adhesion between coating material and wood surface. The degree of coating penetration is an important aspect of coating performance, and it highly depends on type of coating, type of formulation used, and anatomical structure of wood. Richter et al. [70] investigated the effect of surface roughness on paint performance and found better paint performance on sanded wood which needed relatively low quantity of paint. Similar results were reported by Moura and Hernadez [71] who have investigated varnish coating performance for two surfacing methods on sugar maple wood. As mentioned by de Meijer et al. [54], coating penetration not only depends on the anatomical structure of wood but also on the ability of the coating to flow through the lumen of ray cells or tracheid. The coating flow through the wood capillaries is influenced by viscosity, surface tension, drying rate of the coating, the ratio of solid to liquid material, presence of pigments, and diameter of wood capillaries [72]. Rijckaert et al. [73] found that penetration of water-borne paints was less than the solvent borne paints which was well supported by the work of de Meijer and his coworkers [54, 74].

Hora [75] introduced a method for determination of lifetime expectation of exterior wood coatings by the use of water uptake rate and the dynamics of a liquid water drop contact angle. It was also reported that for a short measuring time the contact angle was

proportional to the square root of time and the drop spreading took place due to the isotropic diffusion process.

2.2. Aging of Wood

Within the competitive materials such as concrete, metals, and plastics, wood has a distinguished place due to its physical properties and warm appearance. When exposed to solar irradiation, natural wood undergoes photochemical reactions which lead to significant changes in its appearance such as discoloration, loss of gloss and lightness, roughening and checking of surfaces, and destruction of mechanical and physical properties [11, 26, 29]. There have been many studies in the past on the investigation of the mechanism of wood aging, and it has been clearly shown that the absorption of a UV photon can result in formation of a free radical, and that through the action of oxygen and water, forms hydroperoxide. Both the free radical and hydroperoxide can initiate a series of chain scission reactions to degrade the polymeric components of wood [76].

2.2.1. Factors Affecting Wood Aging

The deleterious effect of wood aging has been ascribed to a complex set of reactions induced by a number of factors. The aging factors responsible for changes in wood surfaces are solar radiation (UV, visible, and IR light), moisture (dew, rain, snow, and humidity), temperature, and oxygen. UV portion of the solar radiation and moisture are the most important parameters contributing to wood aging [24]. UV radiation has sufficient energy to chemically degrade wood's structural components (lignin and carbohydrates)

[33, 77, 78]. The short wavelengths of visible portion of sunlight also cause surface changes in wood [11]. These wavelengths do not directly initiate wood degradation; however, they enhance the photochemical reactions once they are already started [79]. Besides sunlight and water, oxygen molecules are among the most ubiquitous in nature [3,10]. They play a unique role in many photophysical and photochemical processes. In addition, there is considerable evidence that many photo-oxidation reactions involve the low-lying singlet states of oxygen as intermediates [28]. Peroxide formation occurs in cellulose and lignin upon photoirradiation in the presence of oxygen. The deterioration of wood surfaces during the aging process may be the consequence of free radical chain reactions, initiated by active immediates generated by the decomposition of photo-induced hydroperoxides [80]. Heat may not be as critical factor as UV light or water, but as the temperature increases, the rate of photochemical and oxidative reactions increase. Freezing and thawing of absorbed water can also contribute to wood checking [11]. Moreover, an additional aging factor, atmospheric pollutants such as sulfur dioxide, nitrogen dioxide, and ozone in the presence or absence of UV light, also affect the wood aging process [3, 11, 28].

2.2.2. Chemistry of Wood Aging

Among the wood components, lignin is a very good UV absorber due to the presence of chromophores with aromatic conjugated bond systems and carbonyl groups in lignin structure [3, 11]. The ultraviolet portion of the sunlight, which penetrates approximately 75μm, is responsible for the primary photochemical process. Lignin contributes 80–95%,

carbohydrates and extractive contributions are 5–20% and 2%, respectively, to the total UV absorption of wood [33, 78, 81]. Photo-oxidation of lignin refers to a process where this polymer undergoes chemical modifications such as bond cleavage, and hydrogen abstraction resulting in radical formation, formation of peroxides with oxygen and finally decomposition with production of colored and hydrophilic by-products, so called chromophores [11, 27, 28]. Four reaction pathways for lignin have been identified by Schaller and Rogez [8]: (*i*) phenoxyl free radical formation due to direct absorption of UV light by conjugated phenolic groups, (*ii*) abstraction of phenolic hydrogen as a result of aromatic carbonyl triplet excitation to produce a ketyl and phenoxyl free radical, (*iii*) cleavage of non phenolic phenacyl-α-Oarylethers to phenacyl phenoxyl free-radical pairs, and (*iv*) abstraction of benzylic hydrogen of the α-guaiacylglycerol-β-arylether group to form ketyl free-radicals which then undergoes cleavage of the β-O-4 arylether bond to produce an enol and phenoxyl free-radical. The enol eventually tautomerizes to a ketone. Alkoxyl and peroxyl free-radicals produced from the reaction of oxygen and lignin free-radicals, react with the phenoxyl free-radicals to produce colored chromophores, e.g., quinoides, aromatic ketones, aldehydes, and acids as photo degradation products [8]. The mechanism behind natural wood aging is well understood and reported in detail in literature. But very few studies were reported on heat-treated wood aging [24, 26, 82]. Nuopponen and his coworkers [26] found that condensed structure of lignin in heat-treated wood prevents leaching of degradation products which eventually results in enrichment of the heat-treated wood surface with aromatic and conjugated carbonyl products compared to the surface of the reference sample enriched mainly with cellulose after aging. Ayadi et al.

[24] reported an increase in phenolic antioxidants during heat-treatment of wood which, according to them, provides better resistance against aging compared to natural wood.

2.3. Stabilization Methods of Wood Aging

In order to extend the durability of wood, different stabilization methods are reported in literature though very few studies are found on heat-treated wood. In this section, these stabilization methods are discussed.

2.3.1. UV Stabilizers

2.3.1.1. Organic UV stabilizers

The organic chemical additives are of two types -UV absorbers (UV-A) and hindered amine light stabilizers (HALS) (Joint Coatings/Forest Products Committee, 2000).

UV absorbers have been used in order to reduce the damaging effects of UV light and conserve the properties of the materials. In order to offer an effective protection against UV irradiation, one of the requirements for the UV absorber molecules is the ability of transforming the absorbed radiation energy into less damaging thermal energy via a photo-physical process [83]. UV absorbers are organic or inorganic compounds which can absorb, in the best cases, all UV light (λ<400mm). They are transparent for all visible light (λ >400mm) and convert the excitation energy entirely into heat. It was demonstrated by Aloui et al. [84] that UV absorbers can improve the durability of wood clear coating systems by inhibiting the formation of cracks.

UV absorbers must possess an efficient mechanism of energy dissipation other than radiation. Absorption of UV light promotes organic molecules from the electronic ground singlet state S0 into an excited electronic state (S1 or higher). There are different ways to dissipate this energy. The most important energy dissipation mode is internal conversion followed by vibronic relaxation. In contrast to the energy of excited electrons, vibrational energy can be dissipated into heat via collisions with the surrounding medium. The electronic excitation of the UV absorber can be transferred into vibrations via an intra-molecular process called internal conversion. The probability for internal conversion is strongly enhanced when the molecule in its excited electronic state can switch between isomeric structures such as by cis/trans-isomerization or by intra-molecular H-transfer. UV radiation is absorbed and this leads to the excited state S1. Within a very short time, in the order of 10–12 seconds, isomerization takes place. During this short time span no other chemical reactions can be triggered. After the energy is dissipated vibronically, isomerization takes place back to the original ground state S0. This isomerization is also referred to as photo-tautomerism. The structural elements involved are indicated in the Figure 2.2.

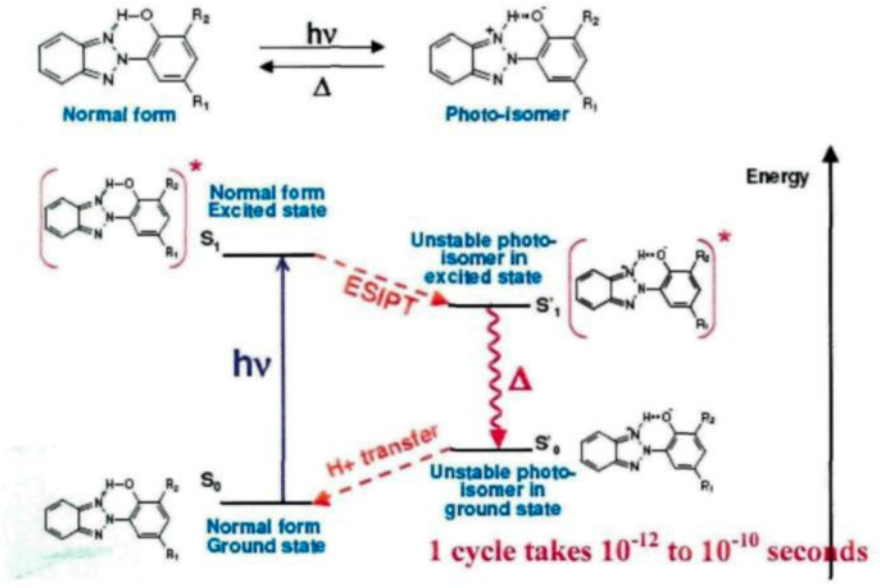

Figure 2.2 Mechanism of dissipation of energy for an UV absorber with an intra-molecular hydrogen bond (webinar ATLAS, 2008)

Light stabilizers are also used to prevent the effect of UV irradiation on color and other properties of materials. A particularly important consideration in the selection of light stabilizers for wood or plastic materials is the permanence of the stabilizer itself, especially under higher intensities of UV-B irradiation. Conceptually, the light stabilizer is slowly depleted on exposure either due to slow leaching out of the organic material or due to photochemical breakdown by UV-B [85].

HALS does not absorb UV radiation, but act to inhibit degradation of the polymer. They slow down the photochemically initiated degradation reactions. Because of the regenerative nature of this radical scavenging process, HALS plays an important role in preventing wood degradation (Figure 2.3).

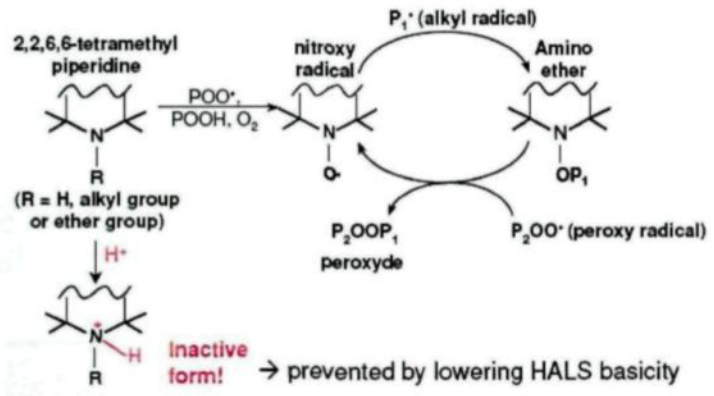

Figure 2.3 Mechanism of HALS action in removing free radicals from photodegrading materials (Webinar, Atlas, 2008)

The susceptibility of clear coating agents to photodegradation and loss of cohesion between coating agents and wood surfaces are generally recognized as the serious limitations for utilization of light stabilizers. Therefore, coating agents with high stability against UV light and a capacity to screen UV light are prerequisites for protection against photodegradation [29]. To enhance the durability of protective coatings, light stabilizer must be effective over a long period of time and must, therefore, not degrade, evaporate from the matrix, be leached out by solvents or removed in any other way from the material [8, 86]. Furthermore, the additive must be uniformly distributed, which requires its compatibility with the polymer. The chemical fixation of light stabilizers can be achieved at various stages and, therefore, the light stabilizers can be classified as [85]

- Light stabilizers which are incorporated during the resin manufacture;
- Light stabilizers which are fixed in post polymerization reactions;
- Light stabilizers, which are fixed during the cross-linking and hardening stage; and

- Light stabilizers, which photo-reacts with the polymer.

Hon et al., have developed a clear acrylic coating containing an internal UV light absorber 2,4-dihydroxybenzophenon in view of need for a stable transparent coating of wood [29]. According to their study, poly(HMHBP) and its co polymers proved to be good protective agents, and the combination of BHT with poly(HMHBP) offered enhanced protection against photodegradation [29].

Decker and Zahouily in 1998 [87] showed that grafting of UV absorbers prior to the coating application on polymeric materials increase the light stabilization of these polymeric materials without affecting the adhesion properties of the coatings. The grafting of UV absorber on wood prior to the clear finish application was studied by Kiguchi et al, [88]. According to their study, grafting of HEPBP is effective in restricting loss of mass and tensile strength of all the wood species during natural aging for fifty days. Grafting of HEPBP significantly improves the performance of clear finishes on wood during artificial aging. They have also grafted new triazine type UV absorber but it results in greater discoloration compared to HEPBP grafted veneers. They concluded that as a commercial pre-treatment method intended to improve the performance of clear finishes on wood, grafting is unsuitable for DYI market. However, it can be conceivably used as an industrial pretreatment method if cost of grafting can be reduced significantly [88].

In 2002, Liu et al. [89] synthesized four monomeric hindered piperidinol derivatives which showed better photo-stabilization characteristics compared to Tinuvin 700 and Tinuvin 292 in UV curable epoxy acrylate coating.

Sundell and Sundholm [90] synthesized polyester binders for wood and found benzotriazole derived UVA as the most effective light stabilizer.

Hayoz et al. [6] developed new UV screeners which had a more pronounced red shift in their absorption spectra than previously used benzophenones and benzotrialzoles since not only UV light but also some portion of visible light affect the photodegradation of wood. In their study, they have shown that effective wood substrate color protection increased with the use of more photo-stable and more red-shift UV screeners. In addition, a hindered amine nitroxyl light stabilizer has been found to provide significant improvement in color stabilization when used in impregnating pre-treatments with subsequent application of a clear topcoat including UV-screener. They have achieved almost total protection against discoloration though their experiments were mainly focused on indoor application [6].

According to Zayat et al, [91] the matrix in which the organic UV absorber embedded was the main factor affecting the stability of the molecule. Basic and polar matrices are capable of forming intermolecular hydrogen bond with the acid phenolic hydroxyl groups, disrupting the intra-molecular H-bonds, therefore, preventing the excited state intra-molecular proton transfer (ESIPT) mechanism to take place.

Schaller and Rogez [9] reported that UV and visible light up to 500nm can cause lignin degradation with chromophore formation and discoloration of pine wood. This means that pale wood species cannot be properly protected by the single use of organic UVA. For this reason, they introduced the utilization of lignin stabilizer which could act as VIS light screeners and were shown to provide improvements in reducing photo-degradation effect

[9]. They, in a later study, reported that HPTs act as effective UVA for most application areas such as automotive, wood, and powder clear coatings [34].

2.3.1.2. Inorganic UV stabilizers

Numerous studies were devoted to the different wood pretreatments methods in the late 80s or early 90s. Among them chromium trioxide stabilized lignin most effectively by forming photo stable lignin complexes which protected wood significantly against aging [27]. But pre-treatment of wood with chromium oxide resulted in unwanted brown coloration initially which turned to green upon natural aging. Also, high toxicity of chromium compounds limited their use as wood pre-treatment agent for photo-stabilization of clear coatings.

Tshabala and her coworkers [12, 92] and Mahlberg et al. [93] studied the aging behavior of wood surface coated with multifunctional alkoxysilanes by sol-gel deposition. They found very little color change of the sol-gel coated wood surfaces after accelerated aging which was directly related to the weight loss of those specimens. The coating derived by Tshabala et al. [12, 92] was not only resistant to water leaching, but also improved the leaching stability of endogeneous wood coloring components and mitigate discoloration of wood which was well supported by the work of Donath et al. [94]. In a later study during the same year [95], they reported that sol-gel deposit on the wood substrates lowered the rates of water and water vapor sorption. They also indicated that the sol-gel process resulted in deposition of polysiloxane networks that were bonded to the wood by polycondensation with surface hydroxyl groups derived mainly from cellulose [95]. In

2005, Tshabala [96] studied the characteristics of wood specimens coated with sol-gel deposited aluminum isopropoxide, titanium isopropoxide, or zirconium propoxide in the presence of methytrimethoxysilane. Both zirconium propoxide and titanium isopropoxide sol-gel deposits reduced water sorption whereas aluminum isopropoxide sol-gel deposit increased water sorption compared to water sorption of uncoated wood specimens. He also concluded that these sol-gel deposits promoted a degradation pathway by affecting both light penetration and permeation rate of oxygen to those wood surface components that were susceptible to photo oxidation.

Thin radiata pine veneers were treated with a range of titanium, zirconium, and manganese compounds and exposed to natural aging. The results revealed the low efficiency of titanates and zirconates in protecting lignin degradation [97].

In 2003, Kundu and Mukherjee [98] derived highly efficient UV absorbing transparent sol-gel coatings on glass and found CeO_2 to be more effective compared to PbO in TiO_2 sol for UV absorption. Cui et al. [99] synthesized TiO_2-CeO_2-SiO_2 coatings by combining UV absorption and optical properties of CeO_2 and amorphous TiO_2 with enhanced UV protective characteristics. They also concluded that low temperature processing ($\leq$100 °C) enabled its use for the protection of inorganic substrates as well as organic materials.

Aloui and his coworkers [100] investigated inorganic iron oxides for the photostabilization of wood clear coating systems and compared the results with that of organic UV absorbers. They found that organic UV absorbers were more efficient compared to inorganic iron oxides which tended to increase the glass transition temperature during aging and, consequently, decreased the flexibility of the films.

Inorganic UV absorbers have been used since long time. Silica, titania, and zinc oxide are the most commonly used inorganic UV absorbers [100-102]. On the other hand, numerous studies are directed their research towards the ceria containing materials due to their wide ranges of applications in solid oxide fuel cells (SOFCs), catalysis, luminescent materials, gas sensors, polishing materials, and ferromagnetic oxides and so on [103-107]. Cerium oxide has almost the same band gap as that of titania (3.0-3.2eV) and shares the same classical UV absorption mechanism. Under UV light, both cerium oxide and titania molecules get excited by absorbing a photon which creates an electron-hole pair.

In case of titania, these electron hole pairs migrate to the surface of the particles and eventually react with oxygen, water or hydroxyls to form free radicals. This process is known as photocatalysis and thus titania particles are not able to prevent the aging of wood. On the contrary, cerium oxides are photocatalytically inactive in nature. The electron-hole pair formation is much lower than that of the titanium oxide due to the presence of higher localized electron in cerium oxide (4f orbital in case of cerium oxide in comparison to 3d orbital for titanium oxide) which leads to more ionic cerium-oxygen bonding. In addition, the electron-hole pair recombines very fast before it can migrate to the particle surface because of the crystal defects and oxido-reduction reaction. Also, cerium oxide has a lower refractive index than that of titanium oxide and is rather transparent to visible light compared to titanium oxide and zinc oxide. Therefore, it seems that it is advantageous to use CeO_2 as UV absorber in coating material; however, it's very high catalytic activity [103] constitutes a major drawback.

In a very recent study, Blanchard and Blanchet [108] compared the effects of inorganic UV absorbers (CeO_2 and ZnO) with the organic UV absorbers for the wood color stabilization in indoor conditions by incorporating them with polyurethane/polyacrylate coating. They reported higher efficiency of these nano particles at medium light exposure whereas highest protection was reported for combination of organic and inorganic materials.

2.3.1.3. Combinations of Organic and Inorganic UV Stabilizers

None of organic or inorganic UV stabilizers can provide 100% UV protection. For this reason, numerous researchers studied towards combined effect of organic and inorganic UV stabilizers.

Improvement of the photo stability using benzophenon(BP)–SiO_2 composites was reported by Miyafuji et al. [109]. This combination prevented discoloration and cell structure degradation of wood better compared to SiO_2 composites. It was also emphasized that this high photo stability of the BP–SiO_2 wood–inorganic composites would be sustainable for a long period because BP was stable against UV light. Mahltig and his coworkers [35] investigated the UV protecting coatings of silica and titania sols in combination with organic UV absorbers, and test results revealed an increase in UV absorption capacity of titania coatings when combined with organic UV absorbers. In 2006, Parejo et al. [83] developed highly efficient UV absorbing sol-gel derived ormosil coating in combination with benzophenon which was successfully applied by Zayat et al. [91] for preventing UV light damage of light sensitive materials.

2.3.1.4. Natural Antioxidants

2.3.1.4.1. Bark Extracts

In recent years, bark has moved increasingly into the centre of interest. Numerous studies on its structure and composition as well as its utilization in different fields are performed [110]. Bark is a highly complex, heterogeneous material composed mainly of a thin, physiologically active inner layer and a relatively inert outer layer whose principal functions are to protect the cambium and to prevent the loss of water. The chemical composition of bark, which differs from wood by its high polyphenols content, determines the properties which are important in view of its utilization. Barks have a different swelling behavior than wood, are less anisotropic, possess slightly lower heat transfer coefficients, and have much weaker mechanical properties compared to wood [110]. However, barks of several tree species are known to contain bioactive chemicals that can add value to this energy resource [111]. The chemicals that give wood its color are extractives: organic compounds of various types that may contain halogens, sulphur, and nitrogen [112]. Extractives are natural products extraneous to a lignocellulose cell wall; though these compounds contribute only a few percent to the total wood mass, they have significant influence in defining some of the properties of wood [33]. They can be removed with inert solvents such as ether, benzene, alcohol, acetone, and water. Natural phenolic compounds have recently received much attention due to their antioxidant properties. It is a growing tendency that natural antioxidant compounds to be used to replace synthetic antioxidants

which are carcinogenic in nature [113]. One of nature's most readily available and most valuable sources of phenolic antioxidants are present in wood, especially in wood knots and barks of several tree species [114, 115]. The major phenolic compounds in plants include flavonoids, phenolic acids, stilbenes, proanthocyanidins, tannins, lignans, and lignin. It is the redox properties of these compounds that accounts for the antioxidant behavior, for example they act as reducing agents, hydrogen donors, and singlet oxygen quenchers. Plant antioxidants also act as peroxide decomposers and enzyme inhibitors [116, 117]. Natural antioxidants can be classified as primary (chain-breaking) antioxidants, which can react directly with lipid radicals and convert them into stable products, or as secondary (preventive) antioxidants, which can lower the rate of oxidation by different mechanisms. Primary antioxidants most often act by donating a hydrogen atom, while secondary antioxidants may act by binding with metal ions which enables them to catalyze oxidative processes by scavenging oxygen, by absorbing UV radiation, by inhibiting enzymes or by decomposing hydroperoxides. The free radical scavenging effect of phenolic compounds has mostly been ascribed to the ability of the compound to donate a phenolic hydrogen radical to the free radical. In turn, the phenolic compound forms a stabilized phenoxyl radical while the free radical is scavenged. This reversible radical trapping stage, which is highly dependent on the molecular structure of the phenolic compound and the bond dissociation energy of the phenolic O–H bond, is followed by a termination stage. In the second stage, the generated phenoxyl radical combines with another radical species to produce stable termination products. The self-redox reaction (disproportionation) of the phenolics should also be considered as an alternative

termination stage. Structural identification of these termination products, as well as kinetic studies of the radical reactions, may give an insight into the antioxidant mechanisms involved at the molecular level. Different lignans have different radical–scavenging activity. The activity can be related to some structural features which makes the tailoring of specific lignan based antioxidants possible. The lignans can scavenge numerous equivalents of free radical [114]. In *Picea mariana*, the total amount of lignans is small in stemwood (less than 0.2% w/w). The knots contained 20-30 times more lignans than the corresponding stemwood [118]. The total amount of lignans in the knots ranged from 1% to 5% (w/w). The identified lignans are the same as in *P. abies* and *P. glauca* with the exception that no α-conidendric acid is detected. In addition to the lignans and oligolignans, all samples of *P. mariana* contained small amounts of 1,3-(bis-guaiacyl)-1,2-propandiol. These same two lignin-like isomers are earlier found also in *P.abies*. The lignans in all spruce species occurred only as free aglycone and no lignan glycosides are detected. Small amounts of flavonoids are present in most samples *P. mariana. P.glauca, P. omorika, P. sitchensis*, and *P. pungens. P. sitchensis*, whose knots also contained the smallest amounts of lignan of all spruces, contained up to five different flavonoids in some samples [118]. The extracts of *Picea glauca* and *Picea mariana* possess similar antioxidant activities, using both assays. The total phenol content of these extracts is also relatively high with concentration ranging from 36g to 59g/100g. Bark of boreal forest conifers is relatively non toxic, rich in phenol, and posses a strong antioxidant activity. The best phenolic extraction yields as well as antioxidant activities with both assays are obtained with *Picea glauca* and *Picea mariana* [119]. Lignans are biologically active polyphenolic

compounds which are defined by the β–β linkage between two phenylpropane units or between their biogenetic equivalents. These compounds are found in the plant kingdom in various structures with different degrees of oxidation of the side chain or with differences in the aromatic substitution pattern [114]. Bark extract of *Picea abies* has the strongest antioxidant potency in the lipid peroxidation tests of the bark extracts. *Picea abies* bark extract contains stilbenes and stilbene glycosides that are known for their potency to inhibit lipid peroxidation. Most lignans are powerful antioxidants with effects as strong as or even stronger than most flavonoids. However, the flavonoid melacacidin possessed the largest trapping capacity of the polyphenols studied by Chou et al. [120]. Results obtained by Nzokou and Kamdem [77] suggested that the presence of extractives slows down this process with polyphenolic water extractives acting as antioxidant protecting the wood surface against photodegradation. It was shown that the rate of whitening and the total discoloration rate of wood specimens are significantly affected by the removal of water extractable compounds from wood [121]. Schultz and Nicholas [122] have found that extractives have very poor fungicidal activities compared to commercial biocides although they have concluded that extractives may protect heartwood against fungicidal activities by their excellent free radical scavenging effect. However, according to Pandey [33], wood species rich in extractives became bleached before the browning happened to be observable.

2.3.1.4.2. Leaf Extracts

Phenolic compounds are commonly found in both edible and nonedible plants. They have been reported to have multiple biological effects including antioxidant activity [115]. Crude extract of leaves, fruits, vegetables are rich in phenolic compounds. Flavonoids are a group of polyphenolic compounds broadly distributed as secondary metabolites in the plant kingdom and represent one of the most important and interesting classes of biologically active compounds [123]. They generally occur as glycosylated derivates in plants although conjugations with inorganic sulphate or organic acid as well as malonylation are also known [124]. The crude extract of leaves contain chlorophylls and their derivatives. The chlorophylls are a group of tetrapyrrolic pigments with common structural elements and functions [125].

Antioxidant Activity of Crude Leaves Extract

Kähakönen et al [115] have reported in their study that tree material extracts have overall good antioxidant activities. The inhibition of conjugated diene hydroperoxides of most active tree extracts (>90% inhibition) decreased in following order: spruce needle > willow leaf) willow bark > silverwillow bark > pine cork > silver birch phloem > pine bark. The inhibition of MeLo-conjugated diene hydroperoxides of most active plant extracts (>90% inhibition) decreased in following order: bog-rosemary > thyme > cloudberry leaf > heather > bulrush stalk. Caraway, flax, and rose seed extracts had only moderate or weak activity (<48% inhibition). All examined tree extracts, excluding birch bark (18%) and pine cork (48%), have antioxidant activity of over 80%. The inhibition

decreased in the following order: silverwillow bark > maple leaf > willow leaf > pine bark > silver birch phloem > willow bark > white birch leaf > aspen leaf > silver birch leaf > silverwillow leaf. The spruce and pine needle extracts are as active as leaf extracts with 98 and 95% inhibitions, respectively. Several flavonoids have been isolated from the needles of Scotch pine and Norway spruce. The flavan-3-ols (+)-catechin and (+)-gallocatechin have been found in both conifer needles. In addition, dimeric and trimeric proanthocyanidins have been reported in pine needles. Dilignols and their glycosides were found in both pine and spruce needles [115]. In another study by Aquino et al. [126] *in vitro* and *in vivo* findings demonstrated that the ethanolic extract of *C. reflexum* leaves (ECR extract) possesses a strong antioxidant/free radical scavenging effectiveness, which is probably due to the presence of phenolic compounds. Furthermore, this polar extract gave excellent photoprotection against UV-B induced skin damage; thus its use could have important therapeutic applications in certain skin diseases caused, initiated or exacerbated by ROS and free radical overproduction. UV-A absorbing capacity of whole leaf methanolic extracts, at least for certain plant species or genera, could be a useful indicator of the ability of abaxial or adaxial epidermis to screening out the UV-A component of the spectrum since a tight link between UV-A related compounds accumulation and UV-A attenuation has been established (at least for abaxial epidermis) [127]. Spectra of NaOH-extracted pigments from UV-B-exposed plants showed a decrease in absorption in the visible region and an increase in the UV region: the former a consequence of the loss of chlorophyll, the latter is probably due to induced synthesis of protective pigments. The

decrease in chlorophyll absorption is an earlier event than the increase in UV absorption [128].

2.3.2. Coatings

2.3.2.1. Soy polymer coatings

Soybeans have a rich history of industrial use, ranging from ancient times when the versatile soybean is used in water-proofing, caulking, mechanical lubrication, leather tanning, soap and fertilizer manufacturing. Soybeans are also utilized to provide lubricants, fuels, coatings, cosmetics, and pharmaceuticals. Soybeans also have a long history of utilization as a protein foodstuff in the orient [129]. Several hundred industrial products made from soybeans are developed in the 1930's and 40's ranging from textile fibers to fire extinguishing foams [130]. However, soy-based products have a number of problems. Moisture absorption properties of soy proteins led to problems with microbial growth and adhesion stability in soy-based glues and plastics. Soy protein is used as adhesive before 1930s, but later it is replaced by petroleum based adhesives due to their greater availability, less complicated chemistry and better product stability, higher gluing strength and better water resistance, and also lower cost [131, 132]. In the late 1980's, interest in environmental balance, product degradability, reduction of hazardous wastes/processing and use of renewable resources has rejuvenated interest in soybean and other plant-based products utilization. New Century Coatings (NCC) has developed a line of soy methyl ester stains, sealers and architectural paints with excellent performance properties. These

stains are user-friendly with deep penetration which extends the life of many different substrates [133]. The stain forms primarily due to the reaction of strong alkali in soybean coating with wood [134]. In the present study, development of a soy based wood coating which can protect wood from UV radiation, consequently, prevents the color change of heat-treated wood is attempted.

2.3.2.2. Acrylic polyurethane coatings

Aliphatic urethane acrylates are one of the most expensive class of materials for coatings industry, but their excellent weather resistance make them an important class of binders for outdoor applications [135].

Masson and his coworkers [136] carried out a kinetic study of the drying and UV-curing of water based urethane-acrylate formulation by means of infrared spectroscopy to quantify the influence of moisture. They found that the softening of water based polyurethane acrylates was directly related to the polar group contents of the polymer due to their high sensitivity towards humidity. But this phenomenon was fully reversible and had no effect on their long term stability. Decker et al. [137] developed a dual cure technique for curing of shadow areas of polyurethane acrylates and compared their light stabilization characteristics with UV cured polyurethane acrylates. Pardini and Amalvy [138] synthesized polyurethane/acrylic hybrids and their characterizations were also presented. Aznar and his coworkers [139] developed glossy topcoat using polyurethane/acrylic hybrid binders which had better optical properties compared to pure acrylic based paints after aging. Ahn et al. [140] modified UV curable polyurethane

dispersions by incorporating multifunctional extender which showed very good mechanical properties and enhanced solvent resistance, and lowered water swell. Tielemans and Blues [141] developed radiation curable polyurethane dispersions for exterior wood applications. They found that use of polycarbonate backbone eventually increased aging resistance of those coatings. The degradation of coated wood prior to the coated neutral substance suggested a modification of coating barrier properties before the destruction of the coating. In a very recent study by Sow and his coworkers [142], the effect of alumina and silica nano particles on mechanical, optical and thermal properties of UV-waterborne nano composite coatings was reported. A poor dispersion of nano particles in UV cured coatings was the main drawback which affected the hardness of the nano composite coatings, but scratch resistance increased significantly, especially with nano silica. The photostability of these nano composite coatings were not published because it was intended to use those coatings for interior applications.

A wide range of studies [143-148] are reported in literature on the photo-oxidation and degradation of acrylic polyurethane coatings. These gave an insight on the chemical and structural modification of these coatings during aging but all of them not necessarily applied to wood.

Although a number of publications are available in literature on the degradation behavior of natural wood coated with different coatings [30, 149-155] only two publications are found on aging behavior of coated heat-treated wood [156, 157]. However, this work seems to be very limited as they only examined few commercially available coatings on

heat-treated wood. Authors did not suggest any improvement to the coatings so that they can be applied to heat-treated wood.

Present work mainly was focused on the development of transparent and non toxic coatings using natural components and minimum amount of chemicals for heat-treated wood which is an eco-friendly product. In general, commercially available coatings are highly pigmented covering the natural texture and look of heat-treated wood. Also, they are mostly toxic and are produced from non renewable petroleum products which have adverse effects on environment as well as human health. Due to the ever increasing environmental legislations which are becoming more stringent with time, development of non toxic environment friendly coatings is very important for heat-treated wood.

Chapter 3

EXPERIMENTAL

The experimental section consists of several subsections. In Section 3.1, the wood sample preparation for accelerated aging test and all other tests are described. In the next two sections (3.2 and 3.3), preparation of different natural extracts (leaf extract, bark extract, and nano organosolv lignin) which have high antioxidant activity are illustrated. These extracts can be added to different base polymers to increase their effectiveness in protecting wood against photodegradation. Since the main aim of this work was to prepare a transparent and non toxic coating, the toxicity of these natural antioxidants are very important. The detailed analyses of cytotoxicity of these natural products are described in Section 3.4. The antioxidant activity measurement technique of these natural antioxidants is reported in the following section (Section 3.5). The subsequent section (Section 3.6) consists of the description of thin layer chromatographic measurement of these natural antioxidants used for evaluating the presence of different phenolic and terpenoid groups. Section 3.7 illustrates the descriptions of three different base polymer coatings. The sol-gel derived coating, soy based polymer coating and acrylic polyurethane coating preparation were explained in detail. Different additives used to improve UV protection characteristics of the acrylic polyurethane coating are summarized in Table 3.1.

The concentration of sol-gel coatings were optimized by transmission tests and details are described in Section 3.8 followed by details of accelerated aging tests given in Section 3.9. The accelerated aging tests were carried out to measure the effectiveness of coatings in protecting different heat-treated wood surfaces from aging as a result of sunlight exposure. These tests facilitates the study of wood aging in shorter time compared to the time of exposure required under natural sun light in order for wood to age to same degree. The surface characterization of coated heat-treated wood surfaces before and after aging is the subject of Section 3.10. The contact angle tests of different coatings and heat-treated wood were carried out to evaluate the wetting behavior of the coatings. In addition, the contact angle between water and coated heat-treated wood samples before and after aging were measured to have an indication of water penetration through the coatings which might be correlated with coating degradation during aging. The color change of the coated heat-treated surfaces were measured before and after aging to evaluate efficiencies of different coatings on heat-treated wood which was then confirmed with visual evaluation. The chemical modifications of coatings during accelerated aging tests were evaluated by ATR-FTIR analyses and XPS analyses whereas the degradations at wood-coating interface were monitored by Fluorescence microscopy analyses and SEM analyses.

The fungal durability of these coatings before and after aging was carried out by two different fungi. This was very important because the accelerated aging chamber can simulate the sunlight and rain, but fungi attack cannot be carried out simultaneously in accelerated aging chamber. Therefore, this test gives an insight against fungal attack on

coated-heat-treated surface before and after aging. The methodology of fungal durability tests is presented in Section 3.11.

3.1. Wood Sample Preparation

3.1.1. Heat Treatment

White birch and quaking aspen wood boards with dimensions of 0.015 m × 0.045 m × 2.44 m were obtained from a local sawmill in Saguenay-Lac-St-Jean (Quebec, Canada). They were pre-dried in air until the moisture content was reduced to 5-17 %. The heat treatment of white birch and quaking aspen was carried out in a prototype furnace of UQAC at Chicoutimi (Quebec, Canada). Heat-treatment was carried out at the maximum temperatures of 210°C and 205°C, respectively, for aspen and birch. The boards were heated to maximum temperature with a heating rate of 15°C/h in a humid and inert gas, and were kept at that temperature for one hour. A detailed description of the thermal modification process is published elsewhere [20]. Heat-treated jack pine thermo wood (210°C) was obtained from Industries ISA, Normandin, Quebec.

The heat-treated wooden boards were then planed followed by sawing. The wood samples for different tests were chosen carefully from the lot without any visible defects or cracks.

3.2. Natural Antioxidant Preparation

In this study, three conifer bark specimens (jack pine, black spruce and balsam fir) were used. The stem of the trees were collected from Lac Simoncouche area of Saguney-Lac-St-Jean region of Quebec. The barks were removed from the tree stem and dried for 3-4 days in an oven at < 50°C. The dried barks were crushed in a grinder with a definite size sieve so that the crushed bark particles had almost uniform dimensions. Barks of 700 g for each species were extracted with methanol-water solutions: [100:0], [80:20], [70:30], respectively. All extractions were performed for 1.5h at 40°C. The extracts were pooled, filtered, and dried under vacuum at 40°C (Figure 3.1).

The branches with needles (jack pine) were collected from Lac Simoncouche area of Saguenay-Lac-St-Jean region of Quebec. Needles were separated from the branches of the trees and washed properly to remove any dirt. The needles were dried at room temperature to remove extra water. The extraction of needles (Figure 3.1) was done with two solvent mixtures: methanol-water: [100:0] and [80:20]. The extracts were then filtered, pooled, and dried under vacuum. The yield was evaluated based on the amount of dry plant material used for extraction.

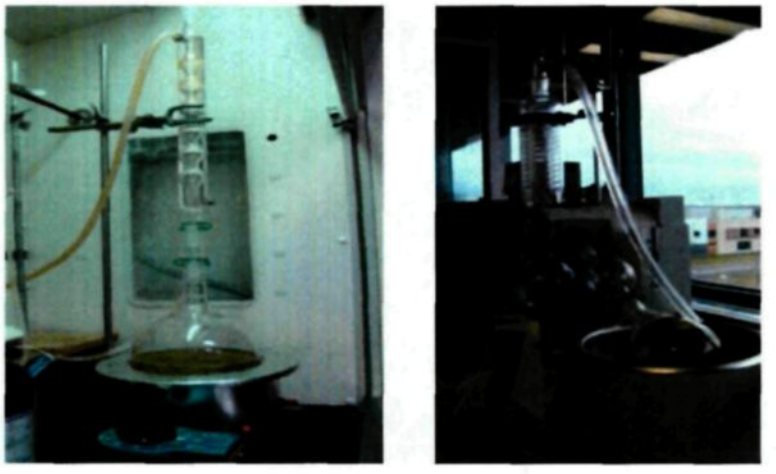

Figure 3.1 Extraction set-up and vacuum rotary evaporator

3.3. Nano-Lignin Synthesis

Powdered organosolv lignin samples of lodge pole pine treated at different temperatures (165°C, 175°C, and 185°C) and one sample of poplar treated at 185°C were received from NSERC Bioconversion Network. The lignin samples were then hydrated overnight mixing by mechanical stirrer and by forming vortex (1 wt% mixture). The samples were then passed through microfluidizer equipped with size sieves (200μ alone-5passes, followed by 200μ and 100μ sieve in series-1 pass followed by 110μ and 87μ sieves in series-maximum 15passes) to prepare nano lignin. The size of the nano particles were detected by zeta plus particle size analyzer and also by scanning electron microscope. Also ATR-FTIR analyses were done to identify the functional groups present in the samples. All these analyses were done at the laboratory of Forest Products Units of AITF, Edmonton, and the SEM analyses were done at University of Alberta, Edmonton.

3.4. Toxicity Test

3.4.1. Cell Culture

Skin fibroblast WS1 (#CRL-1502) cell lines were obtained from the American Type Culture Collection (ATCC, Manassas, USA). Cells line was grown in minimum essential medium containing Earle's salts (Mediatech Cellgro, Herndon, USA), supplemented with 10% fetal calf serum (Hyclone, Logan, USA), 1×solution of vitamins, 1×sodium pyruvate, 1×nonessential amino acids, 100 IU of penicillin and 100 lgmL^{-1} of streptomycin (Mediatech Cellgro). Cells were cultured at 37 °C in a humidified atmosphere containing 5% CO_2.

3.4.2. Cytotoxicity Assay

Exponentially growing cells were plated at a density of 5×10^3 cells per well in 96-well microplates (BD Falcon) in 100 μL of culture medium and were allowed to adhere for 16 h before treatment. Then, the cells were incubated for 48 h in the presence or absence of 100 μL of extracts with increasing concentrations. Fraction of extracts were dissolved in culture medium and DMSO (Dimethyl sulfoxide). The final concentration of DMSO in the culture medium was maintained at 0.25% (v/v) to avoid toxicity. Cytotoxicity was assessed using the Resazurin reduction test and Hoechst test. Fluorescence was measured with an automated 96-well Fluoroskan Ascent Fl™ plate reader (Labsystems) using an excitation wavelength of 530 nm and an emission wavelength of 590 nm. Cytotoxicity was expressed as the concentration of drug inhibiting cell growth by 50% (IC50).

3.5. Oxygen Radical Absorption Capacity

The ORAC (oxygen radical absorption capacity) assay was carried out in 348-well microplates (Costar) on a Fluoroskan Ascent FL^{TM} plate reader (Labsystems) equipped with an automated injector. A gradient of 16 concentrations of the samples was prepared with triplicate. The experiment was conducted at 37.5°C and in pH 7.4 phosphate buffer with a blank sample in parallel. The fluorimeter was programmed to record the fluorescence (λ ex.: 485 nm/em.: 530 nm) of fluorescein every minute after addition of 375 mM 2,2'-azobis(2-amidinopropane) dihydrochloride (AAPH) for a total of 35 min. The final results were calculated using the net area under the curves of the sample concentrations for which a decrease of at least 95% of fluorescence was observed at 35 min and which also presented a linear dose–response pattern (approximately 4-8 concentrations). ORAC values were expressed in micromoles of Trolox equivalents (TE) per miligram (μmol TE/mg).

3.6. Thin Layer Chromatography (TLC)

3.6.1. Sample Preparation

10 mg of extracts were dissolved in 1ml of methanol using ultrasonic bath until complete dissolution. 25μL of the test solution was deposed on silica gel plates (Thin layer chromatography ultrapure silica gel plates, Silicycle). The plates were eluted in the solvent system: chloroform: methanol: water (26:14:3) (vol%), dried, developed and evaluated

under visible and UV (365nm and 254nm) lights (Chromato VUE - Ultraviolet products inc, San Gabriel, CA, USA).

3.6.2. TLC Evaluation of Terpenes

In order to analyze terpenoid compounds, the TLC plates after migration, were sprayed with H_2SO_4 20% in methanol and were heated in oven at 105-110°C for 3-5 minutes. The terpenes were colored in red-violate.

3.6.3. TLC Evaluation of Polyphenols

For polyphenol identification, the plates were sprayed by 1% methanolic diphenylboric acid-β-ethylamino ester (=diphenylbryloxyethylamine) (NP), followed by 5% ethanolic polyethyleneglycol-4000 (PEG). After heating for 1 min at 105-110°C in oven, the plates were evaluated under UV (365nm). The different phenolic compounds were identified with blue, green and yellow colors.

3.6.4. R_f Calculation

The retention factor (R_f) is defined as the distance traveled by the compound divided by the distance traveled by the solvent.

Each component present in the conifer bark or needle extract has their own distinct R_f value for a particular TLC condition. The R_f can provide an evidence as to the identity of a compound which should further be confirmed by adding a standard (co-spot).

3.7. Preparation of Coatings

3.7.1. Sol-Gel Coating Preparation

The inorganic TiO_2 sol was prepared by hydrolysis of equal volume of titanium butoxide ($Ti(OC_3H_7)_4$ obtained from Sigma Aldrich) and pure ethanol (100%) at room temperature by stirring for 15 minutes followed by 72 hours of aging. Different concentrations of sol were prepared by diluting it with pure ethanol (for 5ml concentrated sol 10-25ml pure ethanol). The final coatings were prepared by dissolving Tinuvin5236 and lignostab1198 in diluted sols (0.5-15 wt% tinuvin5236 and 0.1-2 wt% lignostab1198).

3.7.2. Soy Polymer Coating Development

0.9g of NaOH was added to 67.5ml of water to make the solution alkaline as the maximum solubility of soy polymer (Pro-cote obtained from DuPont) is at pH 7. 15 g soy Pro-cote was then added at a very slow rate to avoid build-up of a layer of non-dispersed soy polymer on the top of the solution in order to make 18% Pro-cote solution (Figure 3.2). After mixing for 30min, some lumps were still present in the solution. In order to break those small lumps, the solution was kept in Ultra Sound Bath (Elma, S80H, Elma Sonic, 750 W, U-100-120V/AC, f- 50/60 Hz) at 45°C for almost 30 minutes (till all the lumps were dissolved).

Figure 3.2 Soy polymer preparation setup and soy polymer coating after preparation

3.7.2.1. Preparation of NH_4OH coating

In 85gm of NH_4OH (15% solution) at 60°C, 15gm of 18% Pro-cote solution (already prepared) was mixed by forming high vortex in order to avoid any lump formation. The solution was then cooled down to room temperature before adding any additives to it. In this soy polymer coating different amount of additives (black spruce bark extract, Tinuvin 477DW obtained from CIBA specialty chemicals) were then added and mixed to have a homogeneous solution and their transmittivity was measured using UV-VIS spectrophotometer.

3.7.2.2. Preparation of Urea-formaldehyde Coating

85% of 5% Pro cote solution was mixed with 15 % Urea formaldehyde by a mechanical stirrer for 30min. Different additives were then added to get optimum characteristic.

3.7.3. Acrylic Polyurethane Coatings

Two component sunlight cured water based acrylic polyurethane ((Bayhydrol UV XP 2690 and Bayhydrol 122) was obtained from Bayer Corporation, Germany. The acrylic polyurethane coating consisted of a curing agent-Irgacure 819DW (Ciba Specialty Chemicals), a defoaming agent- Tego Foamex 822 (Goldschmidt Chemical Corporation), a surface tension Reducing agent- Byk 348 (BYK-Chimie USA), and a thickener- Borchigel LW44 (OMG Americas, Inc) to get high performance against aging. The acrylic polyurethane coating was then modified by using different additives like organic antioxidants (bark and leaf extracts, nano lignin), lignin stabilizer (lignostab 1198 obtained from CIBA chemicals), inorganic UV absorbers (CeO_2 nano particles dispersed in water Nano BYK 3810 obtained from Byk Chimie, Titania micro and nano particles, ZnO nano particles obtained from MKNano). Alone or different combinations of these additives have been used and were compared with each other as well as with commercially available organic UV absorber, HALS (tinuvin 123 and tinuvin1130, obtained from CIBA speciality Chemicals) and one commercial coating. The formulations of different coatings are presented in Table 3.1. The coatings found promising are presented in chapter 4. The others are presented in the Appendices as shown in Table 3.1.

Table 3.1 Formulations of different acrylic polyurethane coatings developed during this study

Coating	Description	Presented in
Acrylic polyurethane without UV stabilizers	The base acrylic polyurethane coating	Chapter 4
Acrylic polyurethane with organic UV stabilizers	The base coating + Tinuvin123 + Tinuvin1130	Chapter 4
Acrylic polyurethane with organic UV stabilizers and black spruce bark extracts	The base coating + Tinuvin123 + Tinuvin1130 + black spruce bark extracts	Appendix 3
Acrylic polyurethane with organic UV stabilizers and needle extract	The base coating + Tinuvin123 + Tinuvin1130 + needle extract	Appendix 3
Acrylic polyurethane with organic UV stabilizers and titania micro particles	The base coating + Tinuvin123 + Tinuvin1130 + TiO_2<5μm	Appendix 2
Acrylic polyurethane with organic UV stabilizers and titania nano particles	The base coating + Tinuvin123 + Tinuvin1130 + TiO_2~50nm	Appendix 2
Acrylic polyurethane with organic UV stabilizers and zinc oxide nano particles	The base coating + Tinuvin123 + Tinuvin1130 + ZnO~30nm	Appendix 2
Acrylic polyurethane needle extract and lignin stabilizer	The base coating + needle extract + Lignostab 1198	Appendix 3
Acrylic polyurethane with black spruce bark extracts	The base coating + black spruce bark extracts	Chapter 4
Acrylic polyurethane with lignin stabilizer	The base coating + lignin stabilizer	Chapter 4
Acrylic polyurethane with black spruce bark extracts + lignin stabilizer	The base coating + black spruce bark extracts + Lignostab 1198	Chapter 4
Acrylic polyurethane with CeO_2	The base coating + CeO_2 nano particles~30nm	Chapter 4

Acrylic polyurethane with CeO_2 and bark extract	The base coating + CeO_2 nano particles~30nm + bark extract	Appendix
Acrylic polyurethane with CeO_2 and lignin stabilizer	The base coating + CeO_2 nano particles~30nm + lignin stabilizer	Chapter 4
Acrylic polyurethane with CeO_2, bark extract and lignin stabilizer	The base coating + CeO_2 nano particles~30nm + bark extract + lignin stabilizer	Appendix
Acrylic polyurethane with lignin nano particles BC6	The base coating + organosolv poplar lignin at 185°C	Appendix 4
Acrylic polyurethane with lignin nano particles BC6 and lignin stabilizer	The base coating + organosolv poplar lignin at 185°C + Lignostab 1198	Appendix 4
Acrylic polyurethane with lignin nano particles BC9	The base coating + organosolv lodgepole pine lignin at 185°C	Appendix 4
Acrylic polyurethane with lignin nano particles BC9 and lignin stabilizer	The base coating + organosolv lodgepole pine lignin at 185°C + Lignostab 1198	Appendix 4
Acrylic polyurethane with lignin nano particles BC37 and lignin stabilizer	The base coating + organosolv lodgepole pine lignin at 170°C + Lignostab 1198	Appendix 4

3.8. Transmission Test

The transmission spectra of natural antioxidants (bark extracts and needle extract) and also sol-gel derived coatings at different concentrations were carried out using UV/VIS spectrophotometer (Agilent 8453 UV-VIS spectroscopy system present at UQAC). Different amount of the bark extracts were dissolved in methanol.

3.9. Aging Test

For each species studied, samples (6.6cm×7cm×1.9cm) were coated with three layers (for heat-treated jack pine) and with four layers (for heat-treated aspen and birch) of coatings except for industrial Laurentide coating. For this coating only two layers were used as recommended by the manufacturer. Seven samples were prepared for each coating. Six of these samples were exposed to accelerated aging test and one sample for each coating was kept as a reference. The reference samples were protected from the light exposure.

Accelerated aging tests were conducted in Atlas Xenon Weather-Ometer (with a daylight filter, irradiation 0.35W/m^2 at 340nm, BPT 63±3°C and continuous light cycle with 102min light and 18 min specimen spray with light). All the samples were exposed to UV light for different times. The maximum exposure time was 1500h. A sample for each coating was taken out after 72h, 168h, 336h, 672h, 1008h, and 1500 h exposure.

3.10. Surface Characterizations

3.10.1. Wetting Test

The contact angle tests were performed using FTA200 sessile-drop system. FTA200 consists of a measurement platform, and a frame grabber (video capture) card, and a computer (Figure 3.3). With the help of a computerized syringe pump, 15μL drop of a desired liquid was placed on the wood sample and the images were captured using high resolution camera for a predetermined time. The contact angle measurements of liquid/wood systems and data analysis were carried out using the image analysis software

FTA32. All the contact angle experiments were carried out at room temperatures. In this study, only tangential surface of wood was examined and the contact angle experiments were executed along the veneer grain direction in order to study the affinity of the coatings towards tangential surface of heat-treated jack pine. Also, to investigate the effect of different surface orientation of wood, coating containing bark extract and lignin stabilizer applied to heat-treated jack pine after different surface treatment was examined on radial and tangential surfaces. The contact angles of water and coated jack pine surface were also measured before and after aging. The surface tension of the liquid coatings was measured by pendant drop method using the FTA32 software. At least 6 measurements were carried out for each coating. Contact angles of different probe liquids on coated wood surfaces were measured to calculate solid surface energy. The surface tension components of different probe liquids are presented in Table 3.2.

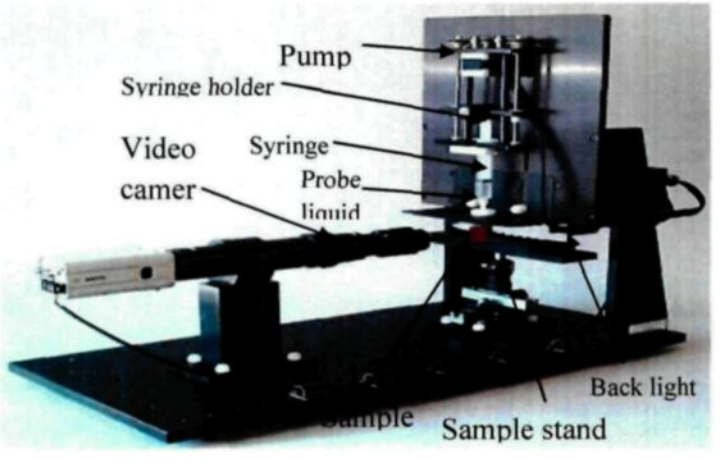

Figure 3.3 FTA200 instrument for contact angle experiment

Table 3.2 The surface tension component and parameters (in mJ/m^2) of probe liquids used for contact angle measurement

Liquids	Liquid index	Interfacial Tension (γ_L)	Dispersive (γ_L^d)	Polar (γ_L^p)	Acid (γ_L^+)	Base (γ_L^-)	Liquid nature
Water	1	72.8	21.8	51	25.5	25.5	Bifunctional
Formamide	2	58	39	19	2.28	39.6	Basic
Ethylene glycol	3	48	29	19	47	1.92	Acidic
Hexane	4	18.4	18.4	0	0	0	Neutral
Pyridine	5	38	37.2	0.8	-	-	
Acetic acid	6	27.8	-	_	_	_	
Nitromethane	7	36.8	_	_	_	_	

3.10.2. Color Measurement

The color of all the samples was measured before and after the aging test using Datacolor CHECK® spectrocolorimeter with diffuse illumination 8° viewing in conformance with CIE publication No.15.2 (Colorimeter based on D65 light source by simulating day light). The CIE L*, a*, b* coordinates were characterized by three parameters. L* axis represented the lightness and it varies from 100 (white) to 0 (black). a* and b* were the chromaticity indices where +a* was the red, -a* was the green, +b* was the yellow, -b* was the blue directions. The color differences were calculated using the equations [3.1] to [3.3] and the total color difference was calculated from equation [3.4] for each sample.

$$\Delta L = L^*_{after\ weathering} - L^*_{before\ weathering} \quad [3.1]$$

$$\Delta a = a^*_{after\ weathering} - a^*_{before\ weathering} \quad [3.2]$$

$$\Delta b = b^*_{after\ weathering} - b^*_{before\ weathering} \quad [3.3]$$

$$\Delta E = \sqrt{\Delta L^2 + \Delta a^2 + \Delta b^2} \quad [3.4]$$

3.10.3. Visual Assessment

The visual assessments were done by taking photographs of coated heat-treated wood surfaces at different aging times. The color change and other changes in surface appearances were carefully noted and reported in the results section.

3.10.4. Chemical Analyses

3.10.4.1. FT-IR-ATR measurement

The chemical modifications of the coated wood samples due to aging were examined by FT-IR spectroscopy (Figure 3.4). IR spectra were collected in the wave number range of 550-4000 cm^{-1} and all the spectra were recorded at 4 cm^{-1} resolution. Each time 20 scans were carried out prior to the Fourier transformation. All spectra were collected using a diamond micro-ATR crystal (Jasco FT/IR 4200). The incident angle of the crystal was 47° corresponding to an analysis depth of 0.2-5 μm, depending on the wave number. This ensured that the recorded FT-IR spectra were solely for the coating and there was no interaction with wood. The diameter of the actual analysis area was ~30μm. All spectra

were analyzed using Jasco spectra manager software. The ATR-FTIR analyses were carried out at the forest products laboratory of Alberta Innovates Technology Future, Edmonton.

Figure 3.4 ATR-FTIR instrument

3.10.4.2. XPS measurement

The XPS measurements of heat-treated and coated wood samples were performed by AXIS Ultra XPS spectrometer (Kratos Analytical) at the Alberta Centre for Surface Engineering and Science (ACSES), University of Alberta (Figure 3.5). The base pressure in the analytical chamber was lower than 2×10^{-8} Pa. Mono-chromate Al Kα (hν = 1486.6 eV) source was used at a power of 210 W. The resolution function of the instrument for the source in hybrid lens mode was 0.55 eV for Ag 3d and 0.70 eV for Au 4f peaks. The photoelectron exit was along the normal of the sample surface with an analysis spot of 400×700 μm. Charge neutralizer was used to compensate sample charging during the

analysis. The survey scans spanned from 1100 eV to 0 eV binding energies which were collected with analyzer pass energy (PE) of 160 eV and a step of 0.35 eV. For the high-resolution spectra the pass-energy of 20 eV with a step of 0.1 eV was used. CASA software was applied in the data processing. A linear background was subtracted from each peak, and then the peak area was evaluated and scaled to the instrument sensitivity factors. The composition was calculated from the survey spectra with sum of all peaks after scaling equal to 100 %. The spectra fitting and component analysis were performed using the high-resolution spectra.

Figure 3.5 AXIS Ultra XPS spectrometer and sample holder for XPS analysis

3.10.5. Morphological Analyses

3.10.5.1. Fluorescence microscopy analysis

The fluorescence microscopy tests were carried out in Laboratoire d'écologie Végétale et Animale, UQAC. Small microcores were cut from the original surface to test with Fluorescence Microscope. Microcores were dehydrated in successive immersions in ethanol and Histo-Clear and embedded in paraffin as recommended by Rossi et al. (2006) [158]. Transverse sections, 7 μm thick, were cut with a rotary microtome, placed on slides and gently stretched with a fine needle. All sections were stained with a 0.5% aqueous solution of Toluidine Blue to enhance the contrast of the wood tissue. To examine the depth of penetration and the pattern of distribution of the coatings, sections were also stained with 1% Sudan IV solution prepared in 95% ethanol [159]. The resulting turquoise color of the wood cell walls contrasts well against the red color of the coating. The transverse sections were fixed on glass slides with the Eukitt histological mounting medium. A camera mounted on an optical microscope was used to record numerical images and measure coating thickness with an image analysis system specifically designed for wood cells (WinCELL).

3.10.5.2. SEM analysis

The samples with dimension of 1cm×1cm×1cm were cut from the original samples for SEM analysis. The tests were performed in CURAL (Centre universitaire de recherche sur l'aluminium), UQAC. The specimens were vacuum dried for one week at room

temperature prior to SEM analysis. Each sample was then sputtered (in three directions-axial, radial and exposed surface) with gold-platinum coating with a plasma current of 10mA, chamber pressure of 6×10^{-2}mbar, and sputtering time of 140s by using a Polaron Range sputter coater. The SEM analysis was done by using JEOL-JSM-6480LV (Figure 3.6) with secondary electron scattering and with a low voltage of 10KV to avoid damage from charging. All the above mentioned surfaces (in three directions) of the samples were examined before and after aging for 72, 672 and 1500h under SEM to find the extent of aging and their effects.

Figure 3.6 JEOL-JSM-6480LV SEM microscope

3.11. Fungal Durability

One brown rot fungi *Poria placenta* and a white rot fungus *Trametes versicolor* purchased from FPInnovations FORINTEK, Québec, Canada were used in this study. Stock cultures of fungi were maintained on malt-agar medium stored at 4°C.

In this study, the methodology used to perform solid state cultures on wood was adapted from EN-113 (1986) standard. Wood samples with dimensions of 0.015 m × 0.005 m × 0.035 m in radial, tangential and axial directions were prepared. The size of wood samples was reduced to accelerate fungal degradation and also to reduce the testing duration from 16 weeks to 8 weeks.

20 ml of sterile medium was prepared by dissolving 40g malt and 30 g agar in 1 liter of distilled water. Petri dishes of 9 cm in diameter were filled with this medium, inoculated with fungus, incubated for 2 weeks at the temperature of 22°C ± 1°C, and the relative humidity of 70% ± 4% so that the mycelium can colonize.

Two sets of each wood sample were placed in different petri dishes. Each experiment was carried out two times to ensure the reproducibility of the results. Incubation was carried out under controlled temperature and humidity (22°C ± 1°C, 70% ± 4% relative humidity) in climatic chamber (Conviron). At the end of each test period, mycelia were removed and the samples were dried at 103°C ± 2°C and the weight loss caused by the fungal decay (WL-FD) was determined. This was expressed as a percentage of the initial oven dried weight of the wood sample as follows:

$$\textbf{WL-FD (\%)} = 100\,((m1 - m2)/m1) \qquad [3.5]$$

where m_1 and m_2 are masses of coated heat-treated wood samples before and after exposure to fungal attack, respectively.

Chapter 4

RESULTS AND DISCUSSIONS

In this chapter results obtained during this work are discussed in detail. This chapter is divided into several main sections. In the first section, different methods of solid surface energy calculations are compared for heat-treated and coated surfaces. This was done to compare different surface forces and Lifshitz van der Waal forces appeared to be the most important component of wood surface energy. During this study, different natural antioxidants were prepared and their characterization is subject of the next section. The detailed discussion about their antioxidant activity is also presented. The bark extract with highest antioxidant activity and a needle extract were chosen to add in the base coatings to study their protective characteristics against accelerated aging of heat-treated wood. Three different coatings are described in the next three subsections. They are sol-gel derived titania coatings, soy based polymer coating and acrylic polyurethane coating. At the beginning of this study titania coatings were developed by sol-gel reaction and different light stabilizers were added to enhance the UV protective characteristic of this coating. The accelerated aging test of these coating on heat-treated jack pine revealed that the sol-gel derived titania coatings were not effective enough to protect discoloration of heat-treated wood against accelerated aging. The soy based polymer coating containing bark extract also showed same trend as sol-gel derived coatings and almost no protection was observed

on heat-treated jack pine against accelerated aging test. In the next attempt, acrylic polyurethane was chosen as the base polymer due to their high resistance against aging and different UV stabilizers were added to it to increase their resistance against aging. This coating in combinations with different UV stabilizers showed promising results against accelerated aging test. Since biological attacks could not be incorporated during the accelerated aging test, the coated and heat-treated samples after aging for different times and before aging were exposed to brown rot and white rot fungi to study their durability against biological attack.

Due to the space limitations, the results for acrylic polyurethane with titania micro and nano particles and ZnO nano particles are presented in Appendix 2. In the Appendix 1 detailed steps for surface energy calculations are presented with one numerical example. The effect of needle extracts on acrylic polyurethane coatings performance is reported in Appendix 3. Characterization of nano lignins and their performance in acrylic polyurethane coating on heat-treated jack pine is subject of Appendix 4. Appendix 5 consists of detailed XPS results for acrylic polyurethane with CeO_2 nano particles and lignin stabilizer. In Appendix 6, the performance of acrylic polyurethanes with black spruce bark extracts and lignin stabilizers; are compared with that of CeO_2 nano particles and lignin stabilizers on heat-treated and un-treated wood species. Finally in Appendix 7, the antifungal activity of different bark extracts on heat-treated jack pine, aspen and birch is compared with that of the coatings without bark extracts.

4.1. Surface Energy Calculation of Coated Wood

4.1.1. General

The contact angle tests and surface energy calculations were performed to understand the interaction of water and other liquids with different coatings and thus to predict the longevity. The contact angle change implies the penetration or spreading properties of the liquid on the coated surface in which facilitates coating characterization (polar or nonpolar).

4.1.2. Zisman Plot

Zisman, in the year 1950, [42] proposed the theory of critical surface tension which is the minimum surface tension below which all the liquids wet the solid surface. The critical surface tension, γ_c, can be estimated by measuring the contact angle of a series of liquids with known surface tensions on the surface of interest. These contact angles are plotted as a function of the surface tension (γ_{LV}) of the test liquids (Table 3.2). The critical surface tension is defined as the intercept of the horizontal line, $\cos\theta = 1$, with the extrapolated straight-line plot of $\cos\theta$ against surface tension of the probe liquids as shown in Figure 4.1.

Zisman [51] measured the contact angle θ for a set of solutions of differing surface tensions γ_{LV}. When the cosines of the contact angles were plotted against the surface tensions, a more-or-less straight line was obtained. From thermodynamic point of view, the critical surface tension of a surface is not identical to its surface energy, but from a

practical point of view, the numbers are very similar. Therefore, many workers use critical surface tension as a usable approximation to surface energy. In the present study, Zisman plot results are used for comparisons for surface energy of coated heat-treated jack pine.

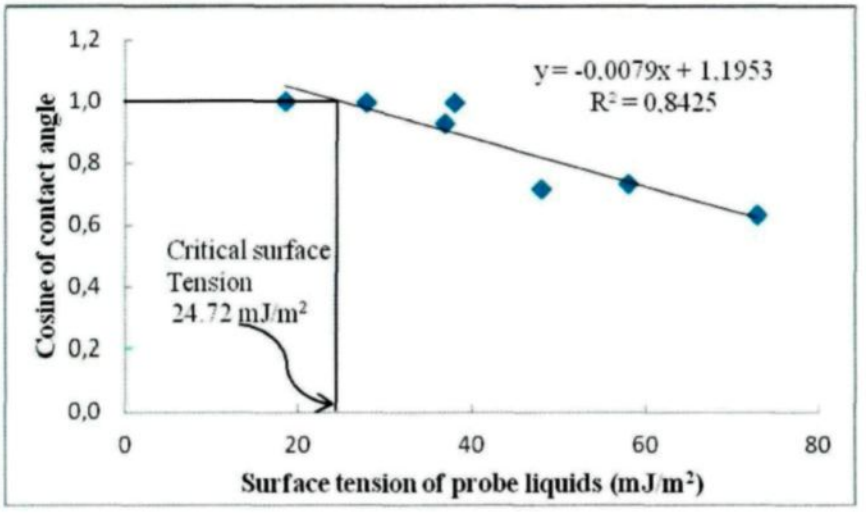

Figure 4.1 Zisman plot for soy polymer embedded with 5% bark extractive coated heat-treated jack pine wood

The critical surface tension values of different wood coating surfaces are tabulated in Table 4.1 and for soy polymer embedded with 5% bark extracts is shown in Figure 4.1. Critical surface tension values varied from 24.6mJ/m^2 for TiO_2 coating embedded with tinuvin5236 to 30.51mJ/m^2 ethanol coating embedded with tinuvin5236. The critical surface tension values for TiO_2 coating embedded with tinuvin5236 and for TiO_2 coating embedded with tinuvin5236 and lignostab1198 were comparable quite favorably with the surface energy values obtained by Lifshitz-van der Waal's acid base approach. However, the critical surface tension for soy polymer coating showed a large deviation from the

surface energy values obtained by Lifshitz-van der Waal's acid base approach (see Table 4.1). It was also very surprising that critical surface tension values for ethanol coatings were higher than the surface energy values obtained by Lifshitz-van der Waal's acid-base approach. It is well known that the choice of probe liquids used to measure the surface tensions can have an effect on the values. In this study, the probe liquids used were mainly chosen for calculating polar-dispersion and acid-base character of the surface and they might not be the best choices for calculating critical surface tension of different coated wood surfaces.

Table 4.1 Surface energy components and parameters obtained by using acid-base approach and critical surface tension values obtained by Zisman plots

Coating	Critical surface tension (mJ/m^2)	Surface Energy (mJ/m^2)				
		Total surface energy	Lifshitz-van der Waal forces	Acid-base forces	Acid	Base
15% tinuvin5236 in ethanol coating	30.51	20.86	19.19	1.67	0.20	3.43
15% tinuvin5236 and 2% lignostab1198 in ethanol	29.99	19.69	19.14	0.55	0.01	5.37
15% tinuvin5236 in TiO_2 coating	24.6	26.25	19.74	6.51	1.28	8.27
15% tinuvin5236 and 2% lignostab in TiO_2 coating	24.72	26.05	19.72	6.33	1.01	9.88
5% bark extractive in soy polymer coating	24.72	39.86	20.14	19.73	2.678	36.32

4.1.3. Owens Wendents' Method

In 1969, based on Fowkes equation (see Eq. 2.10), Owens and Wendt [47] proposed a new expression which divided the surface energy into two components, dispersive and polar and used a geometric mean approach to combine their contributions (see Eqn. 2.12). This concept permits a direct calculation of the unknown solid surface tension components, (γ_s^p and γ_s^d), from contact angle measurements with two liquids with known surface tension components (γ_l^d and γ_l^p). The solution to this equation requires the input from two or more standard high surface tension, non-associating liquids with very different polarities. Water (highly polar) and methyleneiodide (non-polar) are liquids often selected for contact angle experiments when this method is employed. A similar approach was proposed concurrently by Kaelble [160].

In his observations on interfacial tension, Wu also was started with the polar and disperse fractions of the interfacial tension of the participating phases. However, in contrast to Fowkes and Owens and Wendt [45, 47], who used the geometric mean of the interfacial tensions in their calculations, Wu [48] used the harmonic mean (see Eqn. 2.13). Using this relationship, he achieved more accurate results, in particular for high-energy systems. At least two test liquids with known polar and disperse fractions are required for this method; at least one of the liquids must have a polar fraction >0.

The individual contributions of polar and dispersion forces to the total surface energy of the soy polymer coating with 5% bark extracts coated heat-treated jack pine are reported in Figure 4.2. Because of the biological origin of wood and its well-known interactions with water, it was often felt that the polar nature of wood was of primary importance in

understanding its interactions. Both the geometric-mean and harmonic-mean models for surface interaction predicted that dispersion forces were clearly more important than polar forces on coated heat-treated jack pine. Though Gardner [161] observed a higher value of surface energy obtained by the geometric mean method than the values obtained by harmonic mean equation, in the present study opposite observations were recorded.

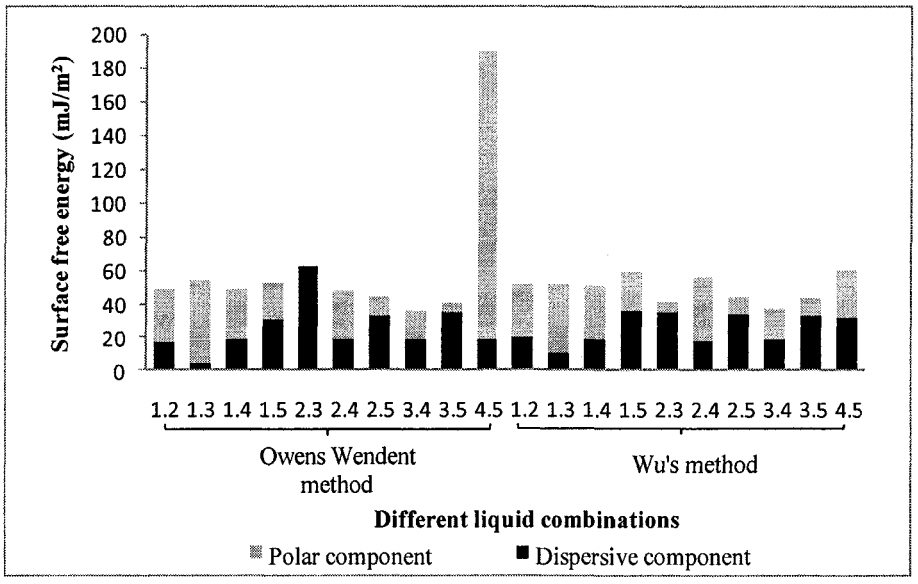

Figure 4.2 Polar and dispersive component of total surface energy of 5% bark extracts in soy polymer coated heat-treated wood by two different approaches

The surface energy values were solely dependent on the choice of liquids. But surface energy values obtained by geometric mean method and using different combinations of liquids, were more divergent than the values obtained by harmonic mean method [46]. This in turn favored use of harmonic mean method for characterizing wood surface

thermodynamics. The surface energy values calculated by using geometric mean method for different liquid combinations varied from 15.02mJ/m^2 for Tinuvin5236 and lignostab1198 embedded ethanol coated wood to 190mJ/m^2 for bark extracts embedded soy polymer coated wood (Figure 4.2). The surface energy values obtained by using Wu's harmonic mean method for different combinations of liquid varied between 20.09mJ/m^2 for Tinuvin and lignostab embedded ethanol coated wood to 60.55mJ/m^2 for bark extracts embedded soy polymer coated wood (Figure 4.2).

4.1.4. Liftshitz Van-der Waals Acid Base Method

Determination of the solid surface energy components γ^{LW}, γ^{+} and γ^{-} for the heat-treated coated wood samples were calculated by using Lifshitz van der Waals (see Eqns 2.14-2.16) acid base approach [49]. If the contact angle, liquid surface tension, and liquid surface tension components are known, the solid surface energy components can be calculated using a set of minimum three simultaneous equations. In this instance, a set of four simultaneous equations representing the four probe liquids (water, formamide, ethylene glycol, and hexane) were utilized to compute the three unknown wood surface energy components. The detailed calculation steps are presented in Appendix 1.

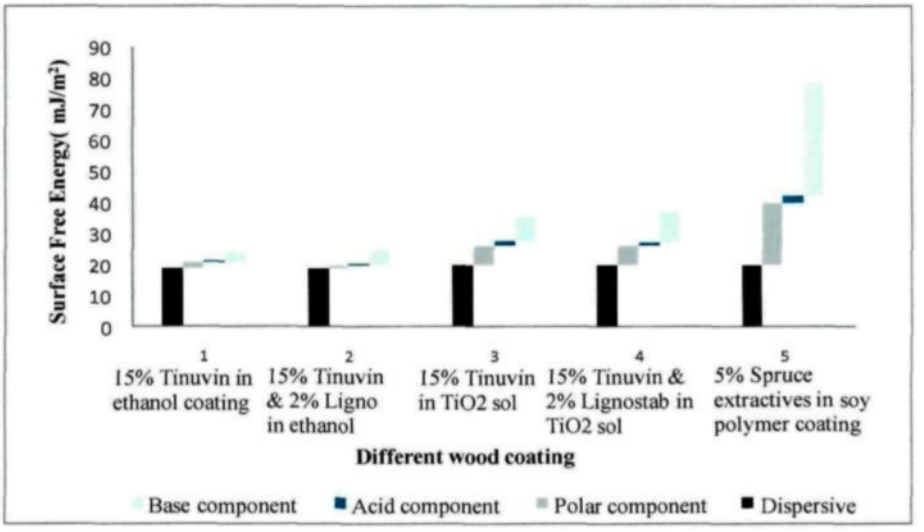

Figure 4.3 Different surface energy components- dispersive, polar, acid and base components of total surface energy for different coated heat-treated jack pine by Lifshitz-van der Waals acid base approach

The surface energy components determined by using Lifshitz-van der Waals acid-base approach is shown in Figure 4.3 and also in Table 4.1. The total surface free energies varied from 19.69mJ/m^2 for tinuvin and lignostab embedded ethanol coating to 39.86mJ/m^2 for bark extracts embedded soy polymer coating. Lifshitz-van der Waal forces appeared to account for the majority of wood surface energy values ranging from 19.14mJ/m^2 for Tinuvin and lignostab embedded ethanol coating to 20.14mJ/m^2 for bark extract embedded soy polymer coating. Acid-base contribution varied from 0.55mJ/m^2 for Tinuvin5236 and lignostab1198 embedded ethanol coating to 19.73mJ/m^2 for bark extract embedded soy polymer coating. It is really important to note that the majority of acid-base character came from the electron donating γ^- sites on the coated heat-treated wood surface.

At first glance, this electron donating behavior goes against conventional wisdom because wood exhibits a slightly acidic pH. However it should be pointed out that pH measurements are usually made on bulk wood, and contact angles are surface sensitive measurement. But for this particular study, the coatings developed were slightly basic in nature.

The contact angle behaviors of different probe liquids on different coated heat-treated jack pine surfaces showed different behavior. Most importantly water on all coatings, except for soy polymer coating, showed high contact angle. This implied hydrophobic character of coatings except for soy polymer coating. The work of adhesion between water and soy polymer coating demonstrated higher value than with other coatings.

The Lifshitz-van der Waals acid base approach provided greater accuracy in calculating wood surface energy components than the geometric mean and harmonic mean equations because it was based on the contribution of contact angles from four liquids versus two liquids. Also, the fact that the acid base character of the solid obtained by using acid-base approach was a marked improvement over the geometric mean and harmonic mean calculations. It is also really important to concentrate on the fact that the calculations depend on the combination of liquids used and different results can be obtained.

According to Gardner [161], the thermodynamic nature of the chemical components comprising the wood surface would prohibit surface tension values greater than $73 mJ/m^2$.

The determinations of critical surface tension values for wood were dependent on choice of probe liquids. In some instances, the critical surface tension of wood obtained by using Zisman plots compared favorably with the total surface tension obtained by the

Lifshitz-van der Waals acid base approach. Therefore, the Zisman approach can still be considered as a useful for understanding how an adhesive or finish will wet the surface. Perhaps, more important, however, is understanding how the acid base character of the wood surface influences adhesive curing mechanisms. The contribution of the γ^- wood surface to fundamental wood –adhesive interactions may have considerable implications in the gluing and finishing technology of wood, and deserves further study.

Lifshitz-van der Waals acid base approach was the most accurate method compared to other methods used during this study to determine surface energy of coated heat-treated jack pine surfaces. Therefore, this method was chosen to determine the surface energy change of acrylic polyurethane coating containing bark extract and lignin stabilizer on heat-treated jack pine during aging. The results (Table 4.2) showed, for initial 72h of aging, the total surface energy decreased along with all the components of surface energy. This was probably due to the curing of acrylic polyurethane coating during initial stages of aging whereas an increase in total surface energy was observed after 1500h of aging. This was due to the degradation occurred during accelerated aging. Also for this coating, it is found that the acid-base character was majorly due to the contribution of base component of surface energy.

Table 4.2 Surface energy components of acrylic polyurethane coating with bark extracts and lignin stabilizer on heat-treated jack pine for different aging time

Aging Time (h)	Surface Energy (mJ/m^2)				
	Total Surface Energy	**Lifshitz-van der Waal forces**	**Acid-base forces**	**Acid**	**Base**
0	45.98	39.27	6.71	0.5	22.52
72	38.13	36.79	1.34	0.02	21.44
1500	56.14	44.72	11.42	1.24	26.33

4.1.5. Concluding Remarks

Further studies are needed in order to evaluate the adhesion forces of these coatings on wood surfaces. The contact angle of water on soy polymer coating was less compared to other coatings and accordingly the adhesion force was quite high for this coating. Generally, work of adhesion increased with time for initial periods and then maintained a constant value. The Lifshitz-van der Waals acid base approach to determine solid surface tension components was more accurate than geometric mean and harmonic man approach. Lifshitz van der Waal forces appeared to be the most important component of wood surface tension, and the electron donating γ^- sites contributed prominently to the acid base character of wood. In some instances critical surface tensions of wood obtained by Zisman plots were in good accordance with the total surface tension obtained using Lifshitz-van der Waals acid base approach.

4.2. Characterizations of Natural Antioxidants

4.2.1. General

The disposal of natural residues (barks or leaves of trees) is a challenging task for wood industry which prompted to investigate the application of these unwanted residues in different areas especially as coating additives due to their high antioxidant activity. Natural polyphenols are well known due to their antioxidant properties. It is a growing tendency to replace synthetic antioxidants which are often carcinogenic with natural antioxidant compounds [113]. One of nature's most readily available and most valuable sources of phenolic antioxidants are present in wood, especially in knots and barks of several tree species [114, 115].

4.2.2. Extraction Yield and Cytotoxicity of Various Conifer Bark Extracts and Needle Extract

Three different species of boreal forest conifers (black spruce, balsam fir, and jack pine) were used for bark extracts whereas only one species (jack pine) was utilized for needle extract. The extraction of each conifer barks were carried out using three different solvent proportions consisting of methanol: water [100:0]; [80:20]; [70:30] whereas first two solvent proportions were used for needle extraction. The total extraction yields of each conifer bark extracts and needle extract are presented in Table 4.3. The extraction yield for conifer bark extracts were ranged from 13.3% to 22.2% while the needle extract (jack pine)

had a very low yield of 3.46%. The highest yield was obtained for black spruce bark extracts (22.19%) whereas lowest yield was observed for jack pine bark extracts.

Table 4.3 The total yield and cytotoxicity of organic UV stabilizers and natural antioxidants

Compounds	**Yield (%)**	**Cell line WS-1**
Tinuvin123	-	>100 μM
Tinuvin1130	-	>100 μM
Balsam Fir bark extracts	16.1	91 ± 7 μg/ml
Jack pine bark extracts	13.3	>200 μg/ml
Black spruce bark extracts	22.2	>200 μg/ml
Needle extract	3.5	>200 μg/ml

WS-1: *human normal skin fibroblasts*

The cytotoxicity of all the bark extracts and needle extract were compared with those of commercially available organic and inorganic UV stabilizers on human skin fibroblast (WS1) by Resazurin reduction test. The cells were incubated in the presence or absence of increasing concentrations of extracts for 48h. The results which were expressed as a concentration inhibiting fifty percent of cell growth (IC_{50}) are presented in Table 4.3. It was clear from the table that Tinuvin123 and needle extract were non toxic on human skin fibroblast cells. Balsam fir bark extracts was slightly active and toxic in nature as the cell

growth was inhibited in dose of less than 100μg/ml. The jack pine bark extracts and the black spruce bark extracts were completely non toxic on human skin fibroblast.

4.2.3. Antioxidant Activity of Extracts

The antioxidant activities of bark extracts and needle extract were evaluated using oxygen radical absorption capacity (ORAC). $ORAC_{FL}$ values were expressed as Trolox equivalent (TE μmol) per mg of extracts. The quercetine was used as positive control with an $ORAC_{FL}$ value of 19.75 μmol TE/mg. All the assays were conducted in triplicate and the mean values are presented in Table 4.4 with standard deviations. Results, presented in Table 4.4, showed that highest antioxidant activity was observed for black spruce bark extracts whereas lowest antioxidant activity was noticed for balsam fir bark extracts. Jack pine bark extracts showed higher antioxidant activity than needle extract.

From the Table 4.4 it is very clear that black spruce bark extracts was about six times more active compared to balsam fir bark extracts and about two times more active compared to jack pine bark extracts radical scavenging activity.

Table 4.4 Antioxidant activity of conifer bark and needle extracts using ORAC assay

Compounds	Oxygen Radical Absorbance Capacity ($ORAC_{FL}$ in 348 well plates)		
	μmol TE / mg	R^2	Number of experiments
Needle extract	3.8 ± 0.5	0.9786	6
Balsam fir bark extracts	2.0 ± 0.4	0.9936	7
Jack pine bark extracts	6.0 ± 0.9	0.9808	5
Black spruce bark extracts	11.6 ± 0.6	0.9862	4
Quercetine	19.8 ± 0.8	0.9941	5
Trolox	3.9 ± 0.2	0.9852	8

4.2.4. UV Absorption Spectra of Tested Extracts

The UV absorption capacity of different conifer bark extracts and needle extract was compared (Figure 4.4) in order to carry out primary screening. The transmission spectra of the black spruce bark extracts at different concentrations (0.5% and 1% w/w) were compared with those of other two conifer bark extracts (balsam fir bark extracts and jack pine bark extracts) and needle extract. The transmission results (Figure 4.4) showed that the balsam fir bark extracts had a poor absorption capacity in the UV range compared to the other three extracts (jack pine bark extracts, black spruce bark extracts, and needle

extract). Less than 1% transmittance was observed up to 337nm and 345nm for 0.5% and 1% of balsam fir bark extracts, respectively. High transmission in the UV range facilitates the UV light to reach to the wood surface and eventually starts to degrade it within a short time period after exposure to outer environment. Negligible transmittance (less than 1%) was detected for jack pine bark extracts (up to 391nm for 0.5% and 396nm for 1%) in the UV region. Conversely, complete blockage of UV light transmission was attained for black spruce bark extracts (less than 1% transmittance up to 401nm for 0.5% and 408nm for 1% black spruce bark extracts). Also, this extract exhibited almost transparent nature throughout visible region. Among all the bark extracts, the black spruce bark extracts fulfilled the primary criteria of UV absorber. On the other hand, the needle extract absorbed all the UV light and some portion of the visible light due to the presence of chlorophyll (green in nature). In addition to their antioxidant activity, black spruce bark extracts and needle extract can also act as UV absorber though their mechanism of energy dissipation is still unknown. However, further tests are necessary to conclude the efficiency of bark extract and needle extract. From UV- VIS spectroscopy and cytotoxicity results black spruce bark extracts and needle extract were chosen for further tests.

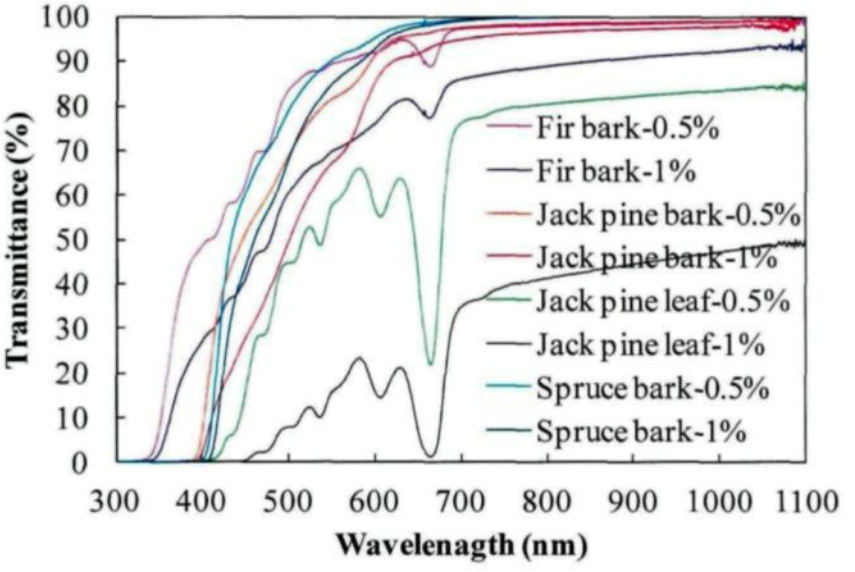

Figure 4.4 Transmissions spectra of different bark extracts and needle extract for two different concentrations

4.2.5. Chromatographic Assessment of Tested Extracts

Of the many chromatographic methods presently available, thin layer chromatography is widely used for separating the components of mixtures due to its rapidity and simplicity. The main advantage of this method is [162] that the qualitative characterization of constituents requires very short time. Other than qualitative detection, the drug quality assessment can also be realized from the semi quantitative information on the chief active constituent provided by TLC.

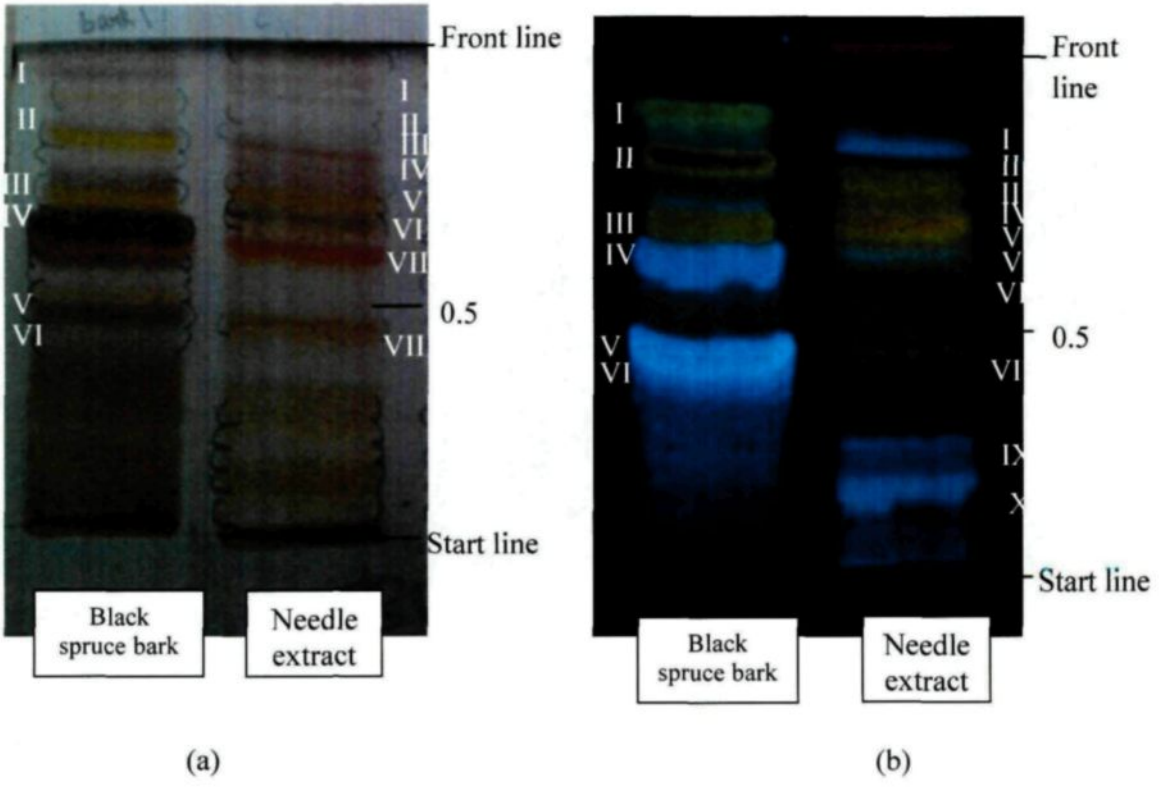

Figure 4.5 TLC of black spruce bark extracts and needle extract on silica gel-coated glass plate (a) terpenes, (b) polyphenols

From the chromatographic tests, it was clear that there were at least seven and six different terpene compounds present in black spruce bark extracts and needle extract, respectively (Figure 4.5a). According to the findings of Lalancette et al. [119] phenolic compunds are mainly responsible for the antioxidant activity of extracts for all conifer species. The black spruce bark extracts consisted of minimum six phenolic compounds and minimum ten phenolic compounds were detected by TLC on silica gel-coated glass plate for the needle extract (Figure 4.5b). Although fewer numbers of phenolic compounds were

present in black spruce bark extracts compared to those of needle extract, they were more prominent than the needle extract phenolics. Quantitatively the black spruce bark extracts had higher number of phenolic compounds compared to those of needle extract whereas qualitatively black spruce bark extracts was richer in phenolics as revealed by TLC (Figure 4.5b). Presence of phenolic acids and flavonoids could be confirmed from TLC results (Figure 4.5b). The R_f values of terpene and phenolic compunds are presented in Table 4.5.

Table 4.5 The R_f values of different phenolic and terpene components of black spruce bark extracts and needle extract

Component Number	**Phenolic Compounds**		**Terpene Compounds**	
			R_f	
	Bark extract	**Needle extract**	**Bark extract**	**Needle extract**
I	0.84	0.77	0.89	0.89
II	0.75	0.72	0.78	0.86
III	0.64	0.67	0.68	0.80
IV	0.57	0.65	0.58	0.74
V	0.48	0.63	0.51	0.53
VI	0.41	0.58	0.42	0.40
VII		0.52	0.33	
VIII		0.41		
IX		0.23		
X		0.16		

4.2.6. Concluding Remarks

The natural antioxidants were extracted successfully. The characteristics of three different bark extracts and one needle extract were evaluated. The UV absorption spectra of different bark extracts and the needle extract showed that the black spruce bark and the needle extracts were the most effective in absorption of light in the UV range as well as lower wavelength of visible region. The highest extraction yield was obtained for the black spruce bark extracts whereas lowest extraction yield was achieved with the needle extract. Other than balsam fir bark extracts, all other extracts were not toxic on normal skin fibroblast cells according to the cytotoxicity results. The highest antioxidant activity was observed for the black spruce bark extracts. Thin layer chromatography revealed minimum six and ten different phenolic compounds present in black spruce bark extracts and needle extract, respectively. Although the black spruce bark extracts and needle extract were rich in phenolic compounds, further tests were needed to study their activity as potential additives in coatings for wood color protection from outer environment. From this point on wards in this thesis, black spruce bark extracts will be marked as bark extract.

4.3. Aging of Sol-Gel Coated Heat-Treated Wood

4.3.1. General

Heat-treated wood is a natural product and no chemicals were used during heat-treatment. To protect this new product from outer environment, a highly effective non toxic coating is necessary. For UV protective coatings, both inorganic and organic UV absorbers can be used. However, no single UV absorber exhibits a complete UV absorption in the desired range (Figure 4.6). Therefore, in order to achieve absorption in this range, organic and inorganic UV absorbers can be combined [35].

4.3.2. Optical Properties of Sol-Gel Coatings

The inorganic oxide coatings were deposited on glass by dip coating method. As the concentration and the thickness of TiO_2 coatings were increased, the wavelength (λ) limit of the region where the transmission of UV was less than 10% ($T<10\%$) was moved from 285nm to 320nm (Figure 4.6). This is in good accordance with the result reported by Mahltig [35]. Also, the interference effect was a good evidence of smoothness of the layers. The titania coatings (Figure 4.6) displayed a high transmission ($T>10\%$) in the UV range (320nm-400nm). The organic UV absorber alone or with lignin stabilizer showed better results but the upper limit was found at near UV region ($T>10\%$ for $\lambda>390$nm). Therefore these coatings could not be used alone as a UV protective coating for wood.

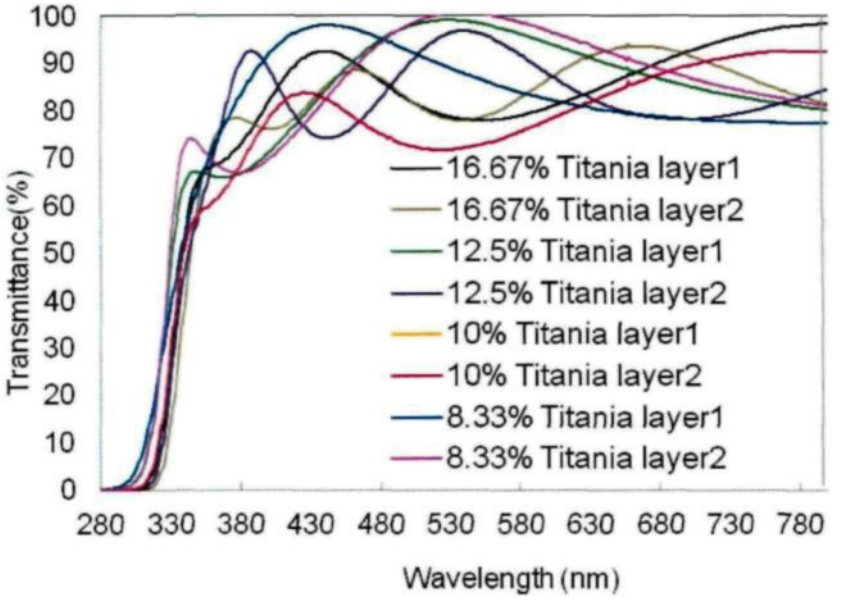

Figure 4.6 UV/VIS spectra of titania coatings on glass as function of concentration and layer thickness

In order to reduce the transmission of UV radiations by the coatings over the whole UV range, organic UV absorbers were embedded into UV absorbing titania coating. The experiments showed that the transmission of UV light decreased rapidly with increasing concentration of Tinuvin 5236. Less than 10% of UV was transmitted below the wave length of 440nm when 15% Tinuvin was used (Figure 4.7). Also as the thickness of the coating (number of layers) was increased the transmission curve was shifted towards red region. When two layers of coating were applied, less than 10% of UV was transmitted at wavelengths less than 470nm (Figure 4.7). Further increase in thickness resulted in fully opaque coatings which were undesirable. Addition of lignin stabilizer did not significantly affect the transmission in UV/VIS spectra. Interference effects were observed only for coatings with low concentration of UV absorber.

The decrease in transmission at a given wave length and also red shift of the minimum could be explained by the formation of complex bonding between the embedded UV absorber and the titania as reported by Mahltig et al. [35]. The transmission tests indicated that the titania nanoparticles embedded Tinuvin5236 alone or together with lignostab could be satisfactorily used as UV protective coatings. However, this has to be verified with aging tests.

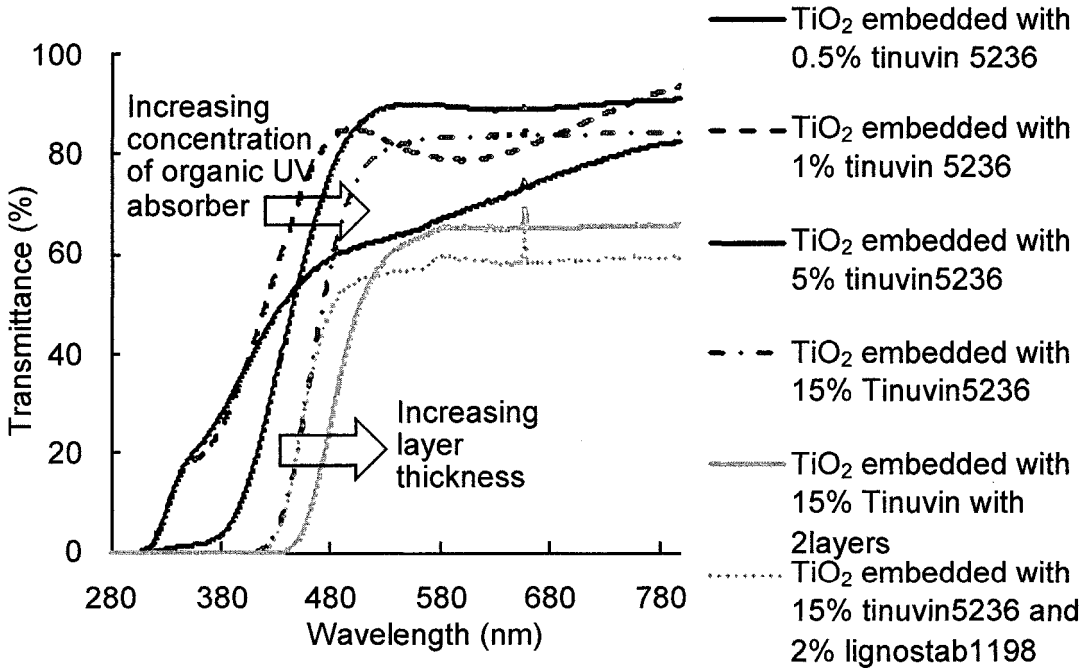

Figure 4.7 UV/VIS spectra of titania nano particles embedded with different concentration of organic UV absorber tinuvin5236

4.3.3. Color Measurement and Visual Assessment

The accelerated aging tests were carried out in order to study the effect of sun exposure on color change of heat-treated wood. Xenon arc source simulates the sun radiation more closely than any other artificial light source. Both the spectral distribution of energy and irradiance control can be adjusted with this system (Atlas aging device) through optical filtering and electrical power management, respectively.

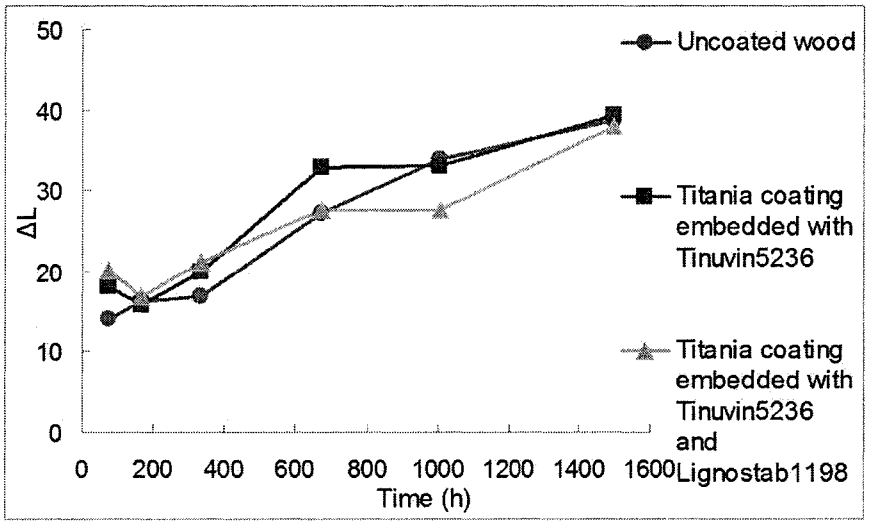

Figure 4.8 Lightness index variation of uncoated and coated heat-treated jack pine as a function of aging time

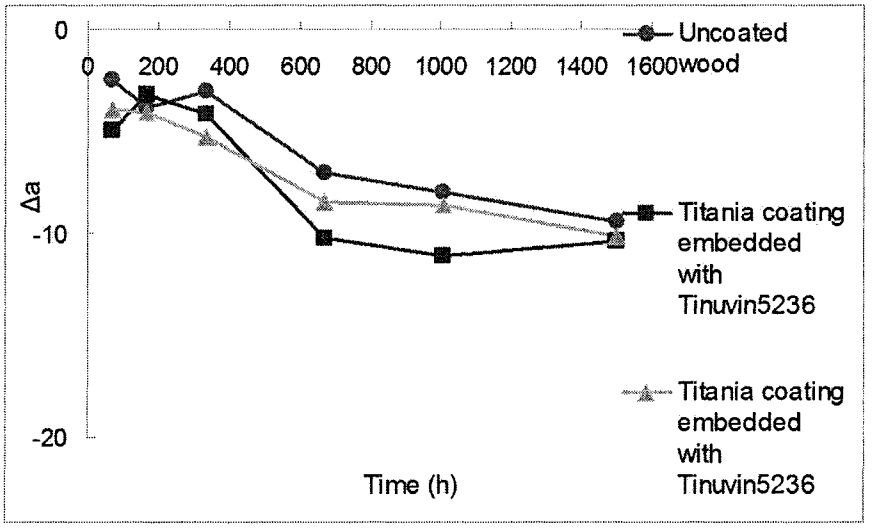

Figure 4.9 Red-green index variation of uncoated and coated heat-treated jack pine as a function of aging time

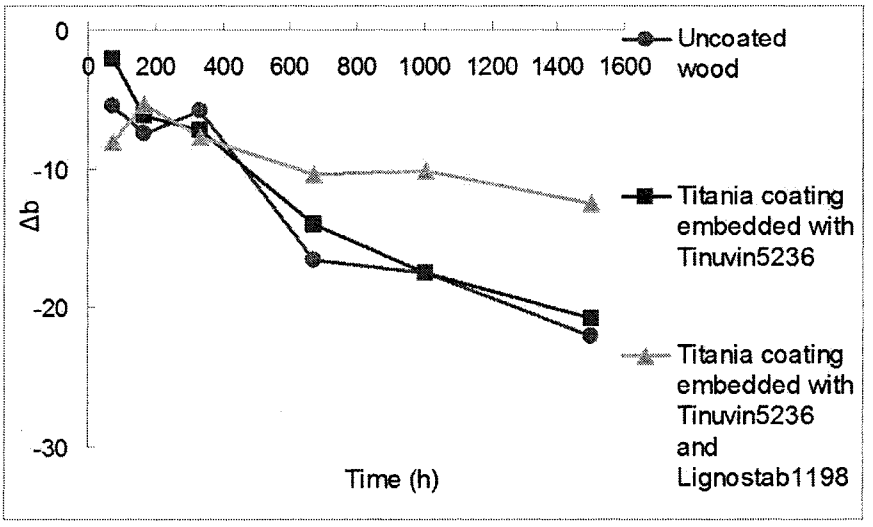

Figure 4.10 Yellow-blue index variation of uncoated and coated heat treated jack pine as a function of aging time

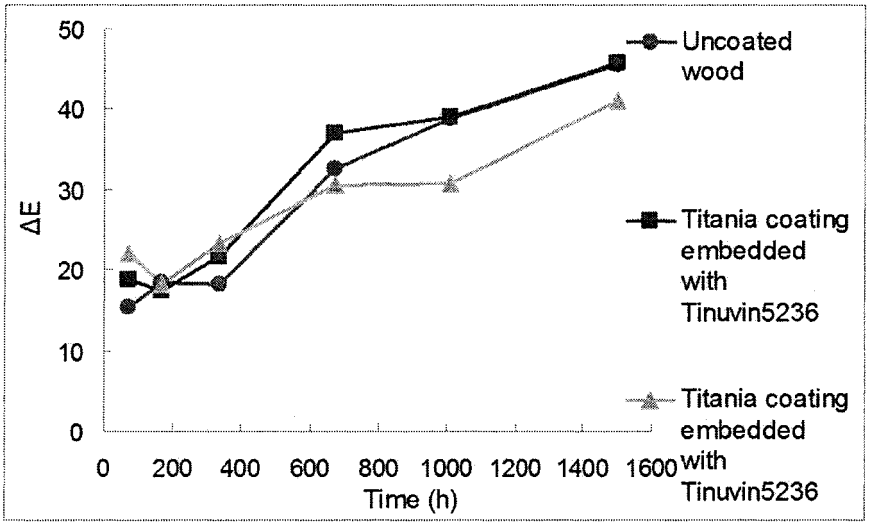

Figure 4.11 Total color variation of uncoated and coated heat-treated jack pine as a function of aging time

The lightness values for coated and uncoated wood were presented in Figure 4.8. The lightness value of uncoated wood was lower than those of the coated ones for the initial period of aging (up to 668h). UV absorber (Tinuvin5236) and lignin stabilizer (Lignostab1198) embedded titania coatings had the lowest lightness value between 668h and 1000h exposure. Although no effect of lignin stabilizer on UV protection could be detected with transmission tests when it was used with titania, artificial aging tests showed that its addition clearly improved the UV protection capacity of the titania containing coatings. After this time, all three curves approached each other. However, lignin stabilizer containing coating always had the lowest lightness value.

Chromaticity coordinates a* and b* over the aging period are presented in Figure 4.9 and Figure 4.10 for coated and uncoated wood samples. The variation of chromaticity

coordinates over the aging period showed similar trends for coated and uncoated wood except at initial aging times. Initially, the uncoated wood was redder than the coated wood. All the samples became greener after aging. Also, it can clearly be seen from Figure 4.10 that UV absorber and lignin stabilizer coated wood was initially more yellowish than uncoated one and the wood coated with UV absorber embedded titania. However, its color was distinctly different (becoming less yellowish) than the other two.

The total color change (Figure 4.11) of uncoated and coated wood samples increased with the exception of initial period of aging (168h). The color change in uncoated wood was lower than that of coated wood for initial 600h but the wood coated with UV absorber and lignin stabilizer embedded titania seemed to be better protected at longer times. Titania coating without lignin stabilizer had no UV protecting effect on wood. Further increase in lignin stabilizer (over 2%) did not affect the protection UV capacity of this coating.

The visual assessments of these two coated jack pine surfaces after different aging times are reported in Figure 4.12. The wood surfaces became white after aging due to degradation of lignin. From the visual assessment also it was clear that better protection was observed for titania sol containing tinuvin5236 and lignostab coated heat-treated jack pine surfaces. But still the coating was not good enough to protect the heat-treated jack pine for longer time period. Since wood is a porous material, coating applied on it tends to penetrate through the pores and after sometime not enough protection is left on the surface. This can be a reason for poor coating performance.

72h 168h 336h 672h 1008h 1500h

(a)

72h 168h 336h 672h 1008h 1500h

(b)

Figure 4.12 Heat-treated jack pine coated with (a) titania sol containing tinuvin 5236, (b) titania sol containing tinuvin5236 and lignostab at different aging times

4.3.4. FTIR Analysis

In the present study, the infrared spectra of coated and uncoated heat-treated wood were studied with FTIR-ATR system before and after aging for different periods. According to the histological observations of Yata and Tamura (1995), the photodegraded zone with grayish color reached 0.2 mm depth from the surface after aging for half a year, and a 0.5mm thick brown zone was found underneath the gray zone. Since the analysis depth of ATR FT-IR spectroscopy is a couple of micrometer, only the surface components of the wood are detected. Different kinds of coatings were applied on wood and their performance was evaluated by following the changes in peak intensity during different exposure times.

The FTIR spectra for heat-treated wood coated with titania coating embedded with Tinuvin 5236 and lignin stabilizer aged for different periods are presented in Figure 4.13. The Figure 4.13 shows the basic structure of wood: a broad but not strong O-H stretching at 3300-3600 cm^{-1} due to high temperature heat treatment of wood, C-H stretching at 2800-3000 cm^{-1} and several distinct peaks in the finger print region between 500 and 1750 cm^{-1}. The peak around 1726 cm^{-1} was assigned to the carbonyl stretching vibration of carboxyl and ester groups, especially acetyl group binding to hemicelluloses, such as xylan in hardwood and glucomannan in softwood [26, 163]. In present study, the peak around 1726 cm^{-1} was the result of chromophores containing carbonyl groups generated during aging and presence of more cellulose on the surface. Decrease in this peak intensity during aging was due to the depletion of chromophores from the wood surface, giving a pale look. Peak intensities around 1505 cm^{-1} and 1595 cm^{-1} were originated from the vibration of aromatic

ring structure of lignin. The band around 1450 cm^{-1} was assigned to asymmetric C-H deformation of lignin [64, 65, 164]. Soft wood lignin showed higher peak intensity at 1505 cm^{-1} and absorption around 1260 cm^{-1}, which is characteristic for aryl alkyl ether bonds. The doublets which might be due to the condensed structure of lignin were noticeable at 1595 cm^{-1} and 1505 cm^{-1}. Disappearance of this doublet after 1500h of aging confirmed that no lignin left on the wood surface. This was the main reason for the coated surface becoming white after aging as shown in Figure 4.12. The peaks at 1367, 1162 and 898 cm^{-1} were mainly due to carbohydrates and have no significant contributions from lignin [86, 165]. The band around 1380cm^{-1} mainly due to conformational changes in the glycosidic bridge [166] remained almost constant.

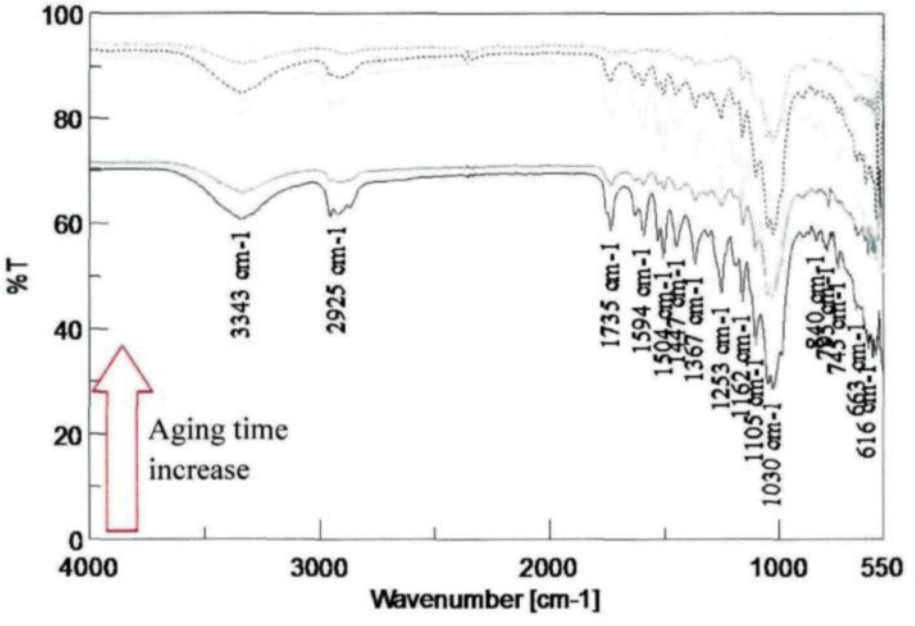

Figure 4.13 FTIR Peaks of 15% Tinuvin5236 and 2% lignin stabilizer in titania coated wood at different aging times

4.3.5. XPS Analysis

The changes in surface chemical compositions were investigated by XPS analyses of tinuvin5236 and lignostab1198 in TiO_2 sol-gel coated heat-treated jack pine surfaces after aging for 72h and 1500h (Figure 4.14a). The survey spectrum of 72h aged coated-wood surface showed prominent peaks of C1s, O1s and Ti2p and small peaks of N1s, Ti3s, Ti3p, OKLL, O2s, Na1s, NaKLL implying presence of titania coating. After 1500h of aging Ti peaks disappeared mainly due to the depletion of titania coating. C1s and O1s peak intensities increased slightly whereas OKLL peak intensity decreased after 1500h of aging. Also the spectra intensity all over the binding energy range decreased after 1500h of accelerated aging (Figure 4.14a). The high resolution spectra of C1s were deconvoluted into four components C1, C2, C3 and C4. The C1 peak is ascribable to hydrophobic bonds such as carbon linked carbon or hydrogen present in lignin and aromatic low molecular weight extractives and fatty acids. The C2 peak corresponds to carbon-oxygen bonds present in hydroxyl or ether group of lignin and polysaccharides of wood. The C3 peak is mainly due to hemiacetal carbon of cellulose and hemicelluloses and to a lower extent to carbonyl groups. The C4 peak corresponds to carbonyl of carboxylic acid or ester functions present in wood [66, 167]. The deconvoluted spectra after 72h of aging (Figure 4.14b) revealed highest contribution from the C1 component followed by C2, C3 and C4. The C2 component contribution was also quite high which was mainly from cellulose. After 1500h of aging C2 component contribution was the highest (Figure 4.14c) as cellulose became the most available component at the wood surface because of aging. At this stage, C1 component contribution decreased considerably as a result of lignin degradation and

depletion of degraded products from the surface due to the presence of moisture and water spray. The contribution of different types of oxygen atoms was more difficult to analyze. According to the literature, the O2 component represents all the oxygen elements in cellulose whereas the oxygen elements in benzyl aryl ether and diaryl ether are ascribed to O1, the oxygen elements in phenolic OH, aliphatic aromatic ether and thioglycolic acid to O3 [2, 168, 169]. The O1s spectrum was decomposed into three components after 72h of aging and four components after 1500h of aging. After 72h of aging O1% was almost 43% and the contribution of O2 and O3 components were almost equal (Figure 4.14d). However, after 1500h of aging a new component was formed and O2% increased to 83% and O1% and O3% decreased extensively (Figure 4.14e). The noteworthy increase in percentage of O2 component clearly showed that after 1500h of aging the wood surface became rich in cellulose. In addition, decrease in contribution of O1 and O3 components illustrated that lignin was degraded and depleted with aging from the wood surface. The formation of a new component O4 demonstrated that oxygenated products were formed due to aging. As illustrated in Table 4.6, the O/C ratio increased from 0.4 (before aging) to 0.55 after 72h of aging and after 1500h of aging to 0.56. The increase in O/C ratio was mainly due to the lignin degradation and production of oxygenated photo products during aging.

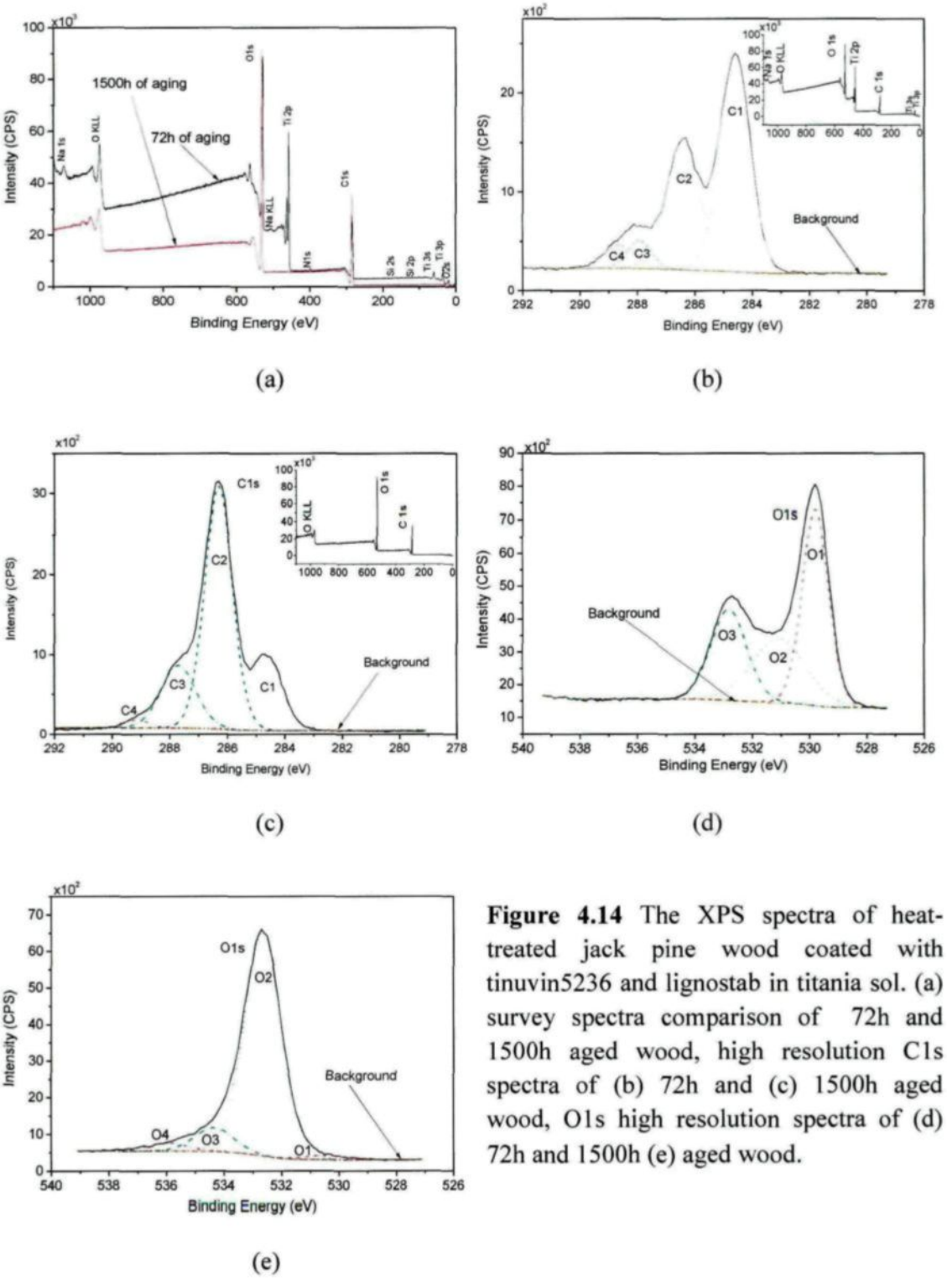

Figure 4.14 The XPS spectra of heat-treated jack pine wood coated with tinuvin5236 and lignostab in titania sol. (a) survey spectra comparison of 72h and 1500h aged wood, high resolution C1s spectra of (b) 72h and (c) 1500h aged wood, O1s high resolution spectra of (d) 72h and 1500h (e) aged wood.

It is well known that all polymers, except saturated hydrocarbons such as polypropylene or polyethylene, have acidic or basic functional sites. In general, most polymers have either an acidic or basic character or both to some extent. Some of the XPS peak shifts may, in principle, be related to the acid-base interactions. Particularly, the high resolution XPS spectrum of the basic oxygen of the surface sites is most helpful in identifying the extent of base interaction. According to Fowke's theory as explained by Shen et al. [170], the total acidity of any surface can be calculated by the contribution of C2 and C4 components and basicity depends on the contribution of C1 and C3 components. It was clear from the Table 4.6 given below that the acidity of the surface increased whereas the basicity decreased with aging. Therefore, it could be concluded that the photo products formed during aging were acidic in nature.

Table 4.6 The O/C ratio and acid/base ratio of heat-treated jack pine coated with tinuvin5236 and lignostab in titania sol

Sample	**O%**	**C%**	**O/C**	**Total Acidity (C2+C4)**	**Total Basicity (C1+C3)**	**A/B**
Before Aging	28.70	71.30	0.40	31.13	68.87	0.45
After 72h of Aging	35.62	64.38	0.55	40.58	59.42	0.68
After 1500h of Aging	35.91	64.09	0.56	60.65	39.35	1.54

4.3.6. SEM Analysis

The most important early structural indication of photo degradation on soft wood surfaces is the damage of bordered pits as explained by Turkulin [171]. For wood surface coated with semitransparent coating, he had reported formation of distinctive cracks of the torus on aspirated pits only after 4days of natural exposure or 10 hours of Fluorescent UV lamps exposure. Whereas such kind of cracks were visible for the present study after 72h of accelerated aging at the surface beneath the sol-gel coated titania nano coating containing Tinuvin5236 and lignin stabilizer (Figure 4.15a). Upon prolonged exposure to accelerated aging test, after 672h of aging, pit dome cracks progressed diagonally, following the microfibril orientation in the domes resulting in the widening in aperture and thinning of the pit dome (Figure 4.15b). Complete destruction of the pit membrane mark was observed in the present study after 1500h of exposure to accelerated aging condition. Simple pits found in late wood of jack pine did not disintegrate as fast as bordered pits. Only after 1500h of aging, SEM micrographs exhibited deep S2 crack in simple pit revealing angle of microfibrils in this layer of secondary cell wall (Figure 4.15c). Along with the longitudinal cracks in S2, horizontal cracks were also evident as a sign of accelerated aging of heat-treated jack pine coated with sol-gel derived titania nano coatings containing Tinuvin5236 and lignin stabilizer after 1500h of exposure (Figure 4.15d).

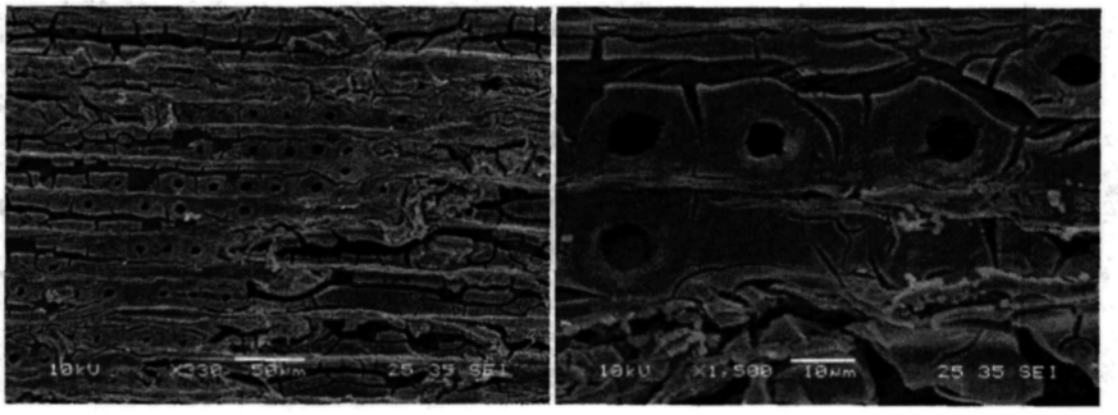
10kU X330 50µm 25 35 SEI
10kU X1,500 10µm 25 35 SEI

(a)

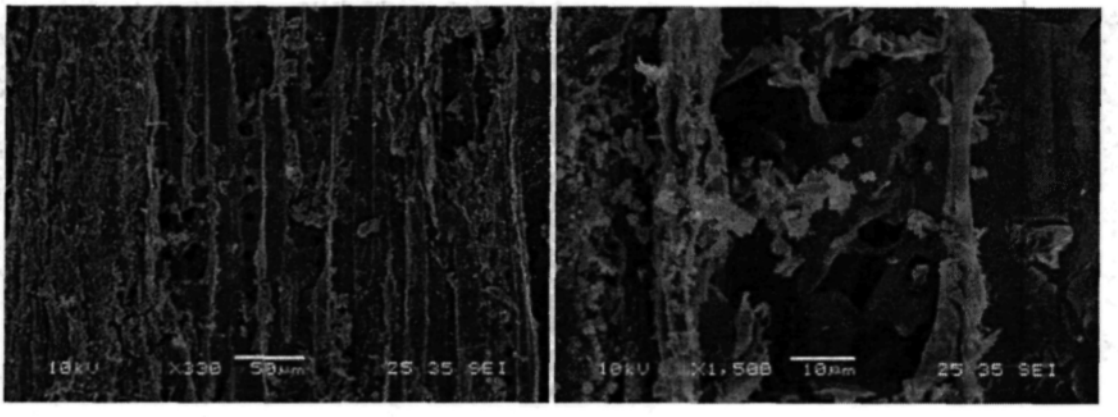
10kU X330 50µm 25 35 SEI
10kU X1,500 10µm 25 35 SEI

(b)

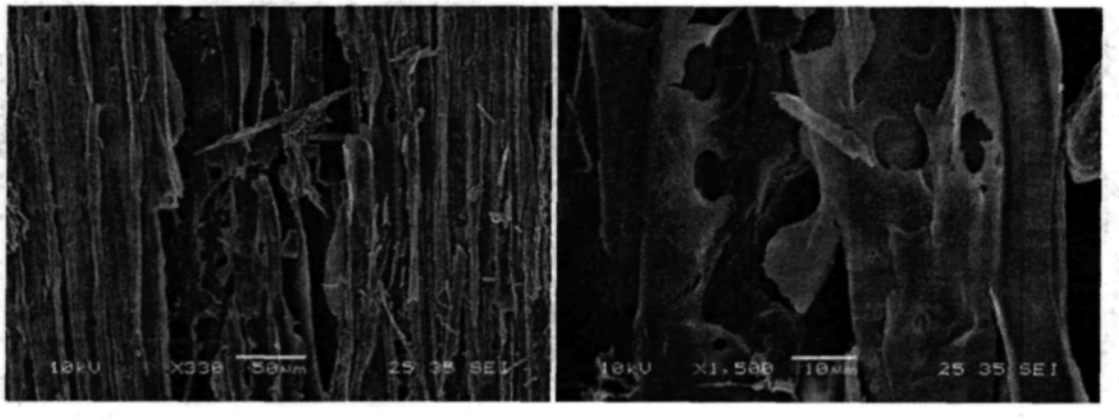
10kU X330 50µm 25 35 SEI
10kU X1,500 10µm 25 35 SEI

(c)

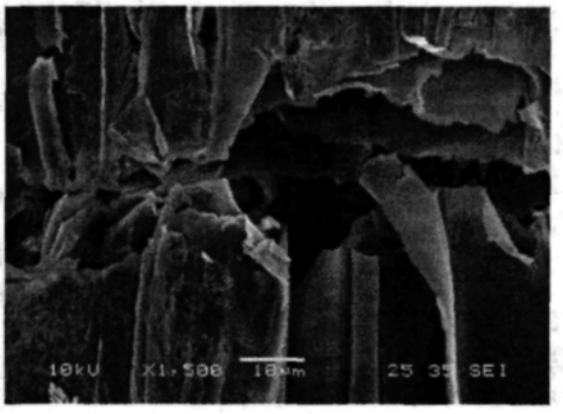

(d)

Figure 4.15 SEM analyses of heat-treated jack pine coated with titania coating containing organic UV absorber and lignin stabilizer after (a) 72h of aging, (b) 672h of aging, (c) and (d) 1500h of aging

4.3.7. Concluding Remarks

The inorganic UV absorbing titania coating and organic UV absorbers did not provide sufficient UV protection for heat-treated jack pine surfaces when used separately. The UV/VIS spectroscopy results for titania particles embedded with UV absorber indicated very promising UV protective characteristics. But the accelerated aging test results did not yield to the same conclusion. The color change diagrams demonstrated that the titania embedded with UV absorber coating did not have a considerable influence on wood color but addition of lignin stabilizer played an important role in protection of wood from UV exposure as they mainly act as radical scavenger. The coatings did not work effectively since they were not thick enough. There was not enough protection left on the surface when the coating fills the pores after the application of a thin layer. The XPS, FTIR

analyses revealed that with aging lignin degraded which resulted in formation of oxygenated acidic products leaving behind a cellulose enriched surface. Further study is needed to investigate the performance of these UV protective coatings incorporated in wood clear coats.

4.4. Aging of Soy Polymer Coated Wood

4.4.1. General

The soy based polymers are non toxic and environment friendly which prompted to choose this polymer for protection of heat-treated wood. No literature was found on their use in outdoor environment as protective coating; therefore, their weather resistance characteristics were unknown. This soy polymer needed to crosslink for better performance and three different ways were available. The first method was to crosslink by using ammonium hydroxide, secondly by using AzeCote and third option was to use urea formaldehyde. The best crosslinking agent was selected by carrying out a 24h water immersion test of these three differently coupled coatings on heat-treated jack pine and investigating the adhesion behavior of them at the end of the test. The azecote coupled soy polymer showed very poor water resistance characteristics whereas ammonium hydroxide and urea formaldehyde demonstrated high water resistivity. Due to the very high toxicity of urea formaldehyde, ammonium hydroxide was chosen as a coupling agent for soy polymer coatings to be tested for their efficiency in protection of heat-treated wood from color change during accelerated aging.

4.4.2. Color Measurement and Visual Assessment

The color measurement results for the heat-treated jack pine coated with soy polymer coating containing bark extracts were compared with commercially available pigmented

solvent borne Laurentide and Cetol coatings on heat-treated jack pine and are presented in Figure 4.16.

The changes in lightness index suggested that the soy polymer coating on heat-treated jack pine did not prevent wood color change during artificial aging and very high lightness index change was observed only after 72h of exposure (Figure 4.16 a). The change in lightness index increased with aging time and after 1008h of aging it became almost constant. The industrial Laurentide coating and industrial Cetol coating showed very small lightness index change even after 1500h of accelerated aging (Figure 4.16a). For the industrial coatings the surface became lighter for initial 336h of aging but then the lightness value started decreasing for both the commercially available coatings. The soy polymer coating became greener with increasing aging time whereas increase in red-green index was observed for both the industrial coatings (Figure 4.16b). The most change in chromaticity indices was noticed for soy polymer based coating on heat-treated jack pine. The soy polymer coated heat-treated jack pine turned to bluish in nature after accelerated aging whereas both the industrial coatings showed yellowish nature up to 1008h of aging (Figure 4.16c). Increase in same index for initial 336h of exposure was observed for both the industrial coatings. The soy polymer coating exhibited almost no protection, and color change was very significant compared to the industrial coatings on heat-treated jack pine (Figure 4.16d).

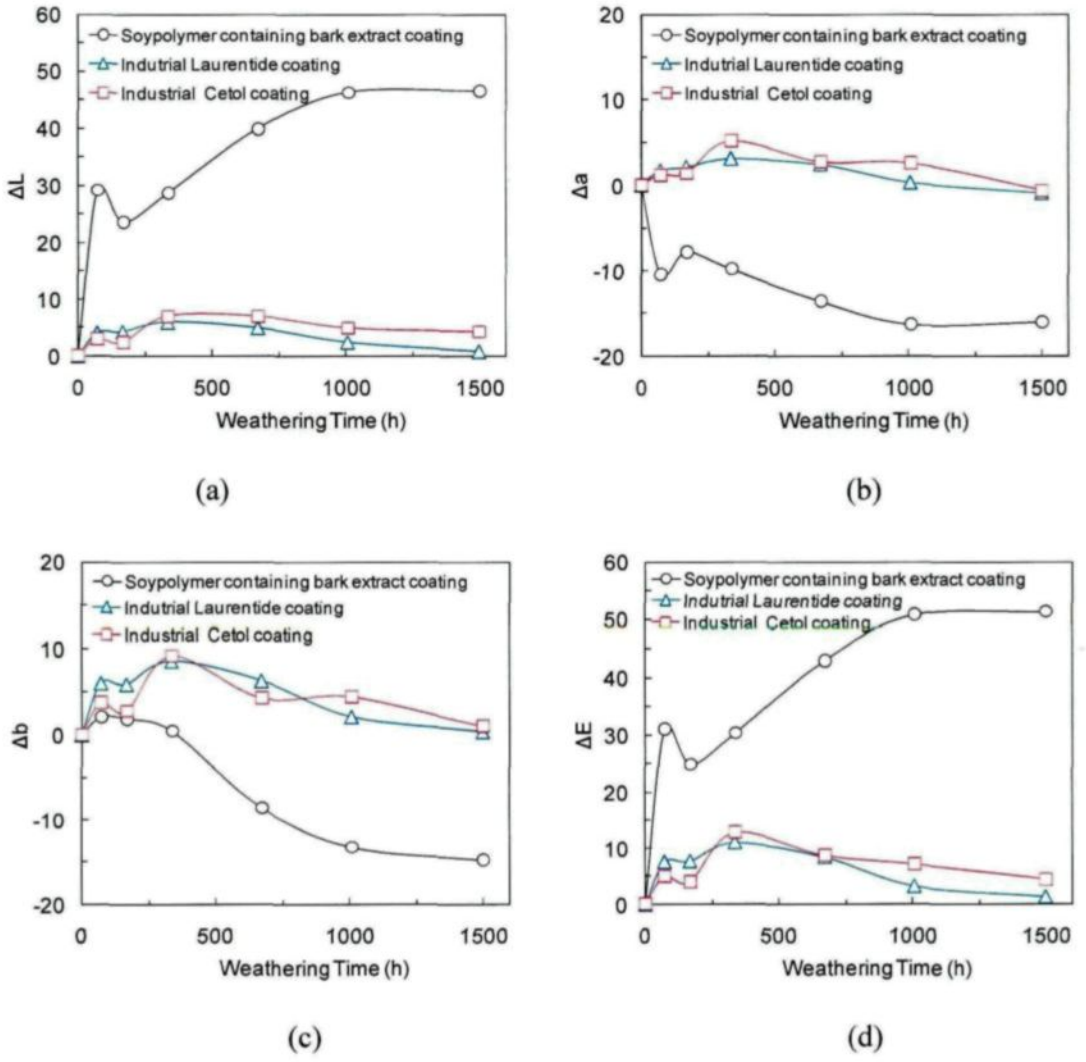

Figure 4.16 Comparison of color change of heat-treated jack pine coated with soy polymer coating and commercially available Laurentide coating and Cetol coating after different aging period (a) lightness index, (b) red-green index, (c) yellow-blue index, and (d) total color change

72h 168h 336h 672h 1008h 1500h

(a)

72h 168h 336h 672h 1008h 1500h

(b)

72h 168h 336h 672h 1008h 1500h

(c)

Figure 4.17 Visual assessment of heat-treated jack pine coated with (a) soy polymer coating, (b) Industrial Laurentide coating, and (c) Cetol coating for different aging periods

A very significant change in color was observed only after 72h of accelerated aging for heat-treated jack pine coated with soy polymer coating containing bark extract as shown in Figure 4.17a. The surface became completely white due to degradation after 672h of accelerated aging for this coating. The industrial coatings on the other hand protected wood better and almost no color change was observed up to 672h of accelerated aging. Small local degradations were visible after 1008h of aging for the both industrial coatings (Figure 4.17). The Cetol coating (Figure 4.17c) degraded more at the end of 1500h of aging compared to industrial Laurentide (Figure 4.17b) coating but significant degradation were noticed for both the coatings at the end of 1500h of aging.

4.4.3. FT-IR Analysis

Soy polymer coating containing bark extracts was prepared in the laboratory and applied on the wood surfaces. The thickness of the coating was very small and sometimes the active components penetrated though the pores of the wood surfaces, resulting in ineffective coating. For this reason, the coated heat-treated jack pine surfaces were degraded only after 72h of aging. A very small peak around 1509 cm^{-1}, which was attributed due to the lignin guaiacyl nuclei, was noticeable after 72h of aging. However, the peak disappeared after 168h of aging (Figure 4.18). The degradation of lignin during aging was confirmed from disappearance of this peak which was accompanied by formation of new carbonyl photoproducts. This was indicated by increasing absorption around 1734 cm^{-1} due to photo oxidation of wood surface [26, 33, 82, 86, 163, 164, 166, 172-174] (Figure 4.18).

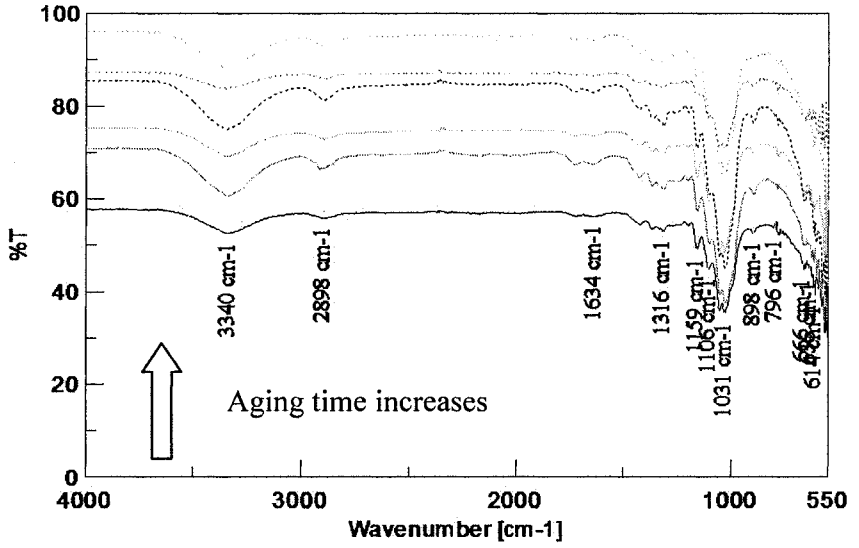

Figure 4.18 ATR-FTIR analyses of heat-treated jack pine coated with soy polymer containing bark extracts for different aging times

4.4.4. XPS Analysis

In the Figure 4.19 the survey spectra of heat treated jack pine coated with soy polymer coating embedded with bark extracts are compared for different aging times. It can be concluded from the survey spectra that both the main peaks, C1s and O1s, increased during aging. There was a slight increase in C1s peak whereas in O1s peak intensity increased quite prominently. Contributions of other components such as N and Si were not important enough to consider (Figure 4.19a). The C1s spectra of the aged wood were deconvoluted into four peaks as C1, C2, C3 and C4. As shown by Figure 4.19, it can be said that there was not enough protection of wood from aging as the C1s spectra after 72h of aging became 'cellulose type' spectra (Figure 4.19b). Among the wood components, lignin is a

very good UV absorber [11] and wood color degradation was mainly due to lignin photo degradation [24]. The O/C ratio was increased from 0.39 to 0.65 with aging mainly due to degradation of lignin and formation of chromophores on the surface. Due to degradation of lignin, C1% decreased significantly while C2% increased (Figure 4.19c). The formation of a cellulose enrich aged layer increased the O/C ratio and the C2 component. The contribution of C3 component increased slightly while C4 contribution decreased. The C1s spectrum of heat-treated jack pine wood before aging was compared with that of coated wood after 72h and 1500h of aging (Figure 4.19d). The highest peak of C1s spectra were shifted to higher binding energy with aging due to the formation of new carbonyl photo products. The C1 peak became narrower while the C2 peak became broader during aging. The C1s spectrum of wood before aging was lignin like while the aged wood spectra were cellulose like. The other important peak O1s was deconvoluted into two components O1 and O2 (Fgure 4.19e). With aging O1% decreased in contrast to O2% (Figure 4.19f), which increased with aging. Also, the contribution of O1% was very small compared to O2% which can be explained with the aging of surface coating as well as underneath lignin on wood surface resulting in formation of various chromophores on the surface.

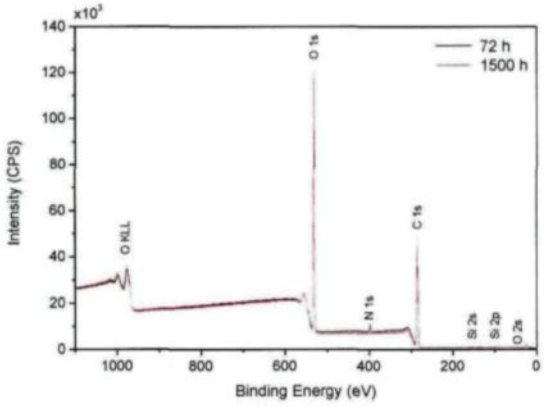
x10³
72 h
1500 h
O 1s
C 1s
N 1s
Si 2s
Si 2p
O 2s
O KLL
Intensity (CPS)
Binding Energy (eV)

(a)

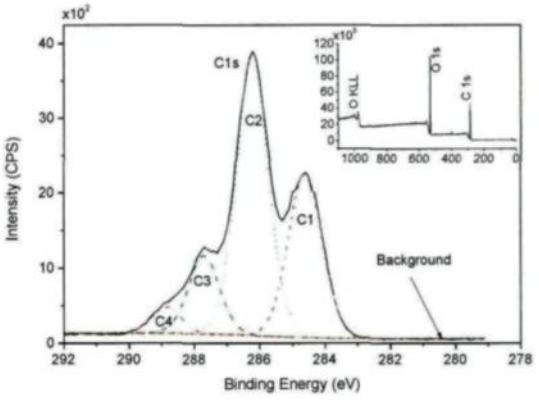
x10²
C1s
C2
C1
C3
C4
Background
O KLL
O 1s
C 1s
Intensity (CPS)
Binding Energy (eV)

(b)

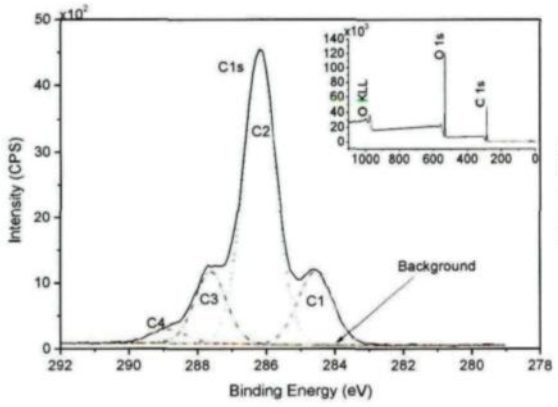
x10²
C1s
C2
C3
C1
C4
Background
O KLL
O 1s
C 1s
Intensity (CPS)
Binding Energy (eV)

(c)

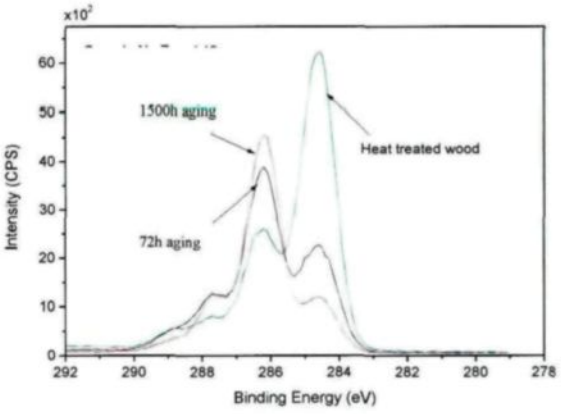
x10²
1500h aging
72h aging
Heat treated wood
Intensity (CPS)
Binding Energy (eV)

(d)

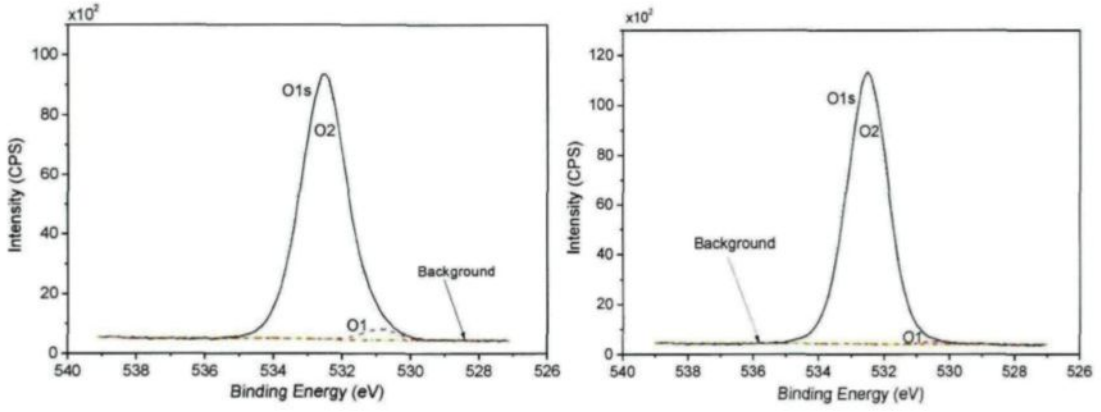

(e) (f)

Figure 4.19 The XPS spectra of heat-treated Jack pine wood coated with bark extracts in soy polymer coating (a) survey spectra comparison of 72h and 1500h aged wood, High resolution C1s spectra of (b) 72h and (c) 1500h aged wood, (d) C1s spectra comparison of wood before and after aging, O1s high resolution spectra of (e) 72h and 1500h (f) aged wood

4.4.5. Concluding Remarks

The soy polymer coating with bark extract did not protect heat-treated jack pine from aging. The wood surface underwent degradation only after 72h of accelerated aging. This was due to the fact that soy polymers, even after cross linking with NH_4OH, had high affinity towards water. The coating depletion took place due to the action of moisture during accelerated aging. Also, bark extracts were soluble in water; therefore, they might migrate from the wood surface as well. The coating thickness was another factor. Due to very low coating thickness and high affinity towards water, even after short span of aging,

no protection was left on the surface. Another important factor could be their (soy polymer coating) highly basic nature which prevented the normal ESIPT mechanism to take place for UV absorbers.

4.5. Aging of Acrylic Polyurethane Coated Wood

4.5.1. General

Water based acrylic polyurethane coatings have wide applications and was chosen for this study because of their high durability characteristics in accelerated aging environment, upgraded film properties, and environmentally friendliness [139, 140, 143]. From durability point of view, colored products are often added to coating materials, but this affects negatively the aesthetic nature of the end product. The transparency of the coating material is one of the most important factors for heat-treated wood from consumer's perspective so that its attractive darker color is preserved for decorative purposes. But, transparent coatings allow sunlight to reach to the wood surface which enables the onset of the photochemical reactions leading to change of color and loss of gloss of the surface. To overcome this shortcoming of transparent coatings, UV stabilizers are often added as an additive to the coating formulations.

In this section, the results are presented for the three heat-treated wood species which were used to test the effectiveness of different coatings with acrylic polyurethane base (acrylic polyurethane with different combinations of bark extracts, CeO_2 nano particles, lignin stabilizer compared with commercially available organic UV stabilizers, and industrial Laurentide coating). One soft wood species (heat-treated jack pine) and two hard wood species (heat-treated aspen and birch) were taken into consideration in order to investigate coating's durability under accelerated aging conditions. The results for the acrylic polyurethane with titania and ZnO particles are presented in Appendix 2 and acrylic

polyurethanes with needle extracts alone or together with lignin stabilizers are reported in Appendix 3.

4.5.2. Affinity of Coatings towards Wood Surface

The wetting characteristics of different acrylic polyurethane coatings on heat-treated jack pine revealed that the contact angle of the acrylic polyurethane coating with CeO_2 nano particles was smallest (better wetting) compared to other acrylic polyurethane coatings (Figure 4.20). This was due to the fact that CeO_2 nano particles were dispersed in water with the help of surfactants. Therefore, addition of CeO_2 nano particles to the coating formulation increased its water content and added some surfactants as well. This lowered the surface tension and also viscosity of the coating which eventually resulted in better wetting. However, the initial contact angles of all the acrylic polyurethane coatings were below 90° showing that there were good contact with heat-treated jack pine and these coatings. For all the coatings, contact angle started changing as soon as coating materials came in contact with wood surface. After approximately 10 s, the contact angle reached to an equilibrium point for all the coatings. The acrylic polyurethane coating with bark extract showed slightly bigger equilibrium contact angle compared to acrylic polyurethane coating with CeO_2 nano particles and almost similar equilibrium contact angle with acrylic polyurethane coating containing CeO_2 nano particles and lignin stabilizer. Bark extract and lignin stabilizer containing acrylic polyurethane coating exhibited slightly larger contact angle compared to that of acrylic polyurethane coating containing bark extract. The largest equilibrium contact angle was observed for the coating with CeO_2 nano particles, lignin

stabilizer and bark extract whereas the coating containing CeO_2 nano particles and bark extract showed slightly smaller contact angle than that of the former coating (Figure 4.20). On the other hand, acrylic polyurethane coating without light stabilizers showed larger equilibrium contact angle compared to that of acrylic polyurethane coatings containing CeO_2 nano particles; bark extracts; lignin stabilizer; CeO_2 nano particles and lignin stabilizers. Larger contact angle means less wetting which also means lower adhesion between coating and wood. The difference in contact angle was mainly due to the difference in percentage of solids (additives) in the coating materials (Figure 4.23) and surface tensions of the coatings. Increase in solid percentage increased the viscosity and higher surface tension of the coating which eventually resulted in larger contact angle and decrease in wetting.

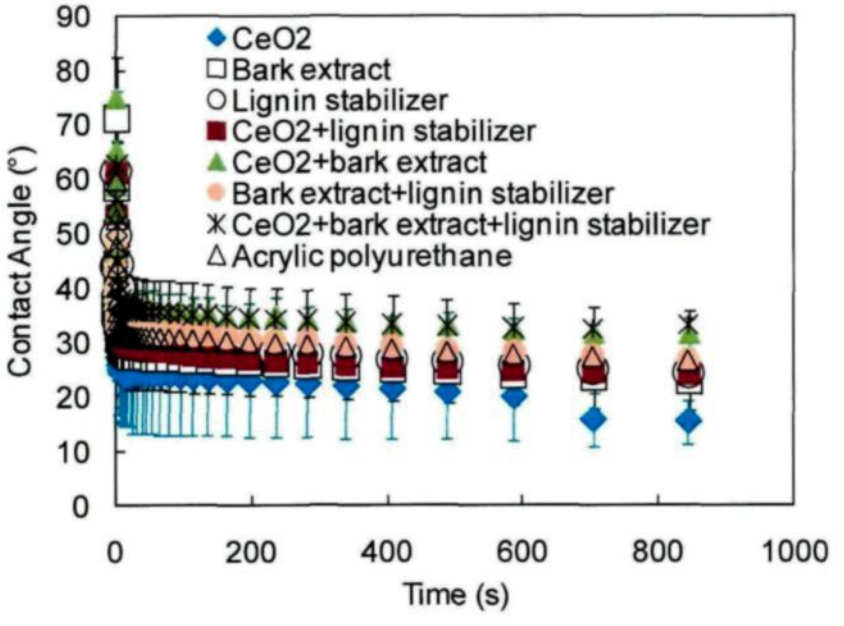

Figure 4.20 Dynamic contact angle of acrylic polyurethane coatings on heat-treated jack pine with or without light stabilizers

These coatings showed similar wettability trends on heat-treated aspen as on heat-treated jack pine, with the exception of acrylic polyurethane containing bark extract and lignin stabilizer (Figure 4.21). This coating surprisingly showed smaller equilibrium contact angle compared to all other coatings, other than acrylic polyurethane with CeO_2 nano particles. Latter coating exhibited smallest contact angle on heat-treated aspen whereas largest contact angle was observed for both CeO_2 nano particles and bark extract containing acrylic polyurethane and CeO_2 nano particles, bark extract, and lignin stabilizer containing acrylic polyurethane. Other than acrylic polyurethane without any light stabilizer and with bark extract and lignin stabilizer, the increase in equilibrium contact angle for all other coatings was found to be directly proportional to their solid content on heat-treated aspen (Figure 4.23).

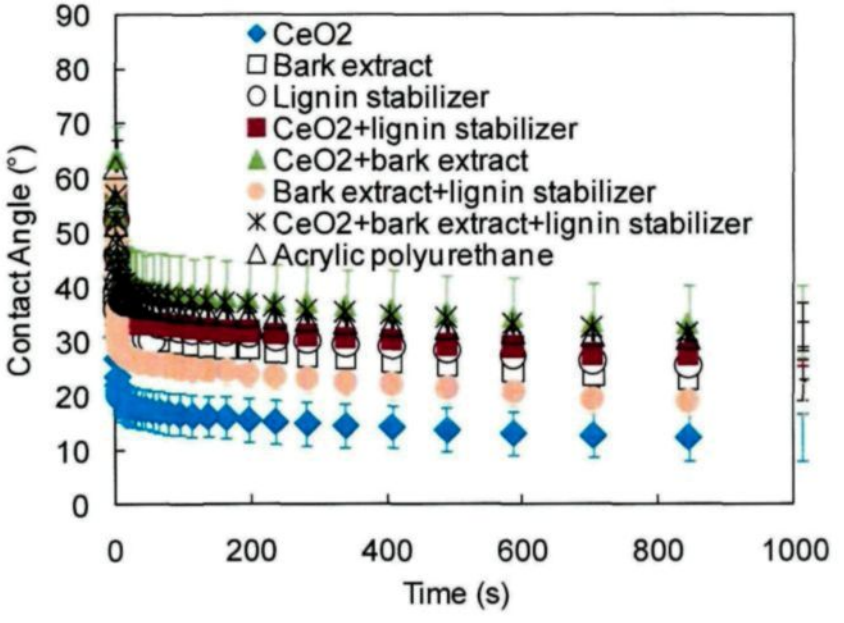

Figure 4.21 Dynamic contact angle of acrylic polyurethane coatings on heat-treated aspen with or without light stabilizers

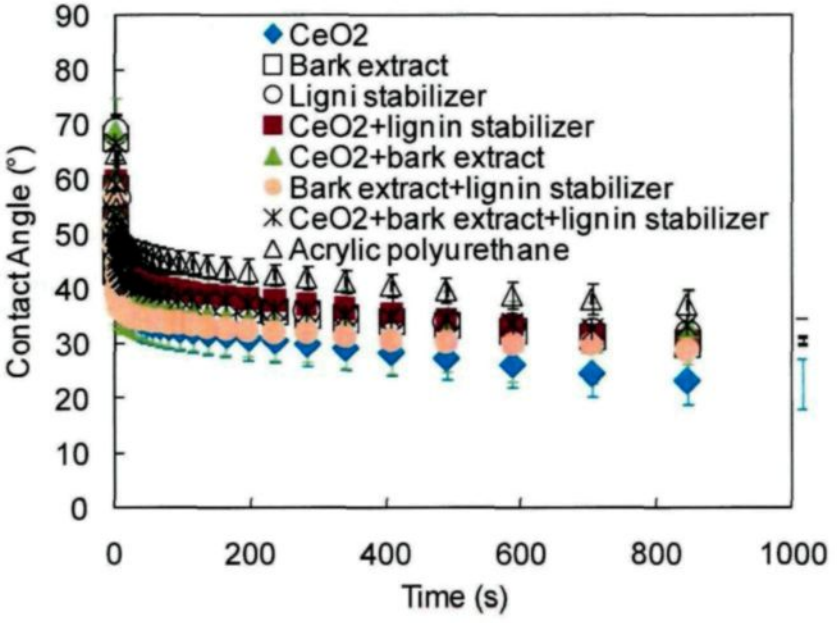

Figure 4.22 Dynamic contact angle of acrylic polyurethane coatings on heat-treated birch with or without light stabilizers

The wetting characteristics of acrylic polyurethane coatings on heat-treated birch did not follow the same trend as on heat-treated jack pine or aspen. After 10s of contact time between coatings and heat-treated birch, contact angle change rate decreased considerably (Figure 4.22). After this point also contact angle decreased slowly with time for all coatings. This was probably due to the ongoing penetration of the coatings through the pores. All the equilibrium contact angles clustered between 35° to 50°. Although smallest equilibrium contact angle was observed for acrylic polyurethane with bark extract and lignin stabilizer, at the end of wetting process, acrylic polyurethane with CeO_2 nano particles exhibited smallest contact angle. Largest contact angle was observed for acrylic polyurethane without light stabilizers.

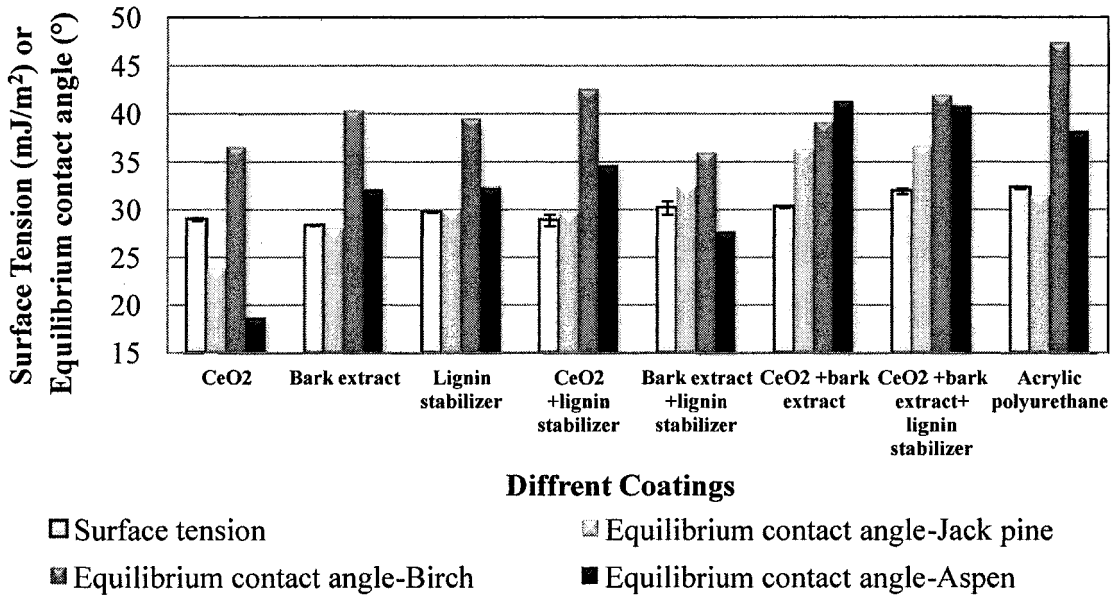

Figure 4.23 Surface tensions and equilibrium contact angles of acrylic polyurethane coatings on heat-treated jack pine, aspen and birch with or without light stabilizers

4.5.2.1. Effect of Capillary Penetration of Coatings

In this section only four coatings (acrylic polyurethane with bark extracts; with lignin stabilizers, with bark extracts and lignin stabilizer and without light stabilizers) and heat-treated jack pine are considered since they were found to be most promising.

The surface tension affects the wetting properties of coatings. Figure 4.23 compares the surface tension of acrylic polyurethane coatings with or without light stabilizers. The surface tension of acrylic polyurethane coating without light stabilizers was found to be higher than the surface tensions of acrylic polyurethane coatings with light stabilizers. This was probably due to the presence of polar groups (OH groups on the surface) in UV

stabilizers. Lowest surface tension was observed for coating containing bark extract whereas highest surface tension was pertained by acrylic polyurethane coating without light stabilizers. With the exception of coating without light stabilizers, equilibrium contact angle increased with increasing surface tension. Other than some small exception, the surface tension increase was directly proportional with the increase in solid content of the coatings. For example, the solid content of acrylic polyurethane coating without light stabilizers was lower compared to that of the coating with light stabilizers; therefore, it had higher surface tension. This was most likely due to the addition of hydrophilic light stabilizers which lowered the surface tension of acrylic polyurethane coatings with bark light stabilizer.

The contact angle of a liquid on a porous substrate depends on interfacial forces and highly affected by capillary penetration as reported in literature [72]. In this study, the degree of capillary penetration was evaluated by monitoring the height and diameter change of the drop as a function of time and also by calculating the drop's volume according to Equations 4.1 and 4.2. The first model (see Eqn 4.1) which uses the height (h) and diameter (d) to calculate the drop volume was proposed by Liptakova and Kudela (1994) [36] whereas Denesuk et al. (1993) [175] derived the second model (see Eqn 4.2) to compute the drop volume using diameter of the drop and contact angle (θ).

$$V_d = \frac{\pi}{6} h \left[3\frac{d^2}{4} + h^2 \right] \qquad [4.1]$$

$$V_d = \frac{\pi}{3}(0.5d^3)\frac{(1-cos\theta)(cos\theta+2)}{sin\theta(cos\theta+1)} \quad [4.2]$$

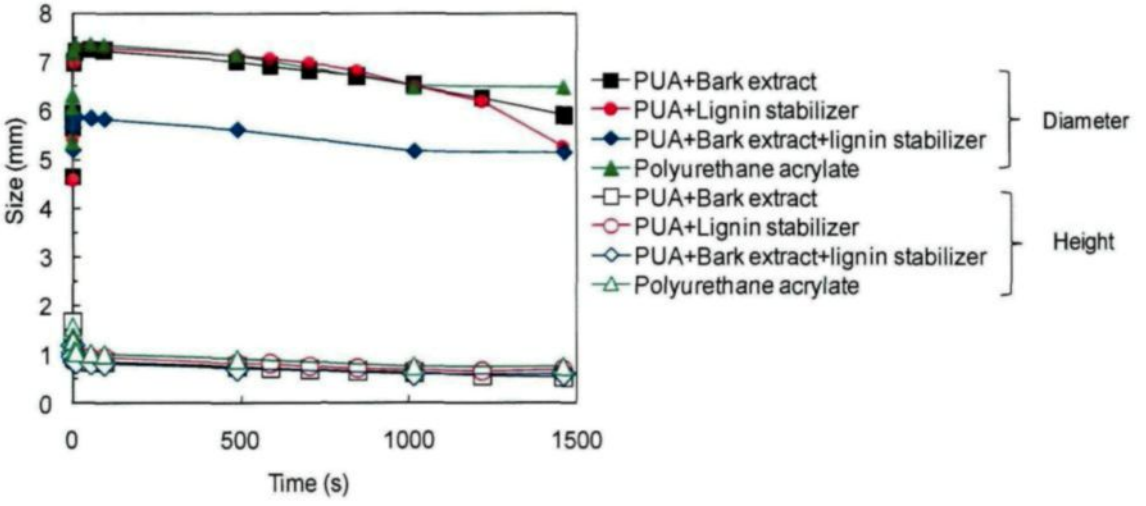

Figure 4.24 The drop height and diameter change with time for acrylic polyurethane coatings with or without light stabilizers

The height of drops started decreasing as soon as the coatings came in contact with the wood surface. As shown in Figure 4.24, the change of drop height with time was found to be similar for all the four coatings. The diameter of drop was initially increased up to about 50s and decreased slightly thereafter for all the four coatings. The increase in diameter was the indication of spreading of the coating drop on wood surface. Decrease in diameter was most probably due to the ongoing penetration of the coating materials into the wood. The least spreading was observed for coating containing bark extract and lignin stabilizer whereas most spreading was noticed for coating containing bark extracts or lignin stabilizer (Figure 4.24). This type of phenomenon was also observed with the alkyd based

high solid containing coating, traditional solvent borne alkyd resin paint, and water borne acrylic binder wetting properties on spruce and pine sapwood as reported by de Meijer et al. (2001) [176]. Since wood is a porous material capillary penetration of the coatings took place along with spreading.

The volumetric changes of the coating drops on heat-treated and planed jack pine with time were calculated using Equations 4.1 and 4.2 and similar results were obtained from both equations (Figure 4.25). Other than acrylic polyurethane coating containing bark extract and lignin stabilizer, the drop volume seemed to increase for initial 10 seconds and after that decreased with increasing contact time. The initial increase in drop volume was due to rapid increase in diameter mainly along the grain of the wood surface for initial time of contact although drop height decreased slightly. The volume of the drop calculated in this study was dependent on the spreading of the drop along the grain. The spreading of the drop along the grain was much higher than across the grain leading to an increase in volume of the drop (assumed spherical but actually elliptical) for initial 10 seconds. The drop volumes of the coating containing bark extract and lignin stabilizer decreased as soon as it came in contact with wood surface. The decrease in volume of the drops was due to the penetration of coatings material into the wood as well as evaporation of water from the coating drops.

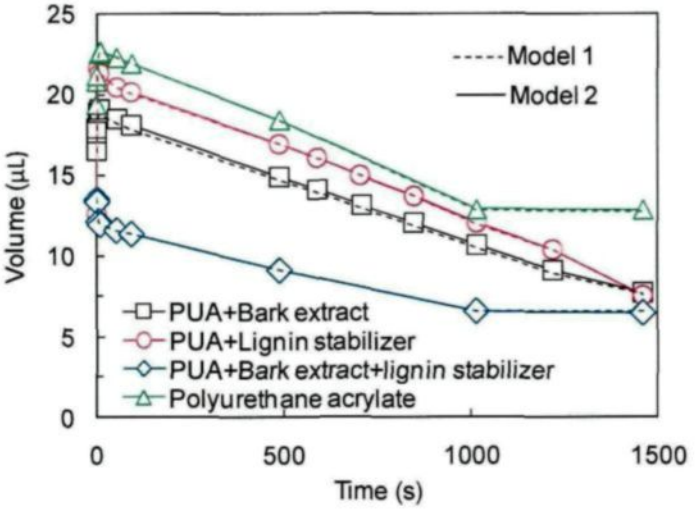

Figure 4.25 Change of drop volume with time for acrylic polyurethane coatings with or without light stabilizers

The model 2 was used to calculate the volumetric changes of the drops vs. contact time as a function of experimentally measured contact angle change (see Eqn. 4.2). The rate of volumetric capillary penetration of the coatings was calculated by using Equation 4.3 [176] are given below.

$$\frac{V_P}{V_0} = \frac{V_0 - V_t}{V_0} = b\sqrt{t} \qquad \text{and} \qquad V_0 = V_t + V_P \qquad [4.3]$$

V_P: volume of coating penetrated into the wood

V_t : volume of drop at time t

V_0: volume of drop at t=0

t: time

b: rate constant

For all the samples, there were fairly good linear relationship between square root of time and fractional penetrated coating volume for initial about 100s with r^2 (correlation coefficient) values of 0.89 or higher. The median rate constant values (s) were calculated because the rate constant values were not normally distributed [176]. This suggested early diffusion of water from the coatings through the cell wall.

The capillary penetration rate varied with different UV stabilizers (Table 4.7). The fastest penetration rate was observed for coating containing bark extract and lowest penetration rate was exhibited by coating containing bark extract and lignin stabilizers. The capillary penetration rate results directly support the contact angle results. Polyurethane acrylate without light stabilizers had lower penetration rate due to the higher surface tension compared to the polyurethane acrylate with bark extract or lignin stabilizer. On the other hand, polyurethane acrylate with bark extract and lignin stabilizer had lower surface tension but lower capillary penetration rate compared to that of the acrylate polyurethane without light stabilizers. This was due to the continuous absorption of water into cell wall and continuous evaporation of water to the environment from the drop which resulted in rapid increase in viscosity and solid matter content in the drop.

Table 4.7 Median rate of capillary penetration for acrylic polyurethane coatings with or without light stabilizers

Coatings	Capillary penetration rate ($s^{-1/2}$)
PUA+Bark extract	-0.024
PUA+Lignin stabilizer	-0.022
PUA+Bark extract+lignin stabilizer	-0.018
Polyurethane acrylate	-0.02

4.5.2.2. Effect of Mechanical Surface treatment

In this section, influence of mechanical surface treatment of heat-treated jack pine on wetting of acrylic polyurethane with bark extract and lignin stabilizer has been discussed. Surface anatomy plays an important role on the wetting process. Two types of surface treatments were scrutinized in this study – sanding and planing. Four different grit papers were used to study the effect of sanding on wetting of the wood by coating. Also, the effect of different surfaces (radial and tangential) along with different mechanical surface treatments on wetting was studied.

Liptakova et al. (1995) [57] compared three different surface treatments – microtoming, milling and grounding and found that mechanical treatments not only change the morphological structure of wood but also the chemical composition of wood surface layer. Sinn et al. (2004) [58] in a later study investigated changes of surface properties of beech and spruce wood due to sanding. The results in this study revealed that contact angle of the acrylic polyurethane coating on heat-treated jack pine reached to equilibrium value both on

tangential (Figure 4.26a) and radial surfaces (Figure 4.26b) irrespective of surface treatments within 10s of contact. Wood cells usually compressed during planing but if the compression is very strong, subsequent expansion of the cells can lead to high grain rising which results in premature cracking of the coating. The mode of wood surface treatment was found to be an important factor in wood/coating wetting process. There was an increase in equilibrium contact angle for both radial and tangential heat-treated jack pine when the surface was sanded by 120 grit paper compared to that of the planed surface. During sanding wood fibers and other cellular elements were torn out, mechanically distorted and even crushed which then were pressed into the pores together with wood dust resulting in lower surface roughness. Increase in equilibrium contact angle was due to the decreased wood surface porosity during sanding compared to planing. This increase was more on radial surface compared to that of tangential surface since radial surfaces were affected more by sanding compared to tangential surfaces. Usually wood surface roughness decreases with increase in grain size of the sand papers. It was quite surprising to notice the lowest equilibrium contact angle on both radial and tangential surfaces at mid grain size sanded wood surface (Figure 4.27). These results are in accordance with the results reported by Sinn et al. (2004) [58]. The equilibrium contact angle was lower after wood surfaces sanded with 150 grit paper compared to 120 grit papers. This was due to the smoothening of the surface which increased the spreading rate. The increase in equilibrium contact angles took place after sanding the wood surface with 180 and 220 grit papers. This could be explained by the fact that although the surface became smoother (faster spreading) with increasing grit number of the sanding papers, the wood pores get

completely blocked which suppressed the penetration of the coatings. Sinn et al. (2004) [58] also noticed that the surface chemistry was altered during sanding which is attributed to increase in lignin content due to the blockage of pores with wood dust.

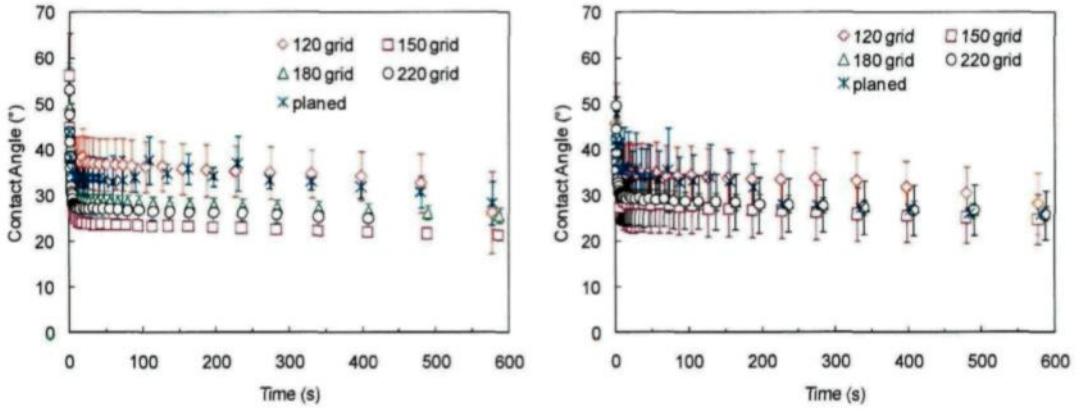

(a) (b)

Figure 4.26 The effect of mechanical surface treatment on wetting of acrylic polyurethane coating containing bark extract and lignin stabilizer-wood system on (a) radial, (b) tangential surfaces

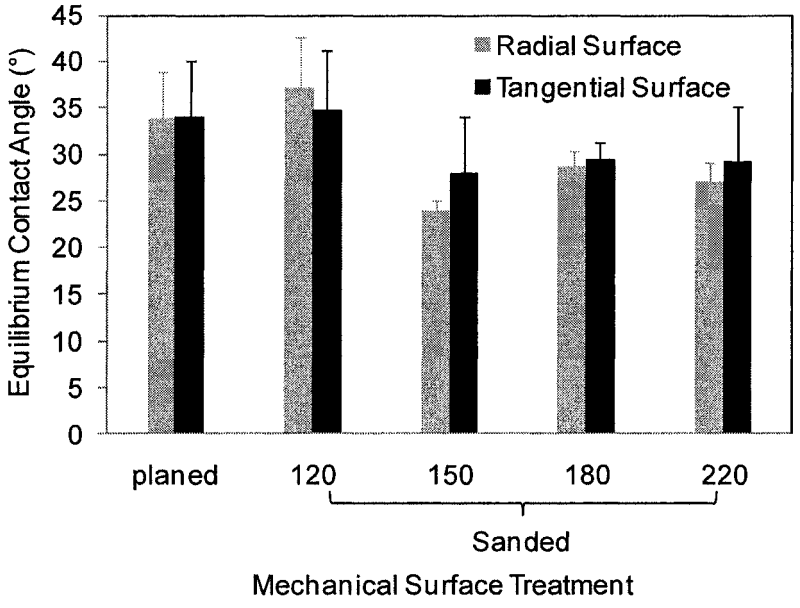

Figure 4.27 The effect of mechanical surface treatment on wetting equilibrium contact angle of acrylic polyurethane coating containing bark extract and lignin stabilizer-wood system

4.5.3. Color Measurement

The accelerated aging tests were carried out in order to study the effect of UV/VIS exposure on color change of coated and heat-treated wood within a shorter time span compared to that of natural aging.

4.5.3.1. Heat-treated Jack Pine

The color measurement data suggested that, other than industrial coating and acrylic polyurethane coating containing CeO_2 nano particles and lignin stabilizer, all the other coatings became greener (Figure 4.28a) with increasing aging time. Only industrial coating and acrylic polyurethane with CeO_2 nano particles and lignin stabilizer became redder. The acrylic polyurethane with CeO_2 nano particles exhibited least variation in red–green index while acrylic polyurethane coating containing organic UV absorber showed most variation of the same index. The acrylic polyurethane coating without light stabilizers, acrylic polyurethane coating containing organic UV stabilizers, and acrylic polyurethane with lignin stabilizer demonstrated bluish nature whereas other coatings showed yellowish nature after 1500h of aging. For acrylic polyurethane coatings with bark extracts, CeO_2 nano particles, bark extracts and lignin stabilizers, and industrial Laurentide coating, the yellow–blue index increased during the initial stages of aging. This was followed by a decrease in the same index though extent of this change was less for industrial coating (Figure 4.28b). The most change in yellow–blue index was observed for base acrylic polyurethane coating, conversely, the least variation of the same index was observed for

the acrylic polyurethane coating containing bark extracts with or without lignin stabilizer, and CeO_2 nano particles.

The lightness of all the coatings increased with aging time; however, lightness variation of industrial Laurentide coating was less for initial 1100h of accelerated aging (Figure 4.28c) compared to those of coatings developed during this study. After 1100h of aging, the acrylic polyurethane coatings containing bark extract or CeO_2 nano particles pertained least lightness variation. The most change in lightness index was observed for the base acrylic polyurethane coating. The acrylic polyurethane coating stabilized with organic UV stabilizers also exhibited very high lightness index change. The acrylic polyurethane coating containing lignin stabilizer showed almost similar lightness variation as the acrylic polyurethane coating containing bark extract and lignin stabilizer; however for initial period of aging, the former coating showed comparatively more variation in lightness index. The acrylic polyurethane with CeO_2 nano particles and lignin stabilizer showed similar lightness index variation as industrial Laurentide coating.

The most color change was detected for the base acrylic polyurethane coating (Figure 4.28d) nevertheless the acrylic polyurethane coating stabilized by organic UV stabilizers also showed a significant total color change after 1500h of aging. The acrylic polyurethane coating containing CeO_2 nano particles pertained highest protection (Figure 4.28d) among all coatings during the accelerated aging test. Although, at the end of 1500h of aging, acrylic polyurethane coating containing bark extracts showed similar total color change as that of acrylic polyurethane with CeO_2 nano particles. Similar protective characteristics were observed for the acrylic polyurethane coating containing bark extract alone or with

lignin stabilizer, acrylic polyurethane with CeO_2 nano particles and lignin stabilizer, and the industrial Laurentide coating during initial 400h of aging but the color of acrylic polyurethane coating containing bark extract and lignin stabilizer varied less compared to the color of the industrial coating and acrylic polyurethane containing CeO_2 nano particles and lignin stabilizer from 400h to 1400h of aging. The acrylic polyurethane coating with bark extract exhibited better protection throughout compared to the industrial coating. The acrylic polyurethane coating containing lignin stabilizer also showed high protective characteristic. High UV/VIS resistance of industrial coating was expected as it is a highly pigmented (almost green and opaque) solvent based coating which tends to cover the natural grain texture of heat-treated jack pine surface completely. Also, this coating contains some toxic substances. On the other hand, the acrylic polyurethane is transparent, non-toxic and water borne coating which contains natural antioxidant or CeO_2 nano particles with or without a very small amount of lignin stabilizer. This study showed that acrylic polyurethane coating containing bark extract, CeO_2 nano particles and lignin stabilizer alone or together can replace effectively the pigments and organic UV stabilizers which are used for slowing down the degradation of wood in outer environment.

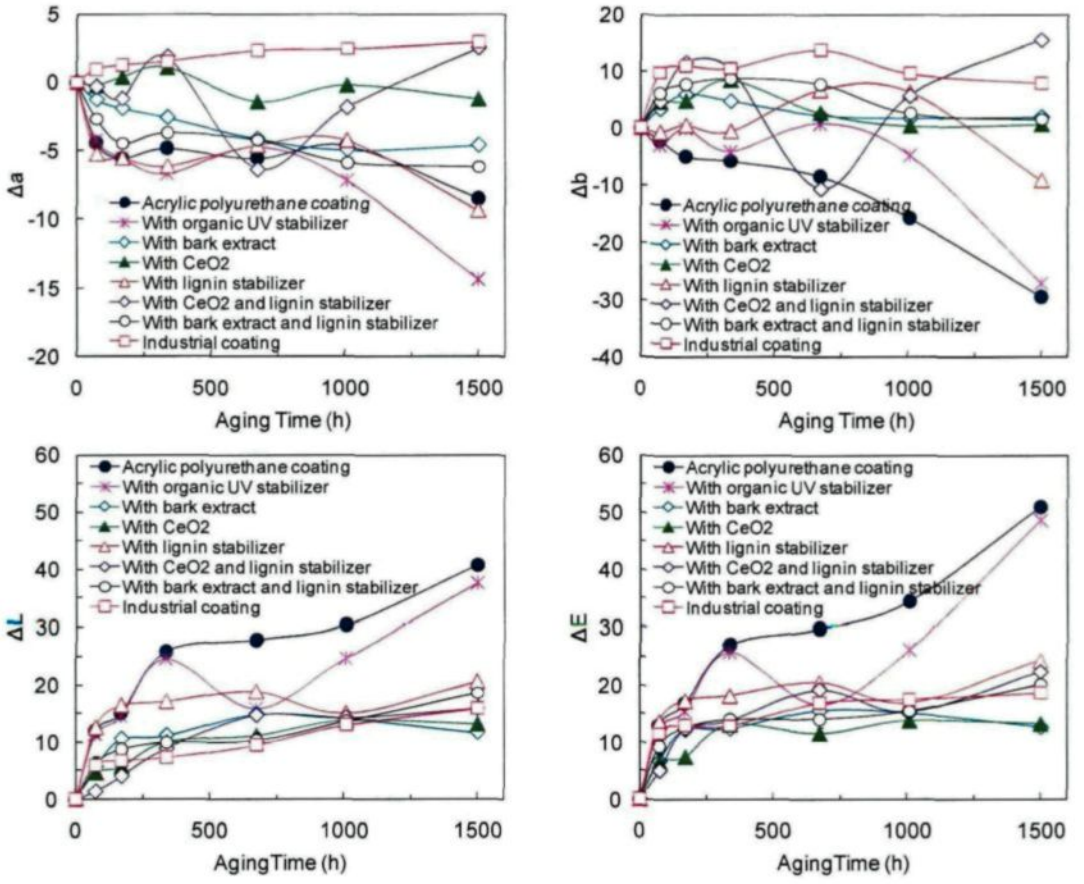

Figure 4.28 Comparison of color change of heat-treated jack pine coated with acrylic polyurethane with or without light stabilizers and commercially available Laurentide coating after different aging period (a) red-green index, (b) yellow-blue index, (c) lightness index, and (d) total color change

4.5.3.2. Heat-treated Aspen

For heat-treated aspen, all the coatings became greener after aging for 1500h (Figure 4.29a). The most change in red-green index was observed for acrylic polyurethane coatings with organic UV stabilizers and lignin stabilizer. The least change in the same index was pertained by acrylic polyurethane coatings with CeO_2 nano particles alone or together with lignin stabilizer. Other than acrylic polyurethane containing CeO_2 nano particle with or without lignin stabilizer and industrial Laurentide coated heat-treated aspen, all the other coatings on heat-treated aspen after accelerated aging for 1500h became bluish in nature whereas former three coatings turned yellowish after aging (Figure 4.29b). The least variation of yellow-blue index was noticed for acrylic polyurethane with bark extract and lignin stabilizer whereas most change in the same index was observed for acrylic polyurethane without light stabilizer and industrial Laurentide coating. After aging all coated heat-treated aspen surfaces became lighter in nature (Figure 4.29c). The most variation in lightness was observed after accelerated aging for acrylic polyurethane with lignin stabilizer with or without bark extracts. The least change in lightness index was exhibited by industrial Laurentide coating. Acrylic polyurethane containing CeO_2 nano particles and lignin stabilizer showed almost similar lightness index variation that of industrial Laurentide coating for final 500h of accelerated aging (after 1000h of aging). The most total color change at the end of accelerated aging was observed for acrylic polyurethane with lignin stabilizer according to color measurement data (Figure 4.29d). Industrial Laurentide coating showed least total color variation for initial 672h of aging, after that acrylic polyurethane containing CeO_2 nano particles and lignin stabilizer

demonstrated least total color change. After 672h of aging, acrylic polyurethane with CeO_2 nano particles also showed less color change compared to industrial Laurentide coating.

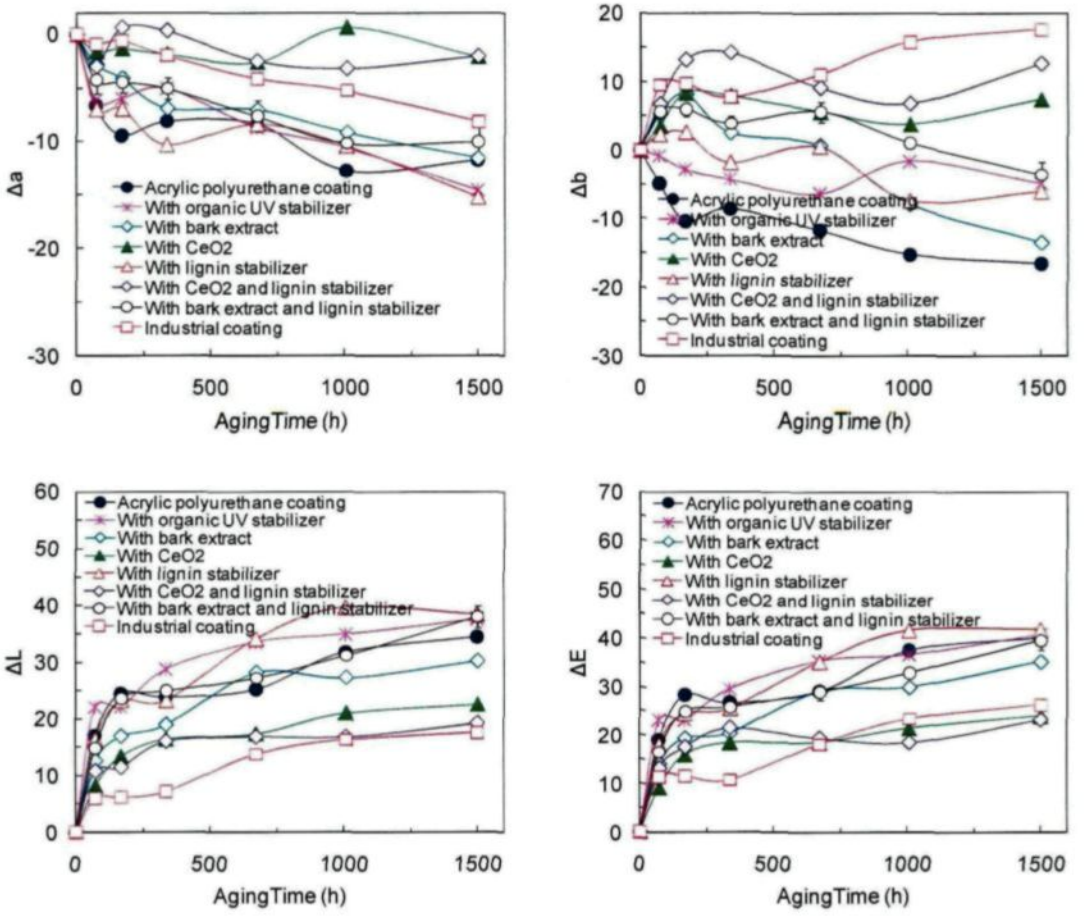

Figure 4.29 Comparison of color change of heat-treated aspen coated with acrylic polyurethane with or without light stabilizers and commercially available Laurentide coating after different aging period (a) red-green index, (b) yellow-blue index, (c) lightness index, and (d) total color change

4.5.3.3. Heat-treated Birch

For heat-treated birch, other than acrylic polyurethane coating with CeO_2 nano particles and lignin stabilizer, all other coated heat-treated birch surface became greener after aging (Figure 4.30a). Least change in this index was displayed by industrial Laurentide coating, whereas most change was observed for acrylic polyurethane without light stabilizers. The acrylic polyurethane coating with CeO_2 nano particles alone or together with lignin stabilizer and industrial Laurentide coated heat-treated birch surfaces demonstrated yellowish nature after aging whereas all other coatings on heat-treated birch exhibited bluish nature (Figure 4.30b). Least change in this index was observed for acrylic polyurethane with bark extract and lignin stabilizer. On the other hand, most change in the same index was noticed for acrylic polyurethane without light stabilizers. The least lightness index change was observed for industrial coating, but for initial 600h of aging acrylic polyurethane with CeO_2 nano particles and lignin stabilizer coated heat-treated birch showed least lightness variation (Figure 4.30c). The most change in lightness variation was noticed for acrylic polyurethane without light stabilizers. Acrylic polyurethane coatings with bark extracts and/or lignin stabilizer also showed very significant lightness index variation. The total color measurement results (Figure 4.30d) revealed least total color variation for acrylic polyurethane with CeO_2 nano particles and lignin stabilizer coated heat-treated birch for initial 1050h of accelerated aging. Thereafter industrial coating showed least total color variation however, the difference between PUA containing CeO_2 with and without lignin stabilizer was not significant. Most color change was observed for acrylic polyurethane without light stabilizers. Acrylic polyurethane with

organic UV stabilizers and bark extracts and/or lignin stabilizers also showed a significant color change at the end of aging test.

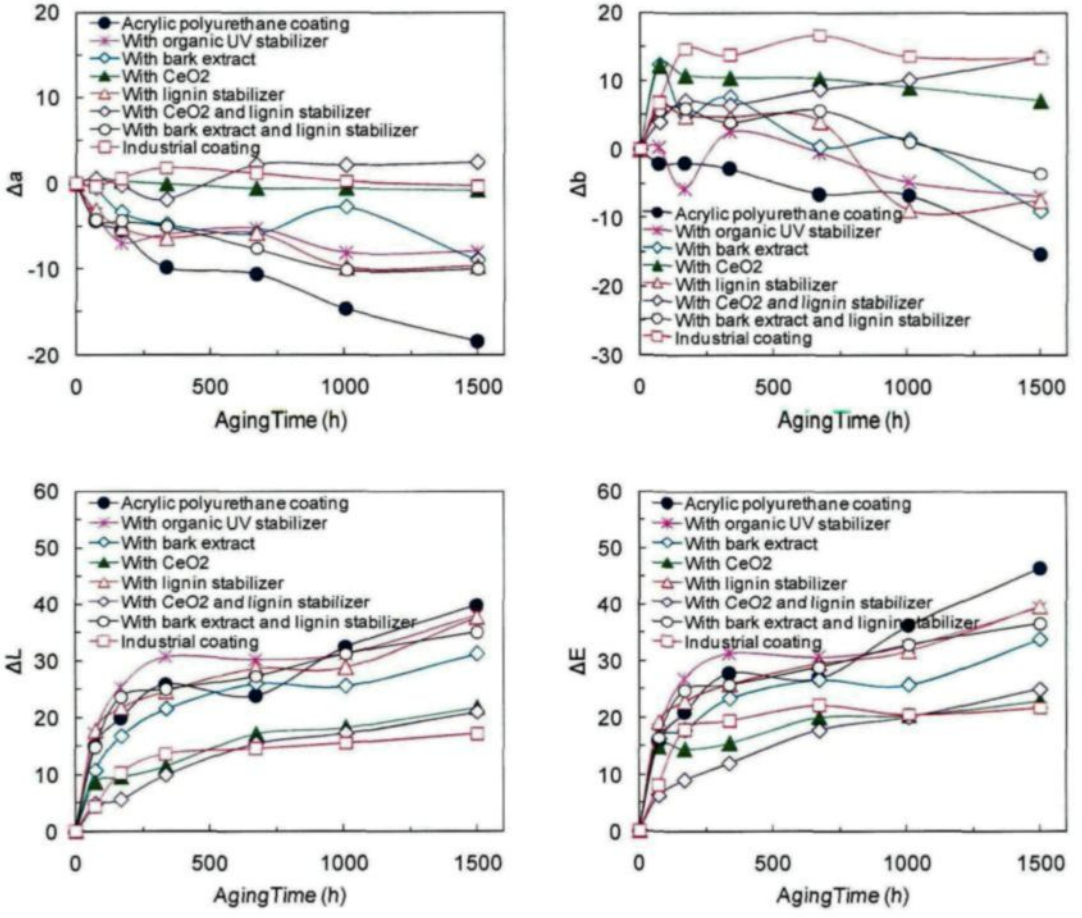

Figure 4.30 Comparison of color change of heat-treated jack birch coated with acrylic polyurethane with or without light stabilizers and commercially available Laurentide coating after different aging period (a) red-green index, (b) yellow-blue index, (c) lightness index, and (d) total color change

Acrylic polyurethane coating containing bark extract alone or together with lignin stabilizer showed slight color change on heat-treated jack pine whereas on heat-treated aspen it exhibited very significant color change and on heat-treated birch, it showed moderate color change. On the contrary, acrylic polyurethane with CeO_2 nano particles alone or together with lignin stabilizer protected well against aging for all the three heat-treated wood species.

Comparing the protective characteristics of the same coatings on heat-treated jack pine with that on heat-treated aspen and birch revealed that coatings worked much better on heat-treated jack pine. There could be several reasons for this difference:

- The total percentage of lignin in heat-treated jack pine (35%) is more than the lignin percentage in heat-treated aspen (26%) and birch (26%).
- Also lignin present in softwood jack pine is generally guaiacyl lignin which is mainly composed of coniferyl alcohol units. Guaiacyl-syringyl lignin, on the other hand, contains monomeric units from coniferyl and sinapyl alcohol which is mainly found in hardwoods (aspen and birch). Pandey and Tapani in 2008 [177] reported that the syringyl moieties of the lignin are more sensitive to UV light than the guaiacyl units which resulted in higher degradation rate of lignin in hardwoods compared to softwoods.
- The extractives present on the jack pine surface are different than those of birch and aspen.

- Due to the porous nature of the aspen and birch (presence of vessels), the coating materials penetrate more and eventually the coating thickness decreases faster on aspen and birch compared to on jack pine.

4.5.4. Visual Assessments

The visual assessment is very important from end user's perspective as this is the main factor which accounts for coating's durability and period for repainting the substrate surface.

4.5.4.1. Jack pine

The visual assessment of different coatings on heat-treated jack pine revealed that the base acrylic polyurethane coating showed poor protective characteristics starting from the initial period of aging and became completely white at the end of 1500h of aging (Figure 4.31). On the other hand, the acrylic polyurethane coating with organic UV absorbers displayed better protection than the base coating but also underwent heavy color loss (Figure 4.31). Small cracks were formed on the surface after 1500h of aging for both of the above mentioned coatings. When the acrylic polyurethane coating was stabilized with bark extract, it became highly efficient in protecting the heat-treated jack pine surface from aging. According to naked eye evaluation, almost no color change was observed for this coating with the exception of two or three local degradation points (small white patches) at the end of 1500h of aging. On the other hand, acrylic polyurethane coating containing lignin stabilizer demonstrated significant degradation at the edges after 1008h of aging and the coating degradation started only after 672h of aging. The acrylic polyurethane coating

containing bark extract and lignin stabilizer was one of the three most efficient coatings for the protection of heat-treated jack pine, developed during this study and no degradation was observed with naked eye for this coating even after 1500h of aging (Figure 4.31). Very small color change (became slightly lighter) was detected for this coating but the color change was homogeneous. Acrylic polyurethane coatings containing CeO_2 nano particles alone or together with lignin stabilizer were other two coatings which showed significant protection against aging of heat-treated jack pine. For coating containing CeO_2 nano particles, no degradation on the surface was found although the surface became slightly lighter at the end of 1500h of aging. In contrast, for coating containing CeO_2 nano particles and lignin stabilizers almost no color change was detected at the end of 1500h of aging. The industrial coating, although it covered fully the heat-treated jack pine surface, did not protect the surface completely. Local degradation started only after 672h of accelerated aging and complete degradation took place after 1500h of aging (Figure 4.31). The cracks and fissures were also observed on the surface after 1008h of aging for this coating.

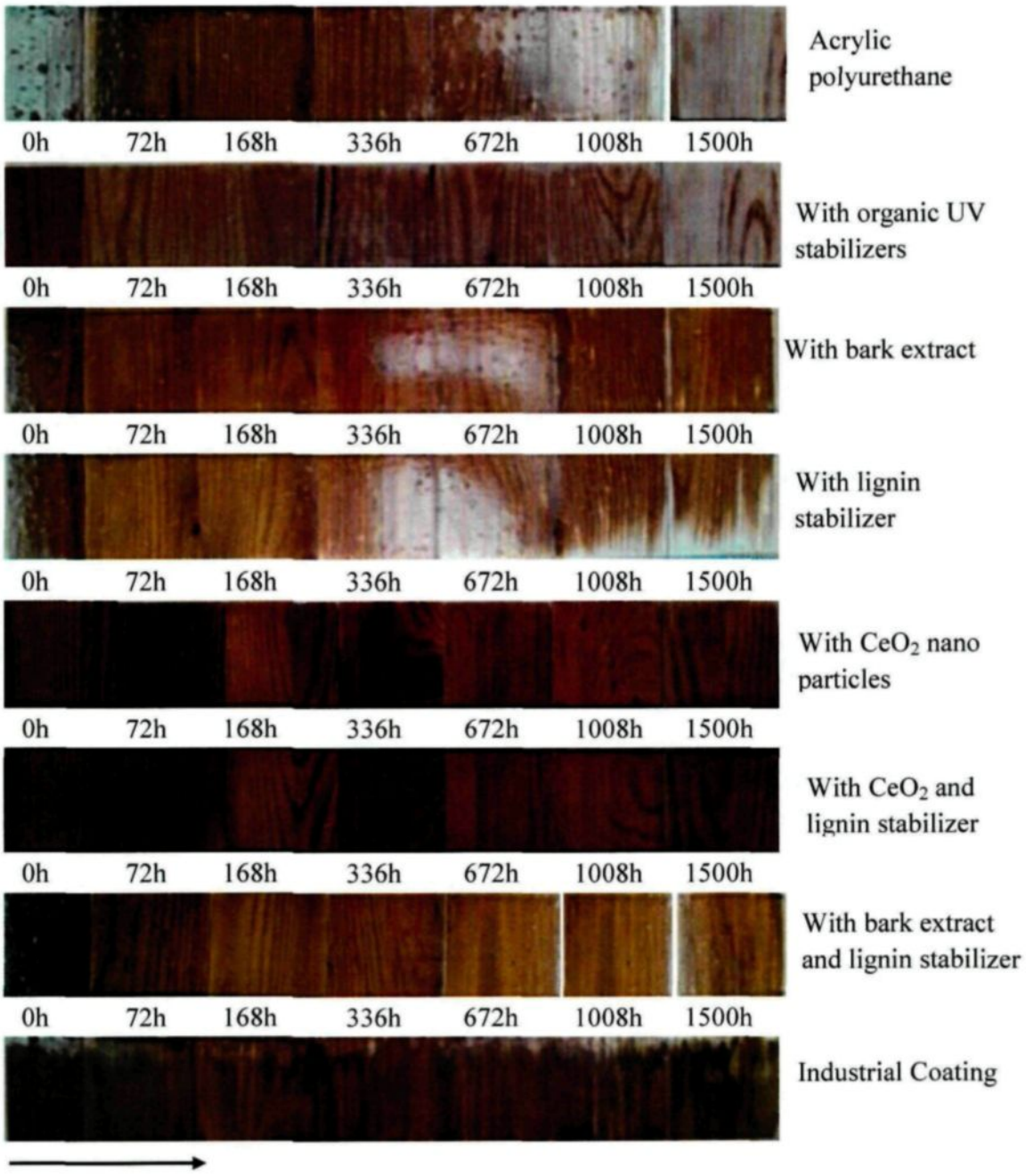

Figure 4.31 Visual assessment of coated heat-treated jack pine for different aging times

4.5.4.2. Aspen

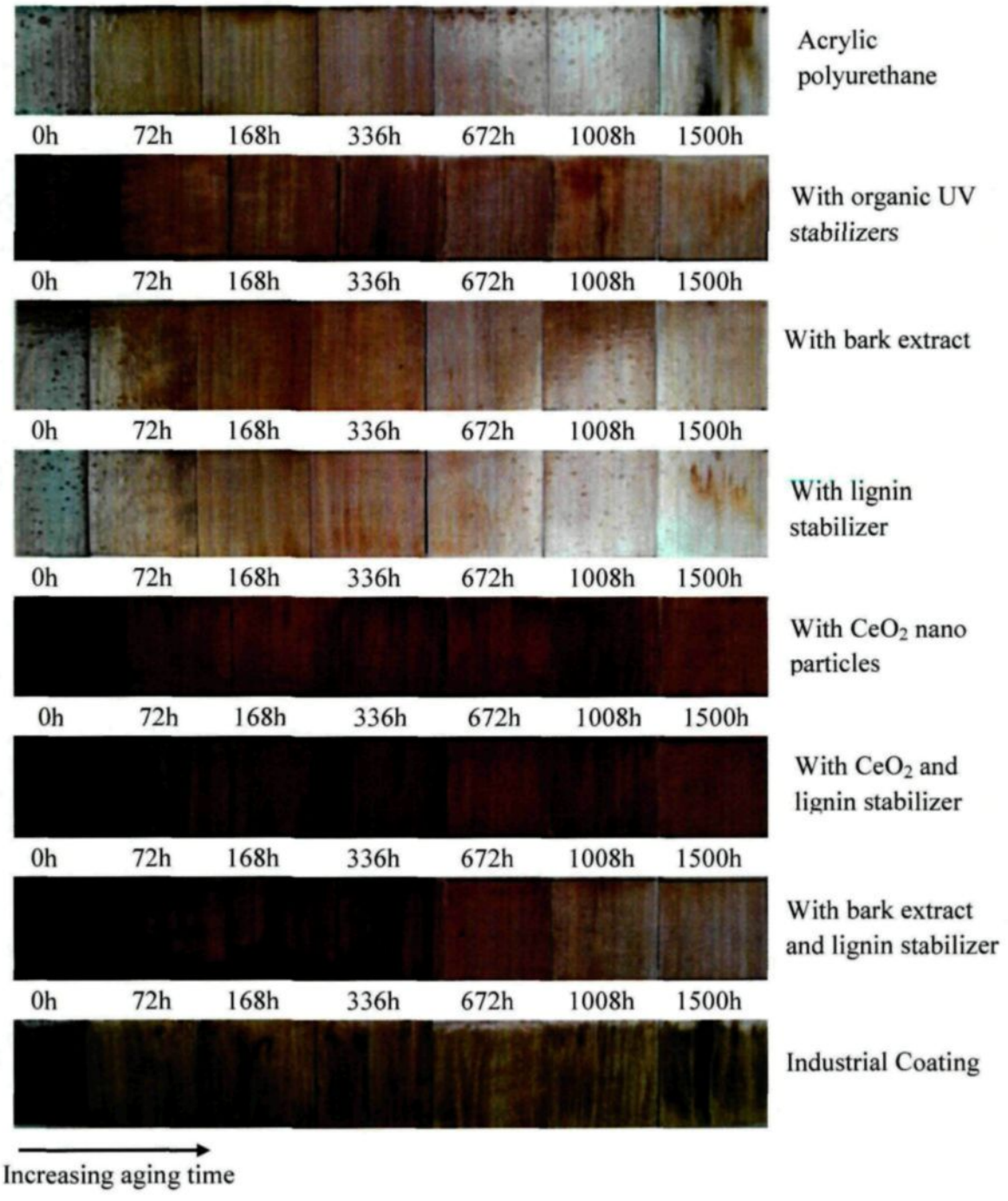

Figure 4.32 Visual assessments of coated heat-treated aspen for different aging times

Acrylic polyurethane with or without UV stabilizers or lignin stabilizer did not protect heat-treated aspen surface and color of wood started to change at the very initial stage of aging (within 72h) and became almost white at the end of 1500h of aging (Figure 4.32). Although acrylic polyurethane with bark extracts showed considerable resistance against accelerated aging on heat-treated jack pine, significant color change was observed for this coating on heat-treated aspen as early as 336h of aging. In contrast, coatings with CeO_2 nano particles alone or together with lignin stabilizer protected aspen well from aging and color changes were minimal (slightly lighter but homogeneous) at the end of 1500h of aging. Acrylic polyurethane with bark extract and lignin stabilizer protected well heat-treated aspen for initial 672h of aging, but the wood surface underwent severe color loss thereafter. Degradation behavior of industrial coating was similar on heat-treated aspen and heat-treated jack pine. Local degradation could easily be noticed for industrial coated heat-treated aspen after 672h of accelerated aging.

4.5.4.3. Birch

Acrylic polyurethane with CeO_2 nano particles alone or together with lignin stabilizer showed best protection against aging on heat-treated birch. No degradation was noticed for these two coatings even after 1500h of aging (Figure 4.33). Behavior of the other acrylic polyurethane coatings was similar on heat-treated birch and heat-treated aspen. Industrial coating protected heat-treated birch slightly better compared to surfaces of heat-treated aspen and jack pine. The local degradation for this coating was visible only after 1008h of aging.

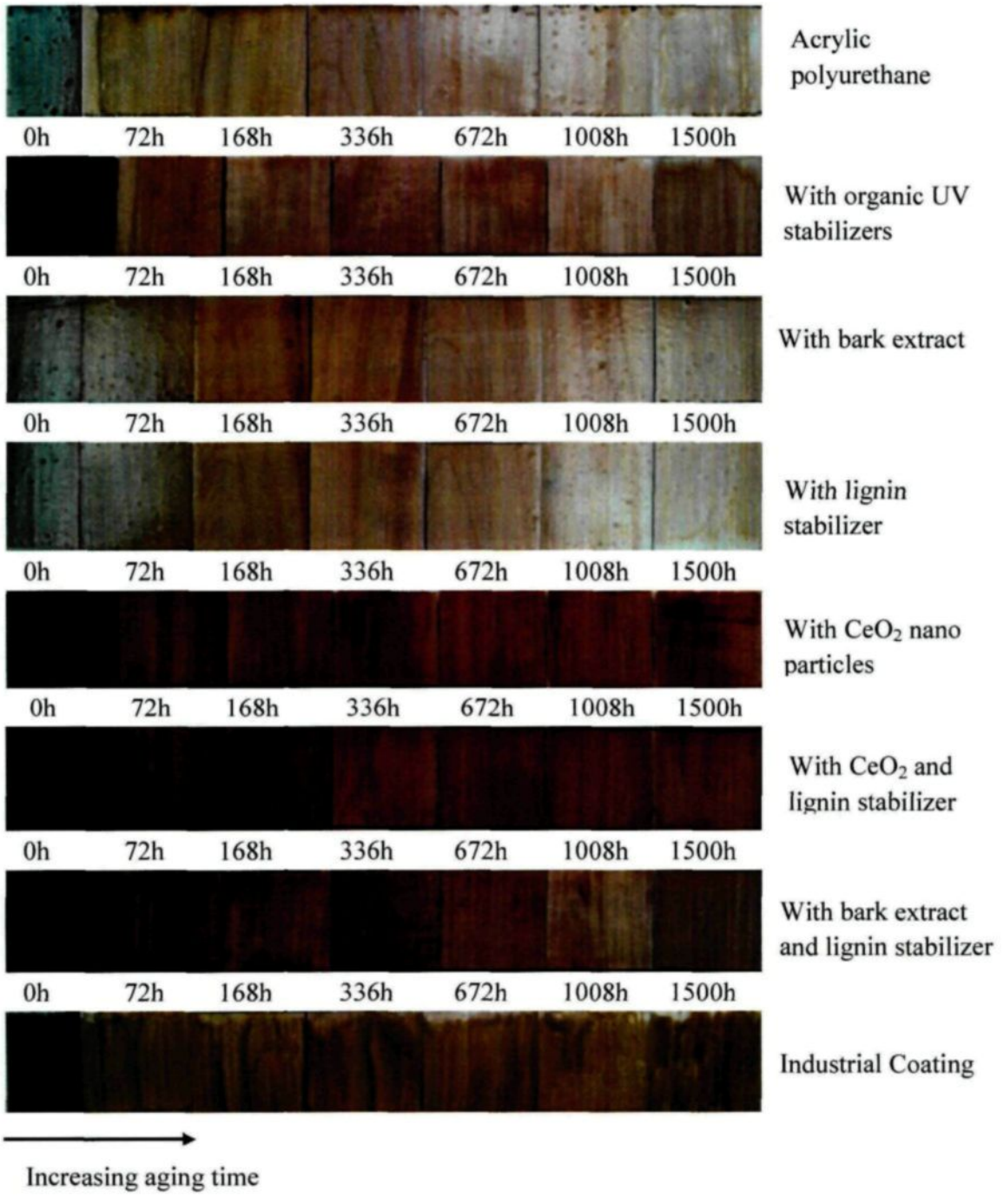

Figure 4.33 Visual assessment of coated heat-treated birch for different aging times

Although acrylic polyurethane coatings containing bark extract alone or together with lignin stabilizer exhibited very good protective characteristic on heat-treated jack pine, it failed to protect heat-treated aspen and heat-treated birch from degradation due to aging. On the contrary, acrylic polyurethane coatings containing CeO_2 nano particles with or without lignin stabilizer were very effective on all the heat-treated wood species investigated during this project. This was probably due to the difference in their protection mechanisms. As explained before, bark extracts enriched with phenolic compounds have high antioxidant properties. Therefore, they mainly act as singlet oxygen quencher or free radical scavenger once the photo degradation starts at wood surface. Lignin content of heat-treated jack pine is much higher compared to that of heat-treated hard wood species (birch and aspen). Probably due to this reason, photodegradation of heat-treated jack pine was much less compared to that of heat-treated aspen and birch. They could also absorb harmful UV light as shown in Figure 4.4. On the other hand, CeO_2 nano particles are highly effective in UV absorption. Thus, they screen harmful UV light before reaching to the wood surface. Also, their low photocatalytic activity facilitates significant protection against aging.

4.5.5. Wetting Characteristics of Coated Wood

The changes in surface polarity of coated wood surfaces during aging were evaluated by measuring contact angles of water drops on coated surfaces at different aging times. The contact angle is a very simple yet insightful measure of coating degradation during aging. The discoloration of coated wood surface underneath the coatings takes place mainly due

to the photodegradation of lignin followed by formation of colored byproducts (chromophores) at the wood surface by the action of UV light. These byproducts are then removed by water diffused through the coatings, leaving behind grey or white texture of wood. Water crosses pores of the superficial layer and reaches the substrate resulting in blisters, cracks, spots, erosion and discoloration [178]. Water penetration through coating is a very important phenomenon for wood discoloration which can be easily measured by contact angle test and water uptake test. The main advantages of contact angle test over water uptake test are precision, repeatability and negligible substrate effect on contact angle dynamics [75].

The results showed that the contact angle started changing as soon as water drop came in contact with coated wood surface. The lowest diffusion rate of water through the coatings was observed for acrylic polyurethane coating with CeO_2 nano particles before aging with the exception of industrial coating (Figure 4.34) whereas highest diffusion rate of water through the coatings was observed for acrylic polyurethane with bark extracts. This was due to the hydrophilic nature of the natural antioxidants and UV stabilizers. Acrylic polyurethane coatings with other additives were more prone to effect of water compared to the coatings with CeO_2 nano particles (Figure 4.34). The acrylic polyurethane coating with bark extract (Figure 4.34a) showed the most hydrophilic nature compared to all other coatings before aging. The contact angle increased with increasing aging time for acrylic polyurethane coatings with bark extracts (Figure 4.34a), lignin stabilizers (Figure 4.34b), bark extracts and lignin stabilizer (Figure 4.34c), CeO_2 nano particles (Figure 74.34g), and CeO_2 nano particles and lignin stabilizer (Figure 4.34h). For acrylic

polyurethane coatings without any additives (Figure 4.34e) and with organic UV stabilizers (Figure 4.34d) the contact angles increased after 72h of aging throughout the contact period. For Industrial Laurentide coating, the contact angles before and after 72h of aging were almost similar. After 1500h of aging contact angle changed drastically, and reached to zero within 50s of contact between water drops and coated wood surfaces for latter three coatings. The highest water repellency characteristic (largest contact angle) was exhibited by coating containing bark extract and lignin stabilizer after 1500h of aging proving the fact that this was most effective coating on heat-treated jack pine.

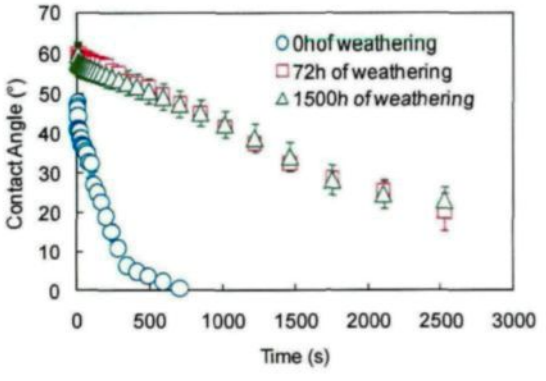

(a)

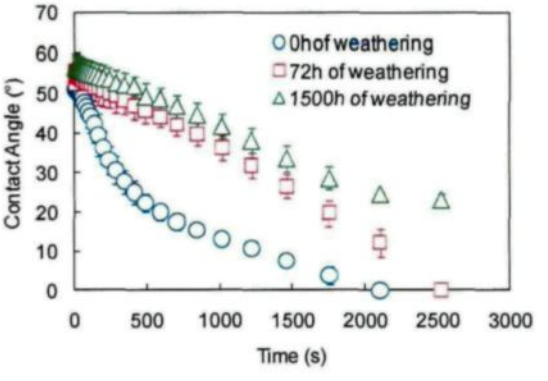

(b)

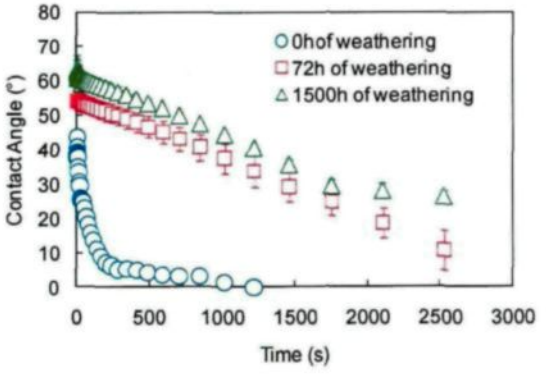

(c)

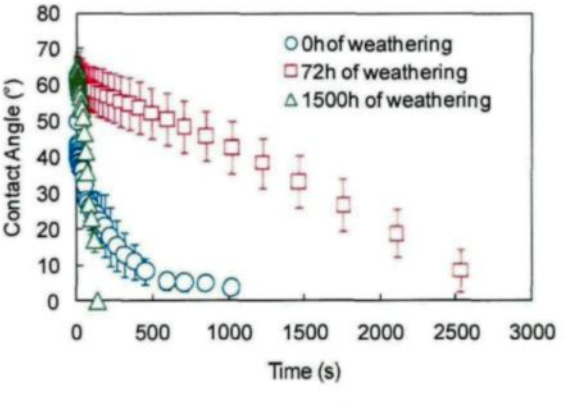

(d)

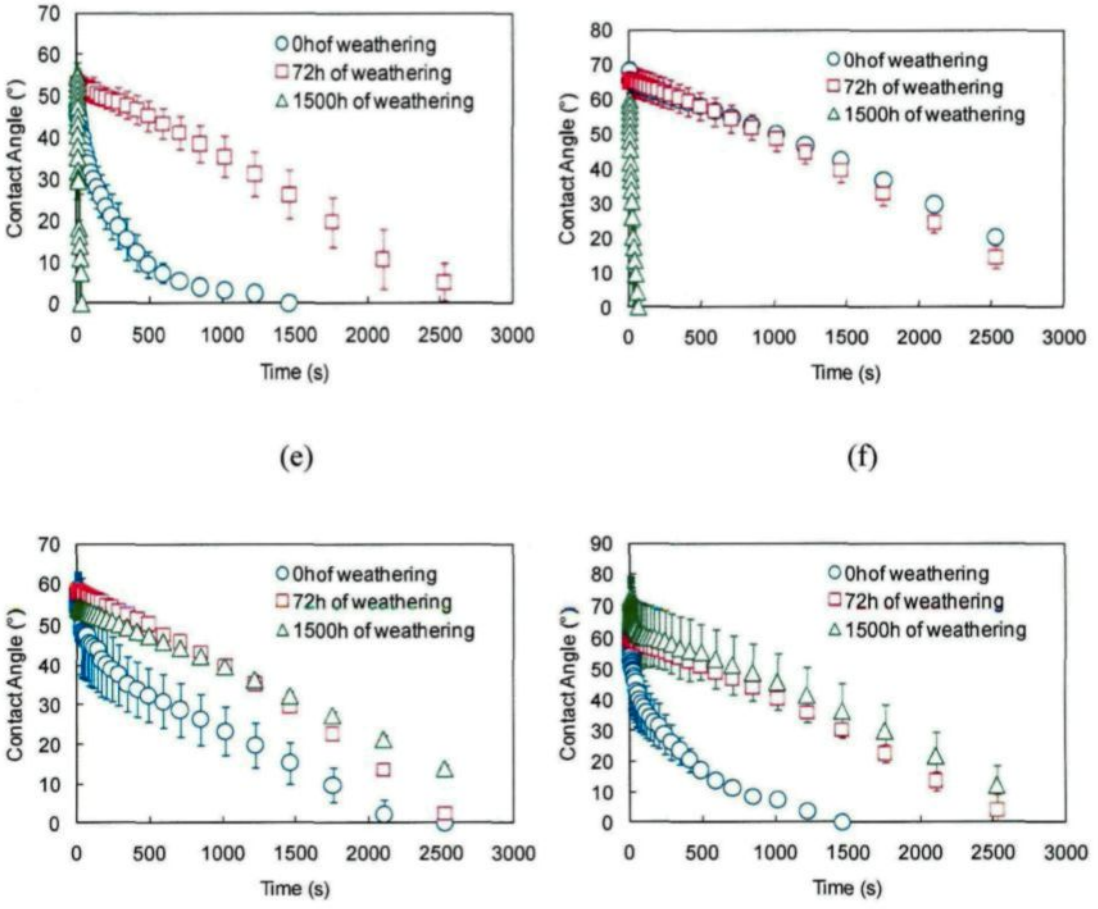

Figure 4.34 Dynamic contact angle of water for different aging times on heat-treated jack pine surface coated with the acrylic polyurethane coating containing (a) only bark extracts, (b) lignin stabilizer, (c) bark extracts and lignin stabilizer, and (d) organic UV stabilizers, (e) acrylic polyurethane without any additives, (f) industrial Laurentide coating, (g) acrylic polyurethane with CeO_2 nano particles, and (h) with CeO_2 nano particles and lignin stabilizer

4.5.6. Chemical Modification

4.5.6.1. ATR-FT-IR analysis

Before the aging test, all the coated samples were cured at 23°C and 15% humidity (laboratory condition) for one week. The effects of different additives on chemical changes of acrylic polyurethane coatings were analyzed using ATR-FT-IR. The FT-IR spectra of the acrylic polyurethane coating containing bark extract and lignin stabilizer coated heat-treated jack pine panels before and after aging for different exposure times are shown in Figures 4.35(a) and 4.35(b). The assignments of the bands were performed based on the literature FT-IR data for acrylic-polyurethane system that is well documented [136-138, 143, 144, 146-148].

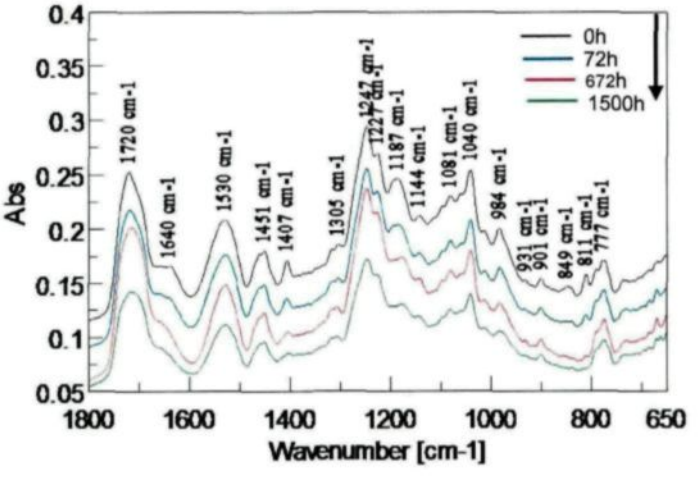

(a)

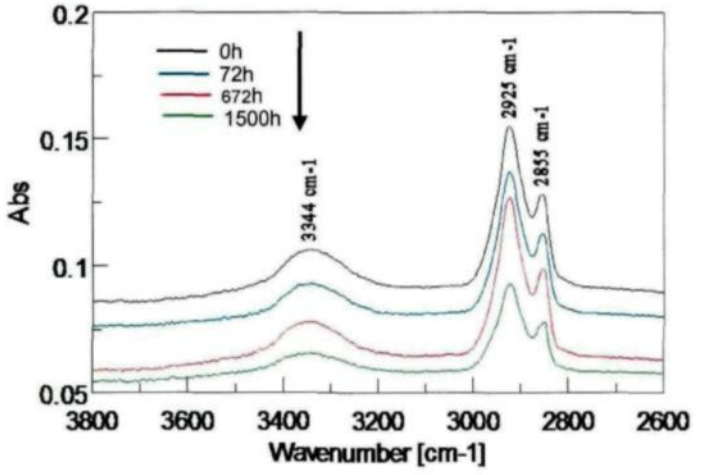

(b)

Figure 4.35 ATR-FTIR analysis of acrylic polyurethane coating containing bark extract and lignin stabilizer on heat-treated jack pine for different exposure times **(a)** 1800-650 cm^{-1} and **(b)** 3800-2600 cm^{-1}

Before the detailed analysis, each spectrum was normalized at the CH bending frequency (1451cm^{-1}) in order to emphasize the oxidation of the polymer matrix [146]. As reported by Perrin et al. [147], CH bending frequency must decrease slightly due to the partial oxidation of the CH_2 in the α-NH position. Semi-quantitative measurements were carried out to comprehend the effect of different additives (Figures 4.36- 4.41) on the aging of acrylic polyurethane coating. Increase in absorption in the carbonyl region (1670-1770 cm^{-1}) for acrylic polyurethane coating containing bark extract with or without lignin stabilizer suggested the formation of several oxidation photoproducts mainly the carboxylic acid (peak at 1715 cm^{-1}) while a decrease in absorption was observed for the acrylic polyurethane coating stabilized with organic UV stabilizers (Figure 4.36). This might be due to the depletion of these photoproducts with the water spray during

accelerated aging test. Carbonyl photoproducts formed either through the direct chain scission or by the radical induced processes upon exposure to the artificial aging conditions [144]. Significant decrease of the absorption in the region of 1605-1670 cm^{-1} (H-bond and C=O stretching of the urethane) was another noticeable phenomenon for all the three stabilized acrylic polyurethane coatings as shown in Figure 4.37. The decrease in the absorption at 1640 cm^{-1} was due to the conversion of urea to urethane linkages [146]. The extent of absorption intensity loss in this region was highest for the acrylic polyurethane coating containing bark extract and a very high loss was also observed for the acrylic polyurethane coating with bark extract and lignin stabilizer. However, relatively small change was observed for the acrylic polyurethane coating stabilized with organic UV absorbers (Figure 4.37). Usually a significant loss in the amide II band (1530 cm^{-1}, as a result of mixed vibration involving C-N and N-H mode) often reported due to the chain scission reaction of the urethane linkages [143]. But in the present study, a small loss in intensity of amide II band (1530 cm^{-1}) was detected for all the three stabilized coating (Figure 4.38). The lowest loss of the urethane group was observed for the acrylic polyurethane coating containing organic UV absorber due to the presence of HALS type UV stabilizer which extends the coating durability as well as the UV absorbers lifetime [143]. The loss of the acrylate double bond (at 1407 cm^{-1}) was attributed to the oxidation reactions initiated by free radicals (Figure 4.39) [136].

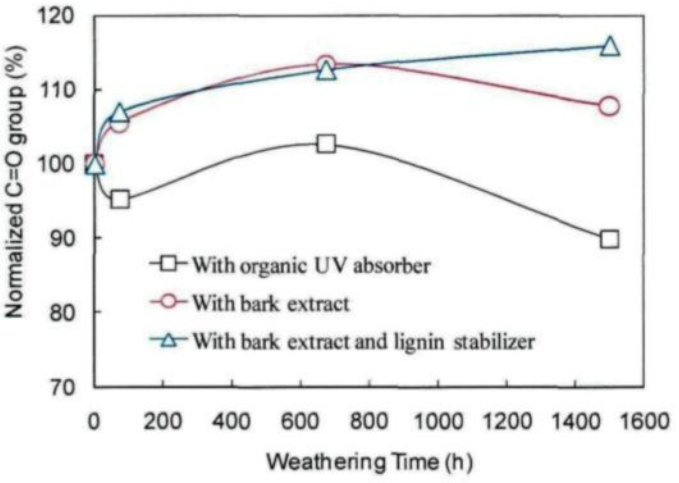

Figure 4.36 Buildup of oxidation products during accelerated aging of acrylic polyurethane coatings stabilized by different additives on heat-treated jack pine

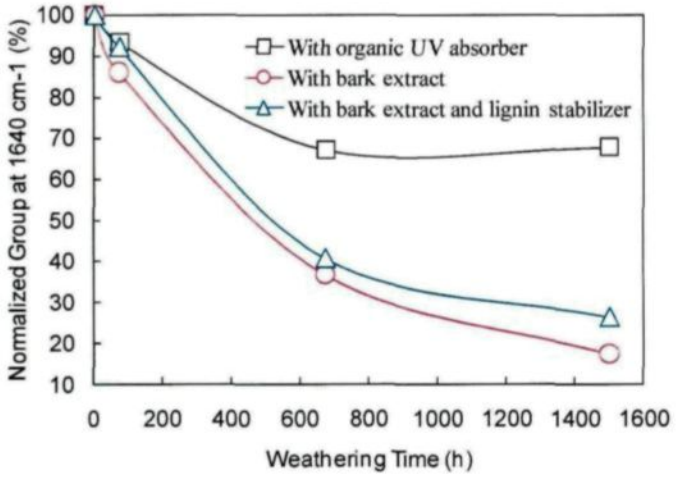

Figure 4.37 Diminution of H-bond and C=O stretching of the urethane during accelerated aging of acrylic polyurethane coatings stabilized by different additives on heat-treated jack pine

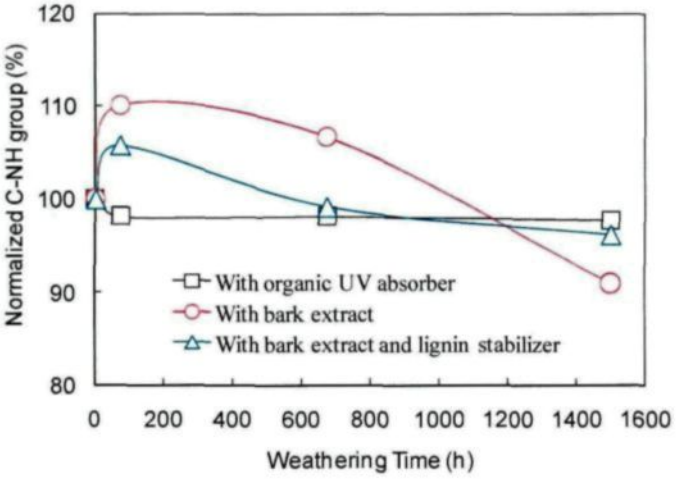

Figure 4.38 Change in urethane group of stabilized acrylic polyurethane coatings during aging on heat-treated jack pine

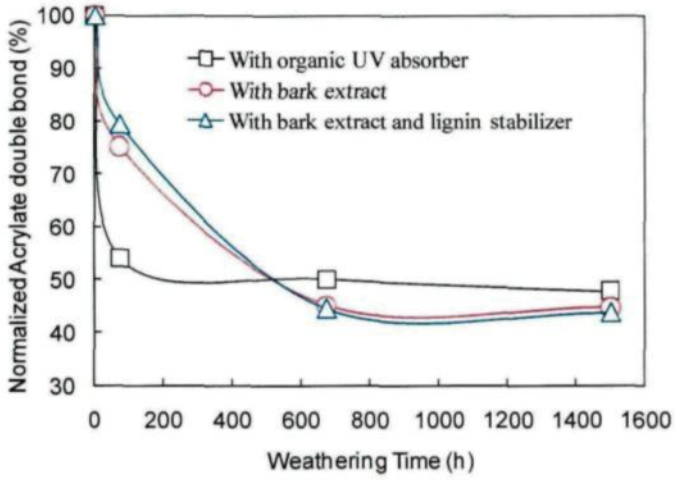

Figure 4.39 Loss of acrylate double bond of acrylic polyurethane coating during aging on heat-treated jack pine

The asymmetric CH group disappeared faster than the symmetric CH group for the acrylic polyurethane coatings with organic UV absorbers and bark extracts. Slight increase

in absorption of symmetric CH was noticed for the acrylic polyurethane coating containing bark extract and lignin stabilizer (Figure 4.40). Slight decrease in OH, NH content (3344 cm^{-1}) during initial 72h of aging was either due to the removal of trapped water molecules inside the coatings or crosslinking between urethane groups. Increase in this absorption band thereafter was due to the formation of hydroxyl groups containing reaction products (Figure 4.41) in addition to the absorption of water in the form of moisture and also due to the formation of polyurea during accelerated aging test.

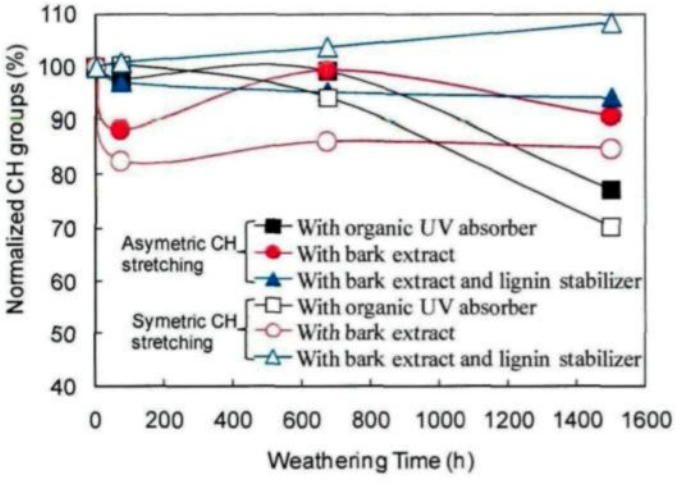

Figure 4.40 Changes in CH stretching of stabilized acrylic polyurethane coatings during accelerated aging on heat-treated jack pine

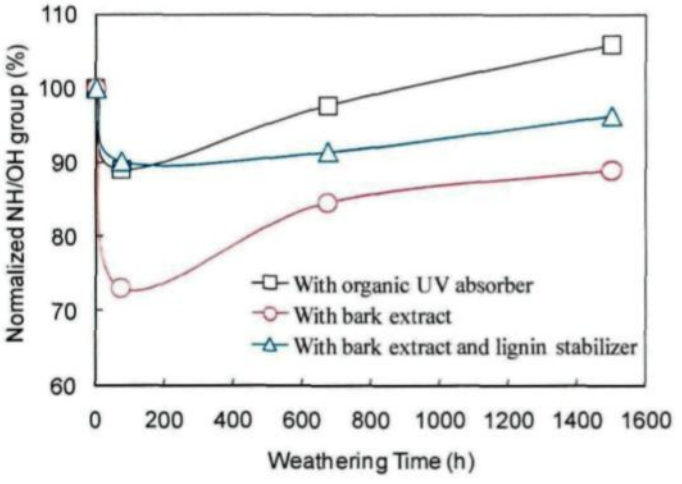

Figure 4.41 Changes in hydroxyl and NH group during accelerated aging for stabilized acrylic polyurethane coatings on heat-treated jack pine

From the FT-IR analyses, it seemed that the coating containing organic UV stabilizers was most stabilized and should be the most durable during accelerated aging test. However, from the accelerated aging test results, it was evident that acrylic polyurethane coating containing bark extract and lignin stabilizer was the most effective coating from the aesthetic and durability point of view for jack pine (Figure 4.29 and Figure 4.31). This might be explained by considering the fact that all the acrylic polyurethane coatings used in this study are transparent or semitransparent in nature. Therefore these coatings cannot prevent the sunlight to reach to the wood surface completely which eventually commences the photodegradation reaction on the wood surface. The bark extract at this stage might be very effective due to its antioxidant properties which can delay the photo oxidation

reaction at the wood surface. At this stage, the UV stabilizers fail to perform as they can only block the harmful UV lights to reach to the wood surface.

Below, the functional changes of acrylic polyurethane with CeO_2 nano particles alone or together with lignin stabilizer and acrylic polyurethane with bark extracts and lignin stabilizer on heat-treated jack pine, aspen and birch are compared for different aging times by using the results of ATR-FTIR analyses.

The ATR-FTIR results revealed that carbonyl peaks (1720 cm^{-1}) shifted towards 1710 cm^{-1} after 1500h of aging for coatings with CeO_2 alone or together with lignin stabilizer, and bark extract and lignin stabilizer on all the three heat-treated wood species. Also, the ATR-FTIR results clearly showed that, with increasing aging time, the C=O stretching of ester at 1720 cm^{-1} became broader which was due to the overlapping of different carbonyl photoproducts formed during aging. Carbonyl photoproducts formed either through the direct chain scission or by the radical induced processes upon exposure to the artificial aging conditions. This is also supported by increase in carbonyl groups during accelerated aging for all the three coatings on heat-treated jack pine, aspen and birch (Figure 4.42). The carbonyl group intensity increased most for the acrylic polyurethane with CeO_2 nano particles compared to the other two coatings (acrylic polyurethane with CeO_2 nano particles and lignin stabilizer, and bark extract and lignin stabilizer). Addition of lignin stabilizer to the coating with CeO_2 nano particles certainly decreased carbonyl formation during accelerated aging due to its radical scavenging properties. On the other hand, the least change in carbonyl group intensity was observed for coating with bark extract and lignin stabilizer due to effect of high antioxidant and singlet oxygen quenching properties

of bark extracts as well as radical scavenging activity of lignin stabilizer. The results also suggested that the most carbonyl formation was higher for any coatings on heat-treated jack pine compared to that of heat-treated aspen or birch. The decrease in the carbonyl groups was noticed for acrylic polyurethane with CeO_2 nano particles and lignin stabilizer and acrylic polyurethane with bark extract and lignin stabilizer on all the three heat-treated wood species. This was probably due to the depletion of the carbonyl photoproducts with water spray during accelerated aging.

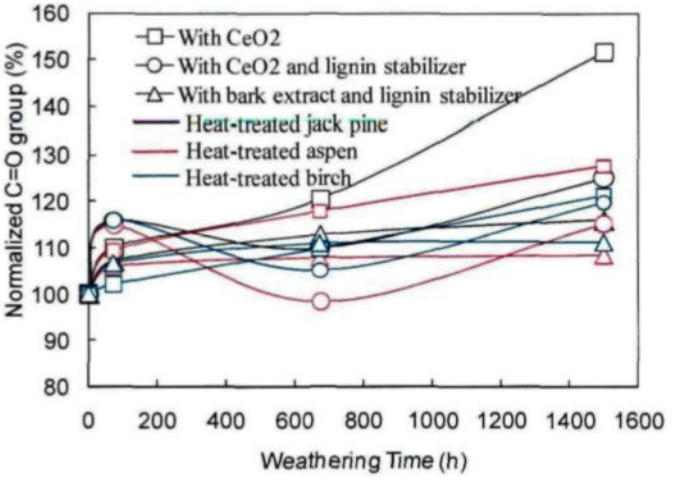

Figure 4.42 Buildup of oxidation products during accelerated aging of acrylic polyurethane coatings stabilized by different additives on different heat-treated wood species

The peak at 1640 cm^{-1} was due to the C=O stretching vibrations of the polyurea. The decrease in 1640 cm^{-1} for acrylic polyurethane with CeO_2 nano particles on heat-treated jack pine was similar to that of heat-treated aspen and birch (Figure 4.43). Similar trends

were noticed for acrylic polyurethane with bark extract and lignin stabilizer on all the heat-treated wood species. Increase in the same group for initial aging periods followed by a decrease for acrylic polyurethane with CeO_2 nano particles and lignin stabilizer was noticed on all the heat-treated wood species (Figure 4.42). Decrease in this peak is directly related to the chain scission of the polyurea. Highest chain scission for polyurea was observed for acrylic polyurethane with CeO_2 nano particles compared to other two coatings. This was due to the absence of lignin stabilizer which has high radical scavenging activity.

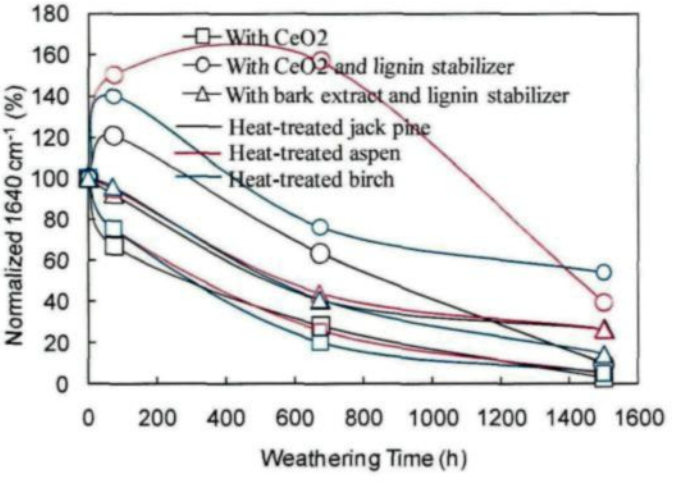

Figure 4.43 Diminution of H-bond and C=O stretching of the urethane during accelerated aging of acrylic polyurethane coatings stabilized by different additives on different heat-treated wood species

It was quite surprising to notice increase in C-NH group of urethane linkages for acrylic polyurethane coating containing CeO_2 nano particles and lignin stabilizer on all the heat-treated wood species (Figure 4.44). This was probably due to the increase in urethane groups on the surface due to the continuous reorientations of the surface functional groups under UV light. The decrease in the same group for acrylic polyurethanes with CeO_2 nano particles and bark extract and lignin stabilizer on all the heat-treated wood species was due to the chain scission reactions at the acrylic urethane linkages. The decrease in C-NH group of urethane was not even 10% for any of the coatings which suggested negligible chain scission of urethane linkages even after 1500h of accelerated aging.

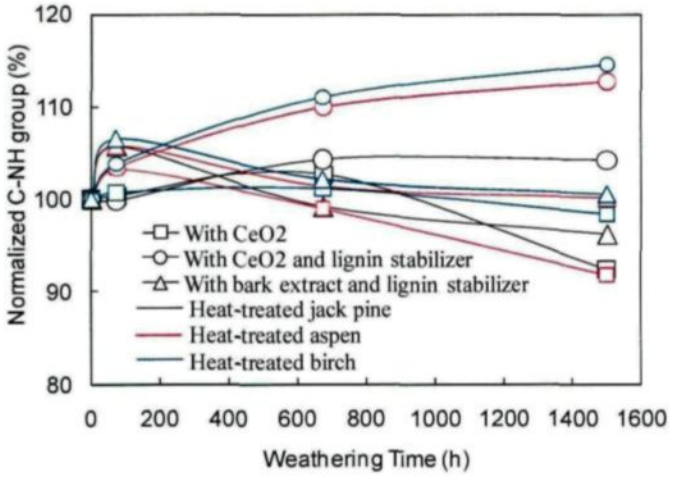

Figure 4.44 Change in urethane group of stabilized acrylic polyurethane coatings during aging on different heat-treated wood species

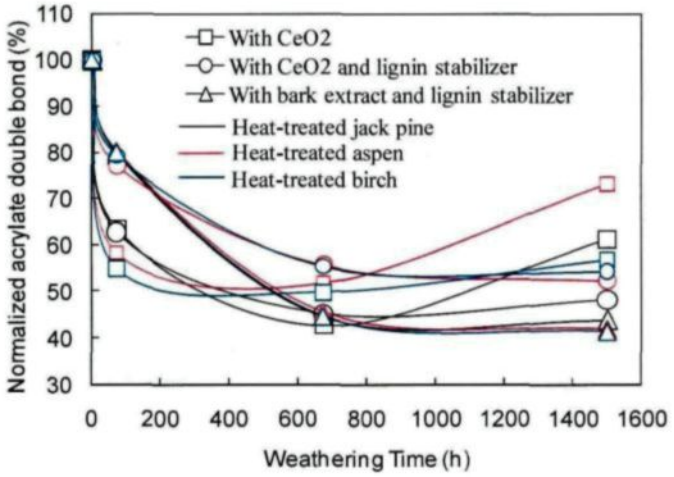

Figure 4.45 Loss of acrylate double bond of acrylic polyurethane coating during aging on different heat-treated wood species

Acrylate double bond was also diminished due the chain scission reactions for all the coatings on heat-treated jack pine, aspen, and birch (Figure 4.45).

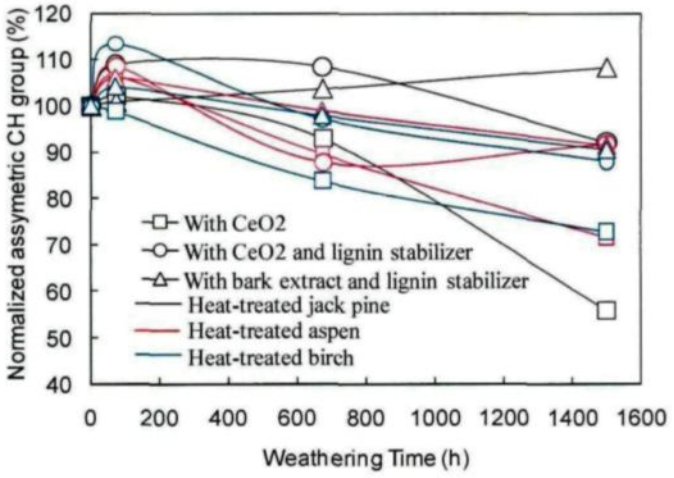

Figure 4.46 Changes in CH stretching of stabilized acrylic polyurethane coatings during accelerated aging on different heat-treated wood species

The assymetric CH groups decreased with increasing aging time. The most change in asymmetric groups was found for acrylic polyurethane with CeO_2 nano particles compared to those of other two coatings which indicated more degradation of this coating compared to other two coatings (Figure 4.46).

The broadening of OH/NH group during accelerated aging was noticed for acrylic polyurethane with CeO_2 nano particles alone or together with lignin stabilizer whereas slight decrease in the same group was observed for acrylic polyurethane with bark extract and lignin stabilizer (Figure 4.47).

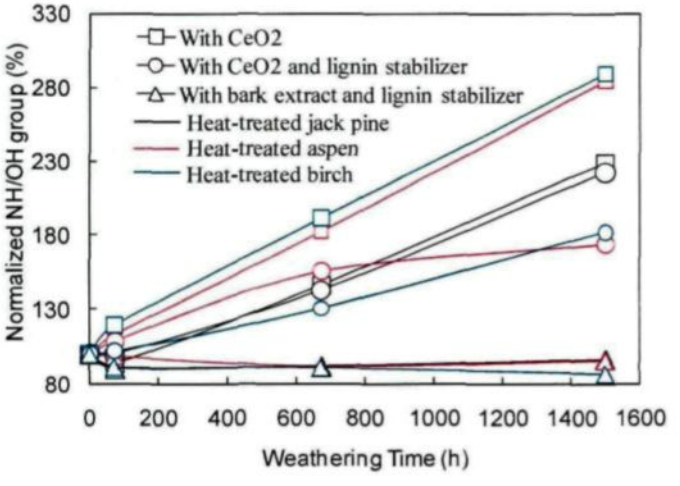

Figure 4.47 Changes in OH and NH groups during accelerated aging for stabilized acrylic polyurethane coatings on different heat-treated wood species

4.5.6.2. XPS analysis

The changes in surface chemical compositions were investigated using XPS analyses. The C1s spectrum for heat-treated jack pine, coated with acrylic polyurethane coating containing bark extract and lignin stabilizer, for different aging times has been shown in Figure 4.48. Atomic percentages of different components for acrylic polyurethane coating containing bark extract and lignin stabilizer for different aging times on heat-treated jack pine, aspen and birch are presented in Table 4.8 along with deconvoluted C1s spectrum and O/C ratio. The XPS results for acrylic polyurethane coating containing CeO_2 nano particles and lignin stabilizer are reported in Appendix 5.

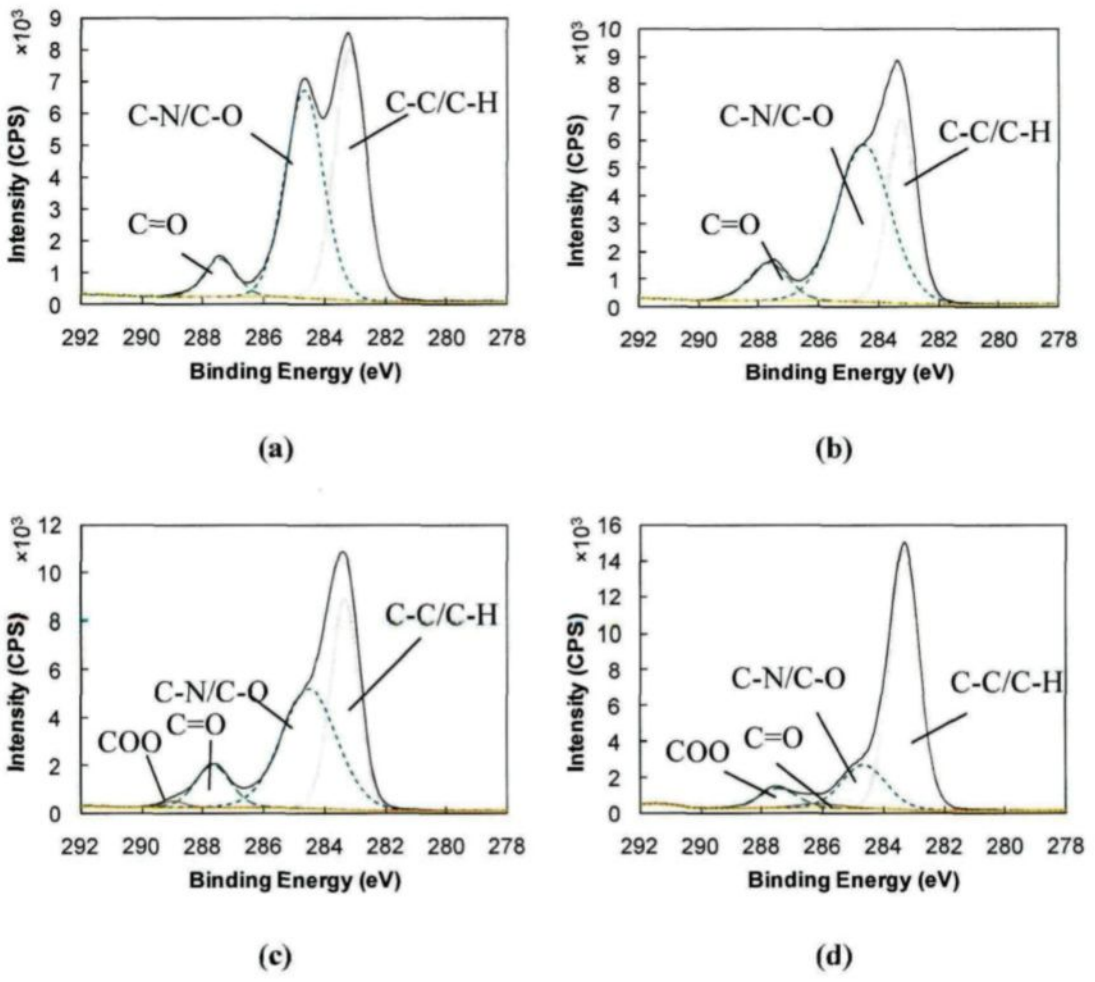

Figure 4.48 C1s spectrum of the acrylic polyurethane coating containing bark extract and lignin stabilizer on heat-treated jack pine: (a) 0h, (b) 72h, (c) 672h, and (d) 1500h of aging

Table 4.8 Atomic percentages of different components of acrylic polyurethane coating containing bark extract and lignin stabilizer on different wood species for different aging times

aging time (h)	Species	C (%)	Carbon Components				O (%)	N (%)	Si (%)	O/C
			C-H/ C-C	C-N/ C-O	C=O	CO O				
0		72.06	42.2	50.36	7.44		22.21	2.18	3.56	0.31
72	Birch	72.28	50.53	39.12	10.35		22.64	2.61	1.88	0.31
1500		75.7	58.43	29.99	11.57		19.86	3.54	0.81	0.26
0		71.71	45.42	47.51	7.07		22.62	2.12	3.55	0.32
72	Aspen	72.69	55.97	34.05	9.99		22.07	2.75	1.93	0.30
1500		79.21	53.32	37.43	9.25		16.93	2.87	0.77	0.21
0		72.16	45.8	46.86	7.33		22.49	1.76	3.59	0.31
72	Jack	74.31	34.22	55.79	9.99		20.43	3.35	1.89	0.27
672	pine	76.48	41.71	46.69	10.5	1.1	19.26	3.98	0.27	0.25
1500		81.88	72.19	18.44	2.19	7.18	14.6	2.46	0.71	0.18

It was evident from XPS results (Table 4.8) that the carbon concentration on the top surface of the coating increased with increasing aging time for all the wood species. On the other hand, O% decreased as aging time increased. This was due to the depletion of oxidation photoproducts during accelerated aging with water spray. The nitrogen concentration also increased as the aging time increased for heat-treated aspen and birch. For heat-treated jack pine, the nitrogen concentration increased for initial 672h of aging followed by a decrease. The increase in nitrogen concentration on the coating surface was attributable to crosslinking whereas decrease of the same component was due to the chain scission reactions. Si concentration decreased during aging which could be due to the depletion of surface tension reducing agent from the polymer matrix.

The high resolution C1s spectra of heat-treated jack pine coated with acrylic polyurethane coating containing bark extract and lignin stabilizer (Figure 4.48) revealed that the C-C/C-H bond linkages increased whereas C-N concentration decreased with increasing aging time. This indicates that there was chain scission of C-O and NH-CO bonds in the polyurethane main chain. A similar behavior was observed for the coated and heat-treated birch, and aspen. Relative increase in C=O was observed for coated aspen, and birch with increasing aging time (Table 4.8) which might correspond to COO carboxyl and N-C=O functions occurred. The carboxyl groups were produced during oxidation of polyurethane coatings and N-C=O function was produced from urea or urethane. Since COO groups are easy to decompose, the increase of the C=O component was probably due to the increase of urethane groups on the surface. For coated jack pine, there was increase in C=O group up to 672h of aging followed by a drastic reduction of the same group. A

separate peak was found for COO carboxyl groups and a drastic increase in the same group was observed after 1500h of aging for jack pine but separate peak of COO was not observed for aspen and birch.

A degradation mechanism shown in Figure 4.49 could be postulated from the chemical analysis of heat-treated surface with acrylic polyurethane coating stabilized by different organic or inorganic UV stabilizer.

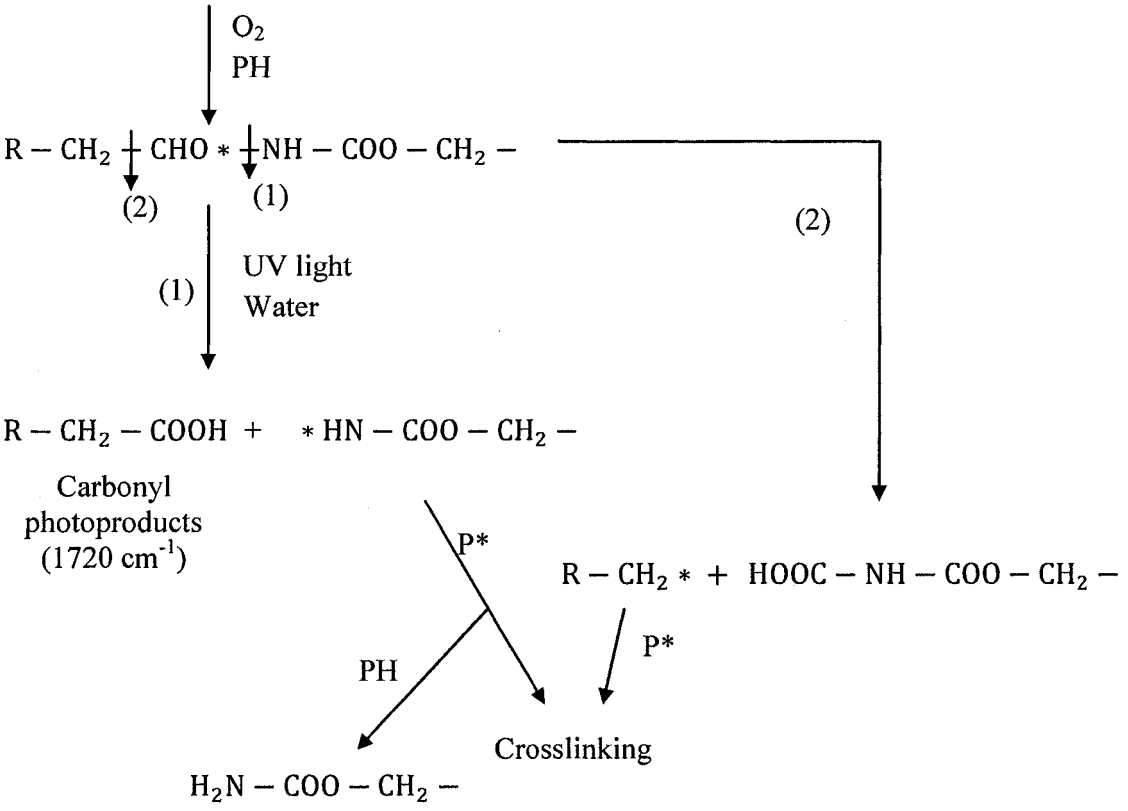

Figure 4.49 Degradation mechanism of acrylic polyurethane coating during accelerated aging

4.5.7. Morphological Analysis

4.5.7.1. Fluorescence Microscopy Assessment

The light microscopy of transverse sections of coated-wood provides useful information on the distribution of the coatings by facilitating the observation of relatively large areas at low magnification, thus, enabling a comparison of coated-wood surfaces at different aging times. Light microscopy observations also facilitate the evaluation of penetration characteristic of different coatings in early wood and late wood regions and coating thickness change with aging.

The light micrographs of transverse section of the coating containing bark extract and lignin stabilizer and heat-treated jack pine, aspen and birch for different aging times have been compared in Figure 4.50. The light microscope pictures revealed good adhesion between heat-treated jack pine, aspen and birch with the coating before aging (Figure 4.50) although almost no penetration was observed for jack pine (Figure 4.50a). On the contrary, considerable penetration was observed for aspen (Figure 4.50c) and birch (Figure 4.50b) due to the presence of vessels which had much bigger radii compared to tracheids present in jack pine. If birch and aspen are compared, the coating material penetrated into aspen more due to its lower density compared to the density of birch. Since the most penetration was detected for aspen, the coating thickness was lower for this species compared to the thickness observed for others at a given number of coating layers. These results could directly be related to contact angle measurement of acrylic polyurethane with different additives on heat-treated jack pine, aspen and birch. The smallest equilibrium contact

angles for coatings were found on heat-treated aspen surface whereas largest equilibrium contact angles were detected on heat-treated birch surface.

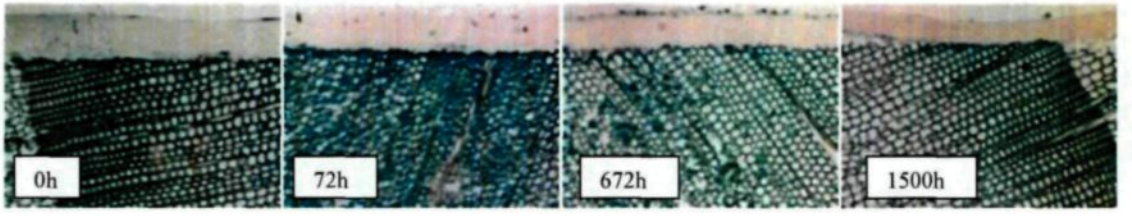

(a)

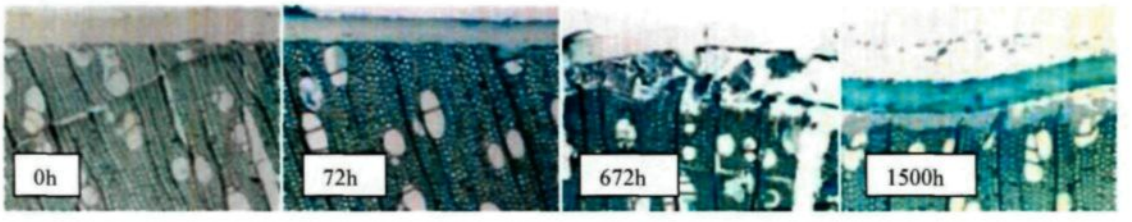

(b)

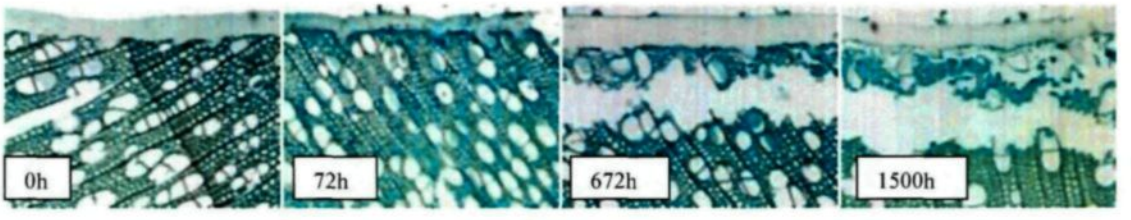

(c)

Figure 4.50 The light micrographs of transverse section of the wood-coating containing bark extract and lignin stabilizer interface for different aging times (a) heat-treated jack pine, (b) heat-treated birch, and (c) heat-treated aspen

It was clear from light micrographs that there was no degradation for jack pine-coating interface even after 1500h of aging, although coating detachment was observed in early

wood region (Figure 4.50a). Complete detachment of the cells from each other for 5-6 cell layers was observed for birch after 672h of aging. The extent of degradation increased further after 1500h of aging and complete detachment of the coating layer was noticed. Same phenomenon was also observed for aspen but the extent of degradation was more important than that of heat-treated birch. After 1500h of aging, not only the middle lamella region but also the cell walls degraded significantly for aspen. Therefore, it can be concluded that coating thickness is a very important parameter in protection of wood from outer environment.

Figure 4.51 compares the light micrographs of acrylic polyurethane with CeO_2 nano particles and lignin stabilizer coated heat-treated jack pine, aspen and birch for different aging times. Negligible degradation was detected at the interface of heat-treated jack pine and acrylic polyurethane containing CeO_2 nano particles and lignin stabilizer after 1500h of aging (Figure 4.51a). Also, no degradation was observed for heat-treated jack pine underneath the acrylic polyurethane coating with bark extract and lignin stabilizer after 1500h of aging. These results directly support the color measurement and visual assessment results which demonstrated that the former coating on heat-treated jack pine was as effective as latter coating. The slight degradation of heat-treated jack pine beneath the acrylic polyurethane with CeO_2 nano particles and lignin stabilizer after 1500h of aging was probably due to more water ingression through this coating compared to the acrylic polyurethane with bark extract and lignin stabilizer which accelerated the photodegradation process. On the other hand, similar degradation behaviors were observed for heat-treated aspen (Figure 4.51c) beneath the acrylic polyurethane coating containing CeO_2 nano

particles and lignin stabilizer and for heat-treated birch underneath the same coating over the complete aging period (Figure 4.51b). After 672h of aging, small degradation was visible for both hard wood species. After 1500h of aging, 5-6 cell layer degradation was observed for heat-treated birch (Figure 4.51b) whereas heat-treated aspen showed 8-9 cell layer degradation beneath the acrylic polyurethane with CeO_2 nano particles and lignin stabilizer. Complete detachment of the cells from each other was not noticed even after 1500h of aging for heat-treated aspen and birch beneath the acrylic polyurethane containing CeO_2 nano particles and lignin stabilizer. This phenomenon was observed for heat-treated birch and aspen only after 672h of aging underneath the acrylic polyurethane with bark extract and lignin stabilizer. The color measurement and visual assessment results are in good agreement with fluorescence microscope results. Color change is directly related to the extent of wood degradation beneath the coatings layers.

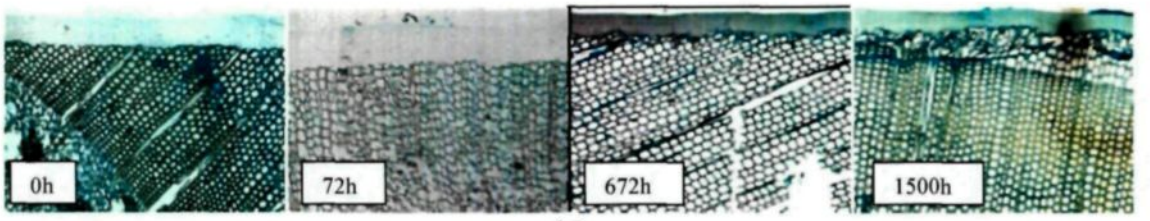

(a)

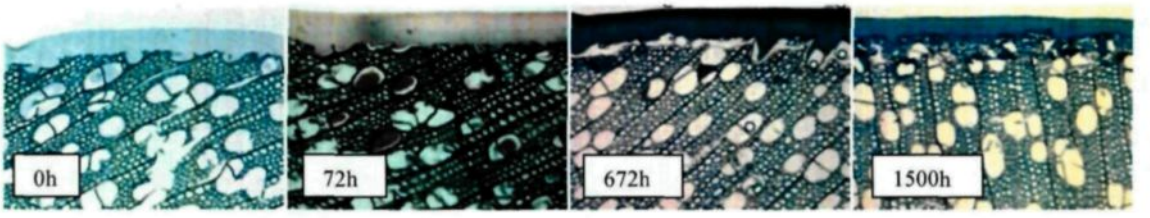

(b)

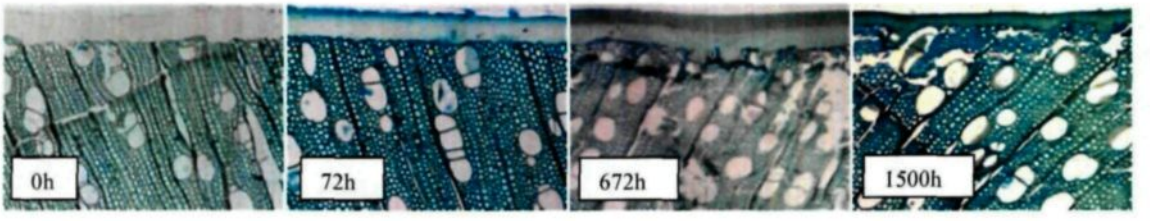

(c)

Figure 4.51 The light micrographs of transverse section of the wood-coating containing CeO_2 nano particles and lignin stabilizer interface for different aging times (a) heat-treated jack pine, (b) heat-treated birch, and (c) heat-treated aspen

In Figure 4.52 the industrial Laurentide coating and heat-treated jack pine, aspen and birch interfaces are compared for different aging times. Color measurement results showed very small color changes throughout the aging period for this coating on all the three heat-treated wood species. On the other hand, visual assessment revealed significant local degradation after 672h of aging and substantial overall degradation after 1500h of aging on heat-treated jack pine. The fluorescence microscopy results directly supports visual

assessment as local degradation was visible after 672h of aging for all the three wood species. Also, very significant degradation of heat-treated jack pine, aspen and birch was noticed at the end of 1500h of aging. For all the three wood species, beneath this coating, cell walls were completely degraded and detached from each other after 1500h of aging.

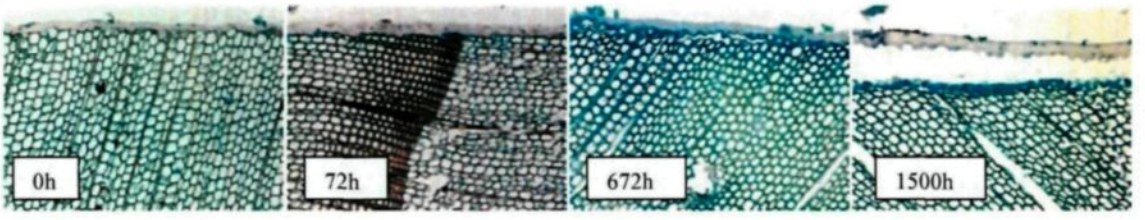

(a)

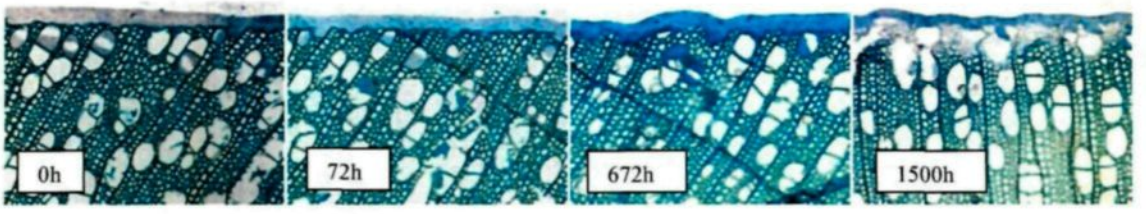

(b)

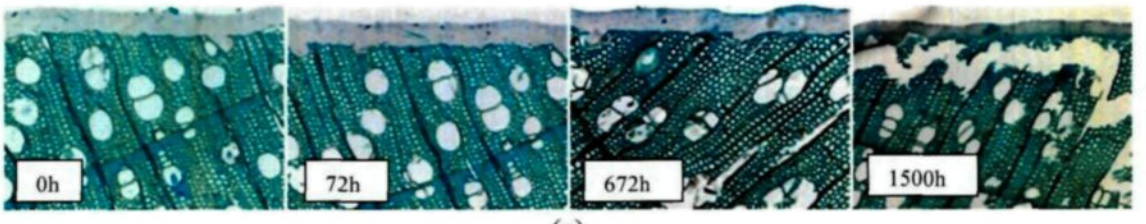

(c)

Figure 4.52 The light micrographs of transverse section of the wood-industrial Laurentide coating interface for different aging times (a) heat-treated jack pine, (b) heat-treated birch, and (c) heat-treated aspen

4.5.7.2. SEM Analysis

The main interest of SEM examination of coated wood is the wood-coating interface. The objective is to investigate the micro-structural changes occurring beneath the coating surface and study the mode of failure of coating. One of the main reasons of coating failure due to aging is adhesion loss. Long service life of coating is possible if the interface of coating and wood are coherent. Adhesion between wood surface and coating has been studied by scanning electron microscopy to detect early evidence of photo degradation as explained by Turkulin [171]. The results of harmful UV transmittance to the wood surface through semitransparent coatings can cause crack formation in the pit membranes, loss of occurrence of radial fibril agglomeration and the development of the brittleness on fractured cross sections of softwood tracheids [154]. The micrographs of aged coated surfaces did not reveal any information about the chalking, porosity and brittleness.

The SEM micrographs of coated (acrylic polyurethane coating containing bark extract and lignin stabilizer) and heat-treated aspen, birch, and jack pine are compared at different aging times in Figure 4.53. It was clear from the SEM micrographs of different wood species that the coating containing bark extract and lignin stabilizer was in good contact with the outer cell layer before aging (Figure 4.53a). After 672h of aging, no structural changes were observed for heat-treated jack pine whereas micro-structural damage was evident for aspen and birch (Figure 4.53b). The damage for aspen was almost doubled in terms of the affected layer after 672h of aging compared to that of birch. Small local degradation was noticed for jack pine after 1500h of aging but only in the early wood regions although the degradation mainly took place in middle lamella region (Figure

4.53c). In contrast, complete destruction of middle lamella region as well as the cell wall was evident for aspen which manifested to coating detachment and also significant color loss (Figure 5.53c). For birch, the depth of degradation after 1500h of aging was almost similar to that after 672h of aging but extent was more than the degradation observed after 672h of aging. Comparison of the degradation of birch and aspen after 1500h of aging (Figure 5.53c) showed that the coating protected the birch better than the aspen. This difference in degradation for these two hardwoods could be explained by the fact that the percentage of syringical lignin was more in birch compared to that of aspen.

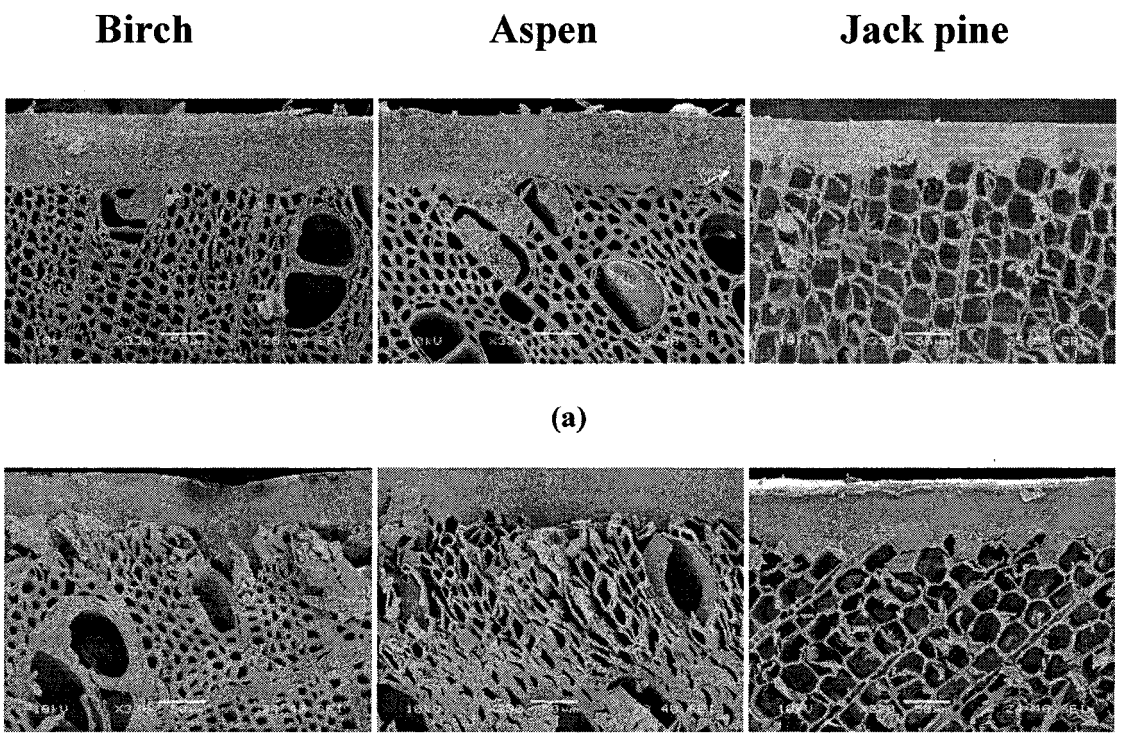

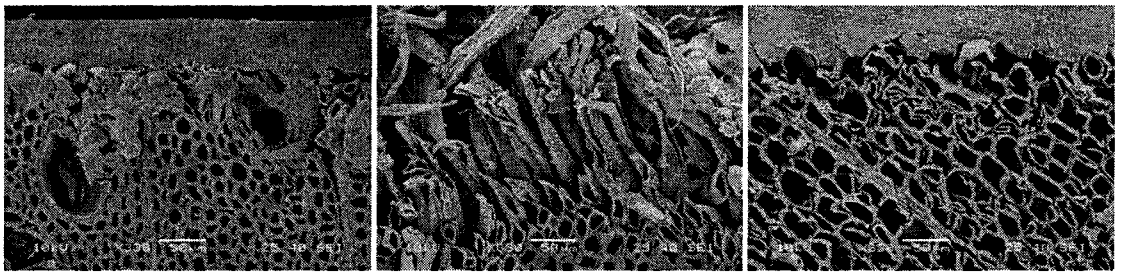

(c)

Figure 4.53 SEM micrographs of transverse sections of heat-treated birch, aspen and jack pine and the coating containing bark extract and lignin stabilizer interface (a) before aging, (b) after 672h of aging and (c) after 1500h of aging

The detailed micro structural changes occurring during accelerated aging in softwood are discussed below. The SEM micrographs showed close contact of the acrylic polyurethane coating containing bark extract and lignin stabilizer with S3 layer of heat-treated jack pine cell before aging. Also, the coating flew through the cracks of cell wall and interlocked cell walls to the middle lamella (Figure 4.54a). Breakdown of the middle lamella during aging often causes cell detachment and this effect was noticed after 1500h of aging for heat-treated jack pine beneath the acrylic polyurethane coating containing bark extract and lignin stabilizer due to the local degradation (Figure 4.54b). In addition, cell wall thinning due to the breakdown of the lignin in the S2 layer of the cell wall was another noticeable phenomenon after 1500h of aging (Figure 4.54b).

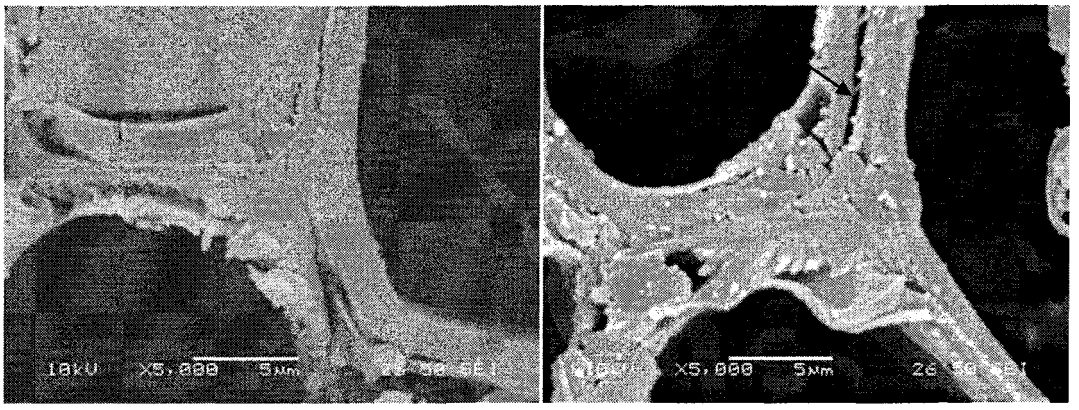

(a) (b)

Figure 4.54 SEM micrographs of the acrylic polyurethane coating containing bark extract and lignin stabilizer and heat-treated jack pine interface **(a)** before aging: The structure reveals that good adhesion of paint to the S3 layer and also penetration of the coating in the cell wall through the cracks **(b)** aged jack pine tracheids after 672h of accelerated aging test

The most important early structural indication of photo degradation on soft wood surfaces is the damage of bordered pits as explained by Turkulin [171]. For wood surface coated with semitransparent coating, he reported formation of distinctive cracks of the torus on aspirated pits only after four days of natural exposure or ten hours of fluorescent UV lamps exposure whereas such kind of cracks were visible for the present study only after 672h of aging at the surface beneath the acrylic polyurethane coating containing bark extract and lignin stabilizer (Figure 4.55b). Figure 4.55a shows no cracks in the bordered pits before aging. Upon prolonged exposure to accelerated aging test, pit dome cracks progressed diagonally, following the microfibril orientation in the domes resulting widening in aperture and thinning of the pit dome (Figure 4.55c) after 1500h of aging.

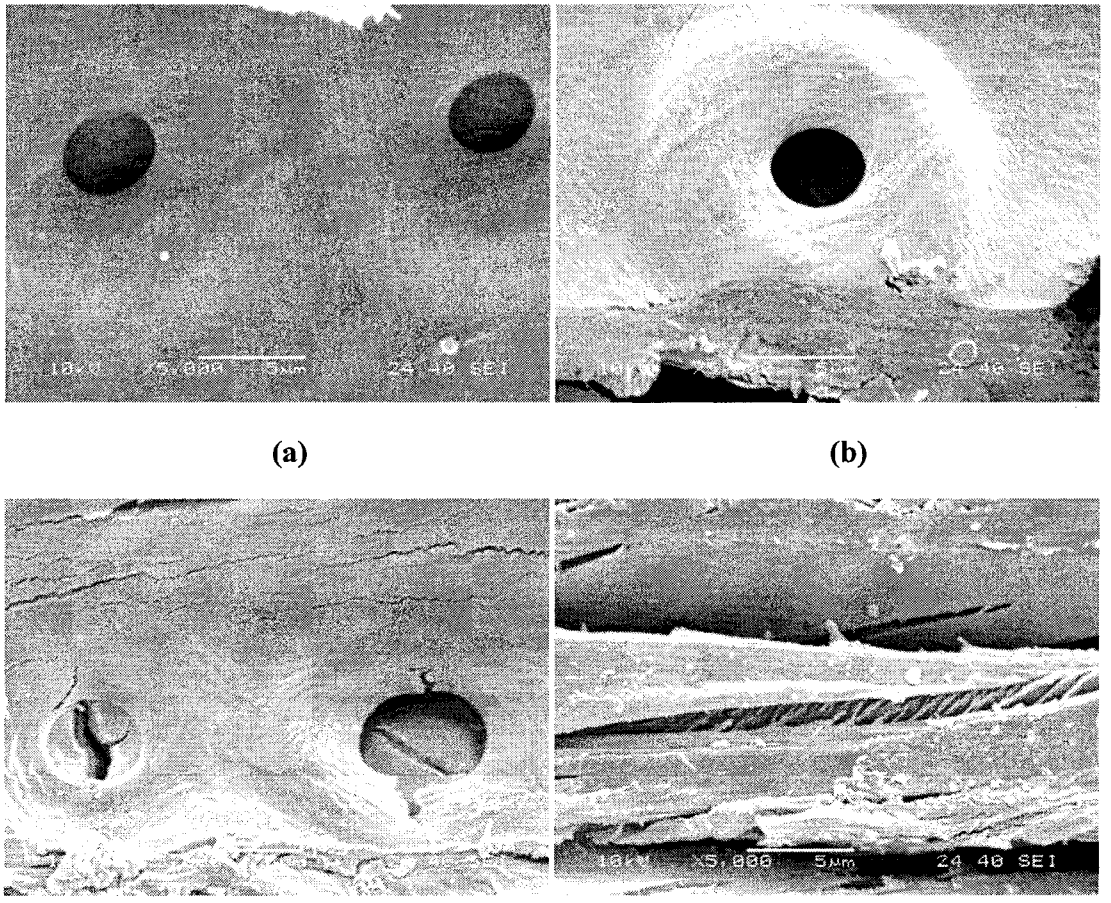

Figure 4.55 SEM micrographs of surface (a) bordered pits beneath the acrylic polyurethane coating with bark extract and lignin stabilizer-radial surface of jack pine wood before aging; development of the structural damage of the bordered pits on radial surface of jack pine coated with acrylic polyurethane with bark extract and lignin stabilizer after (b) 672h and (c) 1500h of aging, (d) structural damage of simple pits on radial surface after 1500h of aging, deep cracks in the S2 layer spread in the direction of the microfibril orientation

Complete destruction of the pit membrane mark was not observed in the present study even after 1500h of aging. Simple pits found in late wood of jack pine did not disintegrate as fast as bordered pits. Only after 1500h of aging, SEM micrographs exhibited deep S2 crack in simple pit revealing angle of microfibrils in this layer of secondary cell wall (Figure 4.54d) although complete wall split was not observed.

4.5.8. Concluding Remarks

The wetting characteristics of the coatings, were not only dependent on the type of additives used and viscosity of the coatings but also on interfacial tensions and capillary penetration. The contact angle started changing as soon as coatings came in contact with wood, but reached to equilibrium for all coatings within 10-15s. The lowest equilibrium contact angle and most capillary penetration were observed for acrylic polyurethane coating with bark extracts. The surface roughness also played an important role in wetting process of wood/coating system. The most wetting was observed if mid grain size sanding paper (grit number 150) was used due to the complex nature of wood surface morphology during sanding. With increasing sanding grit paper number (decreasing grain size) the surfaces became smoother which increased spreadability of the coatings. On the other hand, smoother surfaces had lower porosity resulted in lower penetration characteristic. Therefore, the optimal of spreading and penetration conditions were achieved when the surface was sanded with mid grain size of the sanding papers. The wood surface orientation did not play an important role for these types of highly viscous coatings.

The acrylic polyurethane coating stabilized with bark extract alone or together with lignin stabilizer showed enhanced protection against aging on heat-treated jack pine whereas they failed to provide enough protection on heat-treated aspen and birch. This was due to the presence of more lignin on soft wood species compared to lignin content of hard wood species. But acrylic polyurethane with CeO_2 nano particles alone or together with lignin stabilizer provided very good protection for heat-treated jack pine, aspen and birch. CeO_2 nano particles screened the harmful UV/VIS light during penetration through coating before it reached to the wood surface. The above mentioned coatings performed better in accelerated aging condition compared to industrial Laurentide coating. Water ingression rate through the coatings after aging for different periods proved to be an important factor for wood aging since colored photoproducts derived during accelerated aging could migrate leaving behind pale gray surface. The chemical surface analyses lead to formation of several carbonyl photo products during accelerated aging test, but chain scission reaction of acrylic polyurethane was not very prominent. Therefore, it can be concluded that UV/VIS light penetrates through the coatings and degrades the wood surface beneath it. The morphological studies proved this fact since wood surfaces beneath the coating was found to be degraded even if only minor chemical changes were observed for stabilized acrylic polyurethanes.

4.6. Fungi Test

4.6.1. General

Fungi are organisms which can deteriorate wood in outer environment. Therefore, the effect of fungi on coated heat-treated wood surfaces aged for different times is very important in order to study the efficiency of any coating in outer environment. The fungi decay is a complex process and mainly depends on type of fungi and wood species involved. In this work, the decay resistance of heat-treated jack pine coated with acrylic polyurethane with bark extract and lignin stabilizer was studied by using one brown rot fungus (*P. placenta*) and one white rot fungus (*T.versicolor*). Also, the effect of brown rot fungus on heat-treated jack pine coated with acrylic polyurethane containing bark extract and lignin stabilizer was investigated at different aging times.

4.6.2. Fungal Durability

The weight loss data of acrylic polyurethane containing bark extract and lignin stabilizer coated heat-treated jack pine before and after aging for different times, exposed to a brown rot fungus (*P. placenta*) for 8 weeks are presented in Figure 4.56 . Due to the limitations of number of aged samples, the weight loss data for different exposure periods to fungi could not be monitored. Nevertheless, pictures for different exposure times (2 weeks, 4 weeks, and 8 weeks) were taken to compare the growth of decay fungi on coated heat-treated jack pine before and after aging (Figure 4.57). The weight loss data after 8 weeks of

decay by *P. Placenta* for heat-treated jack pine coated with acrylic polyurethane containing bark extracts and lignin stabilizer suggested that the decay resistance against the brown rot fungus *P. placenta* decreased as the aging time increased (Figure 4.56). This was due the degradation of acrylic polyurethane coating during accelerated aging. The weight loss after 8 weeks of decay for coated heat-treated jack pine after 672h of aging was almost double of the weight loss of the samples recorded before aging. Whereas weight loss after 8 weeks of decay for 1500h aged samples was slightly more than that of 672h aged samples. This indicates that the coating degradation mainly took place within initial 672h of aging. It was observed that the fungal growth of P. placenta on coated heat-treated jack pine surfaces was fast and mycelia covered the coated wood samples before aging almost completely after 2 weeks of exposure to the fungus (Figure 4.57). It was also noticeable that the growth of decay fungus was less on 672h aged coated samples after 2 weeks of exposure compared to that of unaged samples. The growth of P. placenta on 1500h of aged coated samples was slower compared to the growth of the same fungus at different incubation times on samples before aging and 672h aged coated samples, but showed highest mass loss after 8 weeks.

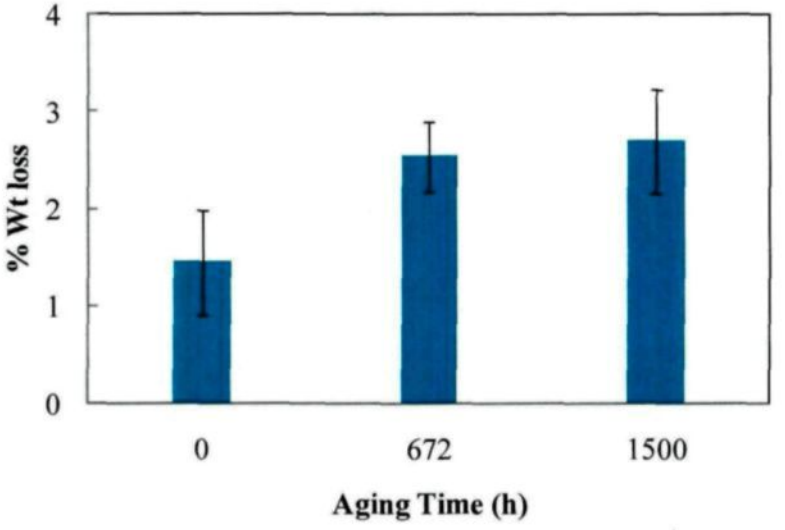

Figure 4.56 Mass loss data of heat-treated jack pine coated with acrylic polyurethane coating containing bark extract and lignin stabilizer for different aging periods after 8 weeks of decay by *P. placenta*

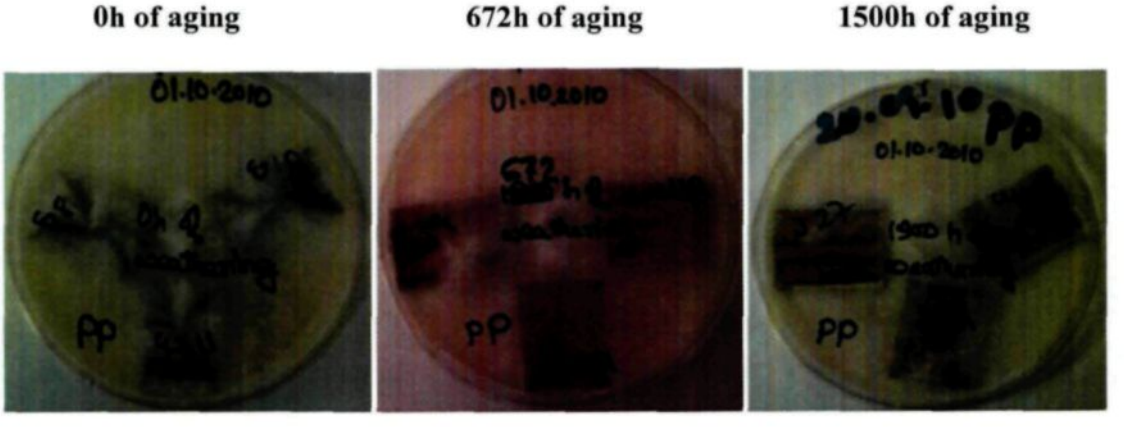

(a)

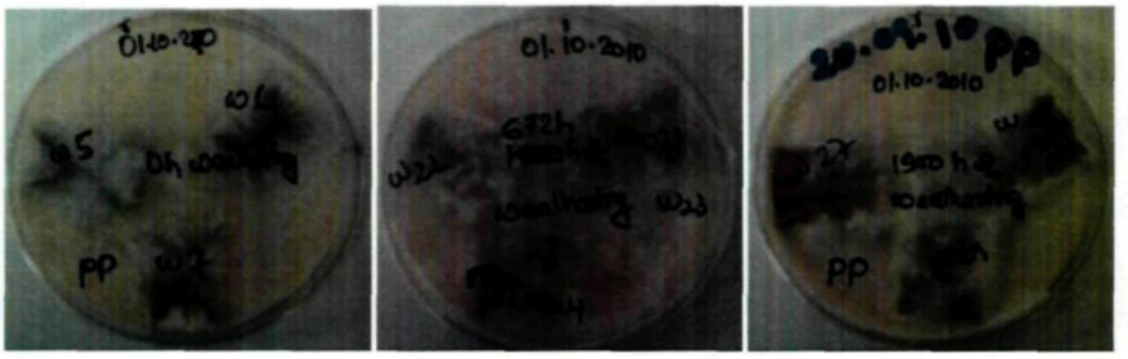

(b)

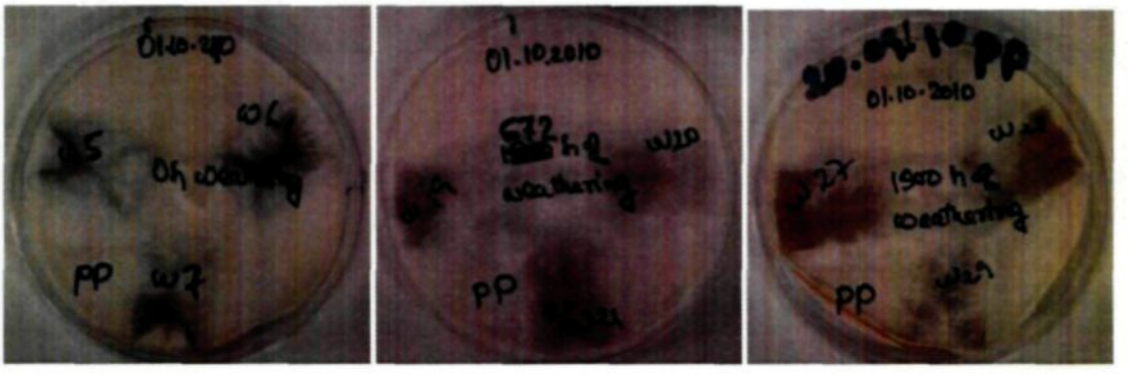

(c)

Figure 4.57 Heat-treated jack pine coated with acrylic polyurethane coating containing bark extract and lignin stabilizer after 2 weeks (a), 4weeks (b), and 8 weeks (c) of decay fungi (*Poria Placenta*) growth for different aging periods

The decay (3.68%) by white rot fungus (*T. versicolor*) of the coated unaged wood after 8 weeks of exposure to the fungus was more than double compared to the decay (1.45%) of the same samples by brown rot fungus (*P. placenta*). The growth of white rot fungus was slower (Figure 4.58) than that of the brown rot fungus but the mass loss (3.68%) was higher by the decay of white rot fungus (*T. versicolor*) compared to mass loss caused by

brown rot fungus (1.45%). This was probably due to the presence of hard wood bark extracts in the acrylic polyurethane coating. White rot fungi degrade hard woods more efficiently compared to brown rot fungi due to the difference in their decay process. Usually white rot fungi degrade lignin and polysaccharides simultaneously whereas brown rot fungi degrade polysaccharides. The bark extracts of hard woods composed of lignins, lignans, stilbenes and different polyphenols. Thus, decay by white rot fungus resulted in higher weight loss compared to weight loss caused by brown rot fungus.

(a) (b) (c)

Figure 4.58 White rot fungus (T. versicolor) growth on heat-treated jack pine coated with acrylic polyurethane coating containing bark extract and lignin stabilizer before aging for different decay periods (a) 2weeks, (b) 4weeks, and (c) 8 weeks

4.6.3. Concluding Remarks

The fungi test results showed more decay by white rot fungus (T. versicolor) compared to that of brown rot fungus (P. placenta) due to the presence of hardwood bark extracts in the acrylic polyurethane coating. Also, with increasing aging time, the fungal durability of heat-treated coated (acrylic polyurethane with bark extracts and lignin stabilizer) jack pine decreased against *P. placenta*. This was due to the degradation of the coatings during accelerated aging.

Chapter 5

CONCLUSIONS AND RECOMMENDATIONS FOR FUTURE WORK

5.1. Conclusions

This thesis mainly concentrates on development of transparent and non toxic protective coatings to prevent or delay the color change of heat-treated wood due to aging. The main challenge was to maintain a balance between aesthetics and protection. From durability point of view, pigmented opaque coatings can protect heat-treated wood surface more efficiently but tends to cover the natural color and texture of heat-treated wood. This value added product attracts the attention of customers mostly because of its color and texture and also due to their increased dimensional stability. On the other hand, transparent coatings are less durable which increases the service cost of this product. Therefore, UV stabilizers are needed to be incorporated in transparent coatings in order to increase their service life. In this work, a variety of organic and inorganic UV stabilizers were considered.

In this thesis, a great effort has been put forth to extract natural antioxidants (bark and needle extracts) which could be used as additives for various coatings and can delay wood aging process. This attempt is justified since most of the organic UV absorbers available in the market are toxic in nature. The black spruce bark extracts had highest yield as well as highest oxygen radical absorbance capacity compared to other extracts. Also, other than

needle extract, highest UV absorption capacity was found in black spruce bark extracts. Although minimum six phenolic compounds were present in black spruce bark extracts compared to minimum nine phenolic compounds present in needle extract as determined from TLC evaluation, concentration of phenolic compounds were much higher in black spruce bark extracts compared to needle extract. The cytotoxicity results showed that these natural antioxidants are non toxic in nature.

The efficiency of these extracts in soy polymer coating on heat-treated jack pine was compared with industrial coatings. The industrial coatings protected heat-treated jack pine well upto 1008h of aging but high surface degradation was noticed after 1500h of aging for the both industrial coatings. The soy based coating with bark extract did not show any protection during accelerated aging due to their highly hygroscopic nature even after crosslinking. Therefore, water could easily diffuse through this coating resulting in delamination, blistering, and flaking of the coating material leading to very significant color change during aging.

A different approach was taken for the protection of the heat-treated wood by sol-gel coating in order to keep different paths open. Since none of the organic and inorganic UV absorbers can absorb UV light completely, combinations of organic and inorganic UV absorbers were used. Although sol-gel derived titania nano coatings containing organic UV absorbers showed very good UV absorption capacity, they could not efficiently protect heat-treated wood. This was probably because of the very thin coating layers left on wood due to penetration of coatings; as a consequence, surface protection was not effective. Also titania has high photocatalytic activity which in turn enhanced photodegradation of wood.

The acrylic polyurethane coatings, on the contrary, are known for their weather resistance capacity. Therefore, the weather resistance characteristic of acrylic polyurethane was enhanced by adding natural antioxidants (bark extracts, needle extracts, and nano lignins), inorganic micro and nano particles and organic UV stabilizers and compared with those of industrial coatings. The acrylic polyurethane coating with black spruce bark extracts alone or together with lignin stabilizers protected best against accelerated aging conditions on heat-treated jack pine compared to all other coatings including Industrial coating. There was not any noticeable degradation at the wood-coating interface even after 1500h of aging. However, this coating failed to perform similarly on heat-treated aspen and birch. This was probably due to the fact that the acrylic polyurethane with bark extract and lignin stabilizer was semitransparent in nature, therefore, the UV/VIS light could easily penetrate and reach to the wood surface. Heat-treated jack pine has higher lignin content than the heat-treated aspen and birch which eventually lead to lower degradation for soft wood species (jack pine) compared to degradation of hard wood species (aspen and birch). This point was further supported by the results of FT-IR analyses which showed minimal degradation (chain scission) of acrylic polyurethane coating containing bark extract and lignin stabilizer during accelerated aging.

Acrylic polyurethanes with CeO_2 nano particles alone or together with lignin stabilizer were other two coatings which showed almost similar protective characteristic as acrylic polyurethane with bark extract alone or together with lignin stabilizer on heat-treated jack pine. Acrylic polyurethane with CeO_2 nano particles also pertained very significant protective characteristic against the discoloration of heat-treated aspen and birch under

accelerated aging conditions. They performed better than the industrial coating when applied to the heat-treated wood species (jack pine, aspen, and birch) studied during this work.

The acrylic polyurethane with black spruce bark extracts and lignin stabilizer showed better decay resistance against the brown rot fungus (*P. placenta*) compared to their resistance against white rot fungus (*T. versicolor*) due to the difference in the decay mechanism of these two fungi. Decay resistance against brown rot fungus decreased with increasing in aging time due to the degradation of coatings during aging.

The main objective of this study was well achieved and some of the coatings developed during this study performed better than the industrial coating under accelerated aging conditions. Therefore, it can be concluded that this work has significantly contributed to the wood coating industry.

5.2. Contribution to Saguenay-Lac-Saint-Jean Region, Quebec and Canadian Economies

The heat-treated wood is a relatively new value-added product and it is very important for the diversification of forestry products in our region. From the end user's perspective, heat-treated wood is a very beneficial product that has good outdoor fungal resistance, improved swelling and shrinkage properties (dimensional stability) compared to those of untreated wood. However, after a short period of utilization it loses its color. With the move towards value-added products and with higher quality product specifications, the discolorations have become an important economic problem. Therefore, color defects are less tolerable and they ultimately lead to a reduction of physical, chemical and biological properties of heat-treated wood. Wood discolorations can affect the natural appearance of many wood species resulting in economic problems for the wood industry. Although this discoloration takes place on a very thin layer of external surface and does not change the total characteristics of the wood product, the user wants a stable color, particularly when it is used for decorative purposes. The protection of heat-treated wood against discoloration is never studied before. This project attempts to bring a solution to the color loss problem of heat-treated wood. Preservation of color improves the quality of the wood product; consequently, it helps both the manufacturer and the customer. Therefore, the project contributes to the regional economy.

5.3. Recommendations

Although highly efficient coatings for the protection of heat-treated wood (jack pine, aspen, and birch) were developed in this study, there is still a lot to be done for their improvement. The results reported in this thesis are based on accelerated aging conditions. Therefore, to perform natural aging of these samples in outer environment would give the actual understanding of these coating's protective behavior. The location of the natural aging tests could be varied in order to study their efficiency under different conditions. This could be one of the pre requisite for the commercialization of any coating.

The cross linking reactions during accelerated aging condition could be studied in detail. This will give an insight to protection mechanism of different light stabilizers used in this study and might lead to identification of more efficient additives.

The efficiencies of the coatings developed during this work were studied on only three heat-treated species. Their protective behavior on other wood species used frequently in North America could be evaluated in future.

In this study only one kind of acrylic polyurethane base was used. Therefore, to evaluate the efficiencies of the natural antioxidants in different base polymers could also be very interesting. This could lead to identification of better bases for coatings.

In this thesis, main emphasis was on the behavior of different coatings under accelerated aging conditions. As a result, the barrier properties (hardness, glass transition temperature, spreading rate, etc.) of the coatings developed during this study was not investigated in detail. To evaluate the barrier properties of these coatings might prove to be valuable from commercialization point of view.

The fungal resistance tests with other heat-treated and coated species could give better understandings and validity of antifungal behavior of these coatings.

REFERENCES

[1] D. Dufour, The canadian lumber industry: Crucial contribution to Canada's prosperity. Catalogue no. 31F0027XIE. Statistics Canada.

[2] G.N. Inari, M. Petrissans, J. Lambert, J.J. Ehrhardt, P. Gérardin, XPS characterization of wood chemical composition after heat-treatment, Surface and Interface Analysis, 38 (2006) 1336-1342.

[3] D.N.S. Hon, S.-T. Chang, Surface degradation of wood by ultraviolet light, Journal of Polymer Science: Polymer Chemistry Edition, 22 (1984) 2227-2241.

[4] G.N. Salaita, F.M.S. Ma, T.C. Parker, G.B. Hoflund, Weathering properties of treated southern yellow pine wood examined by X-ray photoelectron spectroscopy, scanning electron microscopy and physical characterization, Applied Surface Science, 254 (2008) 3925-3934.

[5] G. Sinn, A. Reiterer, S.E. Stanzl-Tschegg, Surface analysis of different wood species using X-ray photoelectron spectroscopy (XPS), Journal of Materials Science, 36 (2001) 4673-4680.

[6] P. Hayoz, W. Peter, D. Rogez, A new innovative stabilization method for the protection of natural wood, Progress in Organic Coatings, 48 (2003) 297-309.

[7] S.Y. Lin, C.W. Dence, Methods in lignin chemistry, Springer-Verlag, 1992.

[8] C. Schaller, D. Rogez, New approaches in wood coating stabilization, Journal of Coatings Technology and Research, 4 (2007) 401-409.

[9] C. Schaller, D. Rogez, Light stabilization of modified wood species, in: The third European Conference on wood modification, Cardiff, Wales UK 2007, pp. 317-324.

[10] E. Sjöström, Wood chemistry: fundamentals and applications, Academic Press, 1993.

[11] D.N.S. Hon, N. Shiraishi, Wood and cellulosic chemistry, Marcel Dekker, 2001.

[12] M. Tshabalala, J. Gangstad, Accelerated weathering of wood surfaces coated with multifunctional alkoxysilanes by sol-gel deposition, Journal of Coatings Technology, 75 (2003) 37-43.

[13] D. Kocaefe, R. Younsi, S. Poncsak, Y. Kocaefe, Comparison of different models for the high-temperature heat-treatment of wood, International Journal of Thermal Sciences, 46 (2007) 707-716.

[14] M. Boonstra, J. van Acker, E. Kegel, M. Stevens, Optimisation of a two-stage heat treatment process: durability aspects, Wood Science and Technology, 41 (2007) 31-57.

[15] B. Esteves, H. Pereira, Wood modification by heat-treatment: A review, BioResources, 4 (2009) 370-404.

[16] M. Hakkou, M. Pétrissans, P. Gérardin, A. Zoulalian, Investigations of the reasons for fungal durability of heat-treated beech wood, Polymer Degradation and Stability, 91 (2006) 393-397.

[17] D.P. Kamdem, A. Pizzi, A. Jermannaud, Durability of heat-treated wood, European Journal of Wood and Wood Products, 60 (2002) 1-6.

[18] D. Kocaefe, S. Poncsak, Y. Boluk, Effect of thermal treatment on the chemical composition and mechanical properties of birch and aspen, BioResources, 3 (2008) 517-537.

[19] D. Kocaefe, S. Poncsak, G. Doré, R. Younsi, Effect of heat treatment on the wettability of white ash and soft maple by water, European Journal of Wood and Wood Products, 66 (2008) 355-361.

[20] S. Poncsák, D. Kocaefe, M. Bouazara, A. Pichette, Effect of high temperature treatment on the mechanical properties of birch (Betula papyrifera), Wood Science and Technology, 40 (2006) 647-663.

[21] S. Poncsák, S.Q. Shi, D. Kocaefe, G. Miller, Effect of thermal treatment of wood lumbers on their adhesive bond strength and durability, Journal of Adhesion Science and Technology, 21 (2007) 745-754.

[22] J. Shi, D. Kocaefe, T. Amburgey, J. Zhang, A comparative study on brown-rot fungus decay and subterranean termite resistance of thermally-modified and ACQ-C-treated wood, European Journal of Wood and Wood Products, 65 (2007) 353-358.

[23] B. Tjeerdsma, M. Boonstra, A. Pizzi, P. Tekely, H. Militz, Characterisation of thermally modified wood: molecular reasons for wood performance improvement, European Journal of Wood and Wood Products, 56 (1998) 149-153.

[24] N. Ayadi, F. Lejeune, F. Charrier, B. Charrier, A. Merlin, Color stability of heat-treated wood during artificial weathering, European Journal of Wood and Wood Products, 61 (2003) 221-226.

[25] G. Nguila Inari, M. Petrissans, P. Gerardin, Chemical reactivity of heat-treated wood, Wood Science and Technology, 41 (2007) 157-168.

[26] M. Nuopponen, H. Wikberg, T. Vuorinen, S.L. Maunu, S. Jämsä, P. Viitaniemi, Heat-treated softwood exposed to weathering, Journal of Applied Polymer Science, 91 (2004) 2128-2134.

[27] P.D. Evans, A.J. Michell, K.J. Schmalzl, Studies of the degradation and protection of wood surfaces, Wood Science and Technology, 26 (1992) 151-163.

[28] D.N.S. Hon, W.C. Feist, Hydroperoxidation in photoirradiated wood surfaces, Wood and Fiber Science, 24 (1992) 448-455.

[29] D.N.S. Hon, S.-T. Chang, W.C. Feist, Protection of wood surfaces against photooxidation, Journal of Applied Polymer Science, 30 (1985) 1429-1448.

[30] M. Roux, E. Wozniak, E. Miller, J. Boxall, P. Böttcher, F. Kropf, J. Sell, Natural weathering of various surface coatings on five species at four european sites, European Journal of Wood and Wood Products, 46 (1988) 165-170.

[31] M. McCusker, A UVA/HALS Primer: Everything You've Ever Wanted to Know About Light Stabilizers-Part I, Anglais, 97 (1999) 51-53.

[32] M. McCusker, A UVA/HALS PRIMER : Everything you've ever wabted to know about light stabilizers-Part III, Anglais, 97 (1999) 38-40.

[33] K.K. Pandey, A note on the influence of extractives on the photo-discoloration and photo-degradation of wood, Polymer Degradation and Stability, 87 (2005) 375-379.

[34] C. Schaller, D. Rogez, A. Braig, Hydroxyphenyl-s-triazines: advanced multipurpose UV-absorbers for coatings, Journal of Coatings Technology and Research, 5 (2008) 25-31.

[35] B. Mahltig, H. Böttcher, K. Rauch, U. Dieckmann, R. Nitsche, T. Fritz, Optimized UV protecting coatings by combination of organic and inorganic UV absorbers, Thin Solid Films, 485 (2005) 108-114.

[36] E. Liptáková, J. Kúdela, Analysis of the Wood-Wetting Process, Holzforschung, 48 (1994) 139-144.

[37] B.M. Collett, A review of surface and interfacial adhesion in wood science and related fields, Wood Science and Technology, 6 (1972) 1-42.

[38] M. Stehr, D.J. Gardner, M.E.P. Wålinder, Dynamic Wettability of Different Machined Wood Surfaces, The Journal of Adhesion, 76 (2001) 185-200.

[39] G. Mantanis, R. Young, Wetting of wood, Wood Science and Technology, 31 (1997) 339-353.

[40] A. Adamson, Physical Chemistry of Surfaces, John Wiley & Sons, New York, 1990.

[41] M.E. Schrader, Contact Angle and Vapor Adsorption, Langmuir, 12 (1996) 3728-3732.

[42] H.W. Fox, W.A. Zisman, The spreading of liquids on low energy surfaces. I. polytetrafluoroethylene, Journal of Colloid Science, 5 (1950) 514-531.

[43] R.J. Good, L.A. Girifalco, A theory for estimation of surface and interfacial energies. iii. estimation of surface energies of solids from contact angle data, The Journal of Physical Chemistry, 64 (1960) 561-565.

[44] L.A. Girifalco, R.J. Good, A Theory for the Estimation of Surface and Interfacial Energies. I. Derivation and Application to Interfacial Tension, The Journal of Physical Chemistry, 61 (1957) 904-909.

[45] F.M. Fowkes, Attractive forces at interfaces, Industrial & Engineering Chemistry, 56 (1964) 40-52.

[46] T. Nguyen, W.E. Johns, Polar and dispersion force contributions to the total surface free energy of wood, Wood Science and Technology, 12 (1978) 63-74.

[47] D.K. Owens, R.C. Wendt, Estimation of the surface free energy of polymers, Journal of Applied Polymer Science, 13 (1969) 1741-1747.

[48] S. Wu, Calculation of interfacial tension in polymer systems, Journal of Polymer Science Part C: Polymer Symposia, 34 (1971) 19-30.

[49] C.J. Van Oss, M.K. Chaudhury, R.J. Good, Interfacial Lifshitz-van der Waals and polar interactions in macroscopic systems, Chemical Reviews, 88 (1988) 927-941.

[50] M.E. Schrader, G.I. Loeb, Modern approaches to wettability: theory and applications, Plenum Press, 1992.

[51] W.A. Zisman, Contact Angle, Wettability, and Adhesion, American Chemical Society, 1964.

[52] M. Šernek, F.A. Kamke, W.G. Glasser, Comparative analysis of inactivated wood surfaces, Holzforschung, 58 (2004) 22-31.

[53] M.E.P. Wålinder, I. Johansson, Measurement of Wood Wettability by the Wilhelmy Method. Part 1. Contamination of Probe Liquids by Extractives, Holzforschung, 55 (2001) 21-32.

[54] M. Meijer, K. Thurich, H. Militz, Comparative study on penetration characteristics of modern wood coatings, Wood Science and Technology, 32 (1998) 347-365.

[55] M.A. Kalnins, C. Katzenberger, S.A. Schmieding, J.K. Brooks, Contact angle measurement on wood using videotape technique, Journal of Colloid and Interface Science, 125 (1988) 344-346.

[56] M. Gindl, G. Sinn, W. Gindl, A. Reiterer, S. Tschegg, A comparison of different methods to calculate the surface free energy of wood using contact angle measurements, Colloids and Surfaces A: Physicochemical and Engineering Aspects, 181 (2001) 279-287.

[57] E. Liptáková, J. Kúdela, Z. Bastl, I. Spirovová, Influence of Mechanical Surface Treatment of Wood on the Wetting Process, Holzforschung, 49 (1995) 369-375.

[58] G. Sinn, M. Gindl, A. Reiterer, S. Stanzl-Tschegg, Changes in the surface properties of wood due to sanding, Holzforschung, 58 (2004) 246-251.

[59] M. Stehr, S. Östlund, An Investigation of the Crack Tendency on Wood Surfaces After Different Machining Operations, Holzforschung, 54 (2000) 427-436.

[60] M. Scheikl, M. Dunky, Measurement of Dynamic and Staue Contact Angles on Wood for the Determination of its Surface Tension and the Penetration of Liquids into the Wood Surface, Holzforschung, 52 (1998) 89-94.

[61] C.-Y. Hse, Properties of phenolic adhesives as related to bond quality in southern pine plywood, Forest Products Journal, 21 (1971) 44-52.

[62] J. Cao, P. Kamdem, Surface energy of preservative-treated southern yellow pine by contact angle measurement, Frontiers of Forestry in China, 2 (2007) 99-103.

[63] M. Pétrissans, P. Gérardin, I.E. bakali, M. Serraj, Wettability of Heat-Treated Wood, Holzforschung, 57 (2003) 301-307.

[64] M. Hakkou, M. Pétrissans, A. Zoulalian, P. Gérardin, Investigation of wood wettability changes during heat treatment on the basis of chemical analysis, Polymer Degradation and Stability, 89 (2005) 1-5.

[65] M. Hakkou, M. Pétrissans, I. El Bakali, P. Gérardin, A. Zoulalian, Wettability changes and mass loss during heat treatment of wood, Holzforschung, 59 (2005) 35-37.

[66] P. Gérardin, M. Petric, M. Petrissans, J. Lambert, J.J. Ehrhrardt, Evolution of wood surface free energy after heat treatment, Polymer Degradation and Stability, 92 (2007) 653-657.

[67] M.A. Kalnins, W.C. Feist, Increase in wettability of wood with weathering, Forest Products Journal, 43 (1993) 55-57.

[68] M. Gindl, G. Sinn, S.E. Stanzl-Tschegg, The effects of ultraviolet light exposure on the wetting properties of wood, Journal of Adhesion Science and Technology, 20 (2006) 817-828.

[69] E. Liptáková, J. Kúdela, Study of the System Wood – Coating Material. Part 2.Wood – Solid Coating Material, Holzforschung, 56 (2002) 547-557.

[70] K. Richter, W.C. Feist, M.T. Knaebe, The effect of surface roughness on the performance of finishes. I: Roughness characterization and stain performance, Forest Products Journal, 45 (1995) 91-97.

[71] L. de Moura, R. Hernández, Evaluation Of Varnish Coating Performance For Two Surfacing Methods On Sugar Maple Wood, Wood and Fiber Science, 37 (2005) 355-366.

[72] M. de Meijer, K. Thurich, H. Militz, Quantitative measurements of capillary coating penetration in relation to wood and coating properties, European Journal of Wood and Wood Products, 59 (2001) 35-45.

[73] V. Rijckaert, M. Stevens, J. Van Acker, M. de Meijer, H. Militz, Quantitative assessment of the penetration of water-borne and solvent-borne wood coatings in Scots pine sapwood, European Journal of Wood and Wood Products, 59 (2001) 278-287.

[74] M. de Meijer, Review on the durability of exterior wood coatings with reduced VOC-content, Progress in Organic Coatings, 43 (2001) 217-225.

[75] G. Hora, The dynamic contact angle : a characteristic to predict the lifetime of a wood topcoat, Journal of Coatings Technology and Research, 66 (1994) 55-59.

[76] W.C. Feist, D.N.-S. Hon, The chemistry of solid wood, American Chemical Society, Washington, DC, Etats-Unis, 1984.

[77] P. Nzokou, D.P. Kamdem, Influence of wood extractives on the photo-discoloration of wood surfaces exposed to artificial weathering, Color Research & Application, 31 (2006) 425-434.

[78] S. Zahri, C. Belloncle, F. Charrier, P. Pardon, S. Quideau, B. Charrier, UV light impact on ellagitannins and wood surface colour of European oak (Quercus petraea and Quercus robur), Applied Surface Science, 253 (2007) 4985-4989.

[79] B. George, E. Suttie, A. Merlin, X. Deglise, Photodegradation and photostabilisation of wood - the state of the art, Polymer Degradation and Stability, 88 (2005) 268-274.

[80] D.N.S. Hon, S.T. Chang, W.C. Feist, Participation of singlet oxygen in the photodegradation of wood surfaces, Wood Science and Technology, 16 (1982) 193-201.

[81] P. Nzokou, D. Kamdem, Influence of Wood Extractives on Moisture Sorption and Wettability of Red Oak (<i>Quercus Rubra</i>), Black Cherry (<i>Prunus Serotina</i>), and Red Pine (<i>Pinus Resinosa</i>), Wood and Fiber Science, 36 (2004) 483-492.

[82] M. Deka, M. Humar, G. Rep, B. Kričej, M. Šentjurc, M. Petrič, Effects of UV light irradiation on colour stability of thermally modified, copper ethanolamine treated and non-modified wood: EPR and DRIFT spectroscopic studies, Wood Science and Technology, 42 (2008) 5-20.

[83] P.G. Parejo, M. Zayat, D. Levy, Highly efficient UV-absorbing thin-film coatings for protection of organic materials against photodegradation, Journal of Materials Chemistry, 16 (2006) 2165-2169.

[84] F. Aloui, A. Ahajji, Y. Irmouli, B. George, B. Charrier, A. Merlin, Photostabilisation of the "wood-clearcoatings" systems with UV absorbers: correlation with their effect on the glass transition temperature, Journal of Physics: Conference Series, 40 (2006) 118-112.

[85] M.A. Shenoy, Y.D. Marathe, Studies on synergistic effect of UV absorbers and hindered amine light stabilisers, Pigment & Resin Technology, 36 (2007) 83-89.

[86] K.K. Pandey, Study of the effect of photo-irradiation on the surface chemistry of wood, Polymer Degradation and Stability, 90 (2005) 9-20.

[87] C. Decker, K. Zahouily, Light-stabilization of polymeric materials by grafted UV-cured coatings, Journal of Polymer Science Part A: Polymer Chemistry, 36 (1998) 2571-2580.

[88] M. Kiguchi, P.D. Evans, J. Ekstedt, R.S. Williams, Y. Kataoka, Improvement of the durability of clear coatings by grafting of UV-absorbers on to wood, Surface Coatings International Part B: Coatings Transactions, 84 (2001) 263-270.

[89] X. Liu, J. Yang, Y. Chen, Reactive-HALS I: Synthesis, characterization, copolymerization reactivity and photo-stabilizing performance applied in UV-curable coatings, Polymers for Advanced Technologies, 13 (2002) 247-253.

[90] P. Sundell, F. Sundholm, Polyester binders for wood containing benzotriazole and HALS light stabilizers, Journal of Applied Polymer Science, 92 (2004) 1413-1421.

[91] M. Zayat, P. Garcia-Parejo, D. Levy, Preventing UV-light damage of light sensitive materials using a highly protective UV-absorbing coating, Chemical Society Reviews, 36 (2007) 1270-1281.

[92] M. Tshabalala, L.-P. Sung, Wood surface modification by in-situ sol-gel deposition of hybrid inorganic–organic thin films, Journal of Coatings Technology and Research, 4 (2007) 483-490.

[93] R. Mahlberg, S. Jamsa, M. Loija, S. Takala, J. Mannila, A. Pahkala, M. Kallio, A.-C. Ritschkoff, Improved UV resistance of wood with nano-hybrid coatings, VTT SYMPOSIUM, 244 (2006) 145-153.

[94] S. Donath, H. Militz, C. Mai, Creating water-repellent effects on wood by treatment with silanes, Holzforschung, 60 (2006) 40-46.

[95] M.A. Tshabalala, P. Kingshott, M.R. VanLandingham, D. Plackett, Surface chemistry and moisture sorption properties of wood coated with multifunctional alkoxysilanes by sol-gel process, Journal of Applied Polymer Science, 88 (2003) 2828-2841.

[96] M.A. Tshabalala, Sol-gen depositoon of inorganic alkoxides on wood surfaces to enhance their durability under exposure to sunlight and moisture, in: J.W. Martin, R.A. Ryntz, R.A. Dickie (Eds.) Surface life prediction: challenging the status quo, Federation of Societies of Coating Technology, Bluebell, PA, 2005.

[97] K.J. Schmalzl, P.D. Evans, Wood surface protection with some titanium, zirconium and manganese compounds, Polymer Degradation and Stability, 82 (2003) 409-419.

[98] D. Kundu, R. Mukherjee, UV absorbing transparent sol-gel derived coatings on glass, Journal of Materials Science Letters, 22 (2003) 1647-1649.

[99] H. Cui, M. Zayat, P.G. Parejo, D. Levy, Highly Efficient Inorganic Transparent UV-Protective Thin-Film Coating by Low Temperature Sol-Gel Procedure for Application on Heat-Sensitive Substrates, Advanced Materials, 20 (2008) 65-68.

[100] F. Aloui, A. Ahajji, Y. Irmouli, B. George, B. Charrier, A. Merlin, Inorganic UV absorbers for the photostabilisation of wood-clearcoating systems: Comparison with organic UV absorbers, Applied Surface Science, 253 (2007) 3737-3745.

[101] A. Becheri, M. Dürr, P. Lo Nostro, P. Baglioni, Synthesis and characterization of zinc oxide nanoparticles: application to textiles as UV-absorbers, Journal of Nanoparticle Research, 10 (2008) 679-689.

[102] M. Lowry, D. Hubble, A. Wressell, M. Vratsanos, F. Pepe, C. Hegedus, Assessment of UV-permeability in nano-ZnO filled coatings via high throughput experimentation, Journal of Coatings Technology and Research, 5 (2008) 233-239.

[103] D. Fauchadour, T. Jeanson, J.-N. Bousseau, B. Echalier, Nanoparticles of Cerium Oxide — Application to Coatings Technologies, in: Nano and Hybrid Coatings conference, Manchester, UK, 2005.

[104] C. Hu, Z. Zhang, H. Liu, P. Gao, Z.L. Wang, Direct synthesis and structure characterization of ultrafine CeO_2 nanoparticles, Nanotechnology, 17 (2006) 5983–5987.

[105] M.F. Montemor, R. Pinto, M.G.S. Ferreira, Chemical composition and corrosion protection of silane films modified with CeO2 nanoparticles, Electrochimica Acta, 54 (2009) 5179-5189.

[106] S. Phoka, P. Laokul, E. Swatsitang, V. Promarak, S. Seraphin, S. Maensiri, Synthesis, structural and optical properties of CeO2 nanoparticles synthesized by a simple polyvinyl pyrrolidone (PVP) solution route, Materials Chemistry and Physics, 115 (2009) 423-428.

[107] L. Yue, X.-M. Zhang, Structural characterization and photocatalytic behaviors of doped CeO2 nanoparticles, Journal of Alloys and Compounds, 475 (2009) 702-705.

[108] V. Blanchard, P. Blanchet, COLOR STABILITY FOR WOOD PRODUCTS DURING USE: EFFECTS OF INORGANIC NANOPARTICLES, BioResources, 6 (2011) 1219-1229.

[109] H. Miyafuji, H. Kokaji, S. Saka, Photostable wood–inorganic composites prepared by the sol-gel process with UV absorbent, Journal of Wood Science, 50 (2004) 130-135.

[110] D. Fengel, G. Wegener, Wood: chemistry, ultrastructure, reactions, W. de Gruyter, 1984.

[111] S. Pietarinen, S. Willför, M. Ahotupa, J. Hemming, B. Holmbom, Knotwood and bark extracts: strong antioxidants from waste materials, Journal of Wood Science, 52 (2006) 436-444.

[112] R.S. Williams, Weathering of wood, in: R.M. Rowell (Ed.) Handbook of wood chemistry and wood composites, CRC Press, 2005.

[113] H. Gao, T. Shupe, T. Eberhardt, C. Hse, Antioxidant activity of extracts from the wood and bark of Port Orford cedar, Journal of Wood Science, 53 (2007) 147-152.

[114] P.C. Eklund, O.K. Langvik, J.P. Warna, T.O. Salmi, S.M. Willfor, R.E. Sjoholm, Chemical studies on antioxidant mechanisms and free radical scavenging properties of lignans, Organic & Biomolecular Chemistry, 3 (2005) 3336-3347.

[115] M.P. Kähkönen, A.I. Hopia, H.J. Vuorela, J.-P. Rauha, K. Pihlaja, T.S. Kujala, M. Heinonen, Antioxidant Activity of Plant Extracts Containing Phenolic Compounds, Journal of Agricultural and Food Chemistry, 47 (1999) 3954-3962.

[116] A. Guri, P. Kefalas, V. Roussis, Antioxidant potential of six pine species, Phytotherapy Research, 20 (2006) 263-266.

[117] H. Zulaica-Villagomez, D.M. Peterson, L. Herrin, R.A. Young, Antioxidant activity of different components of pine species, Holzforschung, 59 (2005) 156-162.

[118] S. Willför, L. Nisula, J. Hemming, M. Reunanen, B. Holmbom, Bioactive phenolic substances in industrially important tree species. Part 1: Knots and stemwood of different spruce species, Holzforschung, 58 (2004) 335-344.

[119] K. Girard-Lalalncette, J. Legault, D. Dufour, Pichette A., Antoxidant potential of bark extracts from boreal forest conifers, Jouranl of Ethnopharmacology, Submitted (2011).

[120] P.-L. Chou, H.-T. Chang, T.-F. Yeh, S.-T. Chang, Characterizing the conservation effect of clear coatings on photodegradation of wood, Bioresource Technology, 99 (2008) 1073-1079.

[121] Y. Yazaki, J. Bauch, R. Endeward, Extractive components responsible for the discoloration of Ilomba wood (Pycnanthus angolensis Exell), European Journal of Wood and Wood Products, 43 (1985) 359-363.

[122] T.P. Schultz, D.D. Nicholas, Naturally durable heartwood: evidence for a proposed dual defensive function of the extractives, Phytochemistry, 54 (2000) 47-52.

[123] F. Bonina, M. Lanza, L. Montenegro, C. Puglisi, A. Tomaino, D. Trombetta, F. Castelli, A. Saija, Flavonoids as potential protective agents against photo-oxidative skin damage, International Journal of Pharmaceutics, 145 (1996) 87-94.

[124] H.W. Heldt, F. Heldt, Plant biochemistry and molecular biology, Oxford University Press, 1997.

[125] H. Scheer, Chlorophylls, CRC Press, 1991.

[126] R. Aquino, S. Morelli, A. Tomaino, M. Pellegrino, A. Saija, L. Grumetto, C. Puglia, D. Ventura, F. Bonina, Antioxidant and photoprotective activity of a crude extract of Culcitium reflexum H.B.K. leaves and their major flavonoids, Journal of Ethnopharmacology, 79 (2002) 183-191.

[127] V. Liakoura, J.F. Bornman, G. Karabourniotis, The ability of abaxial and adaxial epidermis of sun and shade leaves to attenuate UV-A and UV-B radiation in relation to the UV absorbing capacity of the whole leaf methanolic extracts, Physiologia Plantarum, 117 (2003) 33-43.

[128] Å. Strid, R.J. Porra, Alterations in Pigment Content in Leaves of Pisum sativum After Exposure to Supplementary UV-B, Plant and Cell Physiology, 33 (1992) 1015-1023.

[129] W.J. Wolf, Soybean proteins. Their functional, chemical, and physical properties, Journal of Agricultural and Food Chemistry, 18 (1970) 969-976.

[130] D.J. Myers, Industrial applications for soy protein and potential for increased utilization, Cereal foods world, 38 (5) (1993) 355-360.

[131] R. Kumar, V. Choudhary, S. Mishra, I. Varma, Enzymatically modified Soy Protein, Journal of Thermal Analysis and Calorimetry, 75 (2004) 727-738.

[132] S. Xiuzhi, K. Bian, Shear strength and water resistance of modified soy protein adhesives, Journal of the American Oil Chemists' Society, 76 (1999) 977-980.

[133] Soy based paints and coatings, in:

http://www.soynewuses.com/downloads/Tech_Paints.pdf.

[134] A. Lambuth, Soybean, Blood, and Casein glues in: A. Tracton (Ed.) Coatings Technology Handbook, Taylor & Francis, 2006.

[135] T. Jaworek, H.-H. Bankowsky, R. Königer, W. Reich, W. Schrof, R. Schwalm, Radiation curable materials – principles and new perspectives, Macromolecular Symposia, 159 (2000) 197-204.

[136] F. Masson, C. Decker, T. Jaworek, R. Schwalm, UV-radiation curing of waterbased urethane-acrylate coatings, Progress in Organic Coatings, 39 (2000) 115-126.

[137] C. Decker, F. Masson, R. Schwalm, Dual-Curing of Waterborne Urethane-Acrylate Coatings by UV and Thermal Processing, Macromolecular Materials and Engineering, 288 (2003) 17-28.

[138] O.R. Pardini, J.I. Amalvy, FTIR, 1H-NMR spectra, and thermal characterization of water-based polyurethane/acrylic hybrids, Journal of Applied Polymer Science, 107 (2008) 1207-1214.

[139] A.C. Aznar, O.R. Pardini, J.I. Amalvy, Glossy topcoat exterior paint formulations using water-based polyurethane/acrylic hybrid binders, Progress in Organic Coatings, 55 (2006) 43-49.

[140] B.U. Ahn, S.K. Lee, S.K. Lee, H.M. Jeong, B.K. Kim, High performance UV curable polyurethane dispersions by incorporating multifunctional extender, Progress in Organic Coatings, 60 (2007) 17-23.

[141] M. Tielemans, J.P. Bleus, New Radiation-Curable Polyurethane Dispersions for Outdoor Application on Wood, in: 5th International Wood Coatings Congress, Paragues, 2006.

[142] C. Sow, B. Riedl, P. Blanchet, UV-waterborne polyurethane-acrylate nanocomposite coatings containing alumina and silica nanoparticles for wood: mechanical, optical, and thermal properties assessment, Journal of Coatings Technology and Research, 8 (2011) 211-221.

[143] C. Decker, F. Masson, R. Schwalm, Weathering resistance of waterbased UV-cured polyurethane-acrylate coatings, Polymer Degradation and Stability, 83 (2004) 309-320.

[144] J. Hu, X. Li, J. Gao, Q. Zhao, Ageing behavior of acrylic polyurethane varnish coating in artificial weathering environments, Progress in Organic Coatings, 65 (2009) 504-509.

[145] C. Irle, M. Bayona, B. Wade, M. Dvorchak, Waterborne UV-Curing Polyurethane Dispersions for Clear and Pigmented Coatings on Wood, RADTECH REPORT, 18 (2004) 9-13.

[146] C. Merlatti, F.X. Perrin, E. Aragon, A. Margaillan, Natural and artificial weathering characteristics of stabilized acrylic-urethane paints, Polymer Degradation and Stability, 93 (2008) 896-903.

[147] F.X. Perrin, M. Irigoyen, E. Aragon, J.L. Vernet, Artificial aging of acrylurethane and alkyd paints: a micro-ATR spectroscopic study, Polymer Degradation and Stability, 70 (2000) 469-475.

[148] X.F. Yang, C. Vang, D.E. Tallman, G.P. Bierwagen, S.G. Croll, S. Rohlik, Weathering degradation of a polyurethane coating, Polymer Degradation and Stability, 74 (2001) 341-351.

[149] J.E.P. Custódio, M.I. Eusébio, Waterborne acrylic varnishes durability on wood surfaces for exterior exposure, Progress in Organic Coatings, 56 (2006) 59-67.

[150] F.W. Kropf, J. Sell, W.C. Feist, Comparative weathering tests of North American and European exterior wood finishes, Forest Products Journal, 44 (1994) 33-41.

[151] E. Ncube, M. Meincken, Surface characteristics of coated soft- and hardwoods due to UV-B ageing, Applied Surface Science, 256 (2010) 7504-7509.

[152] L. Podgorski, Analysis of the wood coating ageing and prediction of the durability through calorimetric investigations, in: COST E 18 Final seminar, 2004, pp. 1-6.

[153] L. Podgorski, A. Merlin, X. Deglise, Analysis of the Natural and Artificial Weathering of a Wood Coating by Measurement of the Glass Transition Temperature, Holzforschung, 50 (1996) 282-287.

[154] H. Turkulin, M. Arnold, H. Derbyshire, J. Sell, Structural and fractographic SEM analysis of exterior coated wood, Surface Coatings International Part B: Coatings Transactions, 84 (2001) 67-75.

[155] J. Van den Bulcke, J. Van Acker, M. Stevens, Experimental and theoretical behavior of exterior wood coatings subjected to artificial weathering, Journal of Coatings Technology and Research, 5 (2008) 221-231.

[156] S. Jämsä, P. Ahola, P. Viitaniemi, Performance of coated heat-treated wood, Surface Coatings International Part B: Coatings Transactions, 82 (1999) 297-300.

[157] Saila Jämsä, Pirjo Ahola, Pertti Viitaniemi, Long-term natural weathering of coated ThermoWood, Pigment & Resin Technology, 29 (2000) 68 - 74.

[158] S. Rossi, T. Anfodillo, R. Menardi, Trephor: a new tool for sampling microcores from tree stems, IAWA Journal, 27 (2006) 89-98.

[159] A. Singh, B. Dawson, Microscopic assessment of the effect of saw-texture Pinus radiata plywood surface on the distribution of a film-forming acrylic stain, Journal of Coatings Technology and Research, 3 (2006) 193-201.

[160] D.H. Kaelbel, Dispersion-polar surface tension properties of organic solid, Journal of Adhesion 2(1969) 66-81.

[161] D. Gardner, Application of The Lifshitz-van Der Waals Acid-base Approach To Determine Wood Surface Tension Components, Wood and Fiber Science, 28 (1996) 422-428.

[162] H. Wagner, S. Bladt, E.M. Zgainski, Plant Drug Analysis, Springer-Verlag.

[163] Y. Sudiyani, S.-i. Tsujiyama, Y. Imamura, M. Takahashi, K. Minato, H. Kajita, Chemical characteristics of surfaces of hardwood and softwood deteriorated by weathering, Journal of Wood Science, 45 (1999) 348-353.

[164] L. Tolvaj, O. Faix, Artificial Ageing of Wood Monitored by DRIFT Spectroscopy and CIE L*a*b* Color Measurements. 1. Effect of UV Light, Holzforschung, 49 (1995) 397-404.

[165] O. Faix, J. Böttcher, The influence of particle size and concentration in transmission and diffuse reflectance spectroscopy of wood, European Journal of Wood and Wood Products, 50 (1992) 221-226.

[166] X. Colom, F. Carrillo, F. Nogués, P. Garriga, Structural analysis of photodegraded wood by means of FTIR spectroscopy, Polymer Degradation and Stability, 80 (2003) 543-549.

[167] M. Kiguchi, P.D. Evans, Photostabilisation of wood surfaces using a grafted benzophenone UV absorber, Polymer Degradation and Stability, 61 (1998) 33-45.

[168] X. Hua, S. Kaliaguine, B.V. Kokta, A. Adnot, Surface analysis of explosion pulps by ESCA, Wood Science and Technology, 28 (1993) 1-8.

[169] P. Nzokou, D. Pascal Kamdem, X-ray photoelectron spectroscopy study of red oak-(Quercus rubra), black cherry- (Prunus serotina) and red pine- (Pinus resinosa) extracted wood surfaces, Surface and Interface Analysis, 37 (2005) 689-694.

[170] Q. Shen, P. Mikkola, J.B. Rosenholm, Quantitative characterization of the subsurface acid-base properties of wood by XPS and Fowkes theory, Colloids and Surfaces A: Physicochemical and Engineering Aspects, 145 (1998) 235-241.

[171] H. Turkulin, High Performance Wood Coatings Exterior and Interior Performance, in: COST A 18 Final Seminar, Paris, 2004.

[172] H.-T. Chang, T.-F. Yeh, S.-T. Chang, Comparisons of chemical characteristic variations for photodegraded softwood and hardwood with/without polyurethane clear coatings, Polymer Degradation and Stability, 77 (2002) 129-135.

[173] K. Mitsui, A. Murata, L. Tolvaj, Changes in the properties of light-irradiated wood with heat treatment: Part 3. Monitoring by DRIFT spectroscopy, European Journal of Wood and Wood Products, 62 (2004) 164-168.

[174] K. Mitsui, S. Tsuchikawa, Low atmospheric temperature dependence on photodegradation of wood, Journal of Photochemistry and Photobiology B: Biology, 81 (2005) 84-88.

[175] M. Denesuk, G.L. Smith, B.J.J. Zelinski, N.J. Kreidl, D.R. Uhlmann, Capillary Penetration of Liquid Droplets into Porous Materials, Journal of Colloid and Interface Science, 158 (1993) 114-120.

[176] M. de Meijer, B. van de Velde, H. Militz, Rheological approach to the capillary penetration of coating into wood, Journal of Coatings Technology, 73 (2001) 39-51.

[177] K.K. Pandey, T. Vuorinen, UV resonance Raman spectroscopic study of photodegradation of hardwood and softwood lignins by UV laser, Holzforschung, 62 (2008) 183-188.

[178] R. Marie, M. Garay, Aging Test of Coatings for Wood Panel Boards, in: Proceedings of the 51st International Convention of Society of Wood Science and Technology, Chile, 2008.

Appendix 1

Coated Wood Surface Energy Calculation Steps by Lifshitz van-der Waals Acid Base Approach

In this present study, four liquids (Table 3.2) were used to calculate the surface energy of coated wood surfaces by Lifshitz van-der Waals acid base approach (see Eqn. 2.14). γ_L, γ_L^{LW}, γ_L^-, and γ_L^+ are known and are presented in Table 3.2 for each liquid. The contact angle (θ) was obtained by sessile drop experiments and initial contact angles of each liquid/coated wood system were used for these calculations. Following matrix was obtained for any coated wood surface, and the surface energy components were easily obtained from its solution.

$$\begin{bmatrix} a_1 \\ a_2 \\ a_3 \\ a_4 \end{bmatrix} = \begin{bmatrix} b_1 \\ b_2 \\ b_3 \\ b_4 \end{bmatrix} \sqrt{\gamma_S^{LW}} + \begin{bmatrix} c_1 \\ c_2 \\ c_3 \\ c_4 \end{bmatrix} \sqrt{\gamma_S^+} + \begin{bmatrix} d_1 \\ d_2 \\ d_3 \\ d_4 \end{bmatrix} \sqrt{\gamma_S^-} \qquad \textbf{[A1.1]}$$

Where, $\begin{bmatrix} a_1 \\ a_2 \\ a_3 \\ a_4 \end{bmatrix} = (\mathbf{1} + \boldsymbol{cos\theta})\boldsymbol{\Upsilon_L}$

$$\begin{bmatrix} b_1 \\ b_2 \\ b_3 \\ b_4 \end{bmatrix} = \mathbf{2}\sqrt{\boldsymbol{\Upsilon_L^{LW}}}$$

$$\begin{bmatrix} c_1 \\ c_2 \\ c_3 \\ c_4 \end{bmatrix} = 2\sqrt{\boldsymbol{\Upsilon_L^-}}$$

$$\begin{bmatrix} d_1 \\ d_2 \\ d_3 \\ d_4 \end{bmatrix} = \sqrt{\boldsymbol{\Upsilon_L^+}}$$

By solving the above four equations simultaneously, the three unknown can be easily obtained.

The acid base component ($\boldsymbol{\Upsilon^{AB}}$) was calculated using equation 2.16.

The numerical examples given below is for 5% black spruce bark extract on heat-treated jack pine,

$$\mathbf{(1 + cos\ 81.84) \times 72.8 = 2(\sqrt{\Upsilon_S^{LW} \times 21.8} + \sqrt{\Upsilon_S^+ \times 25.5}\ + \sqrt{\Upsilon_S^- \times 25.5})} \qquad \textbf{[A1.2]}$$

$$\mathbf{(1 + cos\ 65.52) \times 58 = 2(\sqrt{\Upsilon_S^{LW} \times 39} + \sqrt{\Upsilon_S^+ \times 39.6}\ + \sqrt{\Upsilon_S^- \times 2.28})} \qquad \textbf{[A1.3]}$$

$$(1 + cos\ 67.34) \times 48 = 2(\sqrt{\gamma_S^{LW} \times 29} + \sqrt{\gamma_S^{+} \times 47} + \sqrt{\gamma_S^{-} \times 1.92}) \quad \textbf{[A1.4]}$$

$$(1 + cos\ 3.23) \times 18.43 = 2(\sqrt{\gamma_S^{LW} \times 18.43} + \sqrt{\gamma_S^{+} \times 0} + \sqrt{\gamma_S^{-} \times 0}) \quad \textbf{[A1.5]}$$

By solving equations A1.2-A1.5 simultaneously, following surface energy components were obtained

$$\gamma_S^{LW} = 20.14\ mJ/m^2$$

$$\gamma_S^{+} = 2.678\ mJ/m^2$$

$$\gamma_S^{-} = 36.32\ mJ/m^2$$

$$\gamma_S^{AB} = 2\sqrt{(2.678 \times 36.32)} = 19.73\ mJ/m^2$$

$$\gamma_s = 19.73 + 20.14 = 39.86\ mJ/m^2$$

Appendix 2

Effect of Titania and ZnO Particles on Aging Performance of Acrylic Polyurethane for Heat-Treated Jack Pine

Coating selection for exterior use often requires a balance between aesthetic (clear coatings) and protection (colored coatings) for a particular application. Water based acrylic polyurethane coatings are highly efficient, non toxic and durable with upgraded film properties. Incorporation of UV absorbers and HALS is necessary for the development of transparent coatings which most of the time are toxic in nature. Increasing pressure of the environmental legislation to reduce the VOC content of the coatings has compelled the development of non toxic organic and inorganic UV absorbers. Among the inorganic UV absorbers titanium dioxide and zinc oxide have a long history of color protection. In this section, the performance characteristic of acrylic polyurethane incorporated with a natural antioxidant (bark extract) and inorganic UV absorbers (nano and micro titania and nano zinc oxide) along with organic UV absorbers are reported. In order to assess the performance of these modified coatings, it is necessary to study their wetting and penetration characteristics into wood and changes occurring at the wood and coating interface due to weathering induced by UV. The service life (durability) of coated-wood surface depends on the chemical composition of coating material, properties of the wood surface (type of species, early wood and late wood region, sap wood or heart wood etc.) and the interaction between the coating materials with the wood at their interface. This

interaction is primarily reflected in the wetting and spreading of the coating material over the wood surface during its application and it determines the contact area and smoothness of the coating layer. The fluorescence microscope is a very important tool to determine the penetration characteristic of different coatings into wood cells. The penetration behavior is well correlated with the adhesion performance of coatings to the wood surface. Also, the changes in the wood-coating interface taking place due to weathering can be characterized using fluorescence microscopy. This analysis gives valuable information on the interaction between wood and coating which could be directly related to the color change during accelerated aging.

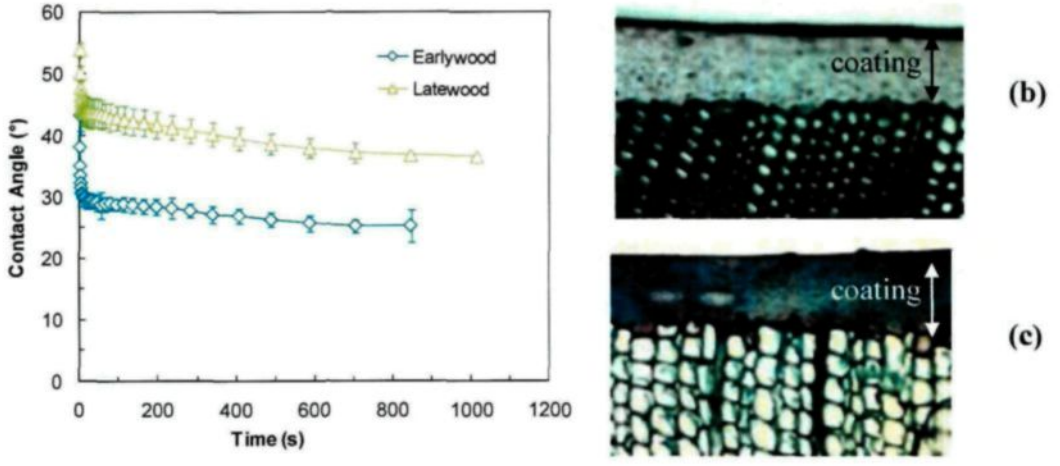

Figure A.2.1 Acrylic polyurethane coating containing bark extract and titania micro particle (a) comparison of contact angle change with time on early wood and late wood regions; penetration characteristic of (b) late wood (c) early wood jack pine studied with fluorescence microscope

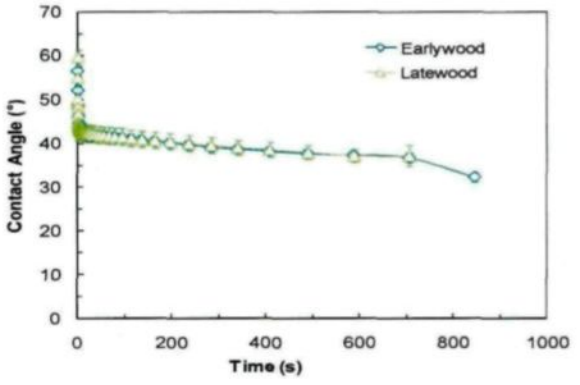

(a)

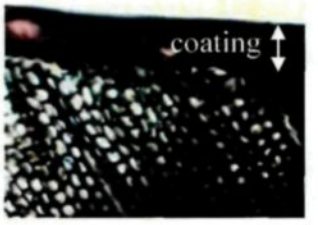

(b)

Figure A.2.2 Acrylic polyurethane coating containing bark extract and titania nano particles **(a)** comparison of contact angle change with time on early wood and late wood regions; penetration characteristic of **(b)** early wood jack pine studied using fluorescence microscope

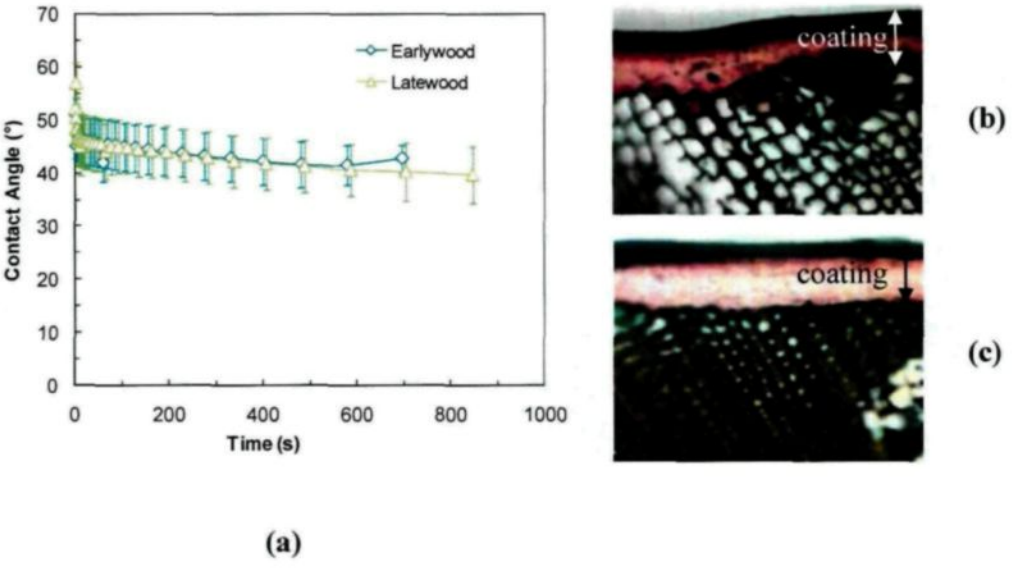

Figure A.2.3 Acrylic polyurethane coating containing bark extract and zinc oxide nano particles **(a)** comparison of contact angle change with time for early wood and late wood region; penetration characteristic of **(b)** late wood **(c)** early wood jack pine studied using fluorescence microscope

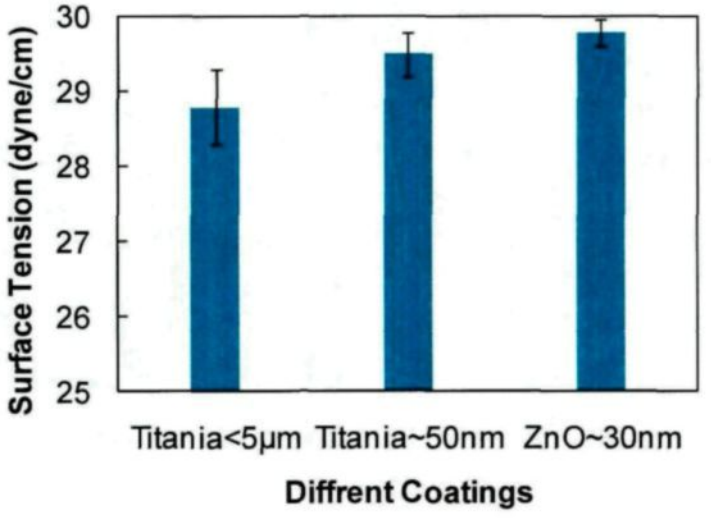

Figure A.2.4 Comparison of surface tension of acrylic polyurethane coating containing titania micro particles, titania nano particles and zinc oxide nano particles

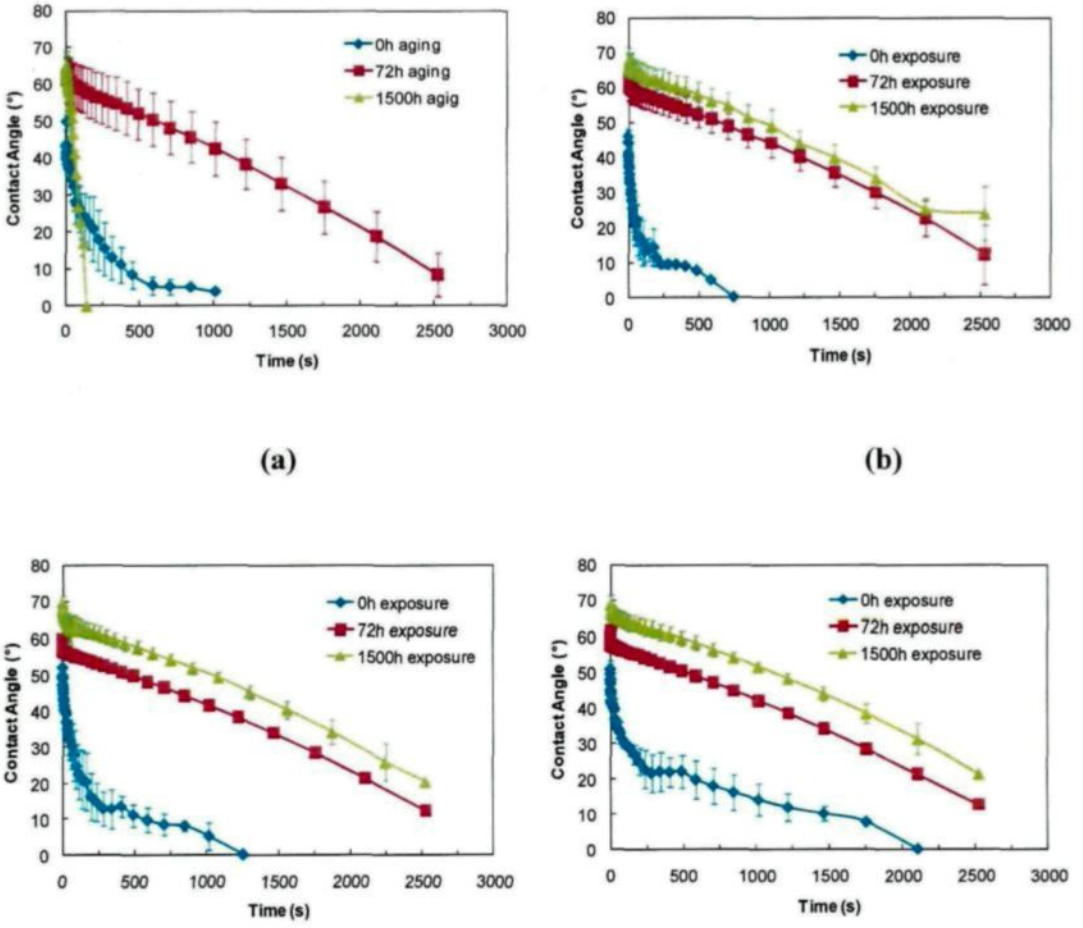

Figure A.2.5 Dynamic contact angle of water for different aging times on jack pine surface coated with the acrylic polyurethane coating containing (a) only organic UV absorbers, (b) titania micro particles, (c) titania nano particles and (d) zinc oxide nano particles

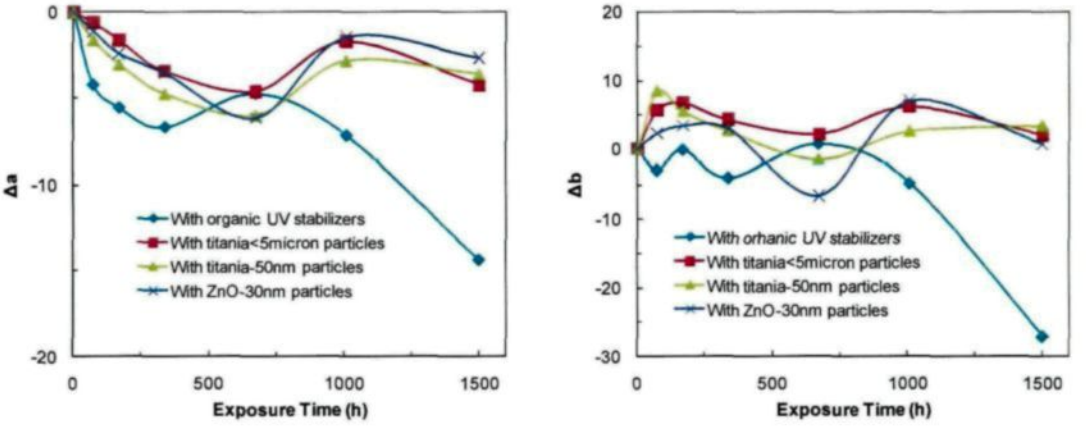

(a)

(b)

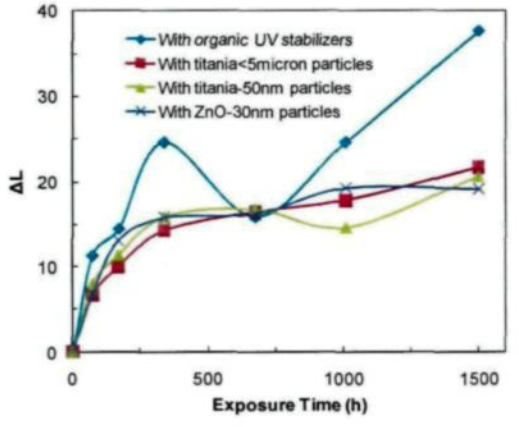

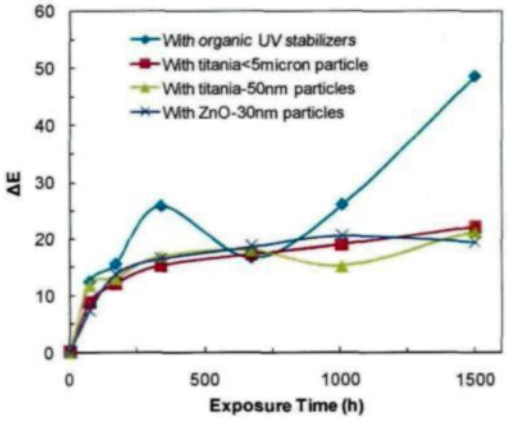

Figure A.2.6 Comparison of color change of heat-treated jack pine coated with acrylic polyurethane with titania micro, titania nano particles, ZnO nano particles, and organic UV stabilizers after different aging periods (a) red-green index, (b) yellow-blue index, (c) lightness index, and (d) total color change

Figure A.2.7 Visual assessment of acrylic polyurethane coated heat-treated jack pine for different aging times

Titania micro particles **Titania Nano particles** **ZnO nano particles**

(a) **(e)** **(i)**

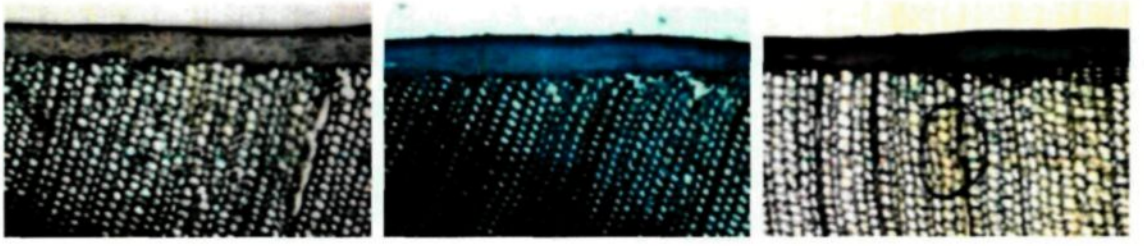

(b) **(f)** **(j)**

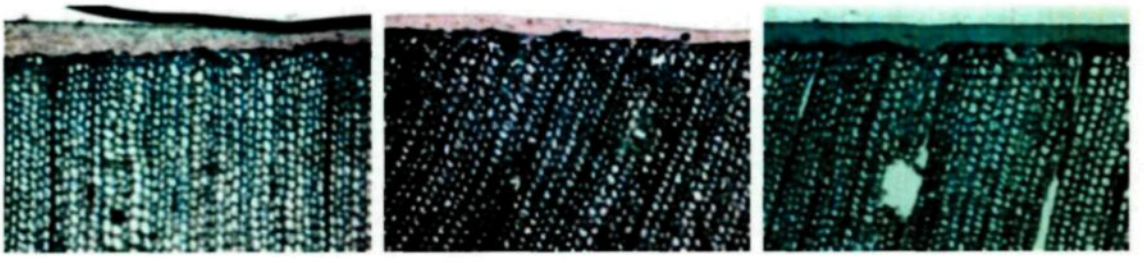

(c) **(g)** **(k)**

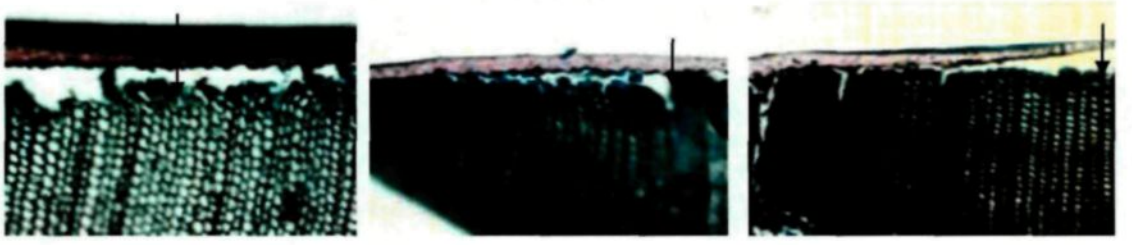

(d) (h) (l)

Figure A.2.8 The light micrographs of transverse section of the coating containing titania micro particles and wood interface for different aging time (a) before aging, (b) after 72h of aging, (c) 672h of aging, (d) 1500h of aging, the coating containing titania nano particles and wood interface for different aging time (e) before aging, (f) after 72h of aging, (g) 672h of aging, (h) 1500h of aging and the coating containing zinc oxide nano particles and wood interface for different aging time (i) before aging, (j) after 72h of aging, (k) 672h of aging, (l) 1500h of aging

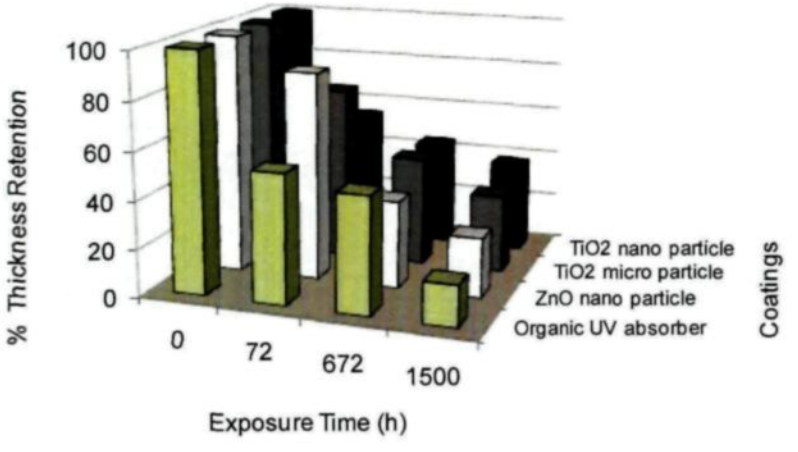

Figure A.2.9 Percentage of coating thickness retention with increasing aging time

There was a notable difference between the contact angle of acrylic polyurethane coating containing titania micro particles and early wood or late wood jack pine whereas for the other two coatings no difference in contact angle had been observed in early wood and late wood regions. The contact angle of the acrylic polyurethane coating containing zinc oxide nano particles/jack pine was highest at all times compared to those of the other two coatings. This could be attributed to its high surface tension. Coating containing titania micro particles had the lowest surface tension. The degree of orientation due to cross linking between polymers under the influence of light increased initial contact angle of coated-wood surface with water during aging for all four coatings. Coating erosion which took place due to the photodegradation of polymeric material of the coating during aging was an important phenomenon noticed for all coated-wood surfaces. Highest change in the coating thickness was observed for the coating containing only organic UV absorbers. Very poor penetration characteristic of all coatings was another important phenomenon revealed by fluorescence microscopy tests. The photodegradation effect on the cell layer just beneath the coating after 1500h of aging was observed for all coatings but for the acrylic polyurethane coating containing only organic UV absorber and the coating containing titania nano particles the degradation started within 672h of aging. The degradation after 672h of aging beneath the coating containing only organic UV absorbers was much severe than the coating containing titania nano particle. Therefore, it was well established that addition of natural antioxidant and inorganic UV absorbers improve the protective characteristic of acrylic polyurethane coating. But among them the coating containing titania nano particles was less effective than the other two coatings for

protecting heat-treated jack pine surface. The delamination was mainly due to the separation of wood cells from each other as a result of degradation of lignin during aging and not to the adhesion loss of the coating material from the wood surface.

Appendix 3

Performance of Needle Extracts as Coating Additives to Delay the Discoloration of Heat-Treated Jack Pine during Aging

In this study, effectiveness of different natural antioxidants has been tested in protecting the heat-treated wood from degradation under accelerated aging conditions. The details of bark extracts performance are reported in the main text. In this section, the performance of needle extract is compared with that of bark extracts incorporated in to acrylic polyurethane coating for the protection of heat-treated wood. The color change data along with visual assessment and ATR-FT-IR analysis revealed that needle extracts are less effective in protection of heat-treated jack pine compared to bark extracts.

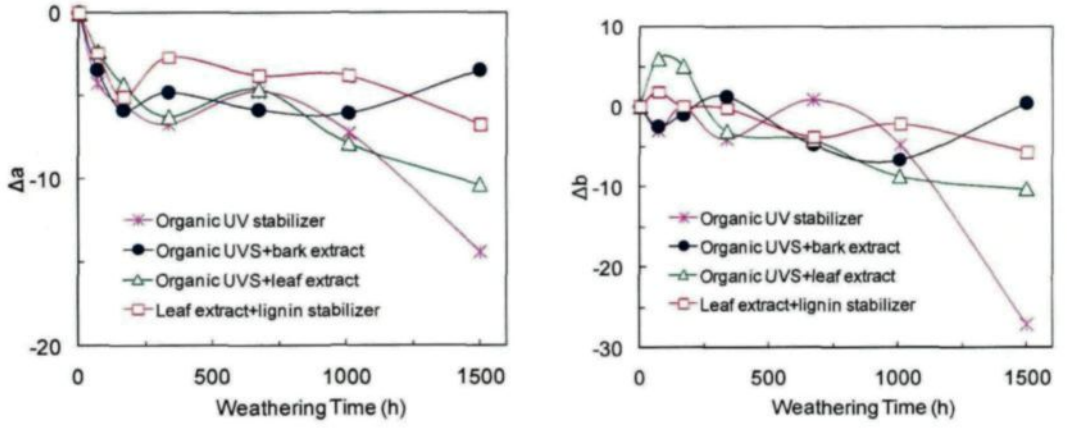

(a) (b)

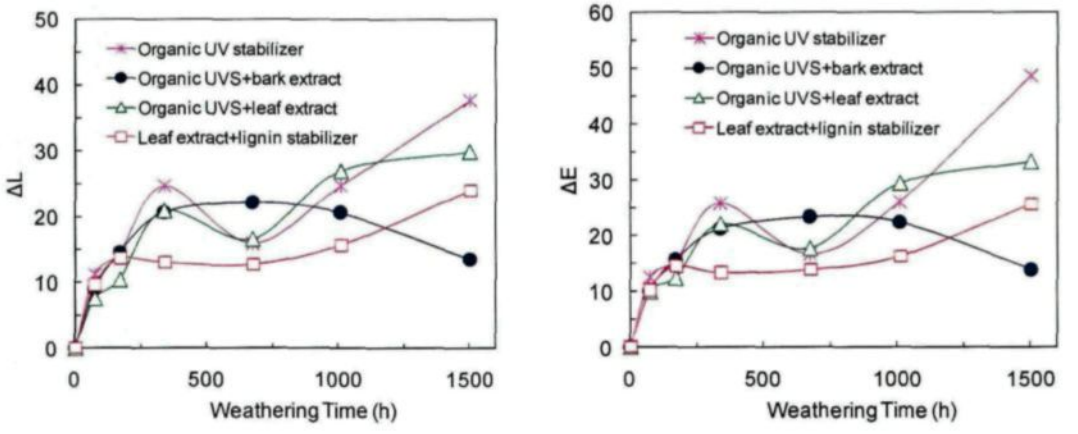

(c) (d)

Figure A.3.10 Comparison of acrylic polyurethane coatings stabilized with different additives (a) red-green index, (b) yellow-blue index, (c) lightness index, and (d) total color change

Figure A.3.2 Heat-treated jack pine coated acrylic polyurethane coatings stabilized by different additives for different aging time

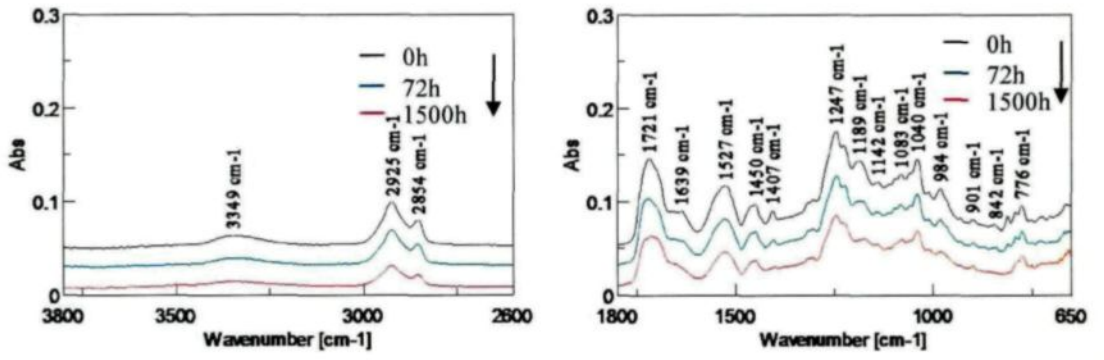

(a) (b)

Figure A.3.3 ATR–FT-IR analysis of acrylic polyurethane coating containing organic UV absorbers and bark extracts on heat-treated jack pine for different exposure times (a) 1800–650cm^{-1} and (b) 3800–2600cm^{-1}

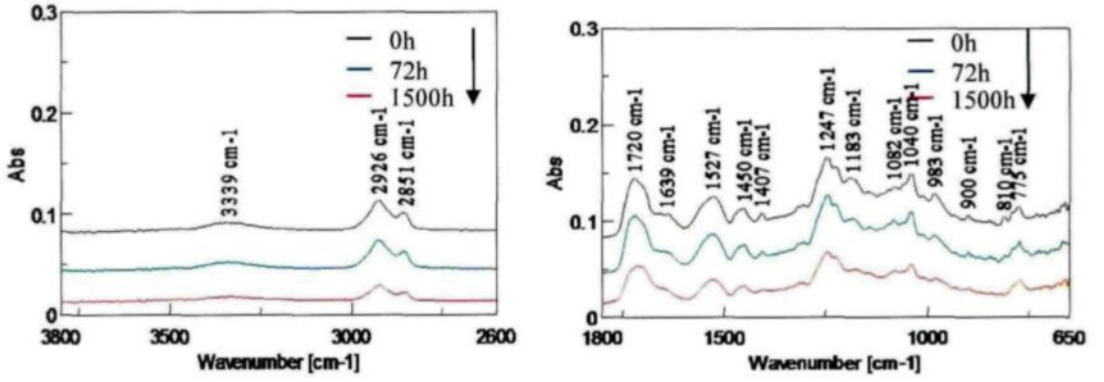

(a) (b)

Figure A.3.4 ATR–FT-IR analysis of acrylic polyurethane coating containing organic UV absorbers and needle extracts on heat-treated jack pine for different exposure times (a) 1800–650cm^{-1} and (b) 3800–2600cm^{-1}

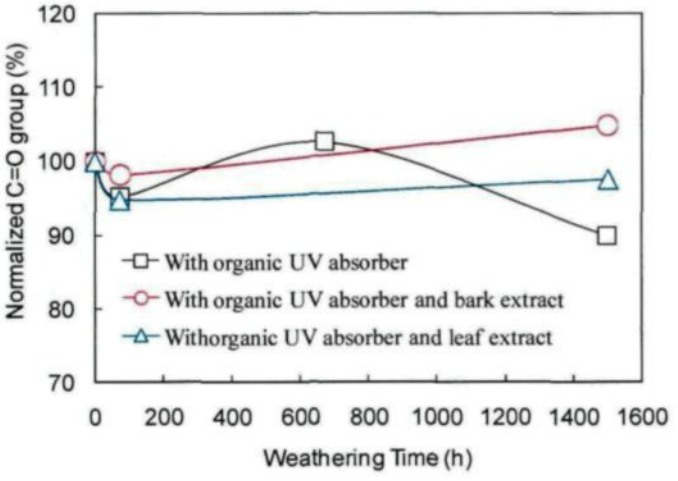

Figure A.3.5 Build-up of oxidation photoproducts during accelerated aging test of acrylic polyurethane coating stabilized with organic UV stabilizers alone or along with needle extract or bark extract

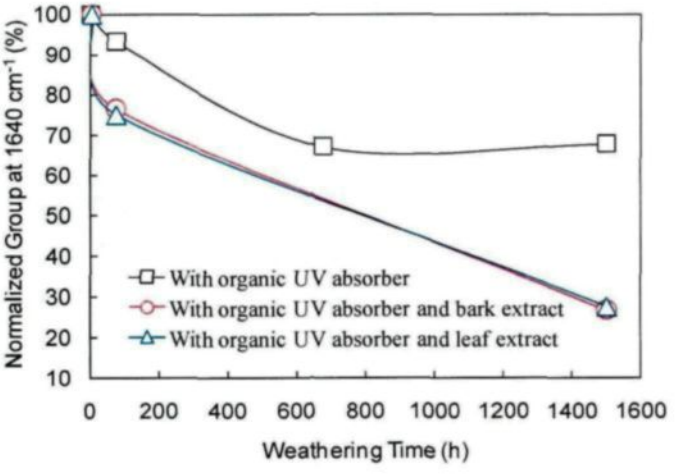

Figure A.3.6 Diminution of H-bond and C=O stretching of the urethane during accelerated aging of acrylic polyurethane coating stabilized with organic UV stabilizers alone or along with needle extract or bark extract

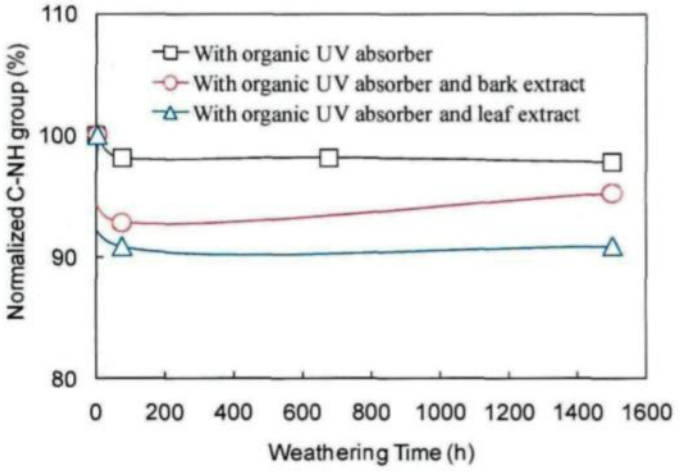

Figure A.3.7 Loss of urethane group for acrylic polyurethane coating stabilized with organic UV stabilizers alone or along with needle extract or bark extract during aging period

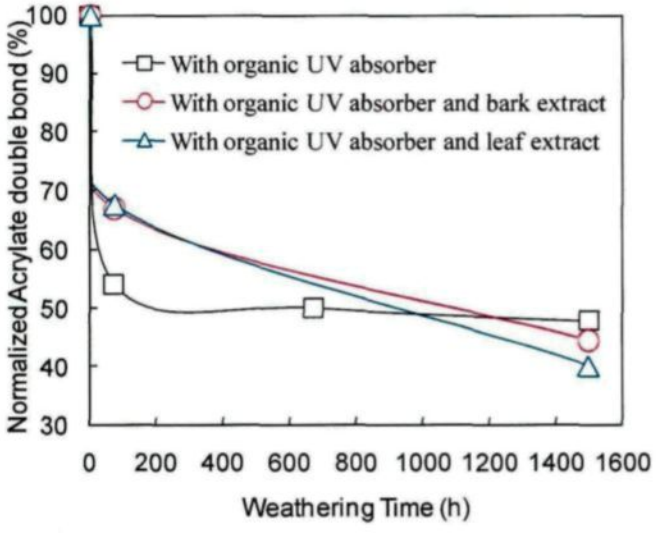

Figure A.3.8 Loss of acrylate double bond for acrylic polyurethane coating stabilized with organic UV stabilizers alone or along with needle extract or bark extract during aging

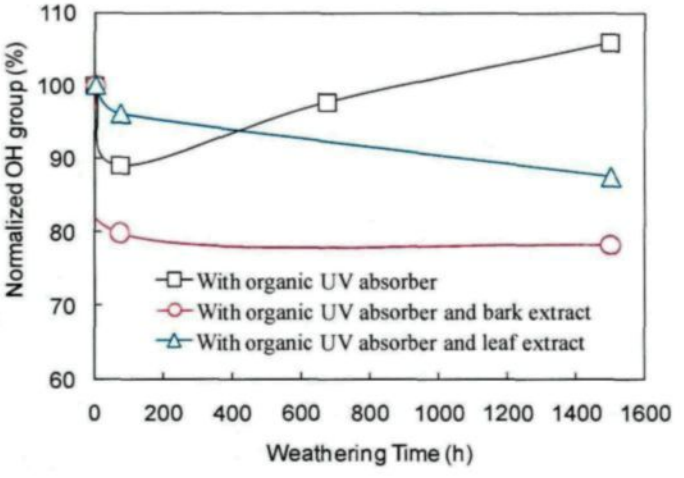

Figure A.3.9 Changes in absorption area under hydroxyl peak for acrylic polyurethane coating stabilized with organic UV stabilizers alone or along with needle extract or bark extract at different aging times

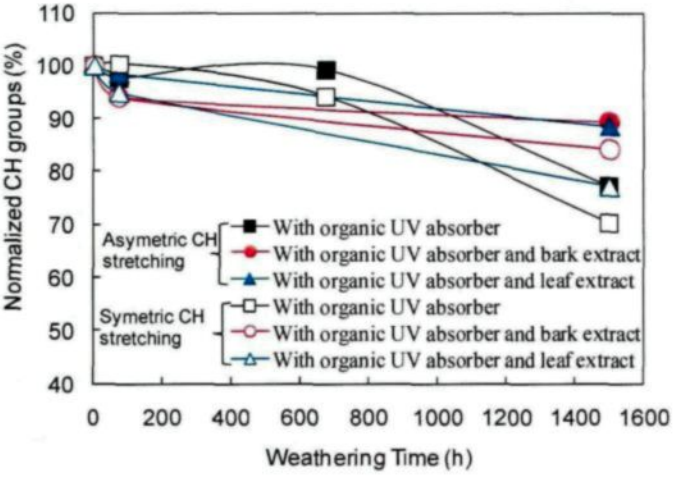

Figure A.3.110 Changes in CH stretching for acrylic polyurethane coating stabilized with organic UV stabilizers alone or along with needle extract or bark extract at different aging times

The color measurement results showed that addition of bark extract and needle extract certainly decreased the color change during accelerated aging but bark extract was more efficient than needle extract. The visual assessment results also proved this statement. Oxidation and loss of acrylate double bond were attributed to the degradation of acrylic polyurethane as divulged by ATR-FTIR analysis. The crosslink scission of acrylic polyurethane was not significant enough. There was depletion of bark extract and needle extract from the polymer matrix during accelerated aging. The natural antioxidants acted mainly as radical scavenger shown by less photodegradation observed for coatings containing natural antioxidants compared to that of organic UV stabilizers.

Appendix 4

Characterization of Lignin Nano Particles and their Efficiency as Coating Additives

Lignin is a very good absorber of UV light. 95% of UV radiation reaches to wood surface are absorbed by lignin. Also it is highly antioxidant in nature due to the presence of phenolic groups in their structure. As a result, it is also a very good source of natural antioxidant. High temperature heat-treatment of wood modifies the lignin structure by demothoxylation and condensation which results in less degradation of heat-treated wood lignin compared to natural wood lignin under aging. Organosolv lignins of lodgepole pine and poplar, heat-treated at different temperatures, were obtained from Bioconversion. They were further treated by microfluidizer in order to get nano sized particles of these organosolv lignins which could be easily distributed homogeneously throughout the acrylic polyurethane coatings. In this section, the particle size distributions of these organosolv lignins are presented along with the SEM images. Also the effectiveness of these lignins in acrylic polyurethane coating for the protection of heat-treated jack pine were studied under accelerated aging conditions and color measurement and visual assessment results are reported in this section.

Effect of sieve size and number of passes on lignin particle diameter

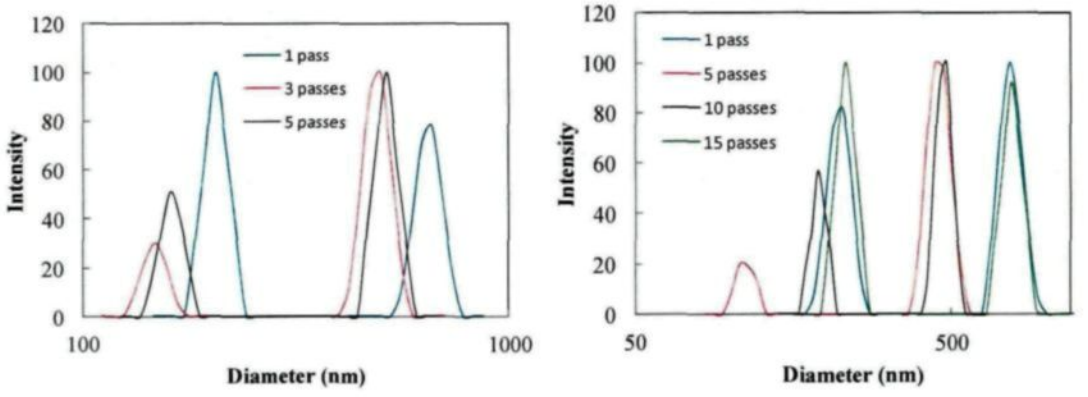

Figure A.4.1 Particle size distribution of poplar lignin after passing through 200μm (a) and 87 μm (b) sieve for different number of passes

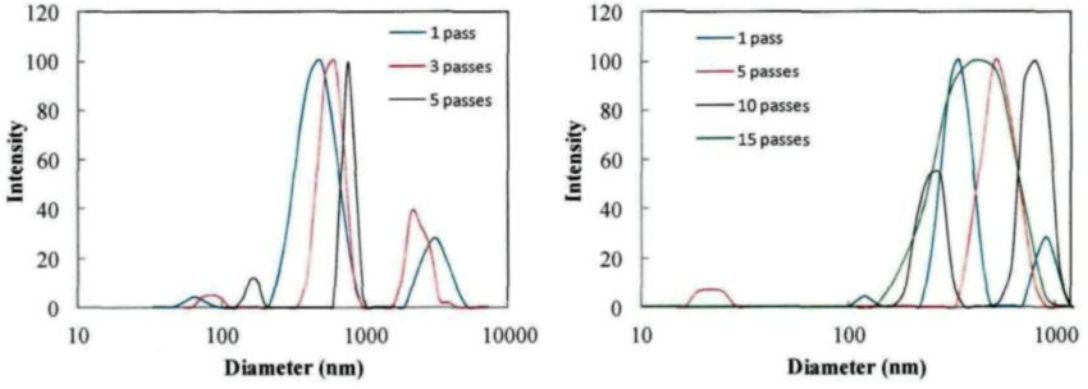

Figure A.4.12 Particle size distribution of lodgepole pine lignin after passing through 200μm (a) and 87 μm (b) sieve for different number of passes

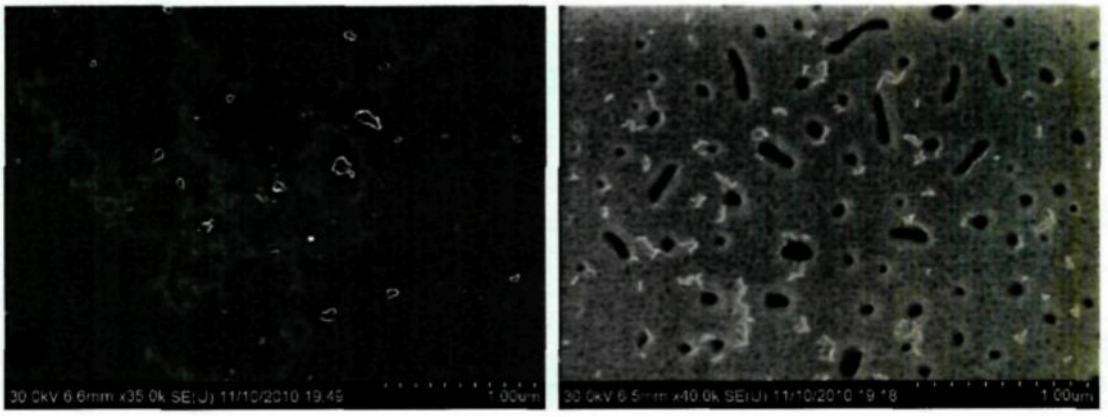

(a) (b)

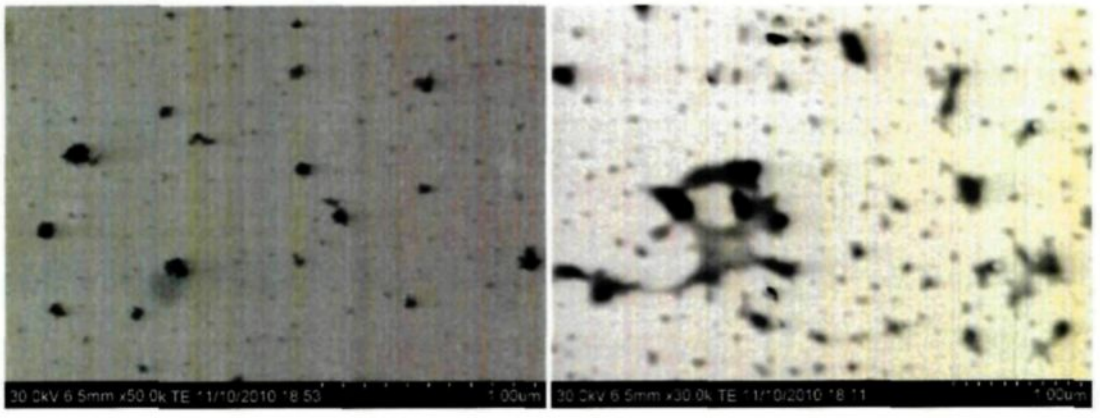

(c) (d)

Figure A.4.3 Lignin nano particles after passing through 200 μm seive for 5 times at 3000 psi (a) and 6000 psi (b) pressure for poplar lignin and 3000 psi(c) and 6000 psi (d) for lodgepole pine lignin in microfluidizer (with increase in pressure lignin nano particles started aggregating)

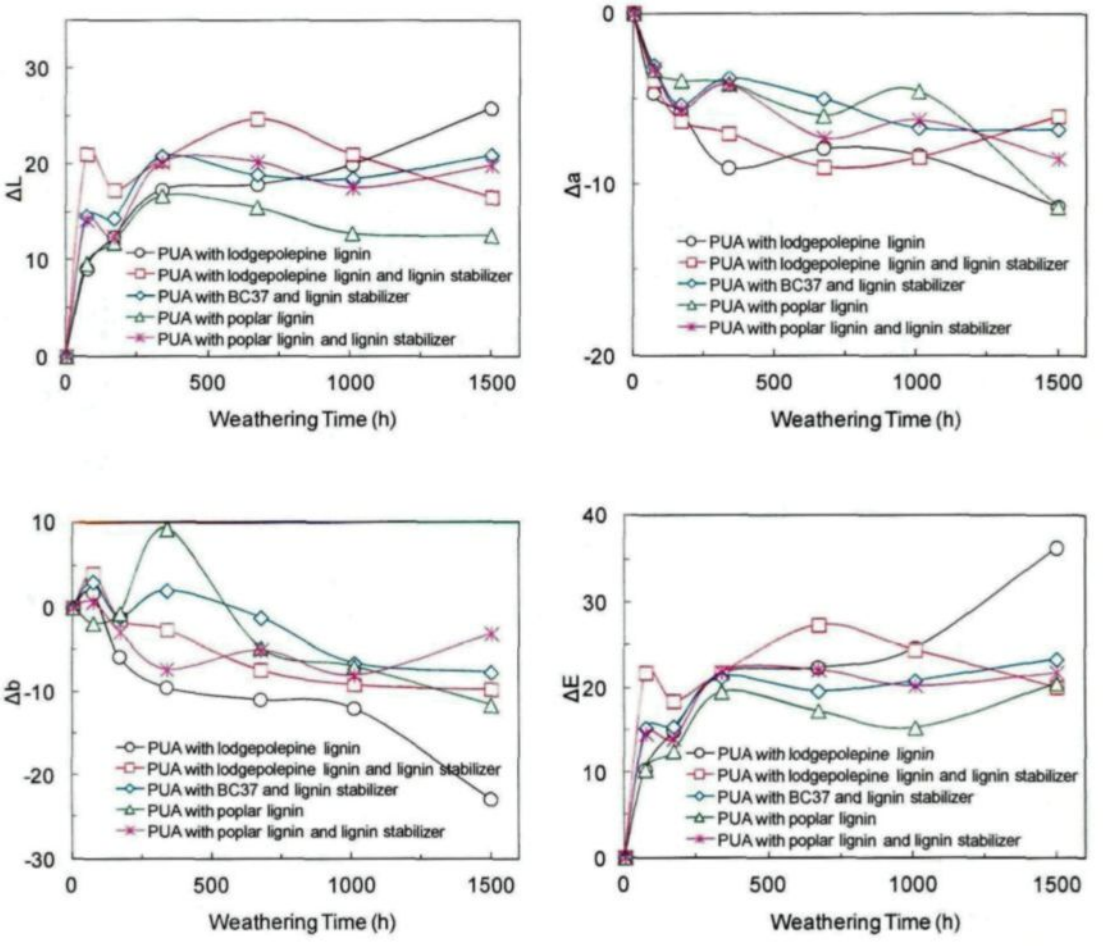

Figure A.4.4 Comparison of color change of acrylic polyurethane coating with different lignin nano particles and/or lignin stabilizer on heat-treated jack pine after different aging periods (a) lightness index, (b) red-green index, (c) yellow-blue index, and (d) total color change

Poplar lignin seemed to be more effective to delay discoloration of heat-treated jack pine compared to lodgepole pine lignins

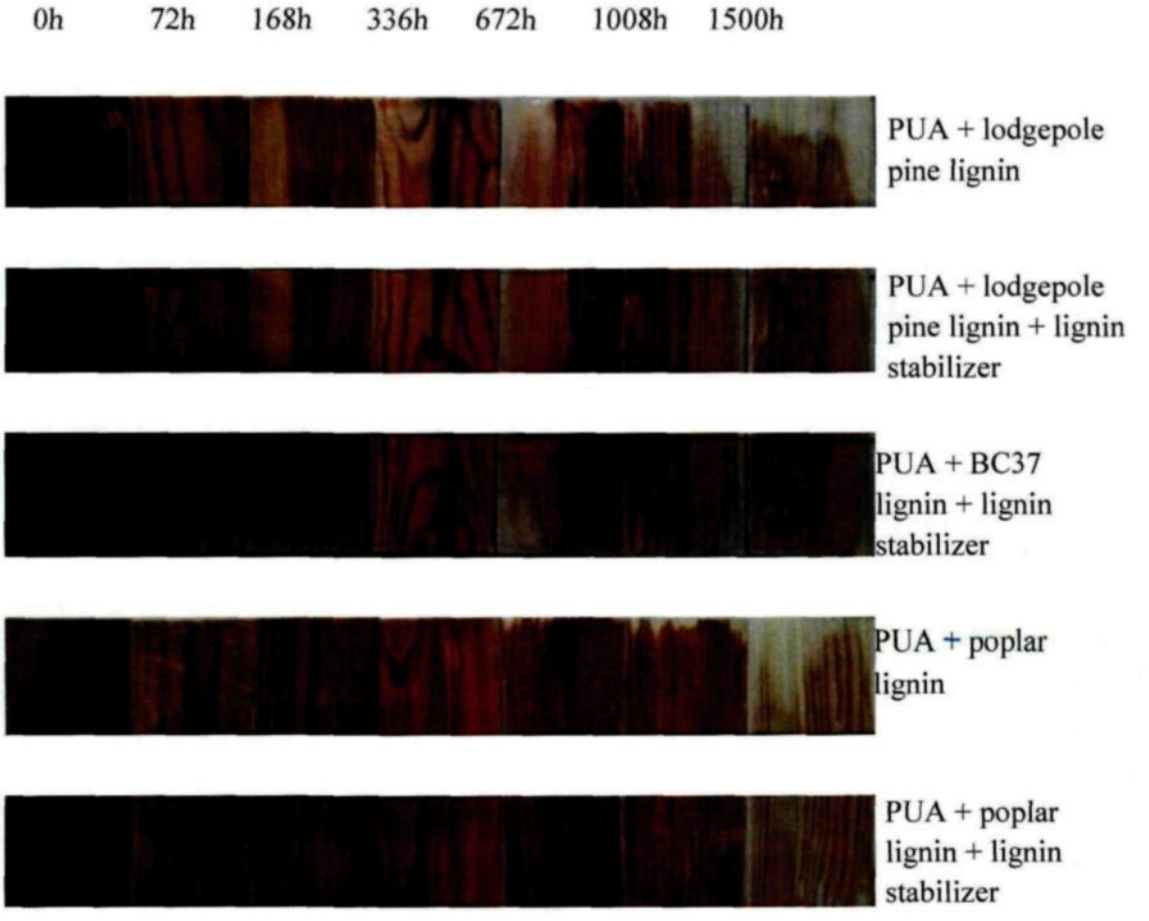

Figure A.4.5 Comparison of protective characteristics of acrylic polyurethane stabilized with lignin nano particles for different aging time

Acrylic polyurethane with poplar lignin alone or together with lignin stabilizer protected heat-treated jack pine till 1008h but at the end of 1500h of accelerated aging both the coatings failed to protect heat-treated jack pine. Acrylic polyurethane with lodge pole pine lignins alone or together with lignin stabilizer underwent high color loss only after 672h of accelerated aging.

Appendix 5

XPS Results for Acrylic Polyurethane Coating with CeO_2 Nano Particles and Lignin Stabilizer

Table A.5.1 Atomic percentage of different components of acrylic polyurethane coating containing CeO_2 nano particles and lignin stabilizer

Aging time (h)	Species	C (%)	Carbon Components				O (%)	N (%)	Si (%)	Ce (%)	O/C	N/C
			C-H/ C-C	C-N	C-O	C=O						
0	Birch	76.48	58.5	29.51	11.99	0	22.24	0	1.29	0	0.29	0.000
72		74.79	61.16	24.38	1.52	12.93	23.21	0.71	1.29	0	0.31	0.009
672		73.16	61.45	26.57	1.92	10.06	21.52	4.07	1.09	0	0.29	0.056
1500		76.59	67.09	20.66	2.74	9.51	19.71	3.68	0	0.03	0.26	0.048
0	Aspen	41.61	57.5	28.51	12.99	0	55.7	1.23	1.46	0	1.34	0.030
72		76.18	46.83	41.33	11.84	0	22.9	0.05	0.86	0	0.30	0.001
672		76.66	61.15	25.31	13.54	0	22.52	0.24	0.58	0	0.29	0.003
1500		77.22	54.61	34.01	11.34	0	18.38	4.14	0	0.27	0.24	0.054
0	Jack pine	76.39	58.47	28.57	0.53	12.44	22.77	0	0.84	0	0.30	0.000
72		76.64	61.74	24.83	0.24	13.19	22.59	0.2	0.57	0	0.29	0.003
672		74.03	61.48	27.4	0.89	10.23	21.77	3.96	0.05	0	0.29	0.053
1500		84.05	80.88	11.52	2.07	5.54	13.76	2.18	0	0.1	0.16	0.026

Appendix 6

Comparison of Acrylic Polyurethane Coatings on Heat-Treated and Untreated Wood Species

This study mainly focuses on the protection of heat-treated wood from UV light. In this section, the effectiveness of the best coatings (acrylic polyurethane with bark extracts and lignin stabilizer; and acrylic polyurethane with CeO_2 nano particles and lignin stabilizer) on heat-treated wood is compared with that on untreated wood. The color measurement results showed that with increase in aging time the acrylic polyurethane with CeO_2 nano particles and lignin stabilizer on all the three heat-treated wood species become darker. This was probably due to the presence of extractives which migrated to the wood surface during aging.

Acrylic polyurethane with bark extracts and lignin stabilizer protected heat-treated jack pine well, even after 1500h of aging, but it failed to perform on untreated jack pine. Significant degradation was observed on the surface of untreated jack pine at the end of 1500h of aging. On the other hand, t could be seen from the fluorescence micrographs that there was almost no degradation at the interface of acrylic polyurethane with CeO_2 nano particles and lignin stabilizer and untreated birch after 1500h of accelerated aging whereas only 4-5 cell layer degradation was observed for untreated aspen. Also, very small degradation was observed at the interface of untreated jack pine and acrylic polyurethane with CeO_2 nano particles and lignin stabilizer after 1500h of aging.

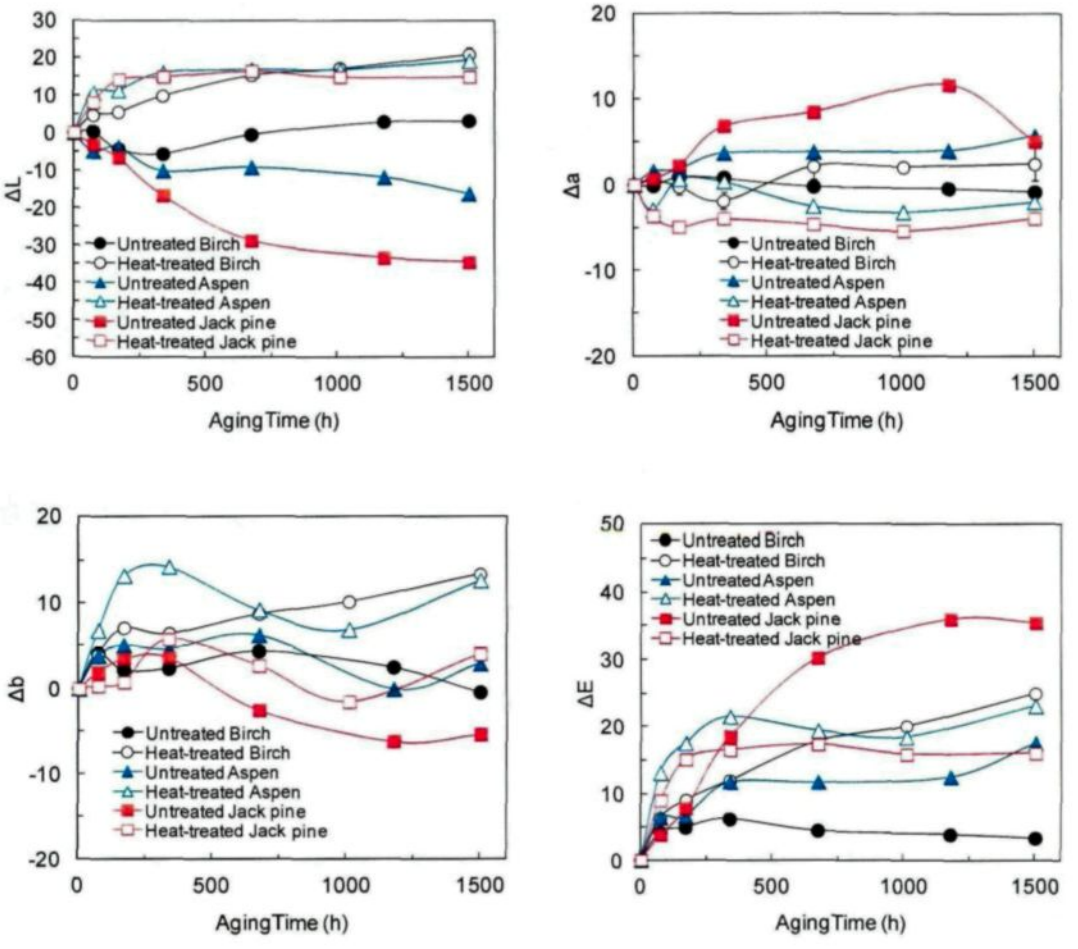

Figure A.6.1 Comparison of color change of acrylic polyurethane containing CeO_2 nano particles and lignin stabilizer on heat-treated and untreated jack pine, aspen, and birch after different aging periods (a) lightness index change, (b) red-green index change, (c) yellow-blue index change, and (d) total color change

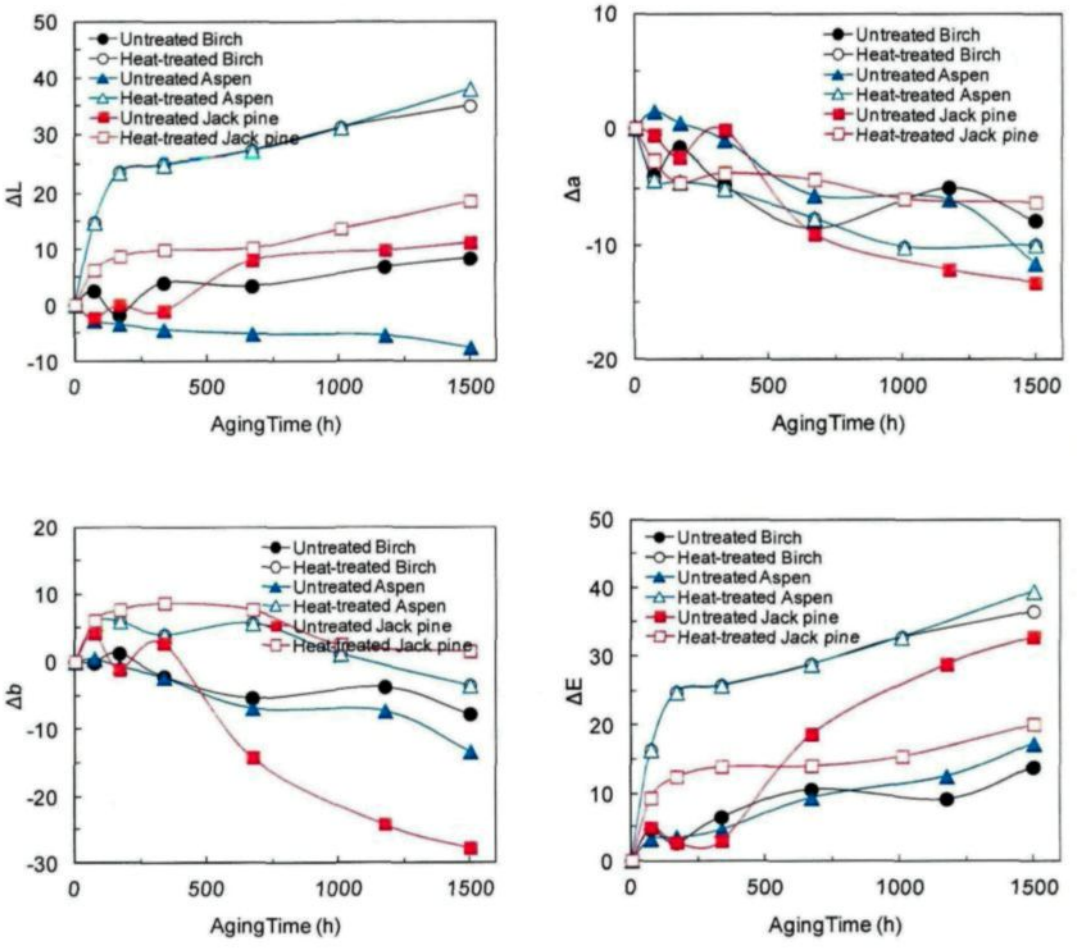

Figure A.6.13 Comparison of color change of acrylic polyurethane containing bark extracts and lignin stabilizer on heat-treated and untreated jack pine, aspen, and birch after different aging periods (a) lightness index change, (b) red-green index change, (c) yellow-blue index change, and (d) total color change

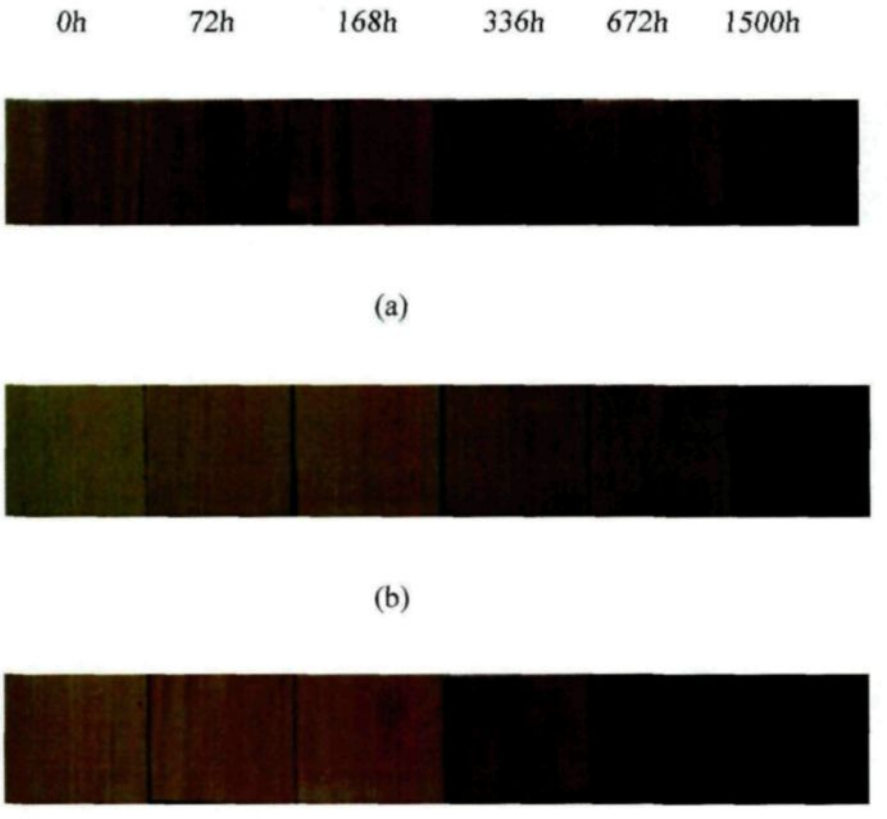

Figure A.6.3 Comparison of protective characteristic of acrylic polyurethane with CeO_2 nano particles and lignin stabilizer on untreated (a) jack pine, (b) aspen, and (c) birch before and after aging for different periods

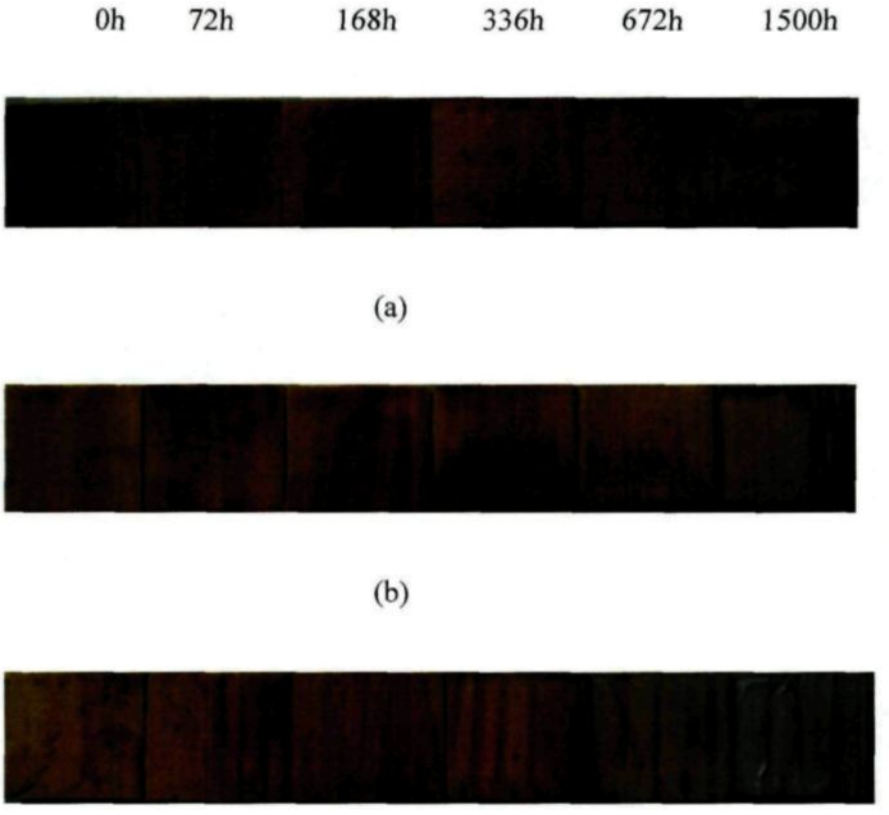

Figure A.6.4 Comparison of protective characteristic of acrylic polyurethane with bark extracts and lignin stabilizer on untreated (a) jack pine, (b) aspen, and (c) birch before and after aging for different periods

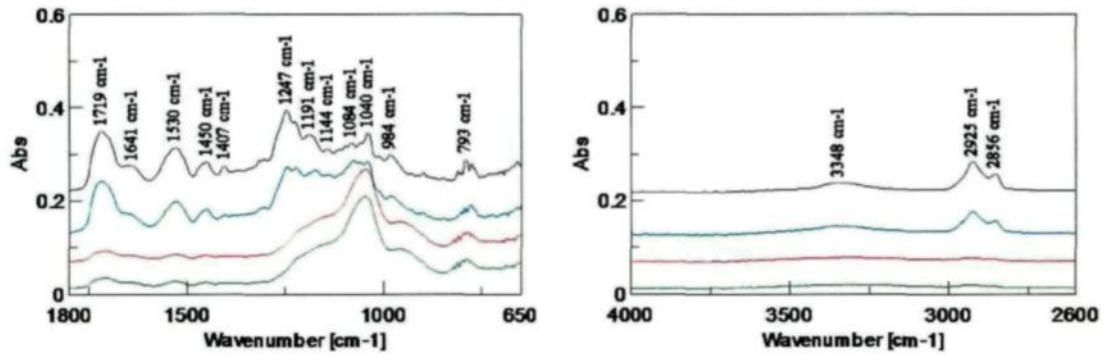

(a) (b)

Figure A.6.5 ATR–FT-IR analysis of acrylic polyurethane coating containing CeO_2 nano particles and lignin stabilizer on untreated birch for different exposure times (a) 1800–650cm^{-1} and (b) 3800–2600cm^{-1}

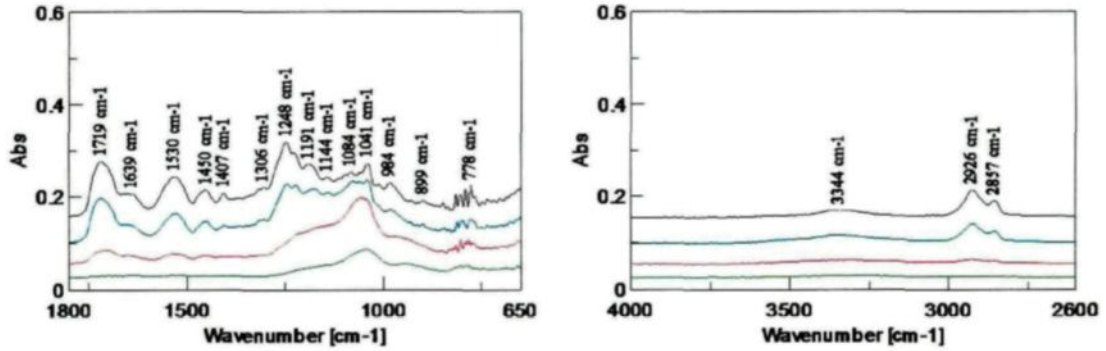

Figure A.6.6 ATR–FT-IR analysis of acrylic polyurethane coating containing CeO_2 nano particles and lignin stabilizer on untreated aspen for different exposure times (a) 1800–650cm^{-1} and (b) 3800–2600cm^{-1}

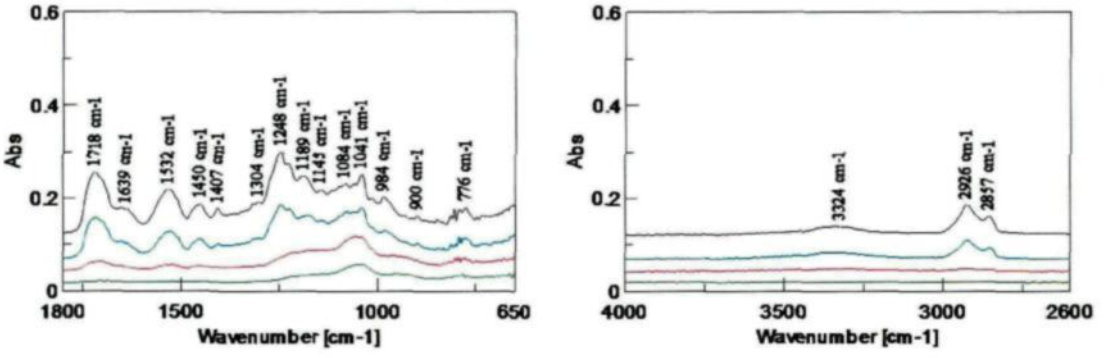

Figure A.6.7 ATR–FT-IR analysis of acrylic polyurethane coating containing CeO_2 nano particles and lignin stabilizer on untreated jack pine for different exposure times (a) 1800–650cm^{-1} and (b) 3800–2600cm^{-1}

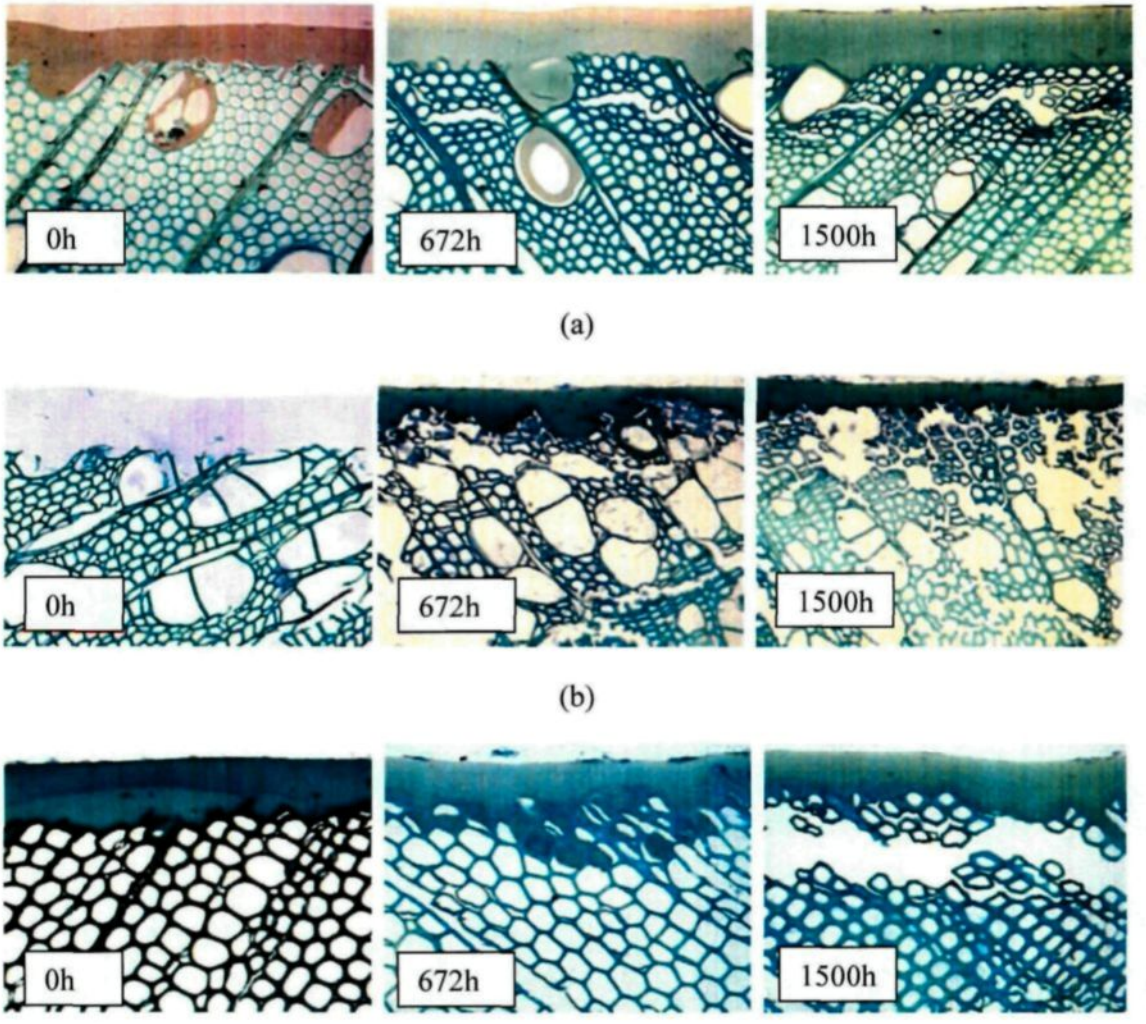

Figure A.6.8 The light micrographs of transverse section of the acrylic polyurethane coating containing CeO_2 nano particles and lignin stabilizer and (a) untreated birch, (b) untreated aspen, and (c) untreated jack pine interface for different aging times

Appendix 7

Antifungal Activity of Different Extracts on Three North American Heat-Treated Wood Species

The efficiency of different bark extracts (jack pine, yellow birch, white birch, larix, white spruce, black spruce) on three heat-treated wood species (jack pine, aspen, birch) were examined for their fungal durability. The heat-treated woods were immersed in 10% methanolic solution of these extract for 24h. They were dried at 40°C for 48h before exposing to fungi. Two different types of fungi were used for this study - a brown rot fungus (*P. placenta*) and a white rot fungus (*T. versicolor*). The mass of these specimens were recorded before and after fungal degradation and the weight loss data were compared and are presented in this section.

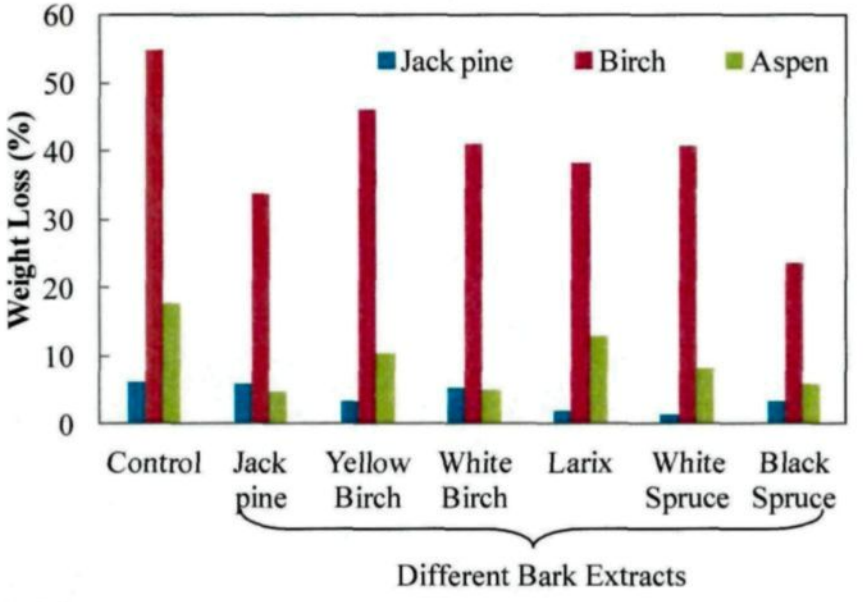

Figure A.7.1 Comparison of mass loss data of different bark extracts on heat-treated jack pine, aspen, and birch with those of heat-treated woods without any extracts (control) after 8 weeks of decay by *P. placenta*

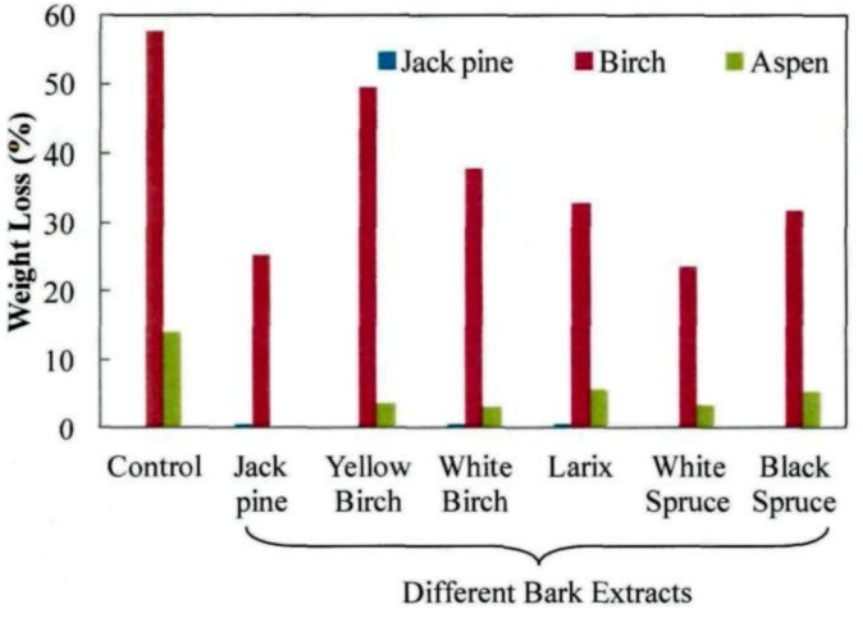

Figure A.7.2 Comparison of mass loss data of different bark extracts on heat-treated jack pine, aspen, and birch with those of heat-treated woods without any extracts (control) after 8 weeks of decay by *T. versicolor*

List of Publications

Journal Papers

- **S. Saha**, D. Kocaefe, D. K. Sarkar, Y. Boluk, A. Pichette (2011) *Effect of TiO_2-containing Nano- coatings on the Color Protection of Heat-treated Jack pine.* J. Coat. Technol. Research. 8 (2) 183-190.

- **S. Saha**, D. Kocaefe, Y. Boluk, A. Pichette (2011) *Enhancing Exterior Durability of Jack Pine by Photo-Stabilization of Acrylic Polyurethane Coating using Bark Extract: Part 1- Effect of UV on Color Change and ATR-FTIR Analysis.* Prog. Org. Coat. 70 (4) 376-382.

- **S. Saha**, D. Kocaefe, C. Krause, T. Larouche (2011) *Effect of Titania and Zinc Oxide Particles on Acrylic Polyurethane Coating Performance*. Prog. Org. Coat. 70 (4) 170-177.

- D. Kocaefe, **S. Saha** (2012) *Comparison of the Protection Effectiveness of Acrylic Polyurethane Coatings Containing Bark Extracts on Three Heat-treated North American Wood Species: Surface Degradation.* Appl. Surf. Sci. 258 (13) 5283-5290.

- **S. Saha**, D. Kocaefe, Y. Boluk, V. Mshvildadze, J. Legault A. Pichette (2011) *Boreal Forest Conifer Extracts: Potential Natural Additives for Acrylic Polyurethane Coatings for the Protection of Heat-Treated Jack Pine.* J. Coat. Technol. Research. (Submitted).

- **S. Saha**, D. Kocaefe, Y. Boluk, A. Pichette (2012) *Surface Degradation of Acrylic Polyurethane Coated Heat-Treated Jack Pine under Accelerated Aging Conditions: Effectiveness of Cerium Oxide Nano Particles* . Appl. Surf. Sci. (Submitted).

- **Sudeshna Saha**, Duygu Kocaefe, Cornelia Krause, Yaman Boluk, Andre Pichette (2011) *Enhancing Exterior Durability of Heat-Treated Jack Pine by Photo-Stabilization by Acrylic Polyurethane Coating using Bark Extract Part 2: Wetting Characteristics and Fluorescence Microscopy Analysis.* Prog. Org. Coat. (Submitted).

- R. Younsi, D. Kocaefe, S. Poncsak, X. Huang, **S. Saha**, (2010) *A High Thermal Treatment of Wood: A Basic Theory and Numerical Modeling,* International Journal of Energy, Environment and Economics. *(In press)*

Book Chapter

- R. Younsi, D. Kocaefe, S. Poncsak, X. Huang, **S. Saha** (2010) *A High Thermal Treatment of Wood: A Basic Theory and Numerical Modeling* in *'Heat Treatment: Theory, Techniques and Applications', pp 201-223, Novapublishers. ISBN: 978-1-61324-684-9.*

Conference Papers

Refereed Conferences

- **S. Saha,** D. Kocaefe, Y. Boluk, A. Pichette (2010) *Photo-stabilization of Acrylic Polyurethane Coatings for Exterior Application on Wood using Bark Extract* . 6th Coatings Science International. 28 June-2 July.

- **S. Saha**, D. Kocaefe, C. Krause, T. Larouche (2010) *Microscopic Assessment of Penetration Characteristics and Coating Thickness Change with Weathering.* 6th Coatings Science International. 28 June-2 July.

- D. Kocaefe, **S. Saha**, Y. Kocaefe, A. Pichette, Y. Boluk (2012) *Effectiveness of Bark Extracts and CeO_2 Nano Particles as Coating Additives for the Protection of Heat-Treated Jack Pine.* HEFAT2012.

Non refereed Conferences

- **S. Saha**, D. Kocaefe, Y. Boluk, A. Pichette (2010) *UV Protective Coatings for Heat-treated Wood.* FPS 64th International Convention June 20-22. Wisconsin, USA .

- X. Huang, D. Kocaefe, **S. Saha**, Y. Boluk, Y. Kocaefe, A. Pichette (2010) *Study on the Discoloration Mechanism of Heat-Treated Wood Due to Weathering.* FPS 64th International Convention June 20-22. Wisconsin, USA.

- **S. Saha,** D. Kocaefe, D. K. Sarkar, Y. Boluk, A. Pichette (2009) *UV Protection of Heat-Treated Jack Pine Using TiO_2 Nano-Coatings.* 8th World Congress of Chemical Engineering, August 23-27, Montreal, Canada.

- **S. Saha**, M. Brisson, D. K. Sarkar, D. Kocaefe, A. Pichette (2009) *Super Hydrophobic Wood and Aluminum Surfaces.* Surface Canada, June 2-5, Hamilton, Canada.

- **S. Saha**, D. Kocaefe, X. Huang, Y. Boluk, A. Pichette (2009) *Characterizing Surface Thermodynamic Properties of Coated and Heat-Treated Wood.* Surface Canada, June2-5 Hamilton, Canada.